Philip Ringrose
Mark Bentley

Reservoir Model Design

A Practitioner's Guide

Springer

Reservoir Model Design

Philip Ringrose • Mark Bentley

Reservoir Model Design

A Practitioner's Guide

Springer

Philip Ringrose
Statoil ASA & NTNU
Trondheim, Norway

Mark Bentley
TRACS International Consultancy Ltd.
Aberdeen, UK

ISBN 978-94-007-5496-6 ISBN 978-94-007-5497-3 (eBook)
DOI 10.1007/978-94-007-5497-3
Springer Dordrecht Heidelberg New York London

Library of Congress Control Number: 2014948780

Cover figure: Multiscale geological bodies and associated erosion, Lower Antelope Canyon, Arizona, USA. Photograph by Jonas Bruneau. © EAGE reproduced with permission of the European Association of Geoscientists and Engineers.

Printed on acid-free paper

Springer is part of Springer Science+Business Media (www.springer.com)

Preface

This book is about the design and construction of subsurface reservoir models. In the early days of the oil industry, oil and gas production was essentially an engineering activity, dominated by disciplines related to chemical and mechanical engineering. Three-dimensional (3D) geological reservoir modelling was non-existent, and petroleum geologists were mostly concerned with the interpretation of wire-line well logs and with the correlation of geological units between wells.

Two important technological developments – computing and seismic imaging – stimulated the growth of reservoir modelling, with computational methods being applied to 2D mapping, 3D volumetric modelling and reservoir simulation. Initially, computational limitations meant that models were limited to a few tens of thousands of cells in a reservoir model, but by the 1990s standard computers were handling models with hundreds of thousands to millions of cells within a 3D model domain.

Geological, or 'static' reservoir modelling, was given a further impetus from the development of promising new geostatistical techniques – often referred to as pixel-based and object-based modelling methods. These methods allowed the reservoir modeller to estimate inter-well reservoir properties from observed data points at wells and to attempt statistical prediction.

3D reservoir modelling has now become the norm, and numerous oil and gas fields are developed each year using reservoir models to determine in-place resources and to help predict the expected flow of hydrocarbons. However, the explosion of reservoir modelling software packages and associated geostatistical methods has created high expectations but also led to periodic disappointments in the reservoir modeller's ability (or failure) to predict reservoir performance. This has given birth to an oft quoted mantra "all models are wrong."

This book emerged from a series of industry and academic courses given by the authors aimed at guiding the reservoir modeller through the pitfalls and benefits of reservoir modelling, in the search for a reservoir model design that is useful for forecasting. Furthermore, geological reservoir modelling software packages often come with guidance about which buttons to press and menus to use for each operation, but very little advice on the objectives and limitations of the model algorithms. The result is that while much time is devoted to model building, the outcomes of the models are often disappointing.

Our central contention in this book is that problems with reservoir modelling tend not to stem from hardware limitations or lack of software skills but from the approach taken to the modelling – the model design. It is essential to think through the design and to build *fit-for-purpose* models that meet the requirements of the intended use. In fact, all models are *not* wrong, but in many cases models are used to answer questions which they were not designed to answer.

We cannot hope to cover all the possible model designs and approaches, and we have avoided as much as possible reference to specific software modelling packages. Our aim is to share our experience and present a generic approach to reservoir model design. Our design approach is geologically based – partly because of our inherent bias as geoscientists – but mainly because subsurface reservoirs are composed of rocks. The pore space which houses the "black gold" of the oil age, or the "golden age" of gas, has been constructed by geological processes – the deposition of sandstone grains and clay layers, processes of carbonate cementation and dissolution, and the mechanics of fracturing and folding. Good reservoir model design is therefore founded on good geological interpretation.

There is always a balance between probability (the outcomes of stochastic processes) and determinism (outcomes controlled by limiting conditions). We develop the argument that deterministic controls rooted in an understanding of geological processes are the key to good model design. The use of probabilistic methods in reservoir modelling without these geological controls is a poor basis for decision making, whereas an intelligent balance between determinism and probability offers a path to model designs that can lead to good decisions.

We also discuss the decision making process involved in reservoir modelling. Human beings are notoriously bad at making good judgements – a theme widely discussed in the social sciences and behavioural psychology. The same applies to reservoir modelling – how do you know you have a fit-for-purpose reservoir model? There are many possible responses, but most commonly there is a tendency to trust the outcome of a reservoir modelling process without appreciating the inherent uncertainties.

We hope this book will prove to be a useful guide to practitioners and students of subsurface reservoir modelling in the fields of petroleum geoscience, environmental geoscience, CO_2 storage and reservoir engineering – an introduction to the complex, fascinating, rapidly-evolving and multidisciplinary field of subsurface reservoir modelling.

Trondheim, Norway — Philip Ringrose
Aberdeen, UK — Mark Bentley

Prologue: Model Design

Successful Reservoir Modelling

This book offers practical advice and ready-to-use tips on the design and construction of reservoir models. This subject is varoiusly referred to as geological reservoir modelling, static reservoir modelling or *geomodelling,* and our starting point is very much the geology. However, the end point is fundamentally the engineering representation of the subsurface.

In subsurface engineering, much time is currently devoted to model building, yet the outcomes of the models often disappoint. From our experience this does not usually relate to hardware limitations or to a failure to understand the modelling software. Our central argument is that whether models succeed in their goals is generally determined in the higher level issue of *model design* – building models which are fit for the purpose at hand.

We propose there are five root causes which commonly determine modelling success or failure:

1. Establishing the model purpose
   - *Why are we logged on in the first place?*
2. Building a 3D architecture with appropriate modelling elements
   - *The fluid-dependent choice on the level of detail required in a model*
3. Understanding determinism and probability
   - *Our expectations of geostatistical algorithms*
4. Model scaling
   - *Model resolution and how to represent fluid flow correctly*
5. Uncertainty handling
   - *Where the design becomes subject to bias*

Strategies for addressing these underlying issues will be dealt with in the following chapters under the thematic headings of model purpose, the rock model, the property model, upscaling flow properties and uncertainty-handling.

In the final chapter we then focus on specific reservoir types, as there are generic issues which predictably arise when dealing with certain reservoirs. We share our experience, gained from personal involvement in over a hundred modelling studies, augmented by the experiences of others shared in reservoir modelling classes over the past 20 years.

Before we engage in technical issues, however, a reflection on the central theme of design.

Reservoir modellers in front of rocks, discussing design

Design in General

Design is an essential part of everyday life, compelling examples of which are to be found in architecture. We are aware of famous, elegant and successful designs, such as *the Gherkin* – a feature of the London skyline designed for the Swiss Re company by Norman Foster and Partners – but we are more likely to live and work in more mundane but hopefully fit-for-purpose buildings. The Gherkin, or more correctly the 30 St. Mary Axe building, embodies both innovative and successful design. In addition to its striking appearance it uses half the energy typically required by an office block and optimises the use of daylight and natural ventilation (Price 2009).

There are many more examples, however, of office block and accommodation units that are unattractive and plagued by design faults and inefficiencies – the *carbuncles* that should never have been built.

This architectural analogy gives us a useful setting for considering the more exclusive art of constructing models of the subsurface.

Norman Foster building, 30 St. Mary Axe (Photograph from Foster & Blaser (1993) – reproduced with kind permission from Springer Science + Business Media B.V.)

What constitutes good design? In our context we suggest the essence of a *good* design is simply that it fulfils a specific purpose and is therefore *fit* for purpose.

The Petter Daas museum in the small rural community of Alstahaug in northern Norway offers another architectural statement on design. This fairly small museum, celebrating a local poet and designed by the architectural firm Snøhetta, fits snugly and consistently into the local landscape. It is elegant and practical giving both light, shelter and warmth in a fairly extreme environment. Although lacking the complexity and scale of the Gherkin, it is equally fit-for-purpose. Significantly, in the context of this book, it rises out from and fits into the Norwegian bedrock. It is an engineering design clearly founded in the geology – the essence of good reservoir model design.

When we build models of oil and gas resources in the subsurface we should never ignore the fact that the fluid resources are contained within rock formations. Geological systems possess their own natural forms of design as depositional, diagenetic and tectonic processes generate intricate reservoir architectures. We rely on a firm reservoir architectural foundation, based on an understanding of geological processes, which can then be quantified in terms of rock properties and converted into a form useful to predict fluid flow behaviour.

The Petter Dass Museum, Alstahaug, Norway (The Petter Dass-museum, © Petter Dass-museum, reproduced with permission)

Good reservoir model design therefore involves the digital representation of the natural geological architecture and its translation into useful models of subsurface fluid resources. Sometimes the representations are complex – sometimes they can be very simple indeed.

References

Foster N, Blaser W (1993) Norman foster sketch book. Birkhauser, Basel
Price B (2009) Great modern architecture: the world's most spectacular buildings. Canary Press, New York

Acknowledgements

Before engaging with this subject, we must acknowledge the essential contributions of others. Firstly, and anonymously, we thank our many professional colleagues in the fields of petroleum geoscience, reservoir engineering, geostatistics and software engineering. Without their expertise and the products of their innovation (commercial reservoir modelling packages), we as users would not have the opportunity to build good reservoir models in the first place. All the examples and illustrations used in this book are the result of collaborative work with others – by its very nature reservoir modelling is done within multi-disciplinary teams. We have endeavoured to credit our sources with reference to published studies where possible. Elsewhere, where unpublished case studies are used, these are the authors' own work, unless explicitly acknowledged.

More specifically we would like to thank our employers past and present – Shell, TRACS and AGR (M.B.) and Heriot-Watt University, Statoil and NTNU (P.R.) – for the provision of data, computational resources and, not least, an invaluable learning experience. The latest versions of this book have been honed and developed as part of the Nautilus Geoscience Training programme (www.nautilusworld.com), as part of a course on Advanced Reservoir Modelling given by the authors. Participants of these courses have repeatedly given us valuable feedback, suggesting improvements which have become embedded in the chapters of this book. Patrick Corbett, Kjetil Nordahl, Gillian Pickup, Stan Stanbrook, Paula Wigley and Caroline Hern are thanked for constructive reviews of the book chapters. Thanks are due also to Fiona Swapp and Susan McLafferty for producing many excellent graphics for the book and the associated courses.

Each reservoir modelling study discussed has benefited from the use of commercial software packages. We do not wish to promote or advocate any one package or the other – rather to encourage the growth of this technology in an open competitive market. We do however acknowledge the use of licenced software from several sources. The main software packages we have used in the examples discussed in this book include the Petrel E&P Software Platform (Schlumberger), the Integrated Irap RMS Solution Platform (Roxar), the Paradigm GOCAD framework for subsurface modelling, the SBED and ReservoirStudio products from Geomodeling Technology Corp., and the ECLIPSE suite of reservoir simulation software tools (Schlumberger). This is not an exhaustive list, just an acknowledgement of the tools we have used most often in developing approaches to reservoir modelling.

And finally we would like to acknowledge our families, who have kindly let us out to engage in rather too many reservoir modelling studies, courses and field trips on every continent (apart from Antarctica). We hope this book is a small compensation for their patience and support.

Contents

Model Purpose

1

Abstract

Should we aspire to build detailed full-field reservoir models with a view to using the resulting models to answer a variety of business questions?

In this chapter it is suggested the answer to the above question is 'no'. Instead we argue the case for building for fit-for-purpose models, which may or may not be detailed and may or may not be full-field.

This choice triggers the question: 'what is the purpose?' It is the answer to this question which determines the model design.

P. Ringrose and M. Bentley, *Reservoir Model Design*, DOI 10.1007/978-94-007-5497-3_1,

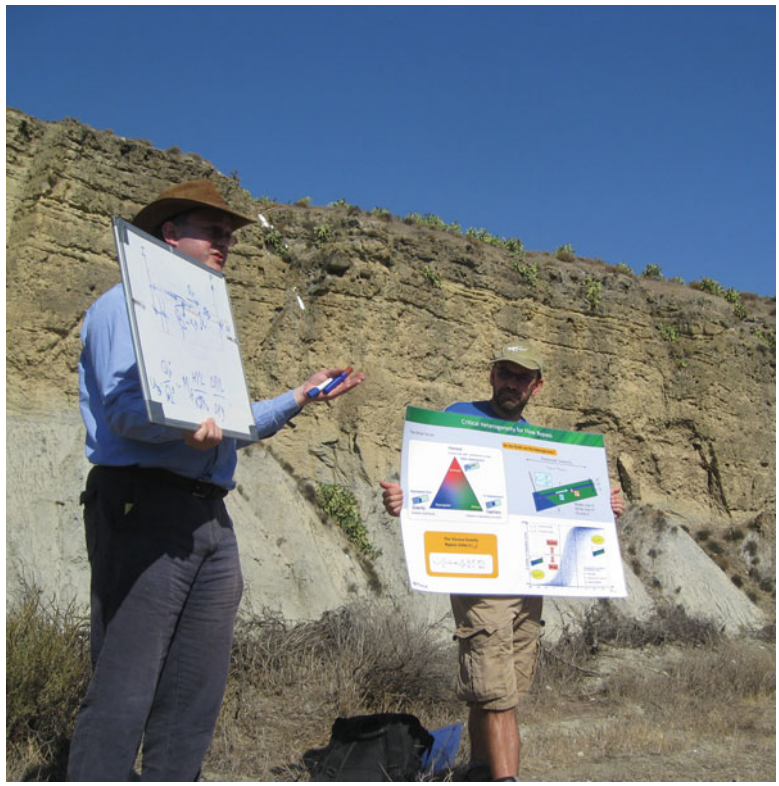

A reservoir engineer and geoscientist establish model purpose against an outcrop analogue

1.1 Modelling for Comfort?

There are two broad schools of thought on the purpose of models:

1. To provide a 3D, digital representation of a hydrocarbon reservoir, which can be built and maintained as new data becomes available, and used to support on-going lifecycle needs such as volumetric updates, well planning and, via reservoir simulation, production forecasting.
2. There is little value in maintaining a single 'field model'. Instead, build and maintain a field database, from which several fit-for-purpose models can be built quickly to support specific decisions.

The first approach seems attractive, especially if a large amount of effort is invested in the first build prior to a major investment decision. However, the 'all-singing, all-dancing' full-field approach tends to result in large, detailed models (generally working at the limit of the available software/hardware), which are cumbersome to update and difficult to pass hand-to-hand as people move between jobs. Significant effort can be invested simply in the on-going maintenance of these models, to the point that the need for the model ceases to be questioned and the purpose of the model is no longer apparent. In the worst case, the modelling technology has effectively been used just to satisfy an urge for technical rigour in the lead up to a business decision – simply 'modelling for comfort'.

We argue that the route to happiness lies with the second approach: building fit-for-purpose models which are equally capable of creating comfort or discomfort around a business decision.

Choosing the second approach (fit-for-purpose modelling) immediately raises the question of

"*what purpose*", as the model design will vary according to that purpose. This section therefore looks at contrasting purposes of reservoir modelling, and the distinctive design of the models associated with these differing situations.

1.2 Models for Visualisation Alone

Simply being able to visualise the reservoir in 3D was identified early in the development of modelling tools as a potential benefit of reservoir modelling. Simply having a 3D box in which to view the available data is beneficial in itself.

This is the most intangible application of modelling, as there is no output other than a richer mental impression of the subsurface, which is difficult to measure. However, most people benefit from 3D visualisation (Fig. 1.1), conscientiously or unconscientiously, particularly where cross-disciplinary issues are involved.

Some common examples are:

- To show the *geophysicist* the 3D structural model based on their seismic interpretations. Do they like it? Does it make geological sense? Have seismic artefacts been inadvertently included?
- To show the *petrophysicist* (well-log specialist) the 3D property model based on the well-log data (supplied in 1D). Has the 3D property modelling been appropriate or have features been introduced which are contrary to detailed knowledge of the well data, e.g. correlations and geological or petrophysical trends?
- To show the *reservoir engineer* the geo-model grid, which will be the basis for subsequent flow modelling. Is it usable? Does it conflict with prior perceptions of reservoir unit continuity?
- To show the *well engineer* what you are really trying to achieve in 3D with the complex well path you have just planned. Can the drilling team hit the target?
- To show the *asset team* how a conceptual reservoir model sketched on a piece of paper actually transforms into a 3D volume.

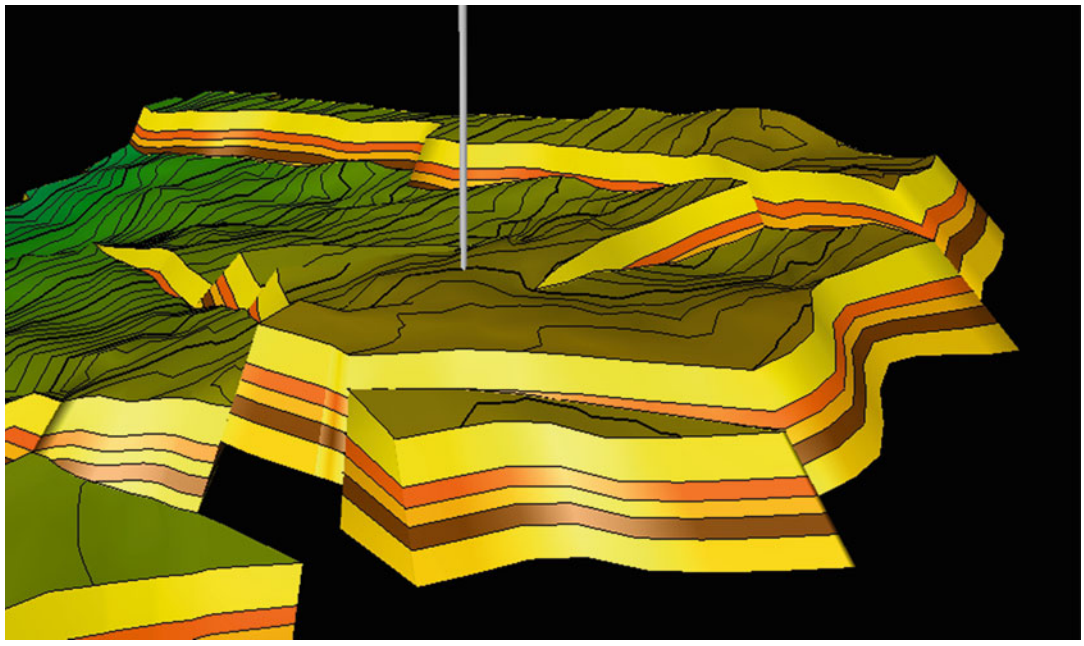

Fig. 1.1 The value of visualisation: appreciating structural and stratigraphic architecture, during well planning

- To show the *senior manager*, or investment fund holder, what the subsurface resource actually looks like. That oil and gas do not come from a 'hole in the ground' but from a complex pore-system requiring significant technical skills to access and utilise those fluids.

Getting a strong shared understanding of the subsurface concept tends to generate useful discussions on risks and uncertainties, and looking at models or data in 3D often facilitates this process. The value of visualisation alone is the improved understanding it gives.

If this is a prime purpose then the model need not be complex – it depends on the audience. In many cases, the model is effectively a 3D visual data base and the steps described in Chaps. 2, 3, 4, 5, and 6 of this book are not (in this case) required to achieve the desired understanding.

1.3 Models for Volumes

Knowing how much oil and gas is down there is usually one of the first goals of reservoir modelling. This may be done using a simple map-based approach, but the industry has now largely moved to 3D software packages, which is appropriate given that volumetrics are intrinsically a 3D property. The tradition of calculating volumes from 2D maps was a necessary simplification, no longer required.

3D mapping to support volumetrics should be quick, and is ideal for quickly screening uncertainties for their impact on volumetrics, as in the case shown in Fig. 1.2, where the volumetric sensitivity to fluid contact uncertainties is being tested, as part of a quick asset evaluation.

Models designed for this purpose can be relatively coarse, containing only the outline fault pattern required to define discrete blocks and the gross layering in which the volumes will be reported. The reservoir properties involved (e.g. porosity and net-to-gross) are statistically additive (see Chap. 3 for further discussion) which means cell sizes can be large. There is no requirement to run permeability models and, if this is for quick screening only, it may be sufficient to run 3D volumes for gross rock volume only, combining the remaining reservoir properties on spreadsheets.

Models designed for volumetrics should be coarse and fast.

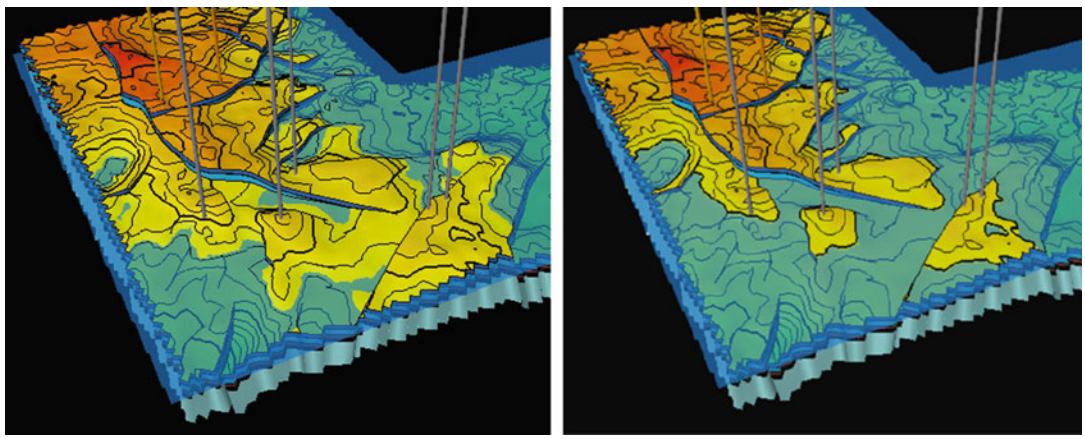

Fig. 1.2 Two models for different fluid contact scenarios built specifically for volumetrics

1.4 Models as a Front End to Simulation

The majority of reservoir models are built for input to flow simulators. To be successful, such models have to capture the essential permeability heterogeneity which will impact on reservoir performance. If the static models fail to capture this, the subsequent simulation forecasts may be useless. This is a crucial issue and will be discussed further at several points.

The requirement for capturing connected permeability usually means finer scale modelling is required because permeability is a non-additive property. Unlike models for volumetrics, the scope for simple averaging of detailed heterogeneity is limited. Issues of grid geometry and cell shape are also more pressing for flow models (Fig. 1.3); strategies for dealing with this are discussed in Chap. 4.

At this point it is sufficient to simply appreciate that taking a static geological model through to simulation automatically requires additional design, with a focus on permeability architecture.

1.5 Models for Well Planning

If the purpose of the modelling exercise is to assist well planning and geosteering, the model may require no more than a top structure map, nearby well ties and seismic attribute maps. Wells may also be planned using simulation models, allowing for alternative well designs to be tested against likely productivity.

It is generally preferable to design the well paths in reservoir models which capture all factors likely to impact a fairly costly investment decision. Most geoscience software packages have good well design functionality allowing for accurate well-path definition in a high resolution static model. Figure 1.4 shows example model for a proposed horizontal well, the trajectory of which has been optimised to access oil volumes (HCIIP) by careful geo-steering with reference to expected stratigraphic and structural surfaces.

Some thought is required around the determinism-probability issue referred to in the prologue and explored further in Chap. 2, because while there are many possible statistical simulations of a reservoir there will only be one final well path. It is therefore only reasonable to target the wells at more deterministic features in the model – features that are placed in 3D by the modeller and determined by the conceptual geological model. These typically include fault blocks, key stratigraphic rock units, and high porosity features which are well determined, such as channel belts or seismic amplitude 'sweet spots.' It is wrong to target wells at highly stochastic model features, such as a simulated random channel, stochastic porosity highs or small-scale probabilistic bodies (Fig. 1.5). The dictum is that wells should only target highly probable features; this means well prognoses (and geosteering plans) can only be confidently conducted on models designed to be largely deterministic.

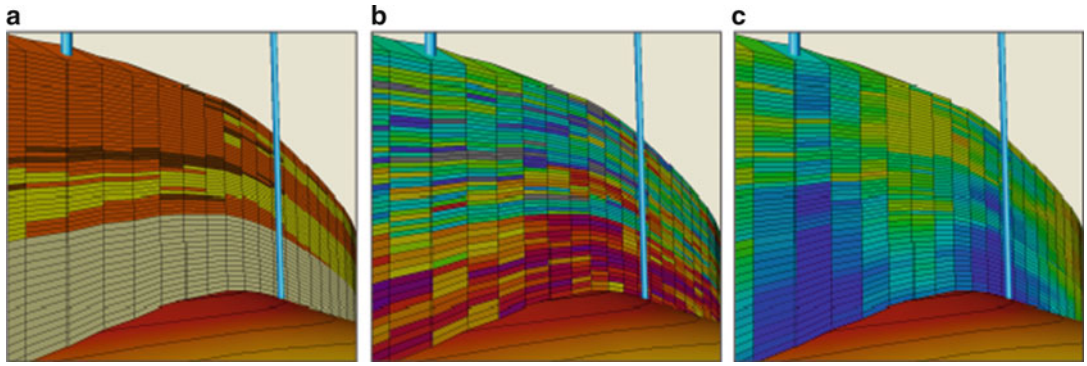

Fig. 1.3 Rock model (**a**) and property model (**b**) designed for reservoir simulation for development planning (**c**)

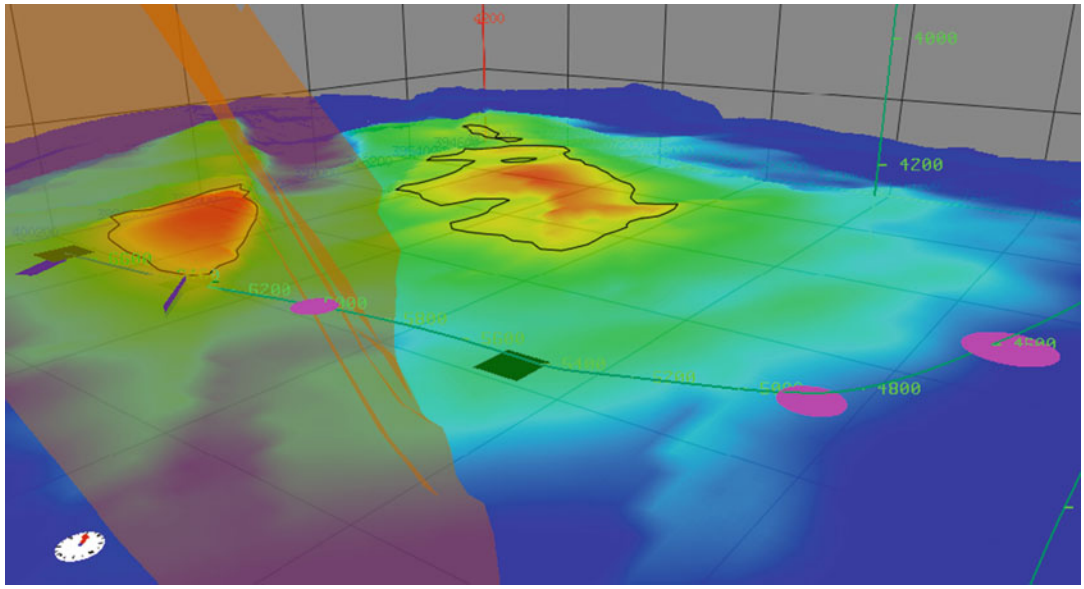

Fig. 1.4 Example planned well trajectory with an expected fault, base reservoir surface and well path targets

Having designed the well path it can be useful to monitor the actual well path (real-time updates) by incrementally reading in the well deviation file to follow the progress of the 'actual' well vs. the 'planned' well, including uncertainty ranges. Using visualisation, it is easier to understand surprises as they occur, particularly during geosteering (e.g. Fig. 1.4).

1.6 Models for Seismic Modelling

Over the last few decades, geophysical imaging has led to great improvements in reservoir characterisation – better seismic imaging allows us to 'see' progressively more of the subsurface. However, an image based on sonic wave reflections is never 'the real thing' and requires translation into rock and fluid properties. Geological reservoir models are therefore vital as *a priori* input to quantitative interpretation (QI) seismic studies.

This may be as simple as providing the layering framework for routine seismic inversion, or as complex as using Bayesian probabilistic rock and fluid prediction to merge seismic and well data. The nature of the required input model varies according to the QI process being followed – this needs to be discussed with the geophysicist.

In the example shown here (Fig. 1.6), a reservoir model (top) has been passed through to the simulation stage to predict the acoustic impedance change to be expected on a 4D seismic survey (middle). The actual time-lapse (4D) image from seismic (bottom) is then compared to the synthetic acoustic impedance change, and the simulation is history matched to achieve a fit.

If input to geophysical analysis is the key issue, the focus of the model design shifts to the properties relevant to geophysical modelling, notably models of velocity and density changes. There is, in this case, no need to pursue the intricacies of high resolution permeability architecture, and simpler (coarser) model designs may therefore be appropriate.

1.7 Models for IOR

Efforts to extract maximum possible volumes from oil and gas reservoirs usually fall under the banner of Improved Oil Recovery (IOR) or Enhanced Oil recovery (EOR). IOR tends to

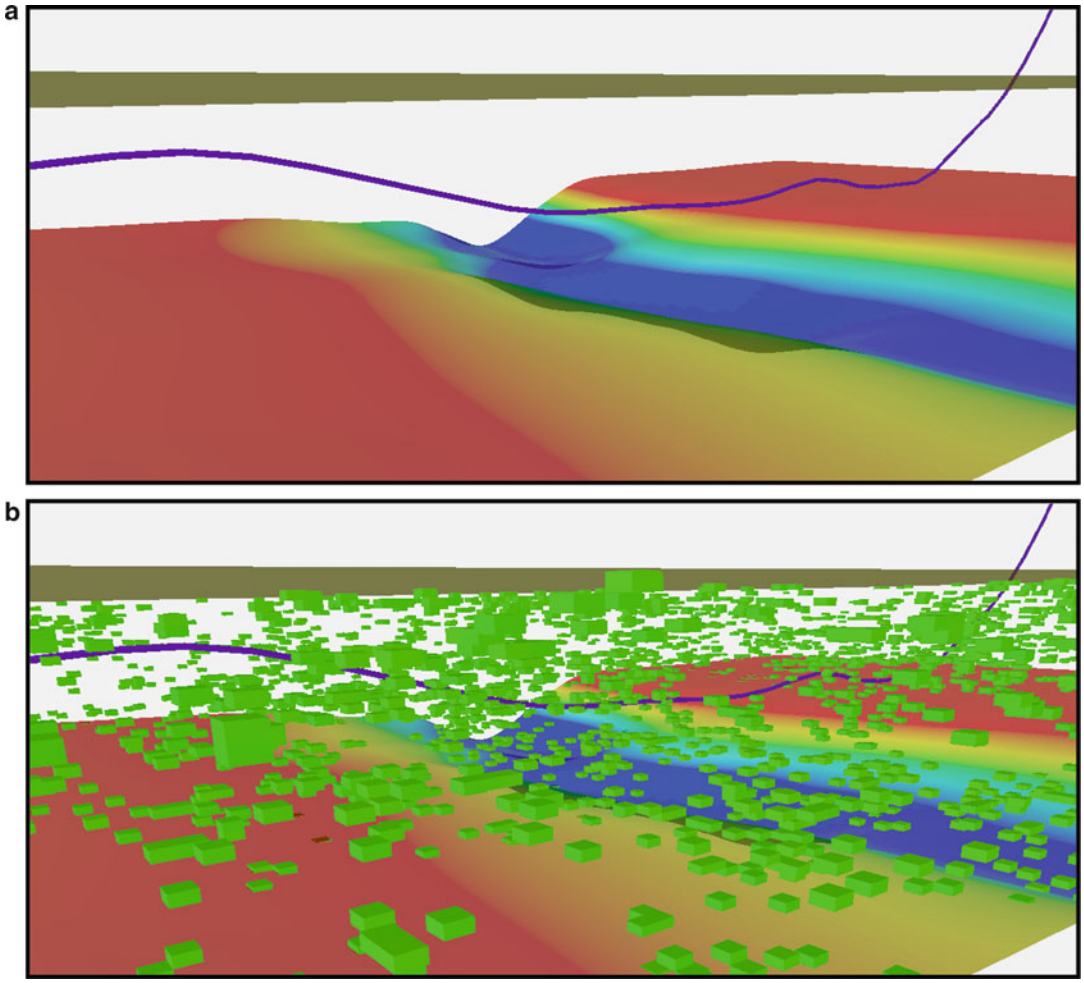

Fig. 1.5 Modelling for horizontal well planning based on deterministic data (**a**) vs. a model with significant stochastic elements (**b**)

include all options including novel well design solutions, use of time-lapse seismic and secondary or tertiary flooding methods (water-based or gas-based injection strategies), while EOR generally implies tertiary flooding methods, i.e. something more advanced than primary depletion or secondary waterflood. CO_2 flooding and Water Alternating Gas (WAG) injection schemes are typical EOR methods. We will use IOR to encompass all the options.

We started by arguing that there is little value in 'fit-for-all purposes' detailed full-field models. However, IOR schemes generally require very detailed models to give very accurate answers, such as 'exactly how much more oil will I recover if I start a gas injection scheme?' This requires detail, but not necessarily at a full-field scale. Many IOR solutions are best solved using detailed sector or near-well models, with relatively simple and coarse full-field grids to handle the reservoir management.

Figure 1.7 shows an example IOR model (Brandsæter et al. 2001). Gas injection was simulated in a high-resolution sector model with fine-layering (metre-thick cells) and various fault scenarios for a gas condensate field with difficult fluid phase behaviour. The insights from this IOR sector model were then used to

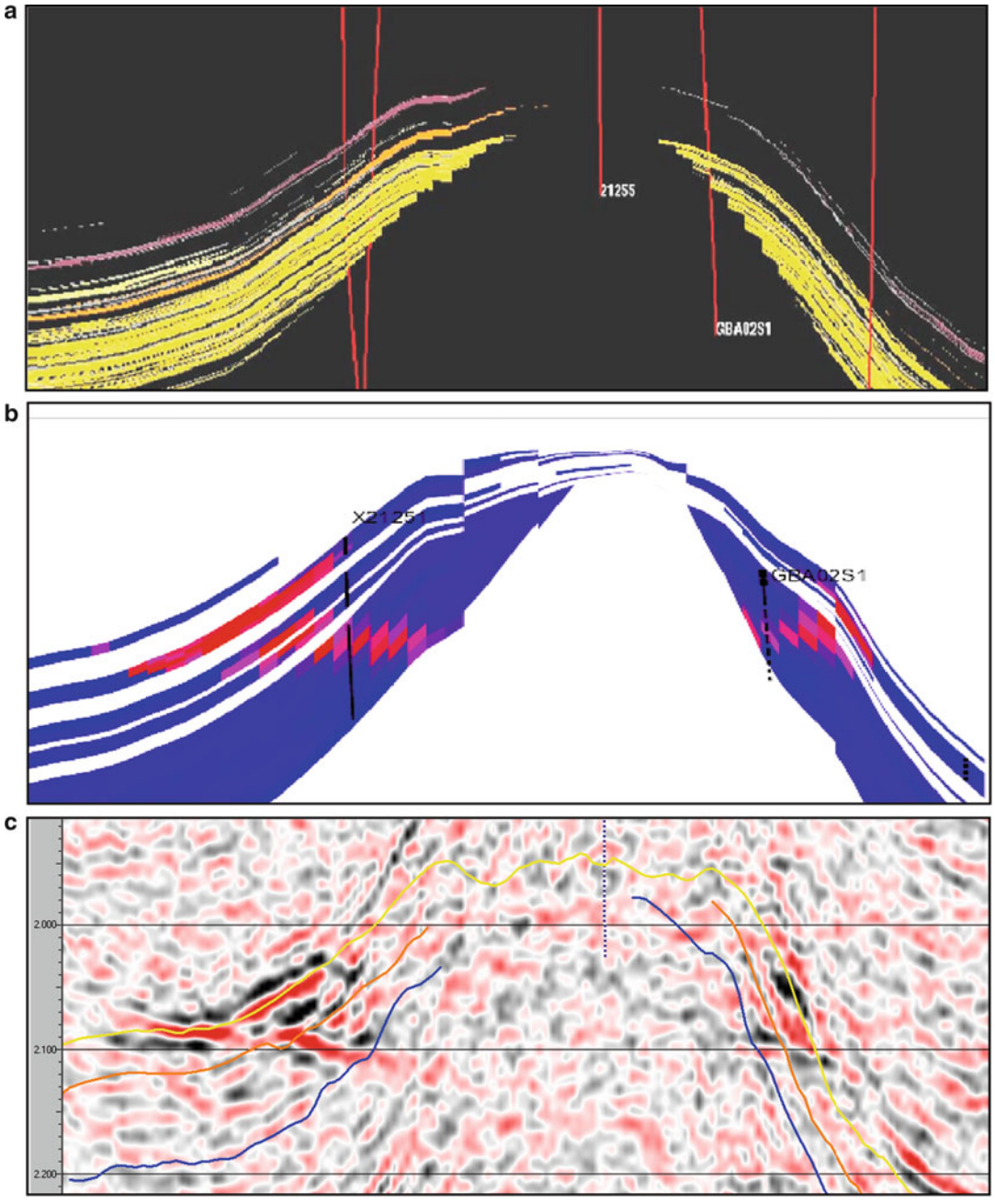

Fig. 1.6 Reservoir modelling in support of seismic interpretation: (**a**) rock model; (**b**) forecast of acoustic impedance change between seismic surveys; (**c**) 4D seismic difference cube to which the reservoir simulation was matched (Bentley and Hartung 2001) (Redrawn from Bentley and Hartung 2001, ©EAGE reproduced with kind permission of EAGE Publications B.V., The Netherlands)

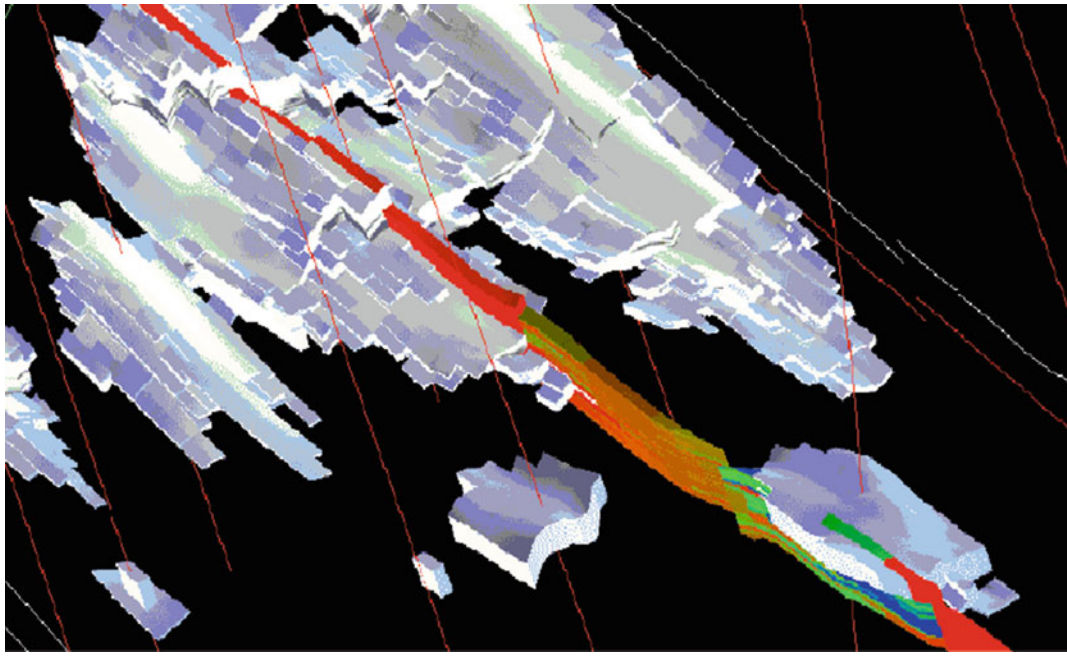

Fig. 1.7 Gas injection patterns (*white*) in a thin-bedded tidal reservoir (*coloured section*) modelled using a multi-scale method and incorporating the effects of faults in the reservoir simulation model

constrain the coarse-grid full-field reservoir management model.

1.8 Models for Storage

The growing interest in CO_2 storage as a means of controlling greenhouse gas emissions brings a new challenge for reservoir modelling. Here there is a need for both initial scoping models (for capacity assessment) and for more detailed models to understand injection strategies and to assess long-term storage integrity. Some of the issues are similar – find the good permeability zones, identify important flow barriers and pressure compartments – but other issues are rather different, such as understanding formation response to elevated pressures and geochemical reactions due to CO_2 dissolved in brine. CO_2 is also normally compressed into the liquid or dense phase to be stored at depths of c.1–3 km, so that understanding fluid behaviour is also an important factor. CO_2 storage generally requires the assessment of quite large aquifer/reservoir volumes and the caprock system – presenting significant challenges for grid resolution and the level of detail required.

An example geological model for CO_2 storage is shown in Fig. 1.8 from the In Salah CO_2 injection project in Algeria (Ringrose et al. 2011). Here CO_2, removed from several CO_2-rich gas fields, has been stored in the down-flank aquifer of a producing gas field. Injection wells were placed on the basis of a seismic porosity inversion, and analysis of seismic and well data was used to monitor the injection performance and verify the integrity of the storage site. Geological models at a range of scales were required, from near-wellbore models of flow behaviour to large-scale models of the geomechanical response.

1.9 The Fit-for-Purpose Model

Given the variety of models described above, we argue that it is best to abandon the notion of a single, all-knowing, all-purpose, full-field model, and replace this with the idea of flexible, faster

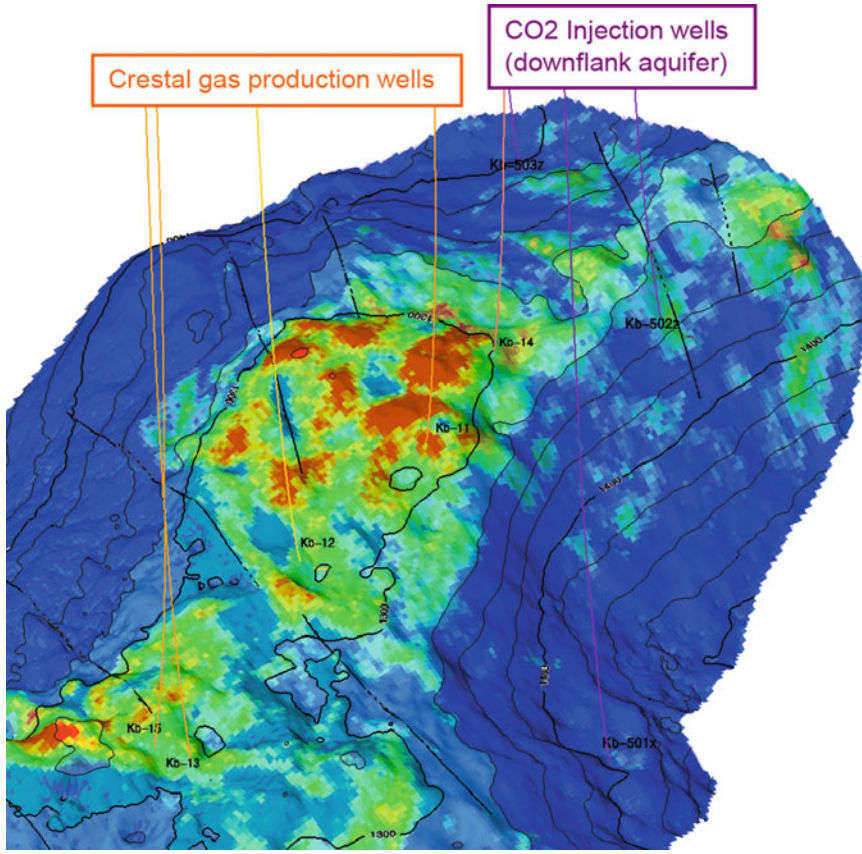

Fig. 1.8 Models for CO_2 storage: Faulted top structure map with seismic-based porosity model and positions of injection wells

models based on thoughtful model design, tailored to answer specific questions at hand. Such models have a short shelf life and are built with specific ends in mind, i.e. there is a clear model purpose. The design of these models is informed by that purpose, as the contrast between the models illustrated in this chapter has shown.

With the fit-for-purpose mind set, the long-term handover items between geoscientists are not a set of 3D property models, but the underlying building blocks from which those models were created, notably the reservoir database (which should remain updated and 'clean') and the reservoir concept, which should be clear and explicit, to the point that it can be sketched.

It is also often practical to hand-over some aspects of the model build, such as a fault model, if the software in use allows this to be updated easily, or workflows and macros (if these can be understood and edited readily). The pre-existing model outputs (property models, rock models, volume summaries, etc.) are best archived.

The rest of this book develops this theme in more detail – how to achieve a design which addresses the model purpose whilst representing the essential features of the geological architecture (Fig. 1.9).

When setting about a reservoir modelling project, an overall workflow is required and this should be decided up-front before significant modelling effort is expended. There is no 'correct' workflow, because the actual steps to be taken are an output of the fit-for-purpose design. However, it may be useful to refer to a general workflow (Fig. 1.10) which represents the main steps outlined in this book.

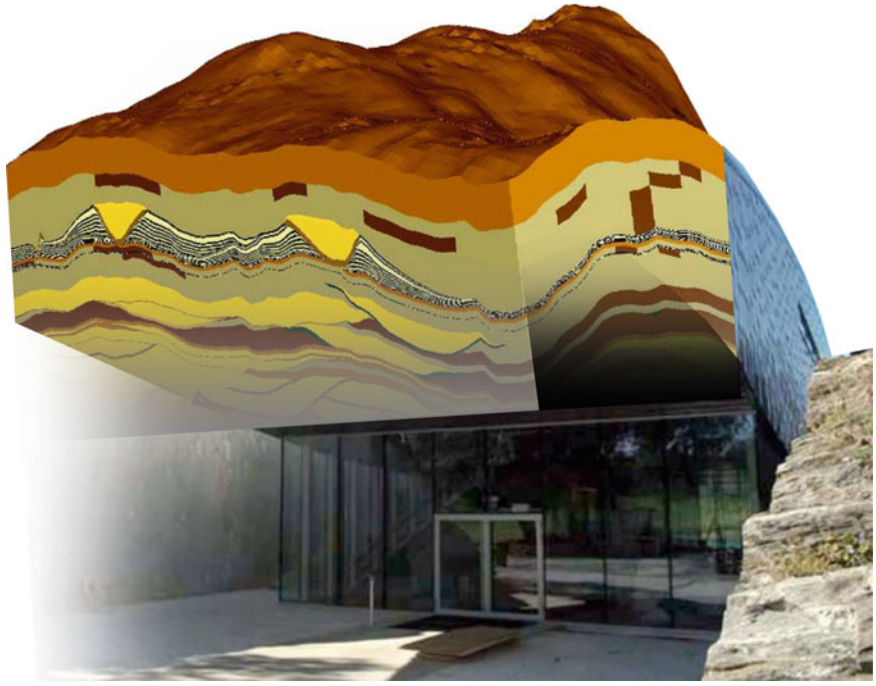

Fig. 1.9 Geological architecture (Image of geomodel built in SBED Studio™ merged with photograph of Petter Dass Museum (Refer Fig. P.2))

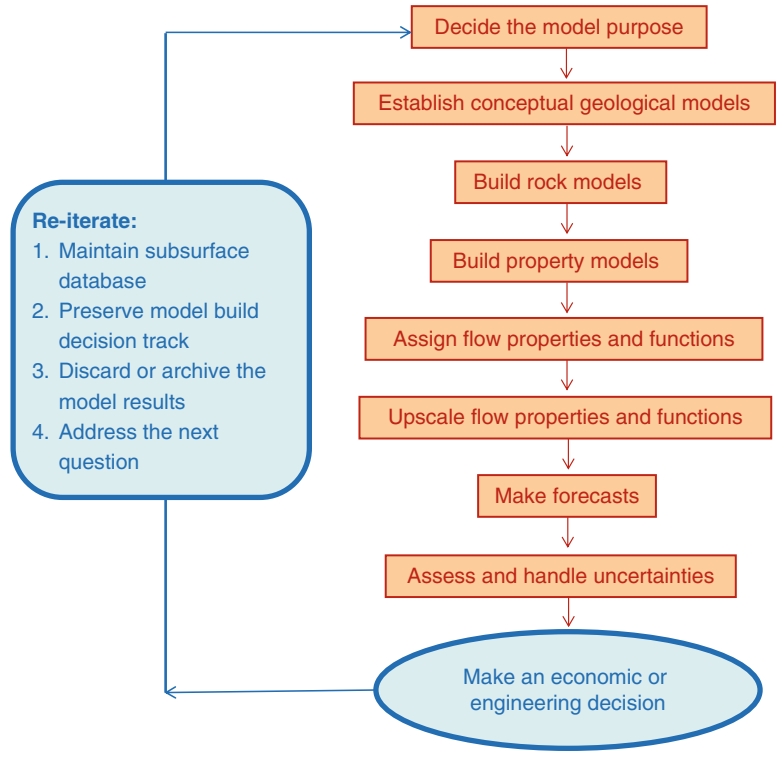

Fig. 1.10 Generic reservoir modelling workflow

References

Bentley MR, Hartung M (2001) A 4D surprise at Gannet B. Presented at 63rd EAGE conference & exhibition, Amsterdam (extended abstract)

Brandsæter I, Ringrose PS, Townsend CT, Omdal S (2001) Integrated modeling of geological heterogeneity and fluid displacement: Smørbukk gas-condensate field, Offshore Mid-Norway. Paper SPE 66391 presented at the SPE reservoir simulation symposium held in Houston, Texas, 11–14 February 2001

Ringrose P, Roberts DM, Raikes S, Gibson-Poole C, Iding M, Østmo S, Taylor M, Bond C, Wightman R, Morris J (2011) Characterisation of the Krechba CO_2 storage site: critical elements controlling injection performance. Energy Procedia 4:4672–4679

The Rock Model

2

Abstract

This topic concerns the difference between a reservoir model and a geological model. *Model representation* is the essential issue – ask yourself whether the coloured cellular graphics we see on the screen truly resemble the reservoir as exposed in outcrop:

WYSIWYG (computing acronym).

Our focus is on achieving a reasonable representation.

Most of the outputs from reservoir modelling are quantitative and derive from property models, so the main purpose of a rock model is to get the properties in the right place – to guide the spatial property distribution in 3D.

For certain model designs, the rock model component is minimal, for others it is essential. In all cases, the rock model should be the guiding framework and should offer predictive capacity to a project.

P. Ringrose and M. Bentley, *Reservoir Model Design*, DOI 10.1007/978-94-007-5497-3_2,

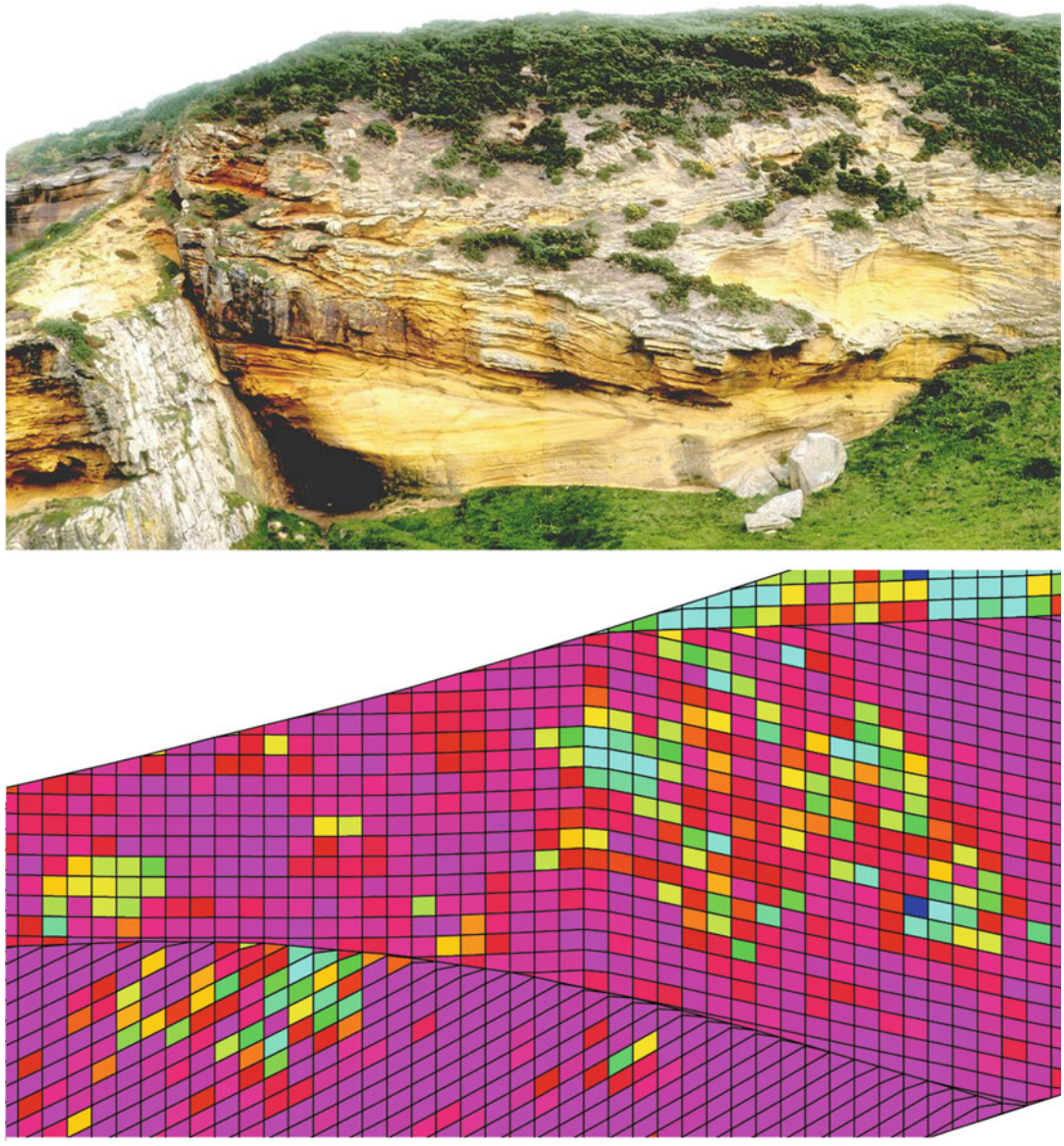

Outcrop view and model representation of the Hopeman Sandstone at Clashach Quarry, Moray Firth, Scotland

2.1 Rock Modelling

In a generic reservoir modelling workflow, the construction of a rock or 'facies' model usually precedes the property modelling. Effort is focussed on capturing contrasting rock types identified from sedimentology and representing these in 3D. This is often seen as the most 'geological' part of the model build along with the fault modelling, and it is generally assumed that a 'good' final model is one which is founded on a thoughtfully-constructed rock model.

However, although the rock model is often essential, it is rarely a model deliverable in itself,

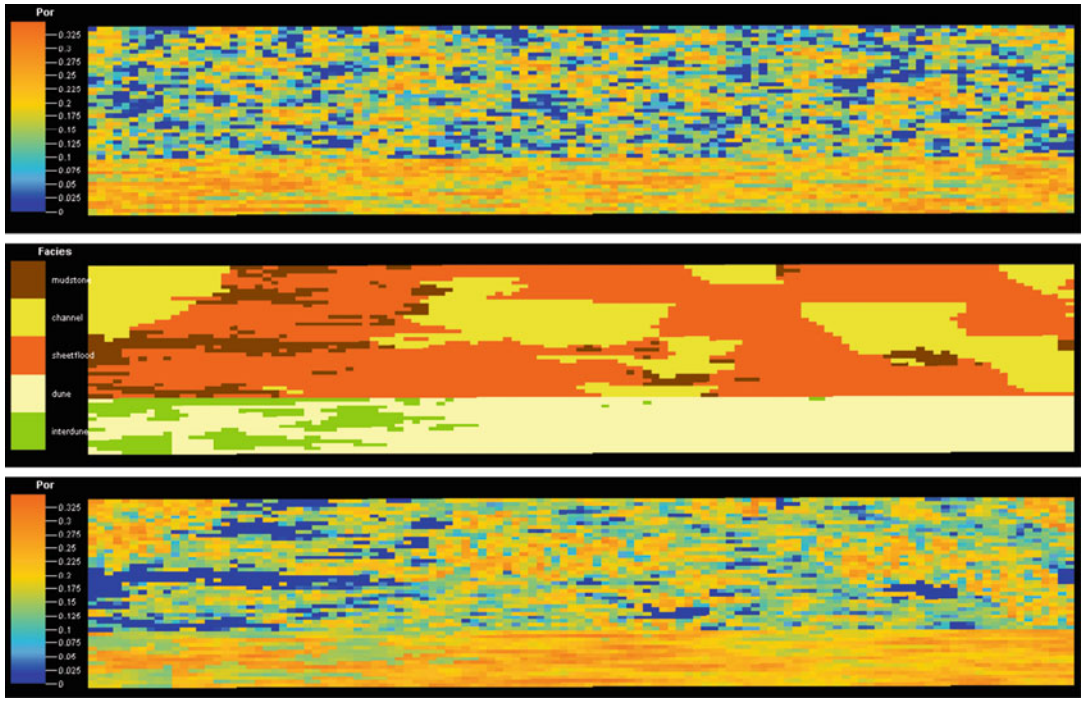

Fig. 2.1 To model rocks, or not to model rocks? *Upper image*: porosity model built directly from logs; *middle image*: a rock model capturing reservoir heterogeneity; *lower image*: the porosity model rebuilt, conditioned to the rock model

and many reservoirs *do not require* rock models. Figure 2.1 shows a porosity model which has been built with and without a rock model. If the upper porosity model is deemed a reasonable representation of the field, a rock model is not required. If, however, the porosity distribution is believed to be significantly influenced by the rock contrasts shown in the middle image, then the lower porosity model is the one to go for. Rock modelling is therefore a means to an end rather than an end in itself, an optional step which is useful if it helps to build an improved property model.

The details of rock model input are software-specific and are not covered here. Typically the model requires specification of variables such as sand body sizes, facies proportions and reference to directional data such as dip-logs. These are part of a standard model build and need consideration, but are not viewed here as critical to the higher level issue of model design. Moreover, many of these variables cannot be specified precisely enough to guide the modelling: rock body databases are generally insufficient and dip-log data too sparse to rely on as a model foundation. Most critical to the design are the issues identified below, mishandling of which is a common source of a poor model build:

- **Reservoir concept** – is the architecture understood in a way which readily translates into a reservoir model?
- **Model elements** – from the range of observed structural components and sedimentological facies types, has the correct selection of elements been made on which to base the model?
- **Model Build** – is the conceptual model carried through *intuitively* into the statistical component of the build?
- **Determinism and probability** – is the balance of determinism and probability in the model understood, and is the conceptual model firmly carried in the deterministic model components?

These four questions are used in this chapter to structure the discussion on the rock model, followed by a summary of more specific rock model build choices.

2.2 Model Concept

The best hope of building robust and sensible models is to use conceptual models to guide the model design. We favour this in place of purely data-driven modelling because of the issue of under-sampling (see later). The geologist should have a mental picture of the reservoir and use modelling tools to convert this into a quantitative geocellular representation. Using system defaults or treating the package as a black box that somehow adds value or knowledge to the model will always result in models that make little or no geological sense, and which usually have poor predictive capacity.

The form of the reservoir concept is not complex. It may be an image from a good outcrop analogue or, better, a conceptual sketch, such as those shown in Fig. 2.2.

It should, however, be specific to the case being modelled, and this is best achieved by drawing a simple section through the reservoir showing the key architectural elements – an example of which is shown in Fig. 2.3.

Analogue photos or satellite images are useful and often compelling but also easy to adopt when not representative, particularly if modern dynamic environments are being compared with ancient preserved systems. It is possible to collect a library of analogue images yet still be unclear exactly how these relate to the reservoir in hand, and how they link to the available well data. By contrast, the ability to draw a conceptual sketch section is highly informative and brings clarity to the mental image of the reservoir held by the modeller. If this conceptual sketch is not clear, the process of model building is unlikely to make it any clearer. If there is no clear up-front conceptual model then the model output is effectively a random draw:

If you can sketch it, you can model it

An early question to address is: *"what are the fundamental building blocks for the reservoir concept?"* These are referred to here as the 'model elements' and discussed further below. For the moment, the key thing to appreciate is that:

model elements ≠ facies types

Selection of model elements is discussed in Sect. 2.4.

With the idea of a reservoir concept as an architectural sketch constructed from model elements established, we will look at the issues surrounding the build of the model framework then return to consider how to select elements to place within that framework.

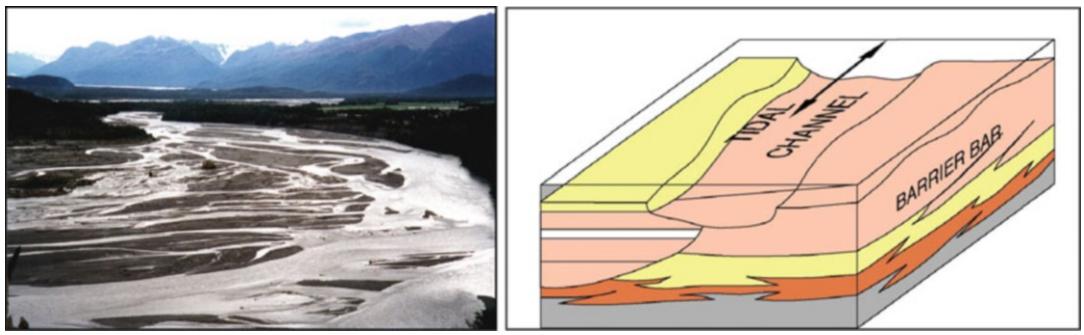

Fig. 2.2 Capturing the reservoir concept in an analogue image or a block diagram sketch

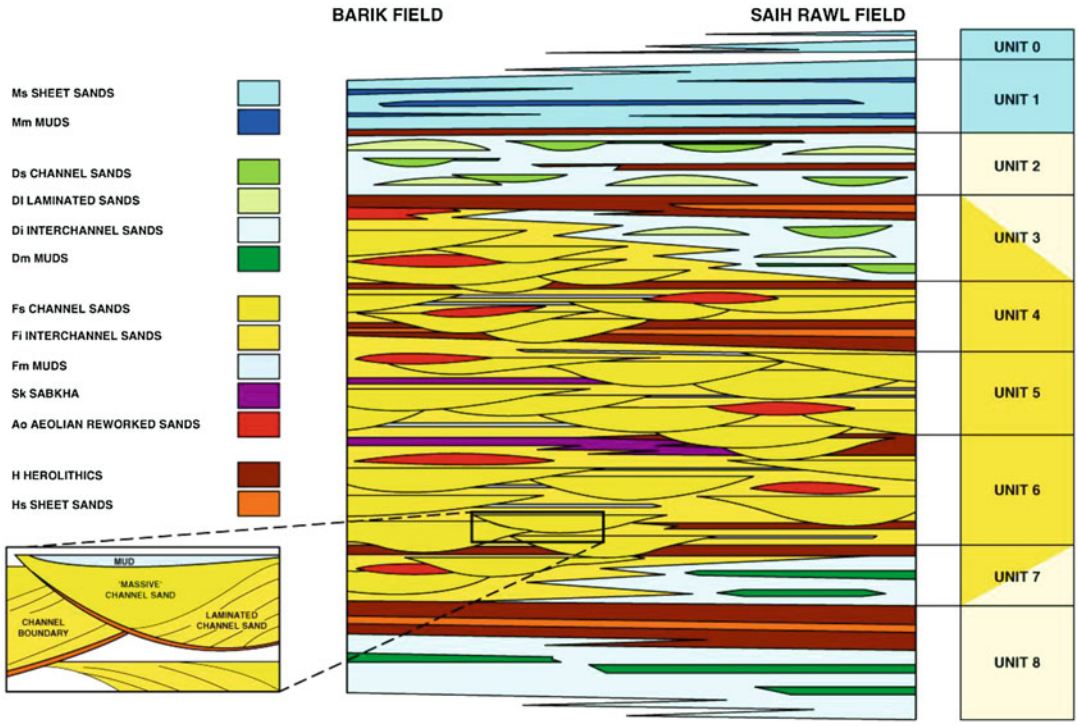

Fig. 2.3 Capturing the reservoir concept in a simple sketch showing shapes and stacking patterns of reservoir sand bodies and shales (From: van de Leemput et al. 1996)

2.3 The Structural and Stratigraphic Framework

The structural framework for all reservoir models is defined by a combination of structural inputs (faults and surfaces from seismic to impart gross geometry) and stratigraphic inputs (to define internal layering).

The main point we wish to consider here is *what are the structural and stratigraphic issues that a modeller should be aware of when thinking through a model design*? These are discussed below.

2.3.1 Structural Data

Building a fault model tends to be one of the more time-consuming and manual steps in a modelling workflow, and is therefore commonly done with each new generation of seismic interpretation. In the absence of new seismic, a fault model may be passed on between users and adopted simply to avoid the inefficiency of repeating the manual fault-building.

Such an inherited fault framework therefore requires quality control (QC). The principal question is whether the fault model reflects the seismic interpretation directly, or whether it has been modified by a conceptual structural interpretation.

A direct expression of a seismic interpretation will tend to be a conservative representation of the fault architecture, because it will directly reflect the resolution of the data. Facets of such data are:

- Fault networks tend to be incomplete, e.g. faults may be missing in areas of poor seismic quality;
- Faults may not be joined (under-linked) due to seismic noise in areas of fault intersections;
- Horizon interpretations may stop short of faults due to seismic noise around the fault zone;

- Horizon interpretations may be extended down fault planes (i.e. the fault is not identified independently on each horizon, or not identified at all)
- Faults may be interpreted on seismic noise (artefacts).

Although models made from such 'raw' seismic interpretations are honest reflections of that data, the structural representations are incomplete and, it is argued here, a structural interpretation should be overlain on the seismic outputs as part of the model design. To achieve this, the workflow similar to that shown in Fig. 2.4 is recommended.

Rather than start with a gridded framework constructed directly from seismic interpretation, the structural build should start with the raw, depth-converted seismic picks and the fault sticks. This is preferable to starting with horizon grids, as these will have been gridded without access to the final 3D fault network. Working with pre-gridded surfaces means the starting inputs are smoothed, not only within-surface but, more importantly, around faults, the latter tending to have systematically reduced fault displacements.

A more rigorous structural model workflow is as follows:

1. Determine the structural concept – are faults expected to die out laterally or to link? Are *en echelon* faults separated by relay ramps? Are there small, possibly sub-seismic connecting faults?
2. Input the fault sticks and grid them as fault planes (Fig. 2.4a)
3. Link faults into a network consistent with the concept (1, above, also Fig. 2.4b)
4. Import depth-converted horizon picks as points and remove spurious points, e.g. those erroneously picked along fault planes rather than stratigraphic surfaces (Fig. 2.4c)
5. Edit the fault network to ensure optimal positioning relative to the raw picks; this may be an iterative process with the geophysicist, particularly if potentially spurious picks are identified
6. Grid surfaces against the fault network (Fig. 2.4d).

2.3.2 Stratigraphic Data

There are two main considerations in the selection of stratigraphic inputs to the geological framework model: *correlation* and *hierarchy*.

2.3.2.1 Correlation

In the subsurface, correlation usually begins with markers picked from well data – *well picks*. Important information also comes from correlation surfaces picked from seismic data. Numerous correlation picks may have been defined in the interpretation of well data and these picks may have their origins in lithological, biostratigraphical or chronostratigraphical correlations – all of these being elements of sequence stratigraphy (see for example Van Wagoner et al. 1990; Van Wagoner and Bertram 1995). If multiple stratigraphic correlations are available these may give surfaces which intersect in space. Moreover, not all these surfaces are needed in reservoir modelling. A selection process is therefore required. As with the structural framework, the selection of surfaces should be made with reference to the conceptual sketch, which is in turn driven by the model purpose.

As a guideline, the 'correct' correlation lines are generally those which most closely govern the fluid-flow gradients during production. An exception would be instances where correlation lines are used to guide the distribution of reservoir volumes in 3D, rather than to capture correct fluid flow units.

The choice of correlation surfaces used hugely influences the resulting model architecture, as illustrated in Fig. 2.5, and in an excellent field example by Ainsworth et al. (1999).

2.3.2.2 Hierarchy

Different correlation schemes have different influences on the key issue of hierarchy, as the stratigraphy of most reservoir systems is inherently hierarchical (Campbell 1967). For example, for a sequence stratigraphic correlation scheme, a low-stand systems tract might have a length-scale of tens of kilometres and might contain within it numerous stacked sand systems

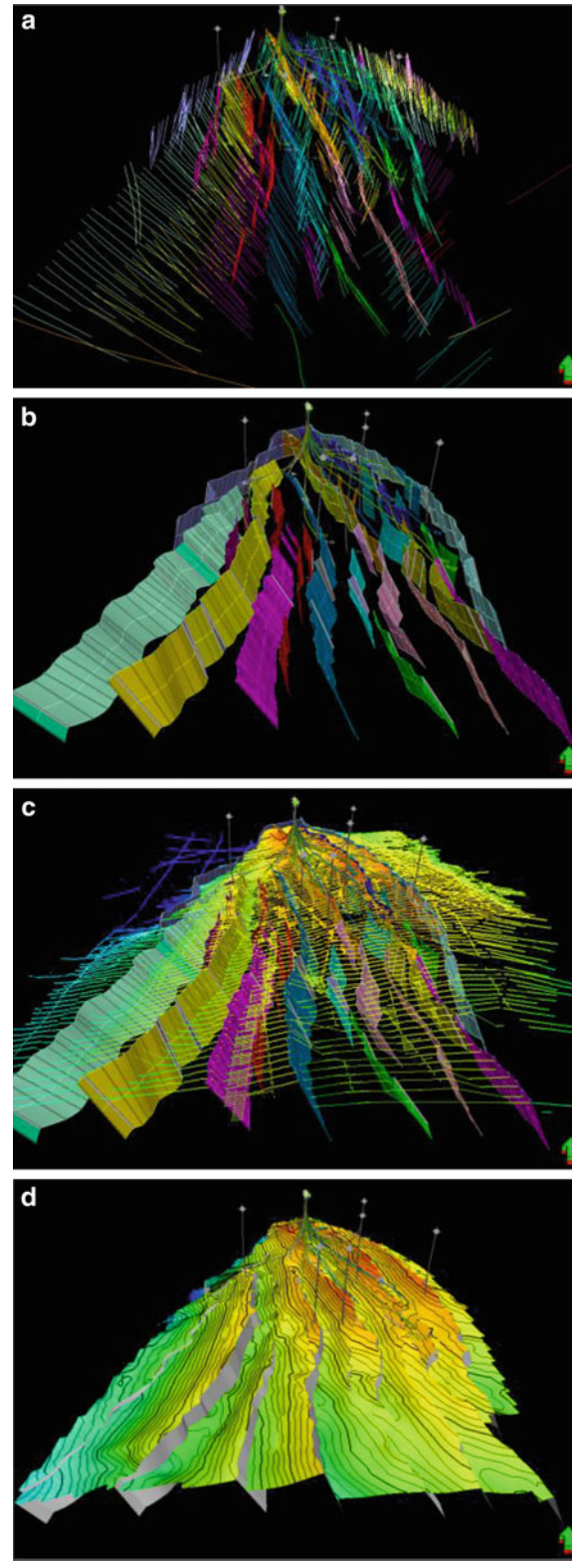

Fig. 2.4 A structural build based on fault sticks from seismic (**a**), converted into a linked fault system (**b**), integrated with depth-converted horizon picks (**c**) to yield a conceptually acceptable structural framework which honours all inputs (**d**). The workflow can equally well be followed using time data, then converting to depth using a 3D velocity model. The key feature of this workflow is the avoidance of intermediate surface gridding steps which are made independently of the final interpreted fault network. Example from the Douglas Field, East Irish Sea (Bentley and Elliott 2008)

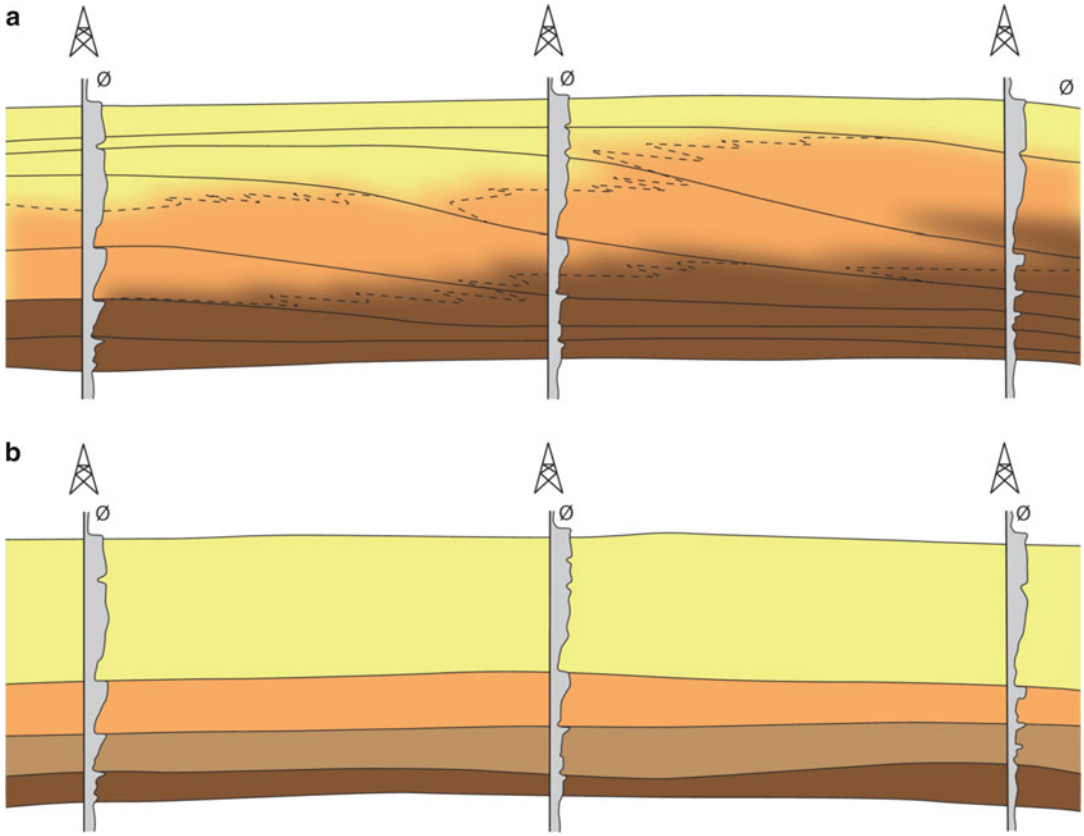

Fig. 2.5 Alternative (**a**) chronostratigraphic and (**b**) lithostratigraphic correlations of the same sand observations in three wells; the chronostratigraphic correlation invokes an additional hierarchical level in the stratigraphy

with a length-scale of kilometres. These sands in turn act as the bounding envelope for individual reservoir elements with dimensions of tens to hundreds of metres.

The reservoir model should aim to capture the levels in the stratigraphic hierarchy which influence the spatial distribution of significant heterogeneities (determining 'significance' will be discussed below). Bounding surfaces within the hierarchy may or may not act as flow barriers – so they may represent important model elements in themselves (e.g. flooding surfaces) or they may merely control the distribution of model elements within that hierarchy. This applies to structural model elements as well as the more familiar sedimentological model elements, as features such as fracture density can be controlled by mechanical stratigraphy – implicitly related to the stratigraphic hierarchy.

So which is the preferred stratigraphic tool to use as a framework for reservoir modelling? The quick answer is that it will be the framework which most readily reflects the conceptual reservoir model. Additional thought is merited, however, particularly if the chronostratigraphic approach is used. This method yields a framework of timelines, often based on picking the most shaly parts of non-reservoir intervals. The intended shale-dominated architecture may not automatically be generated by modelling algorithms, however: a rock model for an interval between two flooding surfaces will contain a shaly portion at both the top and the base of the interval. The probabilistic aspects of the subsequent modelling can easily degrade the correlatable nature of the flooding surfaces, inter-well shales becoming smeared out incorrectly throughout the zone.

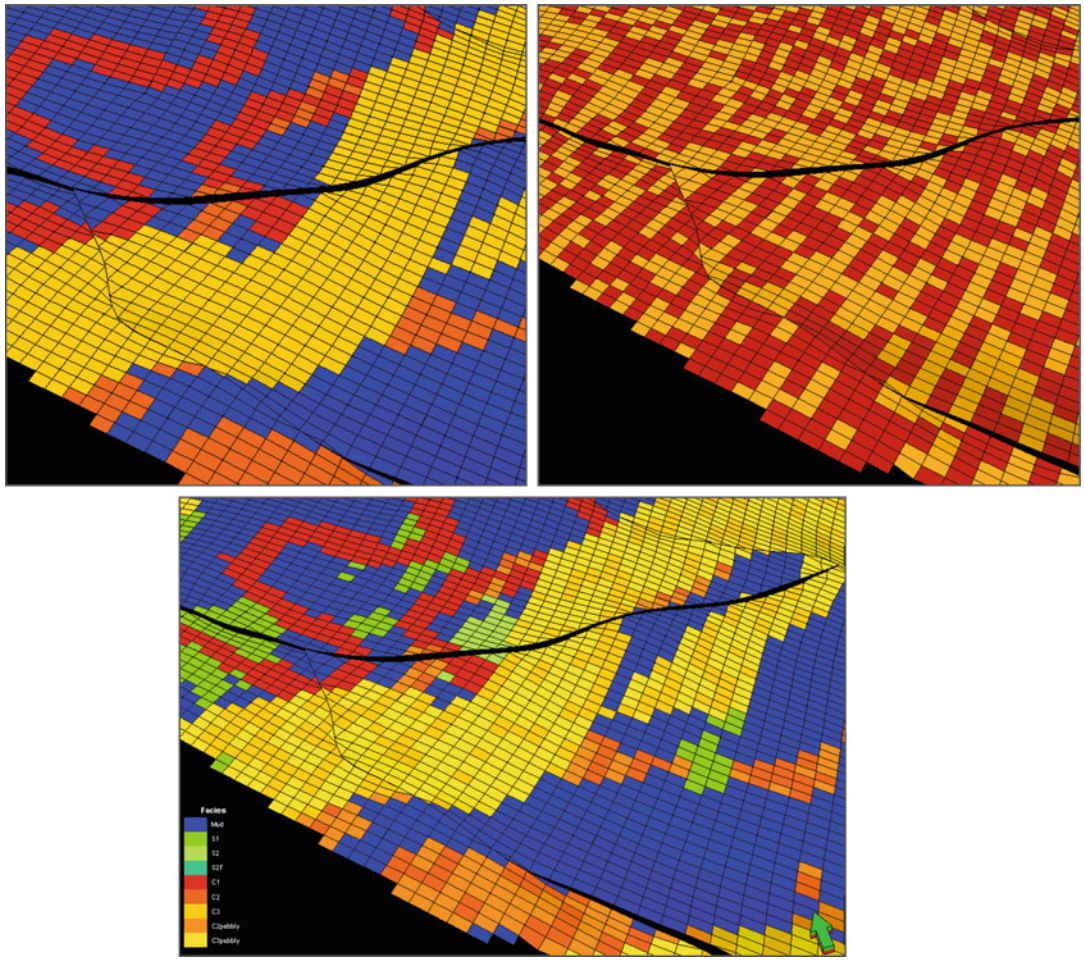

Fig. 2.6 The addition of hierarchy by logical combination: single-hierarchy channel model (*top left*, *blue* = mudstone, *yellow* = main channel) built in parallel with a probabilistic model of lithofacies types (*top right*, *yellow* = better quality reservoir sands), logically combined into the final rock model with lithofacies detail in the main channel only – an additional level of hierarchy

Some degree of hierarchy is implicit in any software package. The modeller is required to work out if the default hierarchy is sufficient to capture the required concept. If not, the workflow should be modified, most commonly by applying logical operations.

An example of this is illustrated in Fig. 2.6, from a reservoir model in which the first two hierarchical levels were captured by the default software workflow: tying layering to seismic horizons (first level) then infilled by sub-seismic stratigraphy (second level). An additional hierarchical level was required because an important permeability heterogeneity existed between lithofacies types *within* a particular model element (the main channels). The chosen solution was to build the channel model using channel objects and creating a separate, in this case probabilistic, model which contained the information about the distribution of the two lithofacies types. The two rock models were then combined using a logical property model operation, which imposed the texture of the fine-scale lithofacies, but only within the relevant channels. Effectively this created a third hierarchical level within the model.

One way or another hierarchy can be represented, but only rarely by using the default model workflow.

2.4 Model Elements

Having established a structural/stratigraphic model framework, we can now return to the model concept and consider how to fill the framework to create an optimal architectural representation.

2.4.1 Reservoir Models Not Geological Models

The rich and detailed geological story that can be extracted from days or weeks of analysis of the rock record from the core store need not be incorporated directly into the reservoir model, and this is a good thing. There is a natural tendency to 'include all the detail' just in case something minor turns out to be important. Models therefore have a tendency to be overcomplex from the outset, particularly for novice modellers. The amount of detail required in the model can, to a large extent, be anticipated.

There is also a tendency for modellers to seize the opportunity to build 'real 3D geological pictures' of the subsurface and to therefore make these as complex as the geology is believed to be. This is a hopeless objective as the subsurface is considerably more complex in detail than we are capable of modelling explicitly and, thankfully, much of that detail is irrelevant to economic or engineering decisions. We are building *reservoir models* – reasonable representations of the detailed geology – *not* geological models.

2.4.2 Building Blocks

Hence the view of the components of a reservoir model as *model elements* – the fundamental building blocks of the 3D architecture. The use of this term distinguishes model elements from geological terms such as 'facies', 'lithofacies', 'facies associations' and 'genetic units'. These geological terms are required to capture the richness of the geological story, but do not necessarily describe the things we need to put into reservoir models. Moreover, key elements of the reservoir model may be small-scale structural or diagenetic features, often (perhaps incorrectly) excluded from descriptions of 'facies'.

Modelling elements are defined here as:

> *three-dimensional rock bodies which are petrophysically and/or geometrically distinct from each other in the specific context of the reservoir fluid system.*

The fluid-fill factor is important as it highlights the fact that different levels of heterogeneity are important for different types of fluid, e.g. gas reservoirs behave more homogeneously than oil reservoirs for a given reservoir type.

The identification of 'model elements' has some parallels with discussions of 'hydraulic units' although such discussions tend to be in the context of layer-based well performance. Our focus is on the building blocks for 3D reservoir architecture, including parts of a field remote from well and production data. It should be spatially predictive.

2.4.3 Model Element Types

Having stepped beyond a traditional use of depositional facies to define rock bodies for modelling, a broader spectrum of elements can be considered for use, i.e. making the sketch of the reservoir as it is intended to be modelled. Six types of model element are considered below.

2.4.3.1 Lithofacies Types

This is sedimentologically-driven and is the traditional way of defining the components of a rock model. Typical lithofacies elements may be coarse sandstones, mudstones or grainstones, and will generally be defined from core and or log data (e.g. Fig. 2.7).

2.4.3.2 Genetic Elements

In reservoir modelling, genetic elements are a component of a sedimentary sequence which are related by a depositional process. These include the rock bodies which typical modelling packages are most readily designed to incorporate, such as channels, sheet sands or heterolithics. These usually comprise several lithofacies, for example, a fluvial channel might

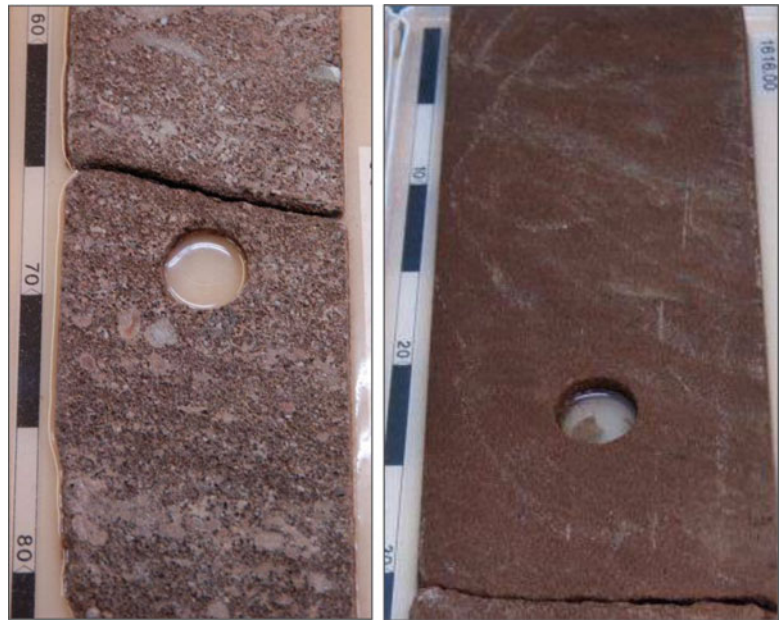

Fig. 2.7 Example lithofacies elements; *left*: coarse, pebbly sandstone; *right*: massively-bedded coarse-grained sandstone

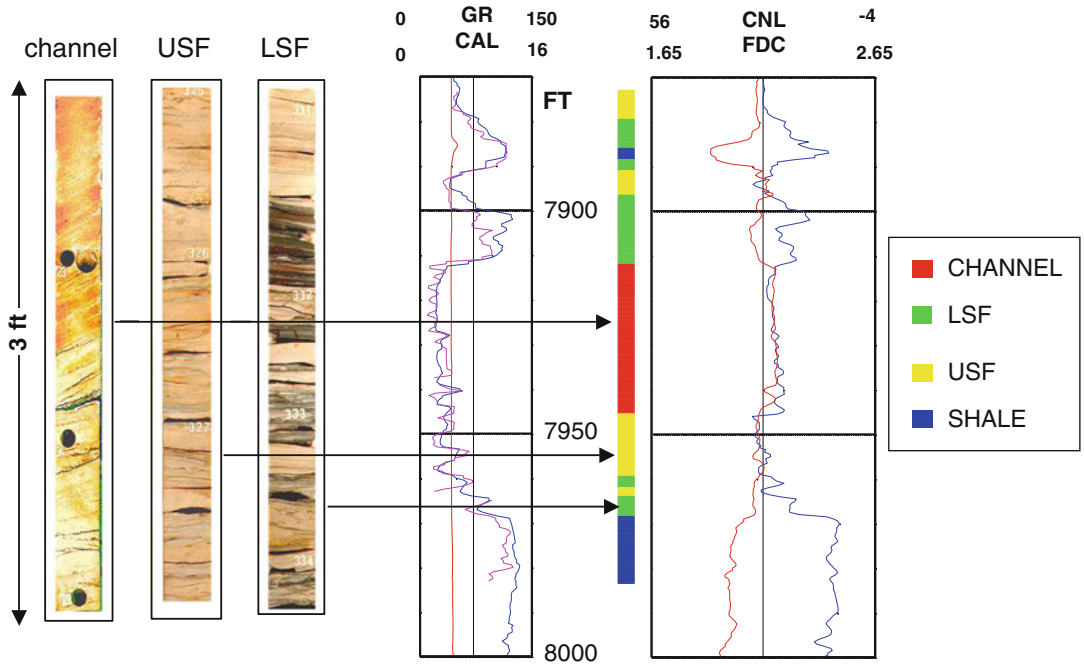

Fig. 2.8 Genetic modelling elements; lithofacies types grouped into channel, upper shoreface and lower shoreface genetic depositional elements (Image courtesy of Simon Smith)

include conglomeratic, cross-bedded sandstone and mudstone lithofacies. Figure 2.8 shows an example of several genetic depositional elements interpreted from core and log observations.

2.4.3.3 Stratigraphic Elements

For models which can be based on a sequence stratigraphic framework, the fine-scale components of the stratigraphic scheme may also be the

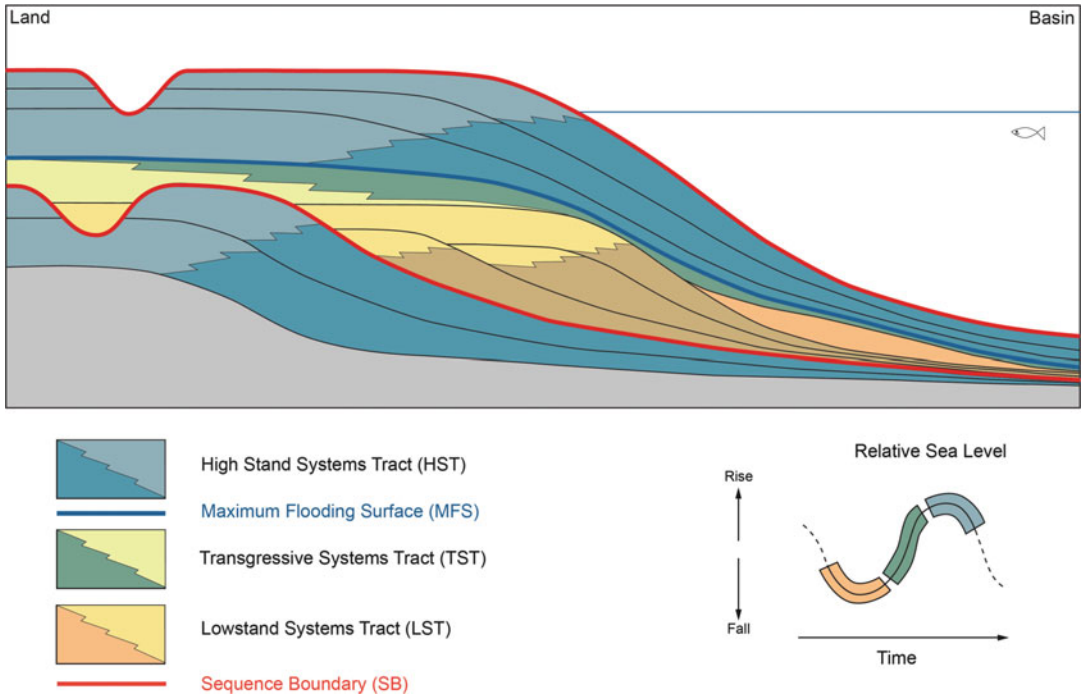

Fig. 2.9 Sequence stratigraphic elements

predominant model elements. These may be parasequences organised within a larger-scale sequence-based stratigraphic framework which defines the main reservoir architecture (e.g. Fig. 2.9).

2.4.3.4 Diagenetic Elements

Diagenetic elements commonly overprint lithofacies types, may cross major stratigraphic boundaries and are often the predominant feature of carbonate reservoir models. Typical diagenetic elements could be zones of meteoric flushing, dolomitisation or de-dolomitisation (Fig. 2.10).

2.4.3.5 Structural Elements

Assuming a definition of model elements as three-dimensional features, structural model elements emerge when the properties of a volume are dominated by structural rather than sedimentological or stratigraphic aspects. Fault damage zones are important volumetric structural elements (e.g. Fig. 2.11) as are mechanical layers (strata-bound fracture sets) with properties driven by small-scale jointing or cementation.

2.4.3.6 Exotic Elements

The list of potential model elements is as diverse as the many different types of reservoir, hence other 'exotic' reservoir types must be mentioned, having their own model elements specific to their geological make-up. Reservoirs in volcanic rocks are a good example (Fig. 2.12), in which the key model elements may be zones of differential cooling and hence differential fracture density.

***

The important point about using the term 'model element' is to stimulate broad thinking about the model concept, a thought process which runs across the reservoir geological sub-disciplines (stratigraphy, sedimentology, structural geology, even volcanology). For avoidance of doubt, the main difference between the model framework and the model elements is that 2D features are used to define the model framework (faults, unconformities, sequence boundaries, simple bounding surfaces) whereas it is 3D model elements which fill the volumes within that framework.

Having defined the framework and identified the elements, the next question is how much information to carry explicitly into the modelling process. Everything that can be identified need not be modelled.

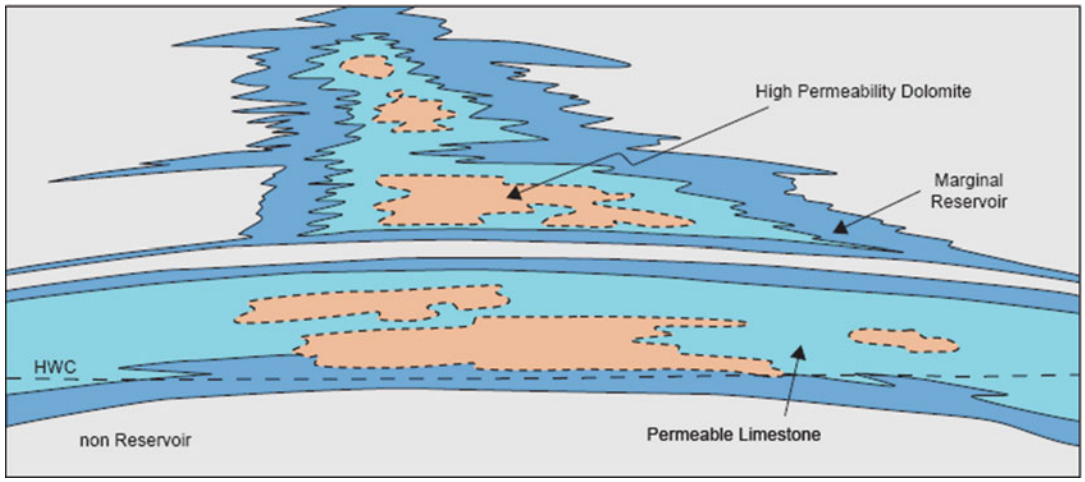

Fig. 2.10 Diagenetic elements in a carbonate build-up; where reservoir property contrasts are driven by differential development of dolomitisation

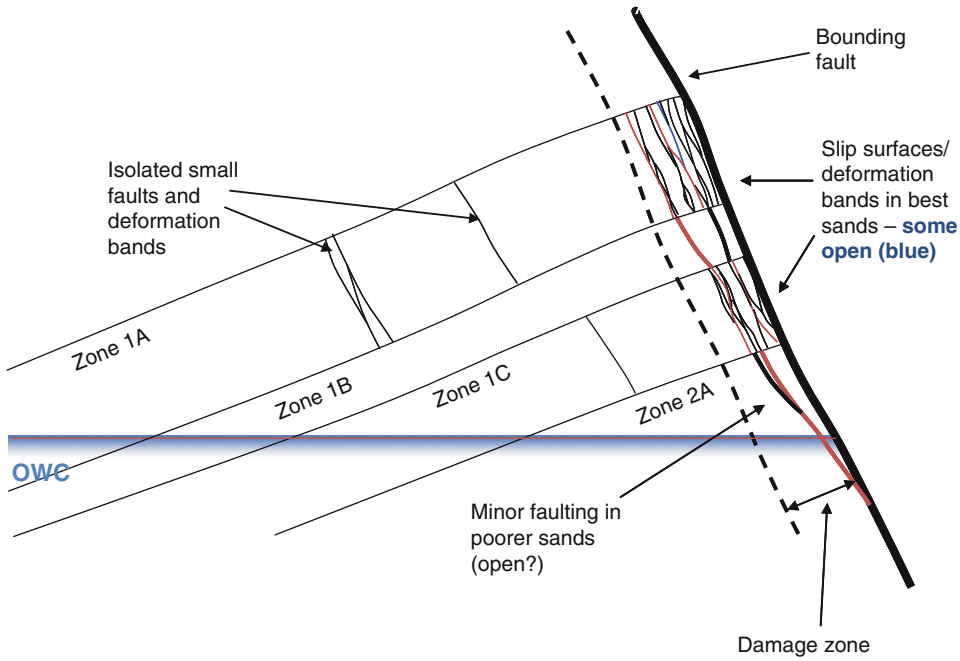

Fig. 2.11 Structural elements: volumes dominated by minor fracturing in a fault damage zone next to a major block-bounding fault (Bentley and Elliot 2008)

2.4.4 How Much Heterogeneity to Include?

The ultimate answer to this fundamental question depends on a combined understanding of geology and flow physics. To be more specific, the key criteria for distinguishing which model elements are required for the model build are:

1. The identification of potential model elements – a large number may initially be selected as 'candidates' for inclusion;

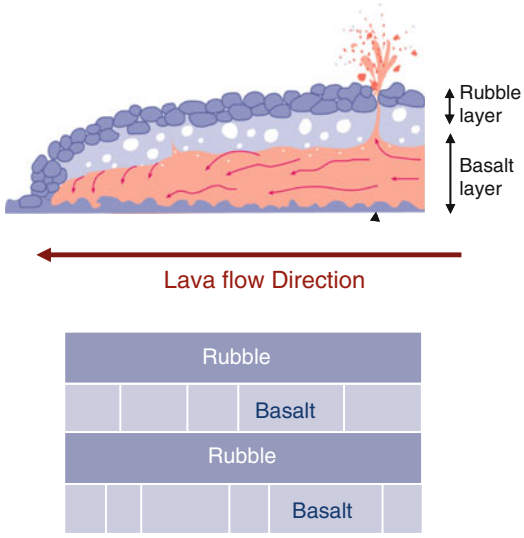

Fig. 2.12 Exotic elements: reservoir breakdown for a bimodal-permeability gas-bearing volcanic reservoir in which model elements are driven by cooling behaviour in a set of stacked lava flows (Image courtesy of Jenny Earnham)

2. The interpretation of the architectural arrangement of those elements represented in a simple sketch – the 'concept sketch';
3. The reservoir quality contrasts between the elements, addressed for example by looking at permeability/porosity contrasts between each;
4. The fluid type (gas, light oil, heavy oil);
5. The production mechanism.

The first steps are illustrated in Fig. 2.13 in which six potential elements have been identified from core and log data (step 1), placed in an analogue context (step 2) and their rock property contrasts compared (step 3). The six candidate elements seem to cluster into three, but is it right to lump these together? How great does a contrast have to be to be 'significant'? Here we can invoke some useful guidance.

2.4.4.1 Handy Rule of Thumb

A simple way of combining the factors above is to consider what level of permeability contrast would generate significant flow heterogeneities for a given fluid type and production mechanism. The handy rule of thumb is as follows (Fig. 2.14):

- Gas reservoirs are sensitive to 3 orders of magnitude of permeability variation per porosity class;
- Oil reservoirs under depletion are sensitive to 2 orders of magnitude of permeability variation per porosity class;
- Heavy oil reservoirs, or lighter crudes under secondary or tertiary recovery, tend to be sensitive to 1 order of magnitude of permeability variation.

This simple rule of thumb, which has become known as 'Flora's Rule' (after an influential reservoir engineering colleague of one of the authors), has its foundation in the viscosity term in the Darcy flow equation:

$$u = \frac{-k}{\mu} \nabla(P) \qquad (2.1)$$

where:
u = fluid velocity
k = permeability
μ = fluid viscosity
∇P = pressure gradient

Because the constant of proportionality between flow velocity and the pressure gradient is k/μ, low viscosity results in a weaker dependence of flow on the pressure gradient whereas higher viscosities give increasingly higher dependence of flow on the pressure gradient. Combine this with a consideration of the mobility ratio in a two-phase flow system, and the increased sensitivity of secondary and tertiary recovery to permeability heterogeneity becomes clear.

Using these criteria, some candidate elements which contrast geologically in core may begin to appear rather similar – others will clearly stand out. The same heterogeneities that are shown to have an important effect on an oilfield waterflood may have absolutely no effect in a gas reservoir under depletion. The importance of some 'borderline' heterogeneities may be unclear – and these could be included on a 'just in case' basis. Alternatively, a quick static/dynamic sensitivity run may be enough to demonstrate that a specific candidate element can be dropped or included with confidence.

Petrophysically similar reservoir elements may still need to be incorporated if they have different 3D shapes (the geometric aspect) if, for example, one occurs in ribbon shapes and another in sheets. The reservoir architecture is influenced by the geometric stacking of such elements.

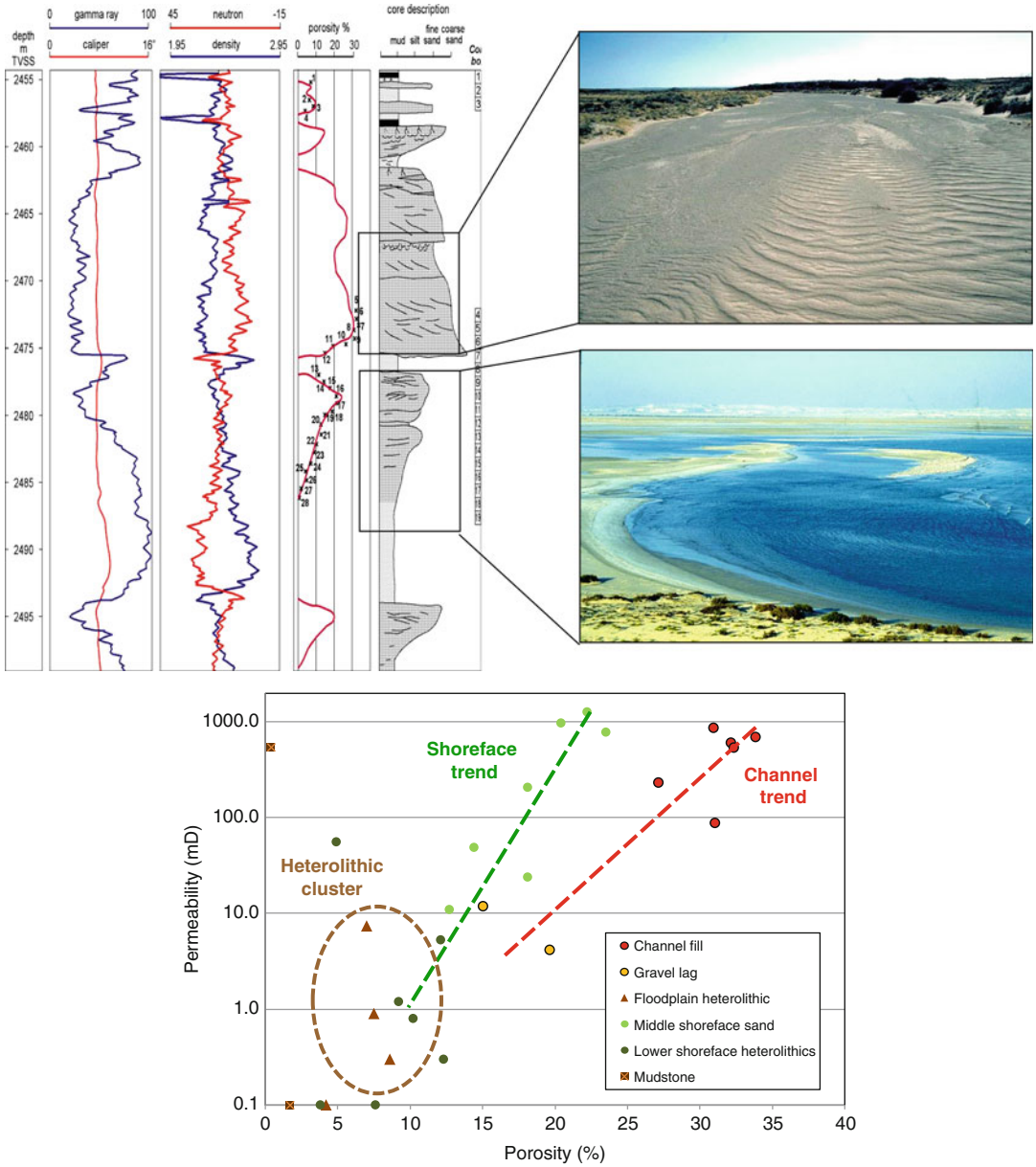

Fig. 2.13 Six candidate model elements identified from core and log data and clustered into three on a k/phi cross plot – to lump or to split?

The outcome of this line of argument is that some reservoirs may not require complex 3D reservoir models at all (Fig. 2.15). Gas-charged reservoirs require high degrees of permeability heterogeneity in order to justify a complex modelling exercise – they often deplete as simple tanks. Fault compartments and active aquifers may stimulate heterogeneous flow production in gas fields, but even in this case the model required to capture key fault blocks can be quite coarse. At the other end of the scale, heavy oil fields under water or steam injection are highly susceptible to minor heterogeneities, and benefit from detailed modelling. The difficulty here lies in assessing the scale of these heterogeneities, which can often be on a very fine, poorly-sampled scale.

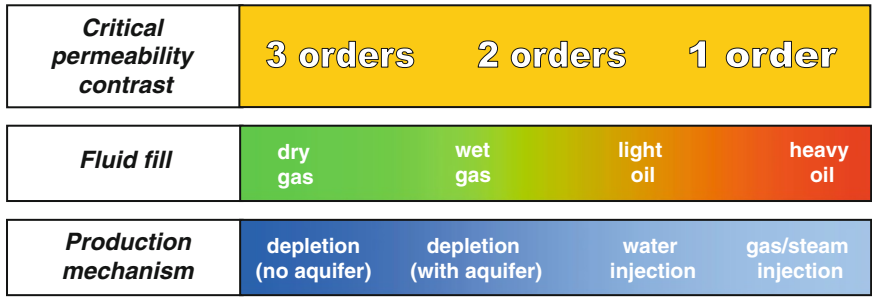

Fig. 2.14 Critical order of magnitude permeability contrasts for a range of fluid and production mechanisms – 'Flora's Rule'

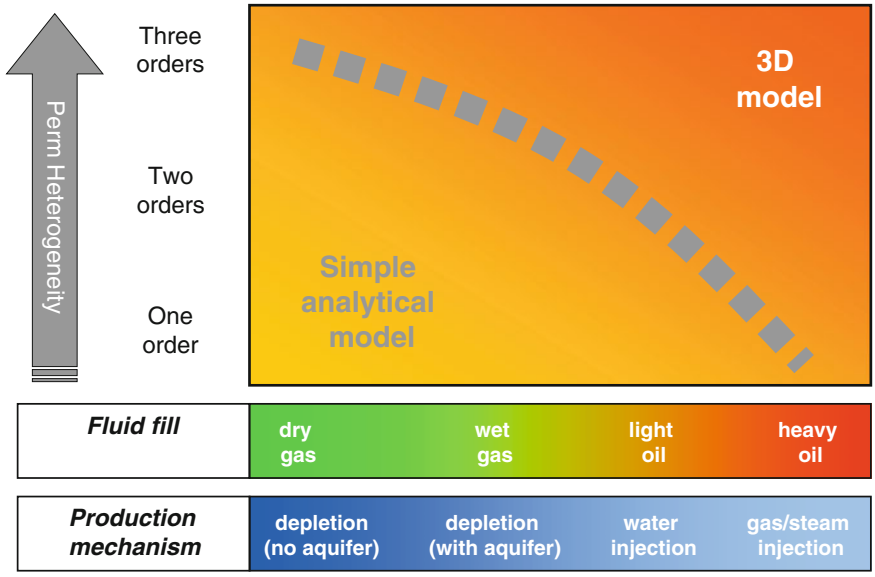

Fig. 2.15 What type of reservoir model? A choice based on heterogeneity and fluid type

The decision as to which candidate elements to include in a model is therefore not primarily a geological one. Geological and petrophysical analyses are required to define the degree of permeability variation and to determine the spatial architecture, but it is the fluid type and the selected displacement process which determine the level of geological detail needed in the reservoir model and hence the selection of 'model elements'.

2.5 Determinism and Probability

The use of geostatistics in reservoir modelling became widely fashionable in the early 1990s (e.g. Haldorsen and Damsleth 1990; Journel and Alabert 1990) and was generally received as a welcome answer to some tricky questions such as how to handle uncertainty and how to represent geological heterogeneities in 3D reservoir models.

However, the promise of geostatistics (and 'knowledge-based systems') to solve reservoir forecasting problems sometimes led to disappointment. Probabilistic attempts to predict desirable outcomes, such as the presence of a sand body, yield naïve results if applied blindly (Fig. 2.16).

This potential for disappointment is unfortunate as the available geostatistical library of tools is excellent for applying quantitative statistical algorithms rigorously and routinely, and is essential for filling the inter-well volume in a 3D

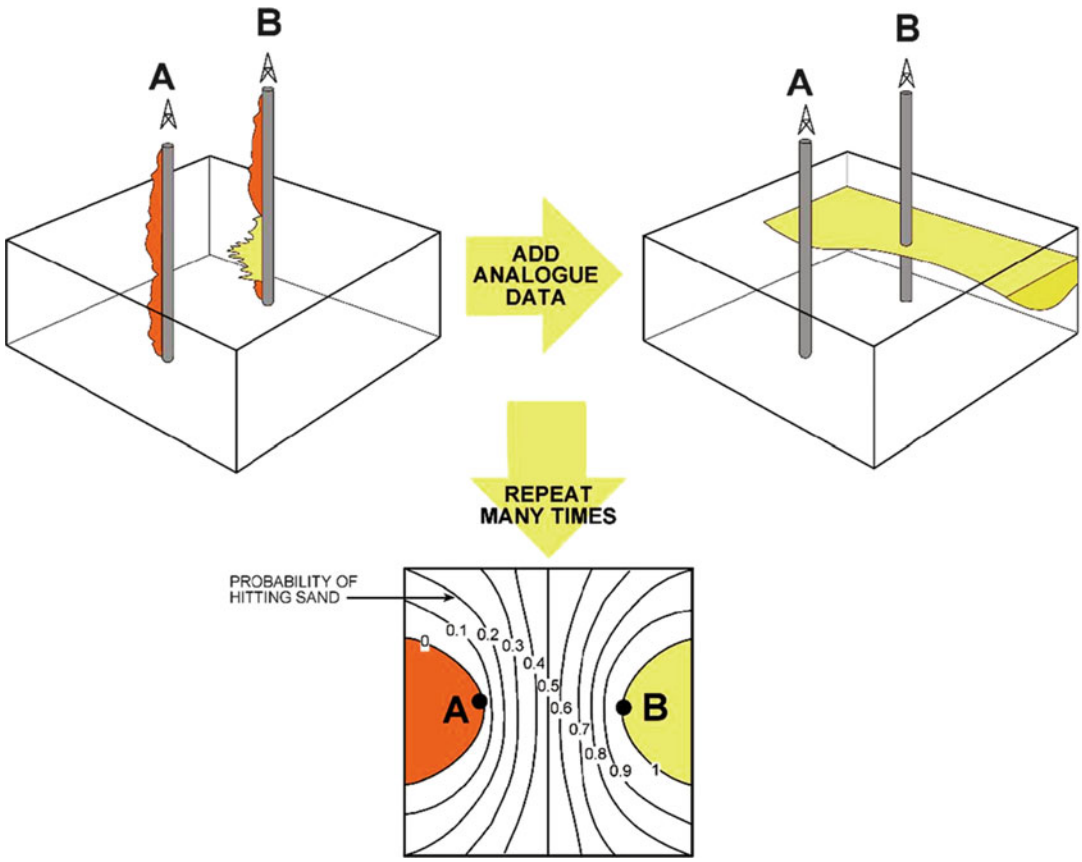

Fig. 2.16 A naïve example of expectation from geostatistical forecasting – the final mapped result simply illustrates where the wells are

reservoir model. Furthermore, geostatistical methods need not be over-complex and are not as opaque as sometimes presented.

2.5.1 Balance Between Determinism and Probability

The underlying design issue we stress is the balance between determinism and probability in a model, and whether the modeller is aware of, and in control of, this balance.

To define the terminology as used here:

- ***Determinism*** is taken to mean an aspect of a model which is fixed by the user and imposed on the model as an absolute, such as placing a fault in the model or precisely fixing the location of a particular rock body;
- ***Probability*** refers to aspects of the model which are specified by a random (stochastic) outcome from a probabilistic algorithm.

To complete the terminology, a *stochastic process* (from the Greek *stochas* for 'aiming' or 'guessing') is one whose behaviour is completely non-deterministic. A *probabilistic* method is one in which likelihood or probability theory is employed. *Monte Carlo* methods, referred to especially in relation to uncertainty handling, are a class of algorithms that rely on repeated random sampling to compute a *probabilistic* result. Although not strictly the same, the terms *probabilistic* and *stochastic* are often treated synonymously and in this book we will restrict the discussion to the contrast between deterministic and probabilistic approaches applied in reservoir modelling.

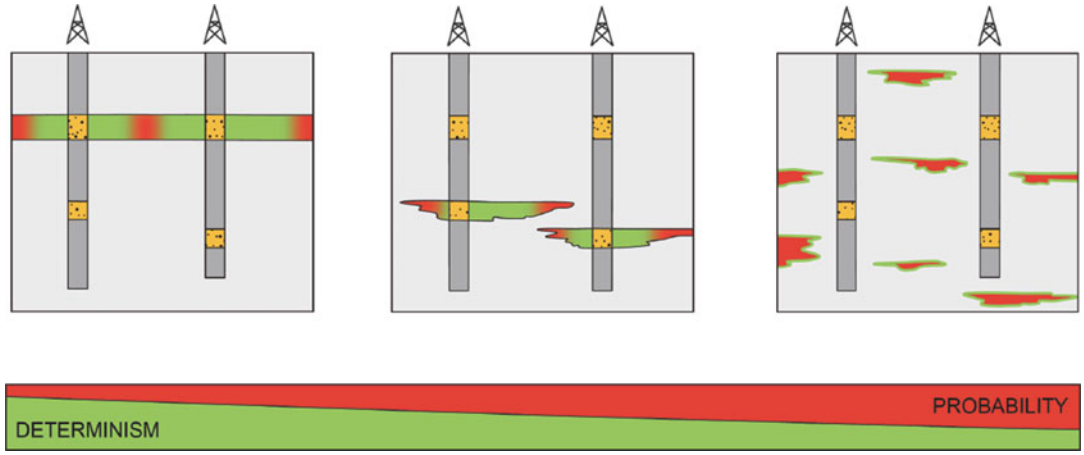

Fig. 2.17 Different rock body types as an illustration of the deterministic/probabilistic spectrum

The balance of deterministic and probabilistic influences on a reservoir model is not as black and white as it may at first seem. Consider the simple range of cases shown in Fig. 2.17, showing three generic types of rock body:

1. *Correlatable bodies* (Fig. 2.17, left). These are largely determined by correlation choices between wells, e.g. sand observations are made in two wells and interpreted as occurrences of the same extensive sand unit and are correlated. This is a deterministic choice, not an outcome of a probabilistic algorithm. The resulting body is not a 100 % determined 'fact', however, as the interpretation of continuity between the wells is just that – an interpretation. At a distance from the wells, the sand body has a probabilistic component.
2. *Non-correlated bodies* (Fig. 2.17, centre). These are bodies encountered in one well only. At the well, their presence is determined. At increasing distances from the well, the location of the sand body is progressively less well determined, and is eventually controlled almost solely by the outcome from a probabilistic algorithm. These bodies are each partly deterministic and partly probabilistic.
3. *Probabilistic bodies* (Fig. 2.17, right). These are the bodies not encountered by wells, the position of which will be chosen by a probabilistic algorithm. Even these, however, are not 100 % probabilistic as their appearance in the model is not a complete surprise. Deterministic constraints will have been placed on the probabilistic algorithm to make sure bodies are not unrealistically large or small, and are appropriately numerous.

So, if everything is a mixture of determinism and probability, what's the problem? The issue is that although any reservoir model is rightfully a blend of deterministic and probabilistic processes, the richness of the blend is a choice of the user so this is an issue of model design. Some models are highly deterministic, some are highly probabilistic and which end of the spectrum a model sits at influences the uses to which it can be put. A single, highly probabilistic model is not suitable for well planning (rock bodies will probably not be encountered as prognosed). A highly deterministic model may be inappropriate, however, for simulations of reservoirs with small rock bodies and little well data. Furthermore, different modellers might approach the same reservoir with more deterministic or more probabilistic mindsets.

The balance of probability and determinism in a model is therefore a subtle issue, and needs to be understood and controlled as part of the model design. We will also suggest here that greater happiness is generally to be found in models which are more strongly deterministic, as the deterministic inputs are the direct carrier of the reservoir concept.

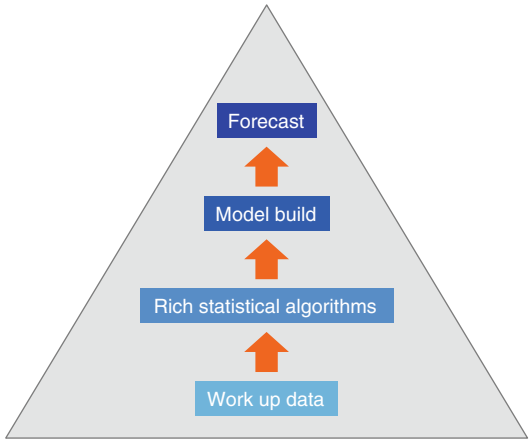

Fig. 2.18 The data-driven approach to reservoir modelling

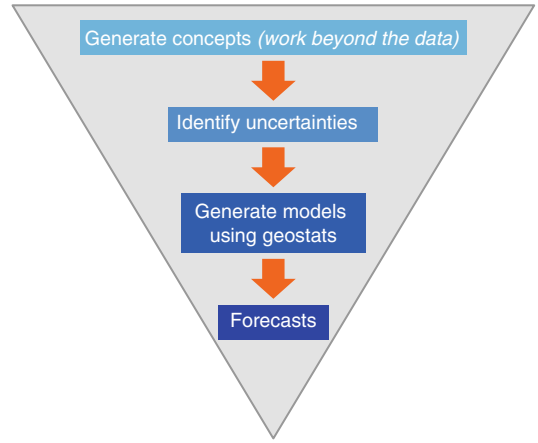

Fig. 2.19 The concept-driven approach to reservoir modelling

2.5.2 Different Generic Approaches

To emphasise the importance of user choice in the approach to determinism and probability, two approaches to model design are summarised graphically (Fig. 2.18).

The first is a data-driven approach to modelling. In this case, the model process starts with an analysis of the data, from which statistical guidelines can be drawn. These guidelines are input to a rich statistical model of the reservoir which in turn informs a geostatistical algorithm. The outcome of the algorithm is a model, from which a forecast emerges. This is the approach which most closely resembles the default path in reservoir modelling, resulting from the linear workflow of a standard reservoir modelling software package.

The limit of a simple data-driven approach such as this is that there is a reliance on the rich geostatistical algorithm to generate the desired model outcome. This in turn relies on the statistical content of the underlying data set, *yet for most of our reservoirs, the underlying data set is statistically insufficient*. This is a critical issue and distinguishes oil and gas reservoir modelling from other types of geostatistical modelling in earth sciences such as mining and soil science. In the latter cases, there is often a much richer underlying data set, which can indeed yield clear statistical guidelines for a model build. In reservoir modelling we are typically dealing with much more sparse data, an exception being direct conditioning of the reservoir model to high quality 3D seismic data (e.g. Doyen 2007).

An alternative is to take a more concept-driven approach (Fig. 2.19). In this case, the modelling still starts with an analysis of the data, but the analysis is used to generate alternative conceptual models for the reservoir. The reservoir concept should honour the data but, as the dataset is statistically insufficient, the concepts are not limited to it. The model build is strongly concept-driven, has a strong deterministic component, and less emphasis is placed on geostatistical algorithms. The final outcome is not a single forecast, but a set of forecasts based on the uncertainties associated with the underlying reservoir concepts.

The difference between the data- and concept-driven approaches described above is the expectation of the geostatistical algorithm in the context of data insufficiency. The result is a greater emphasis on deterministic model aspects, which therefore need some more consideration.

2.5.3 Forms of Deterministic Control

The deterministic controls on a model can be seen as a toolbox of options with which to realise an architectural concept in a reservoir model.

These will be discussed further in the last section of this chapter, but are introduced below.

2.5.3.1 Faulting

With the exception of some (relatively) specialist structural modelling packages, large scale structural features are strongly deterministic in a reservoir model. Thought is required as to whether the structural framework is to be geophysically or geologically led, that is, are only features resolvable on seismic to be included, or will features be included which are kinematically likely to occur in terms of structural rock deformation. This in itself is a model design choice, introduced in the discussion on model frameworks (Sect. 2.3) and the choice will be imposed deterministically.

2.5.3.2 Correlation and Layering

The correlation framework (Sect. 2.3) is deterministic, as is any imposed hierarchy. The probabilistic algorithms work entirely within this framework – layer boundaries are not moved in common software packages. Ultimately the flowlines in any simulation will be influenced by the fine layering scheme and this is all set deterministically.

2.5.3.3 Choice of Algorithm

There are no hard rules as to which geostatistical algorithm gives the 'correct' result yet the choice of pixel-based or object-based modelling approaches will have a profound effect in the model outcome (Sect. 2.7). The best solution is the algorithm or combination of algorithms which most closely reflects the desired reservoir concept, and this is a deterministic choice.

2.5.3.4 Boundary Conditions for Probabilistic Algorithms

All algorithms work within limits, which will be given by arbitrary default values unless imposed. These limits include correlation models, object dimensions and statistical success criteria (Sect. 2.6). In the context of the concept-driven logic described above these limits need to be deterministically chosen, rather than left as a simple consequence of the limits apparent from the (statistically insufficient) well data set.

2.5.3.5 Seismic Conditioning

The great hope for detailed deterministic control is exceptionally good seismic data. This hope is often forlorn, as even good quality seismic data is not generally resolved at the level of detail required for a reservoir model. All is not lost, however, and it is useful to distinguish between *hard* and *soft* conditioning.

Hard conditioning is applicable in cases where extremely high quality seismic, sufficiently resolved at the scale of interest, can be used to directly define the architecture in a reservoir model. An example of this is seismic geobodies in cases where the geobodies are believed to directly represent important model elements. Some good examples of this have emerged from deepwater clastic environments, but in many of these cases detailed investigation (or more drilling) ends up showing that reservoir pay extends sub-seismically, or that the geobody is itself a composite feature.

The more generally useful approach for rock modelling is *soft conditioning*, where information from seismic is used to give a general guide to the probabilistic algorithms (Fig. 2.20). In this case, the link between the input from seismic and the probabilistic algorithm may be as simple as a correlation coefficient. It is the level of the coefficient which is now the deterministic control; and the decision to use seismic as either a hard or soft conditioning tool is also a deterministic one.

One way of viewing the role of seismic in reservoir modelling is to adapt the frequency/amplitude plot familiar from geophysics (Fig. 2.21). These plots are used to show the frequency content of a seismic data set and typically how improved seismic acquisition and processing can extend the frequency content towards the ends of the spectrum. Fine scale reservoir detail, often sits beyond the range of the seismic data (extending the blue area in Fig. 2.21). The low end of the frequency spectrum – the large scale layering – is also typically beyond the range of the seismic sample, hence the requirement to construct a low frequency 'earth model' to support seismic inversion work.

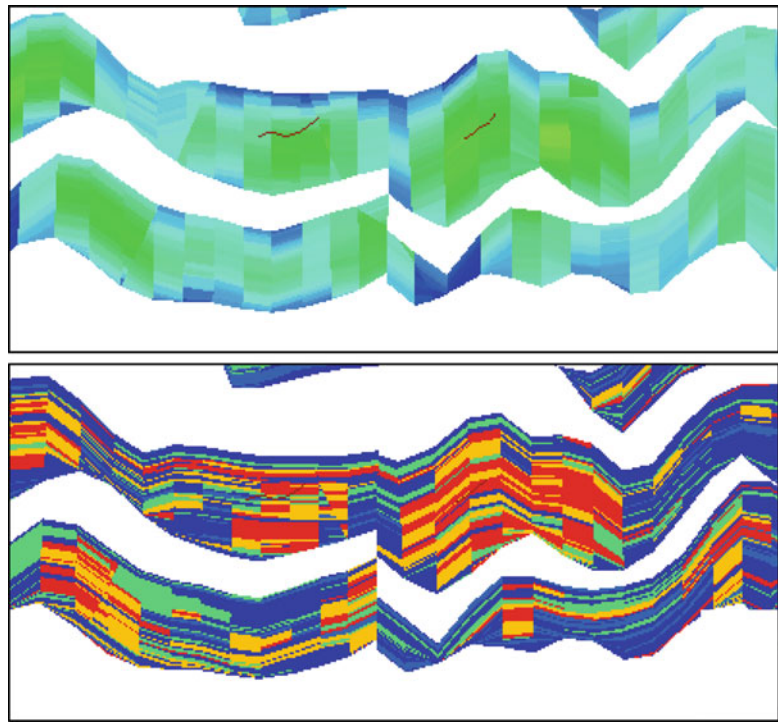

Fig. 2.20 Deterministic model control in the form of seismic 'soft' conditioning of a rock model. *Upper image*: AI volume rendered into cells. *Lower image*: Best reservoir properties (*red*, *yellow*) preferentially guided by high AI values (Image courtesy of Simon Smith)

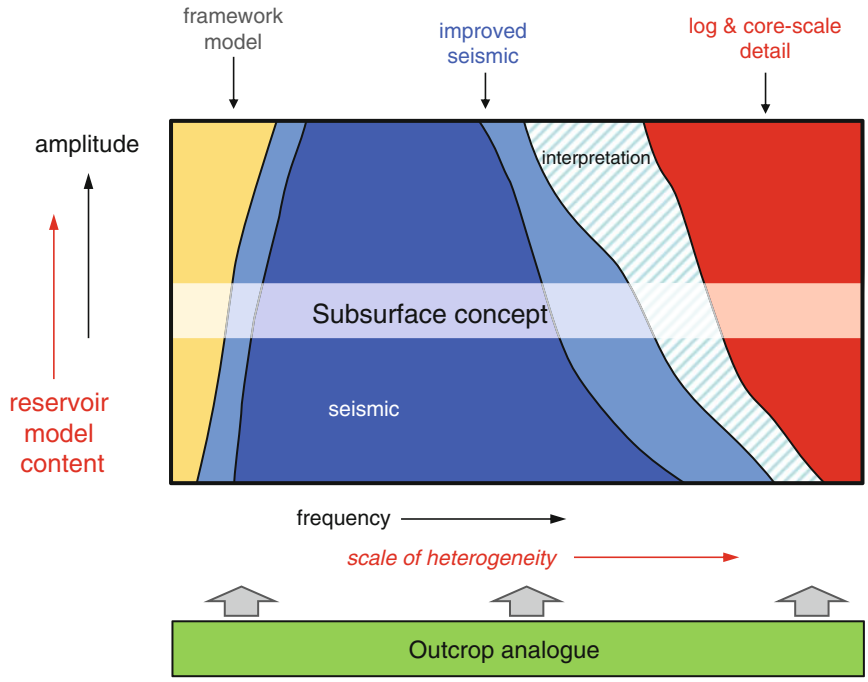

Fig. 2.21 Seismic conditioning: deterministic and probabilistic elements of a reservoir model in the context of frequency & scale versus amplitude & content

The plot is a convenient backdrop for arranging the components of a reservoir model, and the frequency/amplitude axes can be alternatively labelled for 'reservoir model scale' and 'content'. The reservoir itself exists on all scales and is represented by the full rectangle, which is only partially covered by seismic data. The missing areas are completed by the framework model at the low frequency end and by core and log-scale detail at the high frequency end, the latter potentially a source for probabilistic inversion studies which aim to extend the influence of the seismic data to the high end of the spectrum.

The only full-frequency data set is a good outcrop analogue, as it is only in the field that the reservoir can be accessed on all scales. Well facilitated excursions to outcrop analogues are thereby conveniently justified.

Is all the detail necessary? Here we can refer back to Flora's Rule and the model purpose, which will inform us how much of the full spectrum is required to be modelled in any particular case.

In terms of seismic conditioning, it is only in the case where the portion required for modelling exactly matches the blue area in Fig. 2.21 that we can confidently apply hard conditioning using geobodies in the reservoir model, and this is rarely the case.

***

With the above considered, there can be some logic as to the way in which deterministic control is applied to a model, and establishing this is part of the model design process. The probabilistic aspects of the model should be clear, to the point where the modeller can state whether the design is strongly deterministic or strongly probabilistic and identify where the deterministic and probabilistic components sit.

Both components are implicitly required in any model and it is argued here that the road to happiness lies with strong deterministic control. The outcome from the probabilistic components of the model should be largely predictable, and should be a clear reflection of the input data combined with the deterministic constraints imposed on the algorithms.

Disappointment occurs if the modeller expects the probabilistic aspects of the software to take on the role of model determination.

2.6 Essential Geostatistics

Good introductions to the use of statistics in geological reservoir modelling can be found in Yarus and Chambers (1994), Holden et al. (1998), Dubrule and Damsleth (2001), Deutsch (2002) and Caers (2011).

Very often the reservoir modeller is confounded by complex geostatistical terminology which is difficult to translate into the modelling process. Take for example this quotation from the excellent but fairly theoretical treatment of geostatistics by Isaaks and Srivastava (1989):

> *in an ideal theoretical world the sill is either the stationary infinite variance of the random function or the dispersion variance of data volumes within the volume of the study area*

The problem for many of us is that we don't work in an *ideal theoretical world* and struggle with the concepts and terminology that are used in statistical theory. This section therefore aims to extract just those statistical concepts which are essential for an *intuitive* understanding of what happens in the statistical engines of reservoir modelling packages.

2.6.1 Key Geostatistical Concepts

2.6.1.1 Variance

The key concept which must be understood is that of variance. Variance, σ^2, is a measure of the average difference between individual values and the mean of the dataset they come from. It is a measure of the *spread* of the dataset:

$$\sigma^2 = \Sigma(x_i - \mu)^2/N \qquad (2.2)$$

where:

x_i = individual value for the variable in question,

N = the number of values in the data set, and

μ = the mean of that data set

Variance-related concepts underlie much of reservoir modelling. Two such occurrences are summarised below: the use of correlation coefficients and the variogram.

2.6.1.2 Correlation Coefficients

The correlation coefficient measures the strength of the dependency between two parameters by comparing how far pairs of values (x, y) deviate from a straight line function, and is given by the function:

$$\rho = \frac{1/N\sum_{n=1}^{n=N}(x_i - \mu_x)(y_i - \mu_y)}{\sigma_x \sigma_y} \qquad (2.3)$$

where

N = number of points in the data set

x_i, y_i = values of point in the two data sets

μ_x, μ_y = mean values of the two data sets, and

σ_x, σ_y = standard deviations of the two data sets (the square of the variance)

If the outcome of the above function is positive then higher values of x tend to occur with higher values of y, and the data sets are said to be 'positively correlated'. If the outcome is $\rho = 1$ then the relationship between x and y is a simple straight line. A negative outcome means high values of one data set correlate with low values of the other: 'negative correlation'. A zero result indicates no correlation.

Note that correlation coefficients assume the data sets are both linear. For example, two data sets which have a log-linear relationship might have a very strong correlation but still display a poor correlation coefficient. Of course, a coefficient can still be calculated if the log-normal data set (e.g. permeability) is first converted to a linear form by taking the logarithm of the data.

Correlation between datasets (e.g. porosity versus permeability) is typically entered into reservoir modelling packages as a value between 0 and 1, in which values of 0.7 or higher generally indicate a strong relationship. The value may be described as the 'dependency'.

2.6.1.3 The Variogram

Correlation coefficients reflect the variation of values within a dataset, but say nothing about how these values vary spatially. For reservoir modelling we need to express spatial variation of parameters, and the central concept controlling this is the variogram.

The variogram captures the relationship between the difference in value between pairs of data points, and the distance separating those two points. Numerically, this is expressed as the averaged squared differences between the pairs of data in the data set, given by the empirical variogram function, which is most simply expressed as:

$$2\gamma = (1/\mathrm{N})\Sigma\left(\mathrm{z_i} - \mathrm{z_j}\right)^2 \qquad (2.4)$$

where z_i and z_j are pairs of points in the dataset.

For convenience we generally use the semivariogram function:

$$\gamma = (1/2\mathrm{N})\Sigma\left(\mathrm{z_i} - \mathrm{z_j}\right)^2 \qquad (2.5)$$

The semivariogram function can be calculated for all pairs of points in a data set, whether or not they are regularly spaced, and can therefore be used to describe the relationship between data points from, for example, irregularly scattered wells.

The results of variogram calculations can be represented graphically (e.g. Fig. 2.22) to establish the relationship between the separation distance (known as the lag) and the average γ value for pairs of points which are that distance apart. The data set has to be grouped into distance bins to do the averaging; hence only one value appears for any given lag in Fig. 2.22.

A more formal definition of semi-variance is given by:

$$\gamma(h) = \frac{1}{2}E\left\{[Z(x+h) - Z(x)]^2\right\} \qquad (2.6)$$

where

E = the expectation (or mean)

Z(x) = the value at a point in space

Z(x + h) = the value at a separation distance, h (the lag)

Generally, γ increases as a function of separation distance. Where there is some relationship between the values in a spatial dataset, γ shows smaller values for points which are closer together in space, and therefore more likely to have similar values (due to some underlying process such as the tendency for similar rock types to occur together). As the separation distance increases the difference between the paired samples tends to increase.

Fitting a trend line through the points on a semivariogram plot yields a *semivariogram*

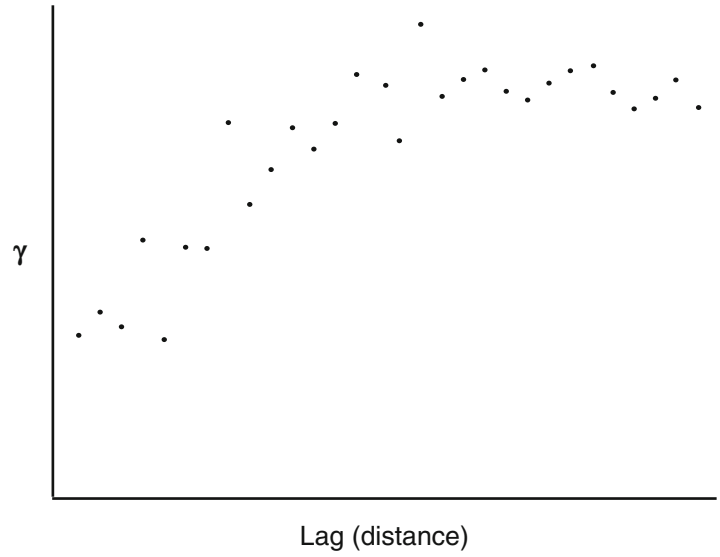

Fig. 2.22 The raw data for a variogram model: a systematic change in variance between data points with increasing distance between those points

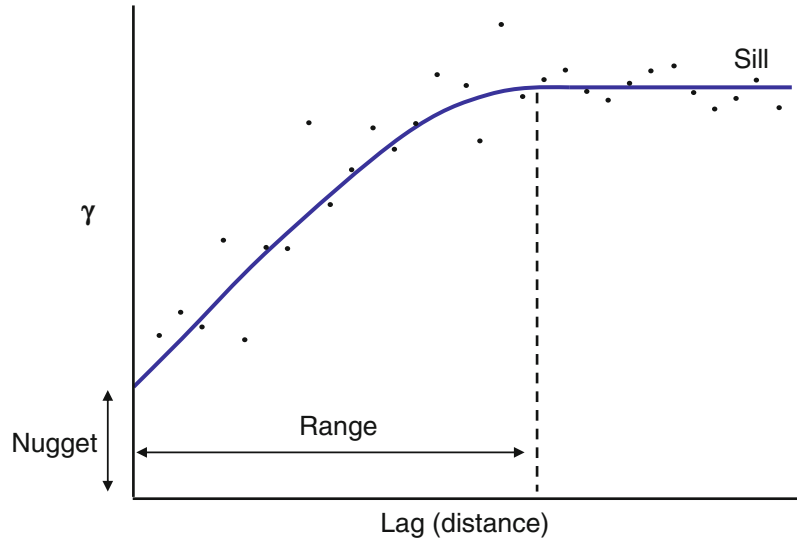

Fig. 2.23 A semivariogram model fitted to the points in Fig. 2.22

model (Fig. 2.23) and it is this model which may be used as input to geostatistical packages during parameter modelling.

A semivariogram model has three defining features:

- *the sill*, which is a constant γ value that may be approached for widely-spaced pairs and approximates the variance;
- *the range*, which is the distance at which the sill is reached, and
- *the nugget*, which is the extrapolated γ value at zero separation.

Now recall the definition of the sill, from Isaaks and Srivastava (1989), quoted at the start of this section. In simpler terms, the sill is the point at which the semivariogram function is equal to the variance, and the key measure for reservoir modelling is the range – the distance at which pairs of data points no longer bear any relationship to each other. A large range means that data points remain correlated over a large area, i.e. they are more homogeneously spread; a small range means the parameters are highly variable over short distances i.e. they are

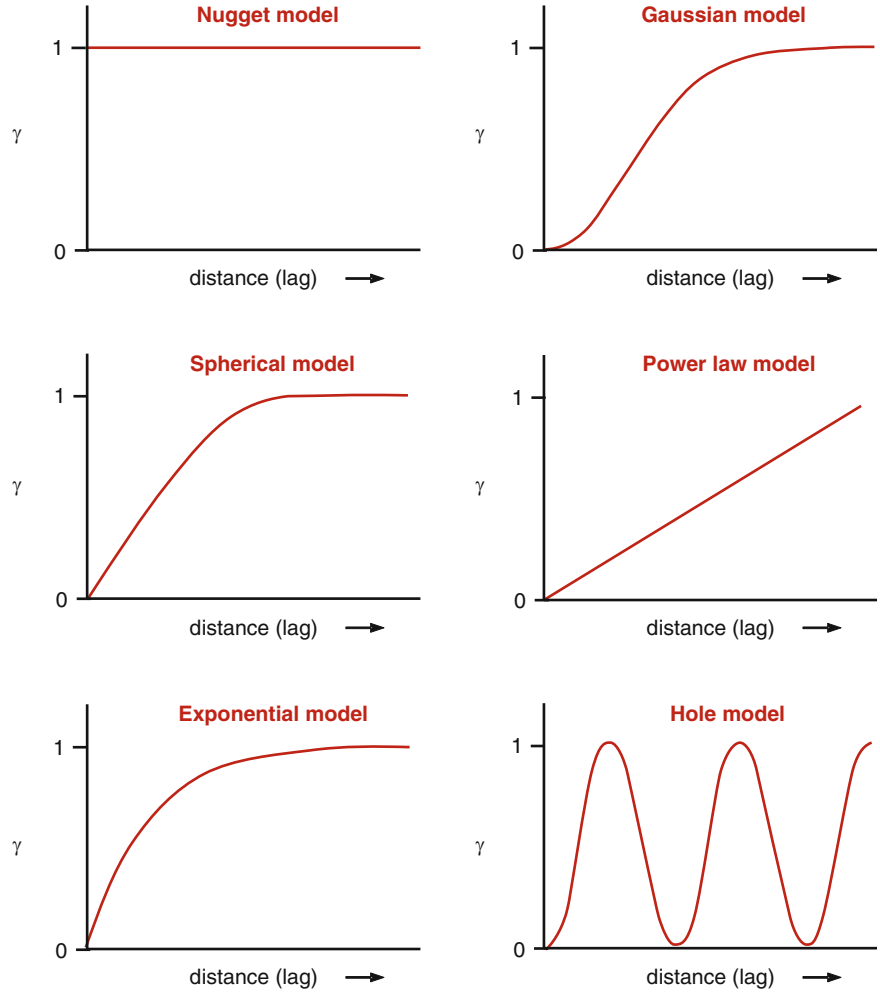

Fig. 2.24 Standard semi variogram models, with γ normalised to 1 (Redrawn from Deutsch 2002, © Oxford University Press, by permission of Oxford University Press, USA (www.oup.com))

spatially more heterogeneous. The presence of a nugget means that although the dataset displays correlation, quite sudden variations between neighbouring points can occur, such as when gold miners come across a nugget, hence the name. The nugget is also related to the sample scale – an indication that there is variation at a scale smaller than the scale of the measurement.

There are several standard functions which can be given to semivariogram models, and which appear as options on reservoir modelling software packages. Four common types are illustrated in Fig. 2.24. The spherical model is probably the most widely used.

A fifth semivariogram model – the power law – describes data sets which continue to get more dissimilar with distance. A simple example would be depth points on a tilted surface or a vertical variogram through a data set with a porosity/depth trend. The power law semivariogram has no sill.

It should also be appreciated that, in general, sedimentary rock systems often display a 'hole effect' when data is analysed vertically (Fig. 2.24e). This is a feature of any rock system that shows cyclicity (Jensen et al. 1995), where the γ value decreases as the repeating bedform is encountered. In practice this is generally not required for the vertical definition of layers in a reservoir model, as the layers are usually created deterministically from log data, or introduced using vertical trends (Sect. 2.7).

The shape of the semivariogram model can be derived from any data set, but the dataset is only a sample, and most likely an imperfect one. For many datasets, the variogram is difficult to estimate, and the modeller is therefore often required to choose a variogram model 'believed' to be representative of the system being modelled.

2.6.1.4 Variograms and Anisotropy

A final feature of variograms is that they can vary with direction. The spatial variation represented by the variogram model can be orientated on any geographic axis, N-S, E-W, etc. This has an important application to property modelling in sedimentary rocks, where a trend can be estimated based on the depositional environment. For example, reservoir properties may be more strongly correlated along a channel direction, or along the strike of a shoreface. This directional control on spatial correlation leads to anisotropic variograms. Anisotropy is imposed on the reservoir model by indicating the direction of preferred continuity and the strength of the contrast between the maximum and minimum continuity directions, usually represented as an oriented ellipse.

Anisotropic correlation can occur in the horizontal plane (e.g. controlled by channel orientation) or in the vertical plane (e.g. controlled by sedimentary bedding). In most reservoir systems, vertical plane anisotropy is stronger than horizontal plane anisotropy, because sedimentary systems tend to be strongly layered.

It is generally much easier to calculate vertical variograms directly from subsurface data, because the most continuous data come from sub-vertical wells. Vertical changes in rock properties are therefore more rapid, and vertical variograms tend to have short ranges, *often less than that set by default in software packages*. Horizontal variograms are likely to have much longer ranges, and may not reach the sill at the scale of the reservoir model. This is illustrated conceptually in Fig. 2.25, based on work by Deutsch (2002). The manner in which horizontal-vertical anisotropy is displayed (or calculated) depends very much on how the well data is split zonally. If different stratigraphic zones are mixed within the same dataset, this can lead to false impressions of anisotropy. If the zones are carefully separated, a truer impression of vertical and horizontal semivariograms (per zone) can be calculated.

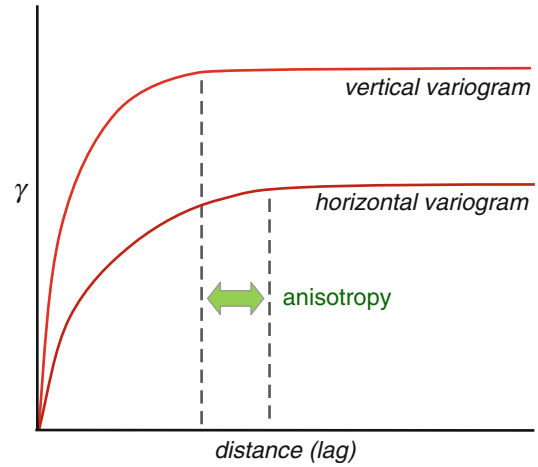

Fig. 2.25 Horizontal-vertical anisotropy ratio in semivariograms (Redrawn from Deutsch 2002, © Oxford University Press, by permission of Oxford University Press, USA (www.oup.com))

Table 2.1 Typical ranges in variogram anisotropy ratios

Element	Anisotropy ratio
Point bars	10:1–20:1
Braided fluvial	20:1–100:1
Aeolian	30:1–120:1
Estuarine	50:1–150:1
Deepwater	80:1–200:1
Deltaic	100:1–200:1
Platform carbonates	200:1–1000:1

From Deutsch (2002)

At the reservoir scale, vertical semivariograms can be easier to estimate. One approach for geostatistical analysis which can be taken is therefore to *measure* the vertical correlation (from well data) and then estimate the likely horizontal semivariogram using a vertical/horizontal anisotropy ratio based on a general knowledge of sedimentary systems. Considerable care should be taken if this is attempted, particularly to ensure that the vertical semivariograms are sampled within distinct (deterministic) zones. Deutsch has estimated ranges of typical anisotropy ratios by sedimentary environment (Table 2.1) and these offer a general guideline.

Fig. 2.26 Image of a present-day sand system – an analogue for lower coastal plain fluvial systems and tidally-influenced deltas (Brahmaputra Delta (NASA shuttle image))

2.6.2 Intuitive Geostatistics

In the discussion of key geostatistical concepts above we have tried to make the link between the underlying geostatistical concepts (more probabilistic) and the sedimentological concepts (more deterministic) which should drive reservoir modelling. Although this link is difficult to define precisely, an intuitive link can always be made between the variogram and the reservoir architectural concept.

In the discussion below we try to develop that link using a satellite image adopted as a conceptual analogue for a potential reservoir system. The image is of a wide fluvial channel complex opening out into a tidally-influenced delta. Assuming the analogue is appropriate, we extract the guidance required for the model design by estimating the variogram range and anisotropy from this image. We assume the image intensity is an indicator for sand, and extract this quantitatively from the image by pixelating the image, converting to a greyscale and treating the greyscale as a proxy for 'reservoir'. This process is illustrated in Figs. 2.26, 2.27, 2.28, 2.29, 2.30, and 2.31.

This example shows how the semivariogram emerges from quite variable line-to-line transects over the analogue image to give a picture of *average* variance. The overall result suggests pixel ranges of 25 in an E-W direction (Fig. 2.30) and 35 in a N-S direction (Fig. 2.31), reflecting the N-S orientation of the sand system and a 35:25 (1.4:1) horizontal anisotropy ratio.

This example is not intended to suggest that quantitative measures should be derived from satellite images and applied simply to reservoir modelling: there are issues of depositional vs. preserved architecture to consider, and for a sand system such as that illustrated above the system would most likely be broken down into elements which would not necessarily be spatially modelled using variograms alone (see next section).

The example is designed to guide our thinking towards an intuitive connection between the variogram (geostatistical variance) and reservoir heterogeneity (our concept of the variation). In particular, the example highlights the role of *averaging* in the construction of variograms. Individual transects over the image vary widely, and there are many parts of the sand system which are not well represented by the final averaged variogram. The variogram is in a sense quite crude and the application of variograms to either rock or property modelling assumes it is reasonable to convert actual spatial variation to a representative average and

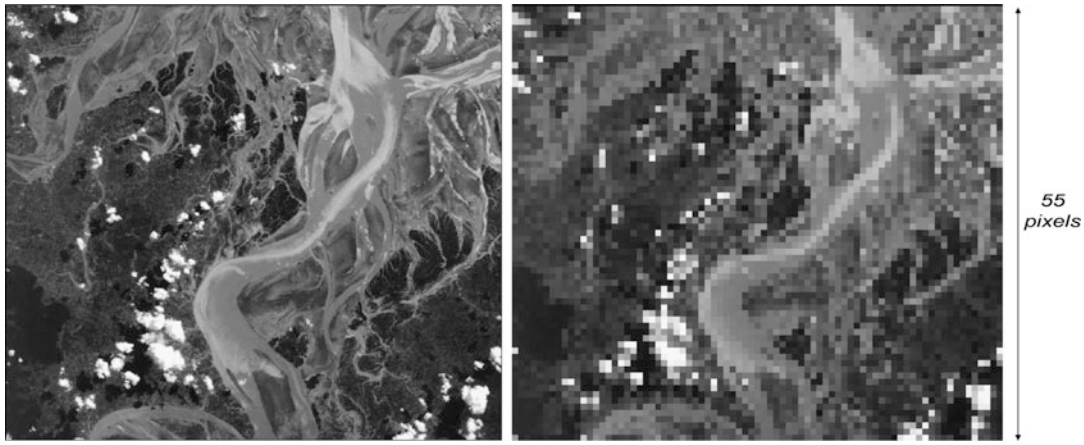

Fig. 2.27 Figure 2.26 converted to greyscale (*left*), and pixelated (*right*)

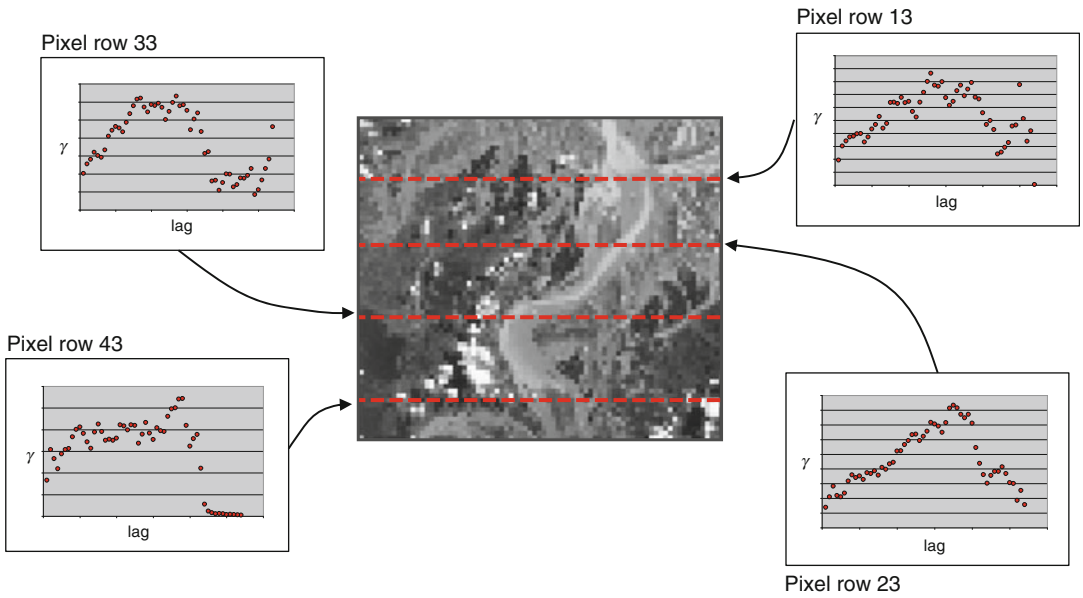

Fig. 2.28 Semivariograms for pixel pairs on selected E-W transects

then apply this average over a wide area. Using sparse well data as a starting point this is a big assumption, and its validity depends on the architectural concept we have for the reservoir. The concept is not a statistical measure; hence the need to make an intuitive connection between the reservoir concept and the geostatistical tools we use to generate reservoir heterogeneity.

The intuitive leap in geostatistical reservoir modelling is therefore to repeat this exercise for an analogue of the reservoir being modelled and use the resulting variogram to guide the geostatistical model, *assuming* it is concluded that the application of an average variogram model is valid. The basic steps are as follows:

1. Select (or imagine) an outcrop analogue;
2. Choose the rock model elements which appropriately characterise the reservoir
3. Sketch their spatial distribution (the architectural concept sketch) or find a suitable analogue dataset;

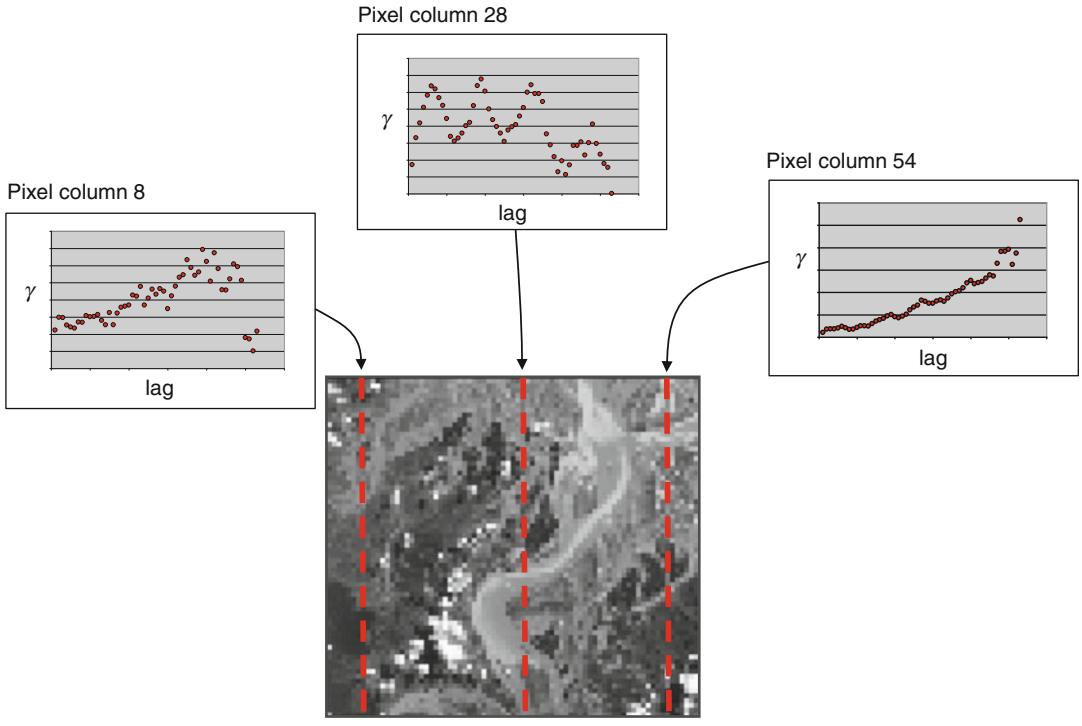

Fig. 2.29 Semivariograms for pixel pairs on selected N-S transects

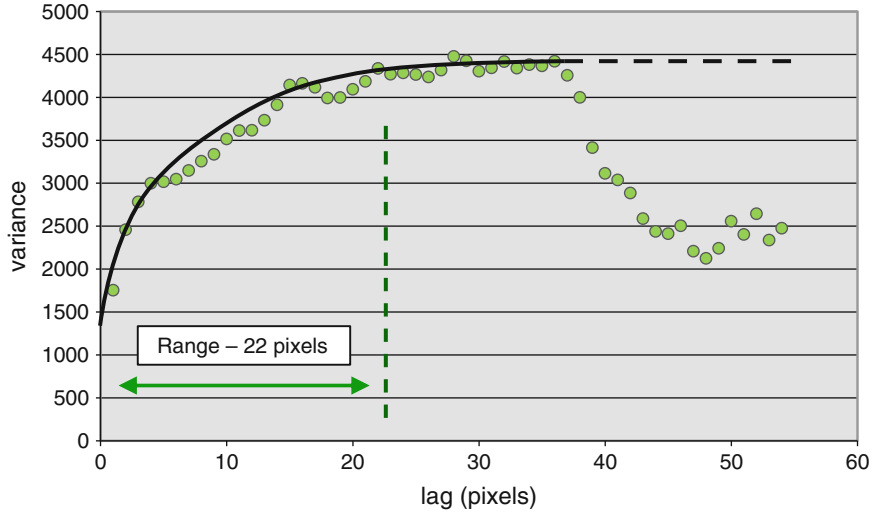

Fig. 2.30 Semivariogram based on all E-W transects

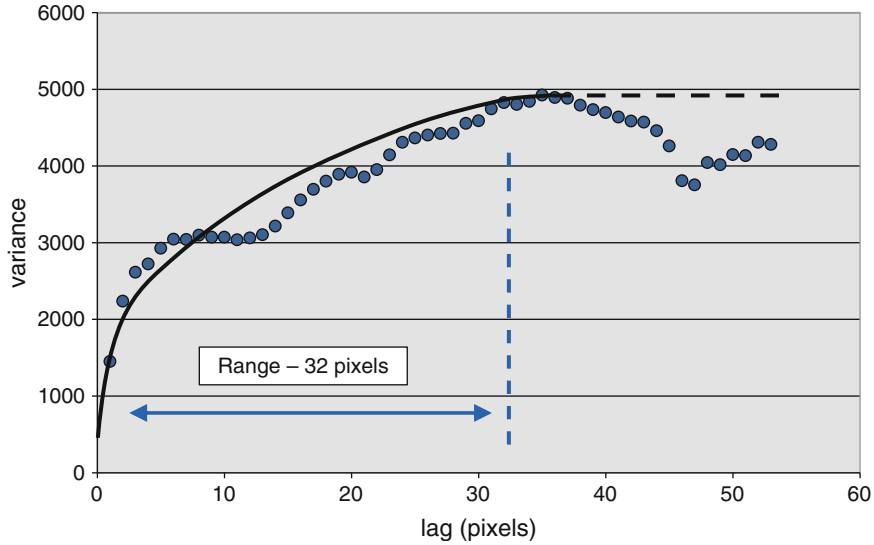

Fig. 2.31 Semivariogram based on all N-S transects

4. Estimate appropriate variogram ranges for individual elements (with different variogram ranges for the horizontal and vertical directions);
5. Estimate the anisotropy in the horizontal plane;
6. Input these estimates directly to a variogram-based algorithm if pixel-based techniques are selected (see next section);
7. Carry through the same logic for modelling reservoir properties, if variogram-based algorithms are chosen.

The approach above offers an intuitive route to the selection of the key input parameters for a geostatistical rock model. The approach is concept-based and deterministically steers the probabilistic algorithm which will populate the 3D grid.

There are some generalities to bear in mind:

- There should be greater variance across the grain of a sedimentary system (represented by the shorter EW range for the example above);
- Highly heterogeneous systems, e.g. glacial sands, should have short ranges and are relatively isotropic in (x, y);
- Shoreface systems generally have long ranges, at least for their reservoir properties, and the maximum ranges will tend to be along the strike of the system;
- In braided fluvial systems, local coarse-grained components (if justifiably extracted as model elements) may have very short ranges, often only a nugget effect;
- In carbonate systems, it needs to be clear whether the heterogeneity is driven by diagenetic or depositional elements, or a blend of both; single-step variography described above may not be sufficient to capture this.

Often these generalities may not be apparent from a statistical analysis of the well data, but they make intuitive sense. The outcome of an 'intuitive' variogram model should of course be sense-checked for consistency against the well data – any significant discrepancy should prompt a re-evaluation of either the concept or the approach to handling of the data (e.g. choice of rock elements). However, this intuitive approach to geostatistical reservoir modelling is recommended in preference to simple conditioning of the variogram model to the well data – which is nearly always statistically unrepresentative.

Exercise 2.1.

Estimate variograms for an outcrop image.

The image below shows an example photo of bedding structures from an outcrop section of a fluvial sedimentary sequence. Redox reactions (related to paleo-groundwater flows) give a strong visible contrast between high porosity (white) and low porosity (red) pore types. Micro channels with lag deposits and soft-sediment deformation features are also present.

Sketch estimated semivariogram functions for the horizontal and vertical directions assuming that colour (grey-scale) indicates rock quality. The hammer head is 10 cm across. Use the grey-scale image and pixelated grey-scale images to guide you.

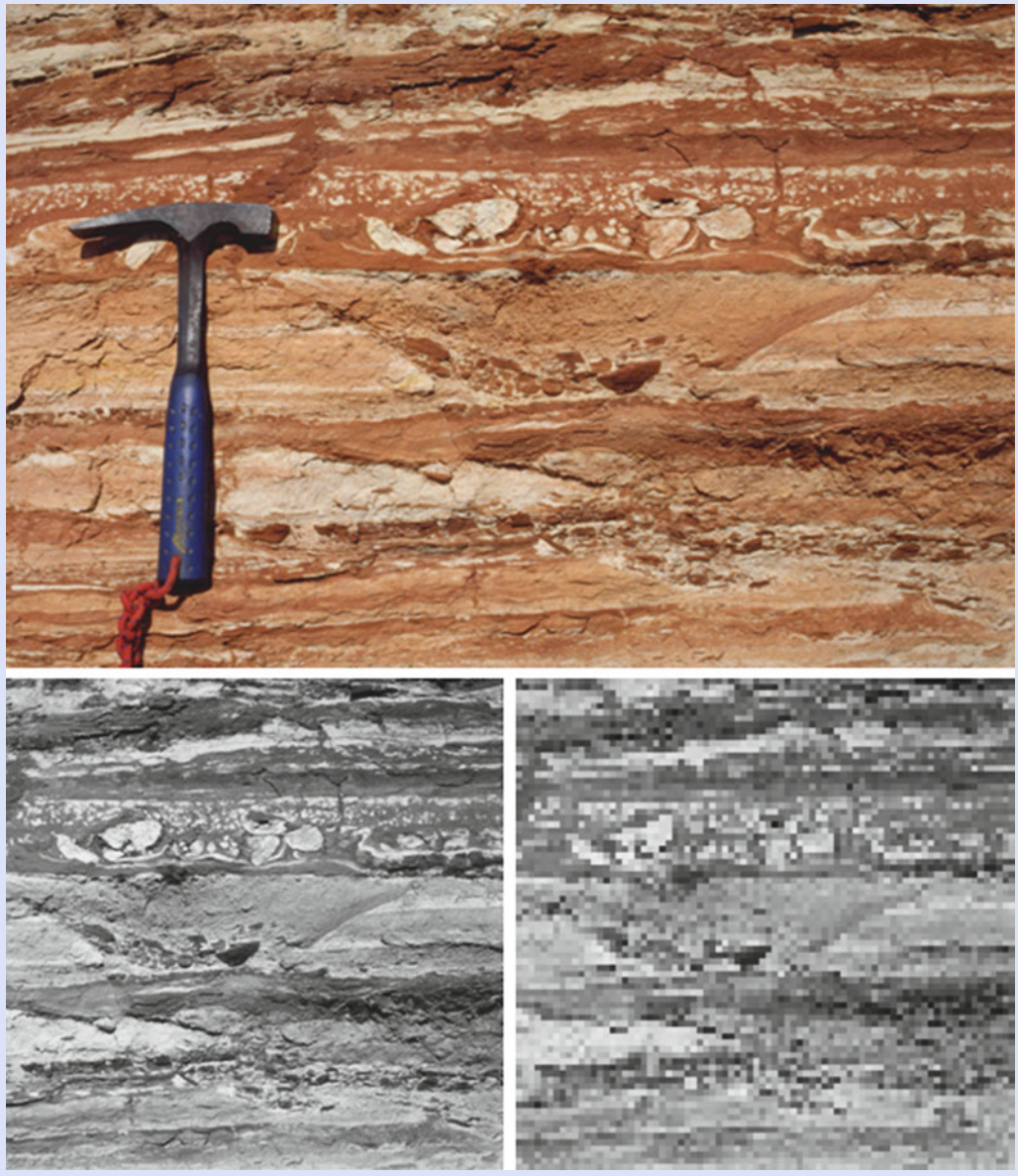

Grey scale image is 22.5 × 22.5 cm; pixelated grey-scale image is 55 by 55 pixels

2.7 Algorithm Choice and Control

The preceding sections presented the basis for the design of the rock modelling process:

- Form geological concepts and decide whether rock modelling is required;
- Select the model elements;
- Set the balance between determinism and probability;
- Intuitively set parameters to guide the geostatistical modelling process, consistent with the architectural concepts.

The next step is to select an algorithm and decide what controls are required to move beyond the default settings that all software packages offer. Algorithms can be broadly grouped into three classes:

– *Object modelling* places bodies with discrete shapes in 3D space for which another model element, or group of elements, has been defined as the background.
– *Pixel-based methods* use indicator variograms to create the model architecture by assigning the model element type on a cell-by-cell basis. The indicator variable is simply a variogram that has been adapted for discrete variables. There are several variants of pixel modelling including sequential indicator simulation (SIS), indicator kriging and various facies trend or facies belt methods which attempt to capture gradational lateral facies changes. The most common approach is the SIS method.
– *Texture-based methods* use training images to recreate the desired architecture. Although this has been experimented with since the early days of reservoir modelling this has only recently 'come of age' through the development of multi-point statistical (MPS) algorithms (Strebelle 2002).

The pros and cons of these algorithms, including some common pitfalls, are explored below.

2.7.1 Object Modelling

Object modelling uses various adaptations of the 'marked point process' (Holden et al. 1998). A position in the 3D volume, the marked point, is selected at random. To this point the geometry of the object (ellipse, half moon, channel etc.) is assigned. The main inputs for object modelling are an upscaled element log, a shape template and a set of geometrical parameter distributions such as width, orientation and body thickness, derived from outcrop data (e.g. Fig. 2.32).

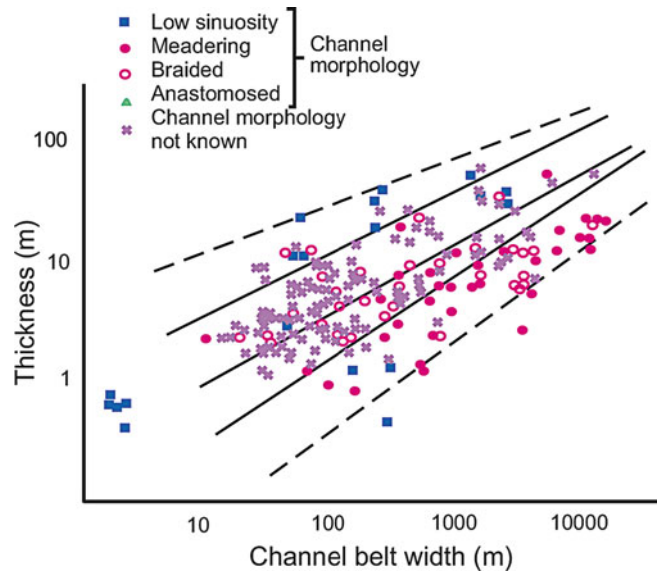

Fig. 2.32 An early example of outcrop-derived data used to define geometries in object models (Fielding and Crane 1987) (Redrawn from Fielding and Crane 1987, © SEPM Society for Sedimentary Geology [1987], reproduced with permission)

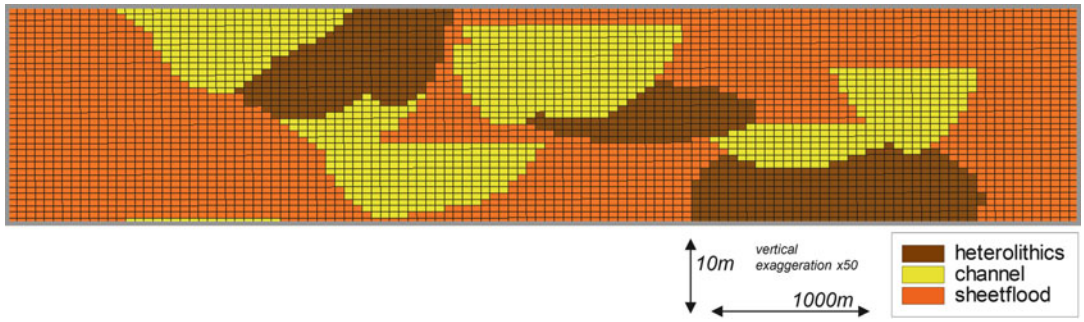

Fig. 2.33 Cross section through the 'Moray Field' model, an outcrop-based model through Triassic fluvial clastics in NE Scotland. Figures 2.35, 2.36, 2.38 and 2.39 follow the same section line through the models and each model is conditioned to the same well data, differing only in the selection of rock modelling algorithm

The algorithms work by selecting objects from the prescribed distribution and then rejecting objects which do not satisfy the well constraints (in statistics, the 'prior model'). For example, a channel object which does not intersect an observed channel in a well is rejected. This process continues iteratively until an acceptable match is reached, constrained by the expected total volume fraction of the object, e.g. 30 % channels. Objects that do not intersect the wells are also simulated if needed to achieve the specified element proportions. However, spatial trends of element abundance or changing body thickness are not automatically honoured because most algorithms assume stationarity (no interwell trends). Erosional, or intersection, rules are applied so that an object with highest priority can replace previously simulated objects (Fig. 2.33).

There are issues of concern with object modelling which require user control and awareness of the algorithm limitations. Firstly, it is important to appreciate that the algorithm can generate bodies that cross multiple wells if intervals of the requisite element appear at the right depth intervals in the well. That is, the algorithm can generate probabilistic correlations without user guidance – something that may or may not be desirable. Some algorithms allow the user to control multiple well intersections of the same object but this is not yet commonplace.

Secondly, the distribution of objects at the wells does not influence the distribution of inter-well objects because of the assumption of stationarity in the algorithm. Channel morphologies are particularly hard to control because trend maps only affect the location of the control point for the channel object and not the rest of the body, which generally extends throughout the model. A key issue with object modelling, therefore, is that things can easily go awry in the inter-well area. Figure 2.34 shows an example of 'funnelling', in which the algorithm has found it difficult to position channel bodies without hitting wells with no channel observations; the channels have therefore been preferentially funnelled into the inter-well area. Again, some intuitive geological sense is required to control and if necessary reject model outcomes. The issue illustrated in Fig. 2.34 can easily be exposed by making a net sand map of the interval and looking for bulls-eyes around the wells.

Thirdly, the element proportions of the final model do *not* necessarily give guidance as to the quality of the model. Many users compare the element ('facies') proportions of the model with those seen in the wells as a quantitative check on the result, but matching the well intersections is the main statistical objective of the algorithm so there is a circular logic to this type of QC. The key thing to check is the degree of 'well match' *and* the spatial distributions *and* the total element proportions (together). Repeated mismatches or anomalous patterns point to inconsistencies between wells, geometries and element proportions.

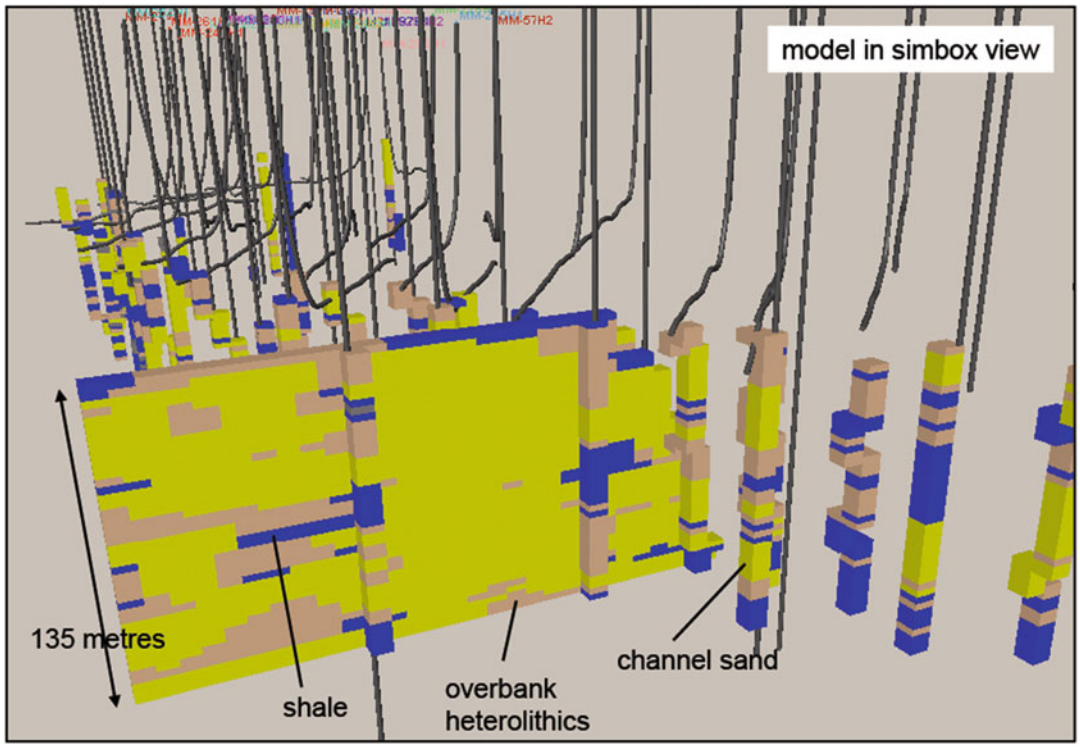

Fig. 2.34 'Funnelling' – over-concentration of objects (channels, *yellow*) in between wells which have lower concentrations of those objects; a result of inconsistencies between well data, guidance of the model statistics and the model concept (Image courtesy of Simon Smith)

Moreover, it is highly unlikely that the element proportions seen in the wells truly represent the distribution in the subsurface as the wells dramatically under-sample the reservoir. It is always useful to check the model element distributions against the well proportions, and the differences should be explainable, but differences should be expected. The 'right' element proportion is the one which matches the underlying concept.

The following list of observations and tips provides a useful checklist for compiling body geometries in object modelling:

1. Do not rely on the default geometries.
2. Remember that thickness distributions have to be customised for the reservoir. The upscaled facies parameter includes *measured* thickness from deviated wells – they are not stratigraphic thicknesses.
3. Spend some time customising the datasets and collating your own data from analogues. There are a number of excellent data sources available to support this; they do not provide instant answers but do give good guidance on realistic *preserved* body geometries.
4. The obvious object shape to select for a given element is not always the best to use. Channels are a good example of this, as the architecture of a channel belt is sometimes better constructed using ellipse- or crescent-shaped objects rather than channel objects *per se*. These body shapes are less extensive than the channel shapes, rarely go all the way through a model area and so reflect the trend map inputs more closely and are less prone to the 'bull's eye' effect.
5. There may be large differences between the geometry of a modern feature and that preserved in the rock record. River channels are a good example: the geomorphological expression of a modern river is typically much narrower and more sinuous that the geometry of the sand body that is preserved. This is

because the channels have a component of lateral migration and deposit a broader and lower sinuosity belt of sands as they do so. Carbonate reservoirs offer a more extreme example of this as any original depositional architecture can be completely overprinted by subsequent diagenetic effects. Differential compaction effects may also change the vertical geometry of the original sediment body.

6. Do not confuse uncertainty with variability. Uncertainty about the most appropriate analogue may result in a wide spread of geometrical constraints. It is incorrect, however, to combine different analogue datasets and so create spuriously large amounts of variation. It is better to make two scenarios using different data sets and then quantify the differences between them.
7. Get as much information as possible from the wells and the seismic data sets. Do well correlations constrain the geometries that can be used? Is there useful information in the seismic?
8. We will never know what geometries are correct. The best we can do is to use our conceptual models of the reservoir to select a series of different analogues that span a plausible range of geological uncertainty and quantify the impact. This is pursued further in Chap. 5.

2.7.2 Pixel-Based Modelling

Pixel-based modelling is a fundamentally different approach, based on assigning properties using geostatistical algorithms on a cell-by-cell basis, rather than by implanting objects in 3D. It can be achieved using a number of algorithms, the commonest of which are summarised below.

2.7.2.1 Indicator Kriging

Kriging is the most basic form of interpolation used in geostatistics, developed by the French mathematician Georges Matheron and his student Daniel Krige (Matheron 1963). The technique is applicable to property modelling (next chapter) but rock models can also be made using an adaptation of the algorithm called *Indicator Kriging*.

The algorithm attempts to minimise the estimation error at each point in the model grid. This means the most likely element at each location is estimated using the well data and the variogram model – there is no random sampling. Models made with indicator kriging typically show smooth trends away from the wells, and the wells themselves are often highly visible as 'bulls-eyes'. These models will have different element proportions to the wells because the algorithm does not attempt to match those proportions to the frequency distribution at the wells. Indicator kriging can be useful for capturing lateral trends *if* these are well represented in the well data set, or mimicking correlations between wells.

In general, it is a poor method for representing reservoir heterogeneity because the heterogeneity in the resulting model is too heavily influenced by the well spacing. For fields with dense, regularly-spaced wells and relatively long correlation lengths in the parameter being modelling, it may still be useful.

Figure 2.35 shows an example of indicator Kriging applied to the Moray data set – it is first and foremost an interpolation tool.

2.7.2.2 Sequential Indicator Simulation (SIS)

Sequential Gaussian Simulation, SGS is most commonly used for modelling continuous petrophysical properties (Sect. 3.4), but one variant, Sequential Indicator Simulation (SIS), is quite commonly used for rock modelling (Journel and Alabert 1990). SIS builds on the underlying geostatistical method of kriging, but then introduces heterogeneity using a sequential stochastic method to draw Gaussian realisations using an indicator transform. The indictor is used to transform a continuous distribution to a discrete distribution (e.g. element 1 vs. element 2).

When applied to rock modelling, SIS will generally assume the reservoir shows no lateral or vertical trends of element distribution – the principle of stationarity again – although trends can be superimposed on the simulation (see the important comment on trends at the end of this section).

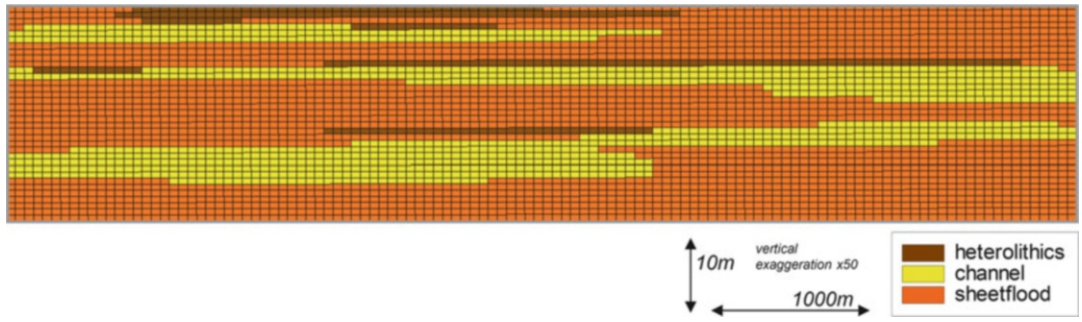

Fig. 2.35 Rock modelling using indicator kriging

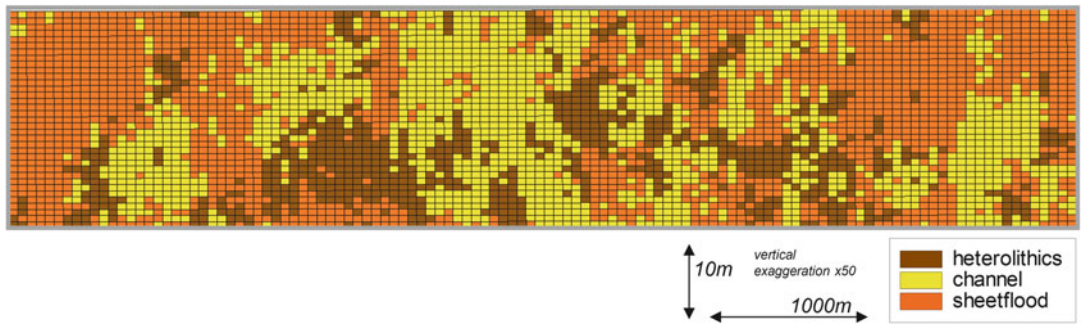

Fig. 2.36 Rock modelling using SIS

Models built with SIS should, by definition, honour the input element proportions from wells, and each geostatistical realisation will differ when different random seeds are used. Only when large ranges or trends are introduced will an SIS realisation differ from the input well data.

The main limitation with such pixel-based methods is that it is difficult to build architectures with well-defined margins and discrete shapes because the geostatistical algorithms tend to create smoothly-varying fields (e.g. Fig. 2.36). Pixel-based methods tend to generate models with limited linear trends, controlled by the principal axes of the variogram. Where the rock units have discrete, well-defined geometries or they have a range of orientations (e.g. radial patterns), object-based methods are preferable to SIS.

SIS is useful where the reservoir elements do not have discrete geometries either because they have irregular shapes or variable sizes. SIS also gives good models in reservoirs with many closely-spaced wells and many well-to-well correlations. The method is more robust than object modelling for handling complex well-conditioning cases and the funnelling effect is avoided. The method also avoids the bulls-eyes around wells which are common in Indicator Kriging.

The algorithm can be used to create correlations by adjusting the variogram range to be greater than the well spacing. In the example in Fig. 2.37, correlated shales (shown in blue) have been modelled using SIS. These correlations contain a probabilistic component, will vary from realisation to realisation and will not necessarily create 100 % presence of the modelled element between wells. Depending on the underlying concept, this may be desirable.

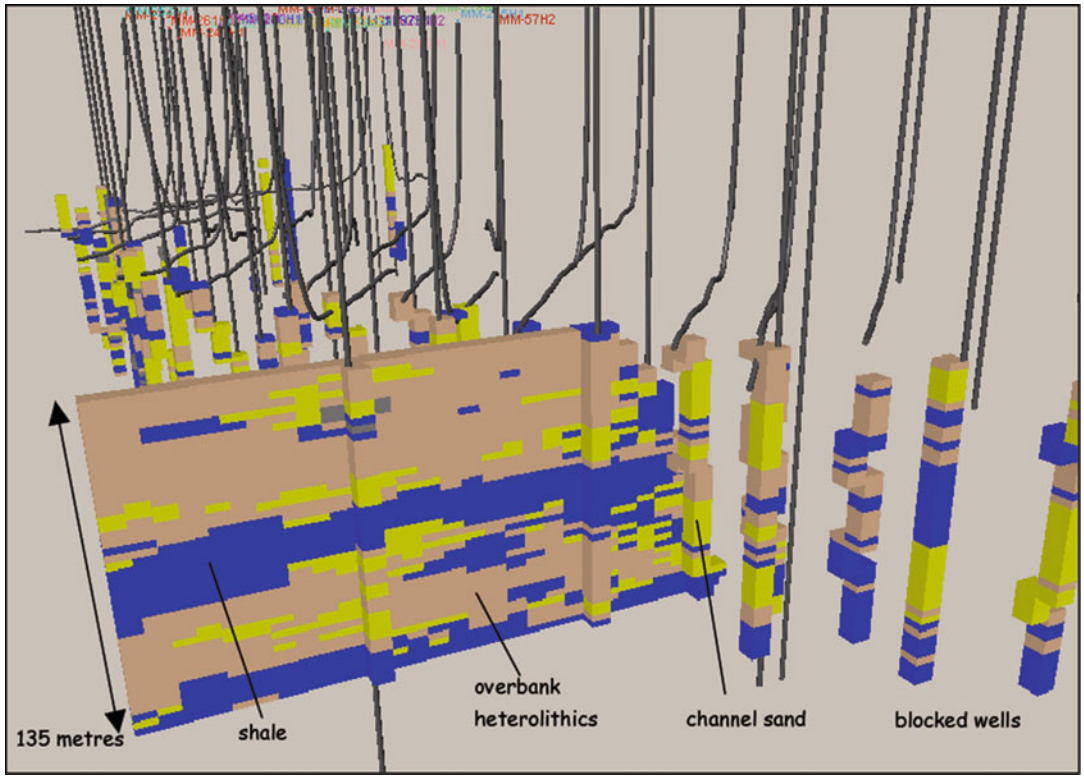

Fig. 2.37 Creating correlatable shale bodies (shown in *blue*) in a fluvial system using SIS (Image courtesy of Simon Smith)

When using the SIS method as commonly applied in commercial packages, we need to be aware of the following:

1. Reservoir data is generally statistically insufficient and rarely enough to derive meaningful experimental variograms. This means that the variogram used in the SIS modelling must be derived by intuitive reasoning (see previous section).
2. The range of the variogram is not the same as the element body size. The range is related to the *maximum* body size, and actual simulated bodies can have sizes anywhere along the slope of the variogram function. The range should therefore *always* be set larger than your expected average body size, as a rule of thumb – twice the size.
3. The choice of the type of kriging used to start the process off can have a big effect. For simple kriging a universal mean is used and the algorithm assumes stationarity. For ordinary kriging the mean is estimated locally throughout the model, and consequently allows lateral trends to be captured. Ordinary kriging works well with large numbers of wells and well-defined trends, but can produce unusual results with small data sets.
4. Some packages allow the user to specify local azimuths for the variogram. This information can come from the underlying architectural concept and can be a useful way of avoiding the regular linear striping which is typical for indicator models, especially those conditioned to only a small number of wells.

2.7.2.3 Facies Trend Algorithms

The facies trend simulation algorithm is a modified version of SIS which attempts to honour a logical lateral arrangement of elements,

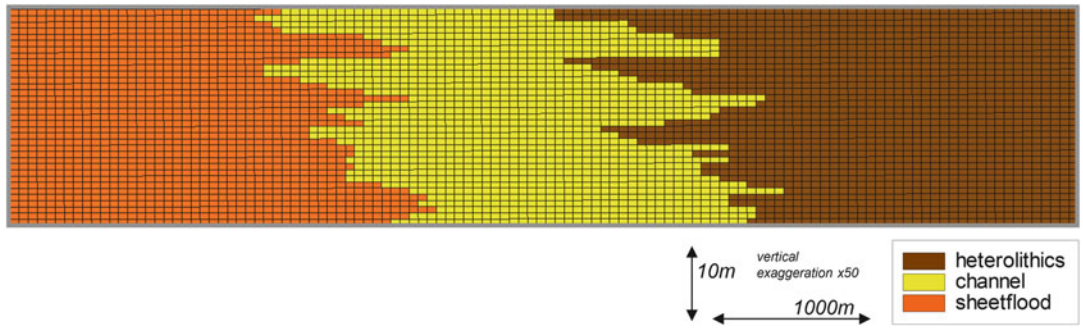

Fig. 2.38 Rock modelling using facies trend simulation

for example, an upper shoreface passing laterally into a lower shoreface and then into shale.

Figure 2.38 shows an example applied to the Moray data set. The facies trend approach, because it uses SIS, gives a more heterogeneous pattern than indicator kriging and does not suffer from the problem of well bulls-eyes. The latter is because the well data is honoured at the well position, but not necessarily in the area local to the well.

The user can specify stacking patterns, directions, angles and the degree of inter-fingering. The approach can be useful, but it is often very hard to get the desired inter-fingering throughout the model. The best applications tend to be shoreface environments where the logical sequence of elements, upper to lower shoreface, transition on a large scale. Similar modelling effects can also be achieved by the manual application of trends (see below).

2.7.3 Texture-Based Modelling

A relatively new development is the emergence of algorithms which aim to honour texture directly. Although there are parallels with very early techniques such as simulated annealing (Yarus and Chambers 1994, Ch. 1 by Srivistava) the approach has become more widely available through the multi-point statistics (MPS) algorithm (Strebelle 2002; Caers 2003).

The approach starts with a pre-existing training image, typically a cellular model, which is analysed for textural content. Using a geometric template, the frequency of instances of a model element occurring next to similar and different elements are recorded, as is their relative position (to the west, the east, diagonally etc.). As the cellular model framework is sequentially filled, the record of textural content in the training image is referred to in order to determine the likelihood of a particular cell having a particular model content, given the content of the surrounding cells.

Although the approach is pixel-based, the key step forward is the emphasis on potentially complex texture rather than relatively simple geostatistical rules. The term 'multi-point' statistics compares with the 'two-point' statistics of variography. The prime limitation of variogram-based approaches – the need to derive simple rules for *average* spatial correlation – is therefore surmounted by modelling instead an average texture.

In principle, MPS offers the most appropriate algorithm for building 3D reservoir architecture, because architecture itself is a heterogeneous textural feature and MPS is designed to model heterogeneous textures directly.

In spite of this there are two reasons why MPS is not necessarily the algorithm of choice:

1. A training image is required, and this is a 3D architectural product in itself. MPS models are therefore not as 'instantaneous' as the simpler pixel-based techniques such as SIS, and require more pre-work. The example shown in Fig. 2.39 was built using a training data set which was itself extracted from a

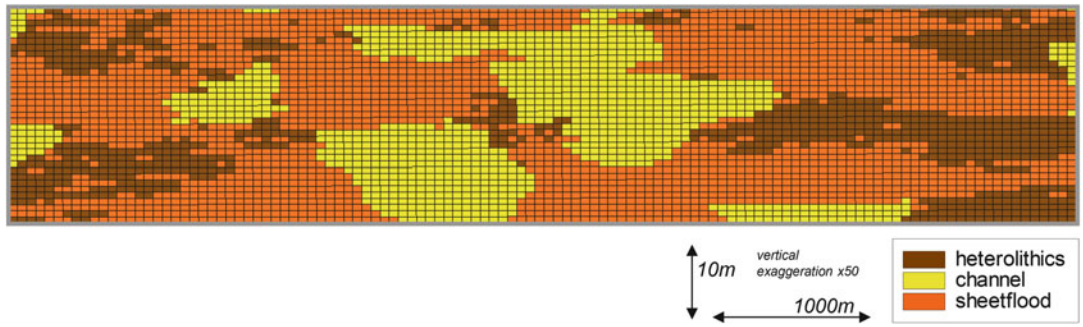

Fig. 2.39 Rock modelling using MPS

model combining object- and SIS-based architectural elements. The MPS algorithm did not 'work alone.'

2. The additional effort of generating and checking a training image may not be required in order to generate the desired architecture.

Despite the above, the technique can provide very realistic-looking architectures which overcome both the simplistic textures of older pixel-based techniques and the simplistic shapes and sometimes unrealistic architectures produced by object modelling.

2.7.4 The Importance of Deterministic Trends

All of the algorithms above involve a probabilistic component. In Sect. 2.5 the balance between determinism and probability was discussed and it was proposed that strong deterministic control is generally required to realise the desired architectural concept.

Having discussed the pros and cons of the algorithms, the final consideration is therefore how to overlay deterministic control. In statistical terms, this is about overcoming the *stationarity* that probabilistic algorithms assume as a default. Stationarity is a prerequisite for the algorithms and assumes that elements are randomly but homogeneously distributed in the inter-well space. This is at odds with geological systems, in which elements are heterogeneously distributed and show significant non-stationarity: they are commonly clustered and show patterns in their distribution. Non-stationarity is the geological norm, indeed, *Walther's Law* – the principle that vertical sequences can be used to predict lateral sequences – is a statement of non-stationarity.

Deterministic trends are therefore *required*, whether to build a model using object- or pixel-based techniques, or to build a training image for a texture-based technique.

2.7.4.1 Vertical Trends

Sedimentary systems typically show vertical organisation of elements which can be observed in core and on logs and examined quantitatively in the data-handling areas of modelling packages. Any such vertical trends are typically switched *off* by default – the assumption of stationarity.

As a first assumption, observed trends in the form of vertical probability curves, should be switched *on*, unless there are compelling reasons not to use them. More significantly, these trends can be manually adjusted to help realise an architectural concept perhaps only partly captured in the raw well data.

Figure 2.40 shows an edited vertical element distribution which represents a concept of a depositional system becoming sand-prone upwards. This is a simple pattern, common in sedimentary sequences, but will not be integrated in the modelling process by default.

Thought is required when adjusting these profiles because the model is being consciously steered away from the statistics of the well data. Unless the well data is a perfect statistical sample

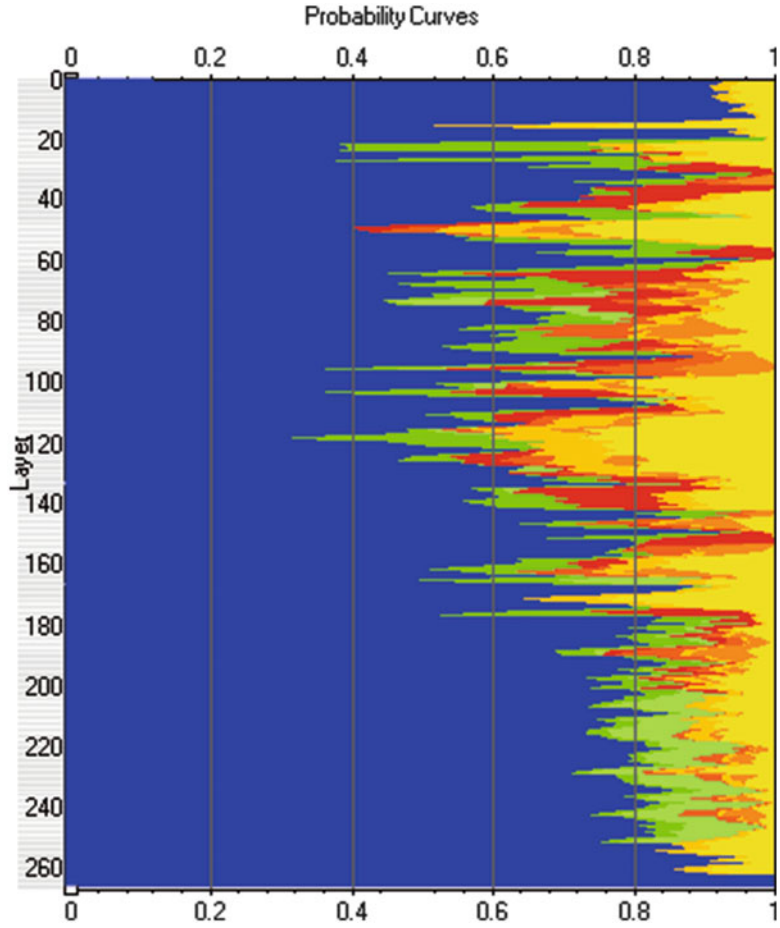

Fig. 2.40 Vertical probability trends; each colour represents a different reservoir element and the probability represents the likelihood of that element occurring at that point in the cell stratigraphy (*blue* = mudstone; *yellow* = sandstone)

of the reservoir (rarely the case and never provable) this is not a problem, but the modeller should be aware that hydrocarbon volumes are effectively being adjusted up and down away from well control. The adjustments therefore require justification which comes, as ever, from the underlying conceptual model.

2.7.4.2 Horizontal Trends

Horizontal trends are mostly simply introduced as 2D maps which can be applied to a given interval. Figure 2.41 shows the application of a sand trend map to a low net-to-gross system following the steps below:

1. Sand elements are identified in wells based on core and log interpretation;
2. A net-to-gross (sand) value is extracted at each well and gridded in 2D to produce a map illustrating any sand trend apparent from well data alone;
3. The 2D map is hand-edited to represent the desired concept, with most attention being paid to the most poorly sampled areas (in the example shown, the trend grid is also smoothed – the level of detail in the trend map should match the resolution of the sand distribution concept);
4. The trend map is input to, in this case, an SIS algorithm for rock modelling;
5. As a check, the interval average net-to-gross is backed-out of the model as a map and compared with the concept. The map shows more heterogeneity because the variogram ranges have been set low and the model has been tied to the actual well observations; the desired deterministic trends, however, clearly control the overall pattern.

The influence of the trend on the model is profound in this case as the concept is for the sand system to finger eastwards into a poorly drilled, mud-dominated environment. The oil

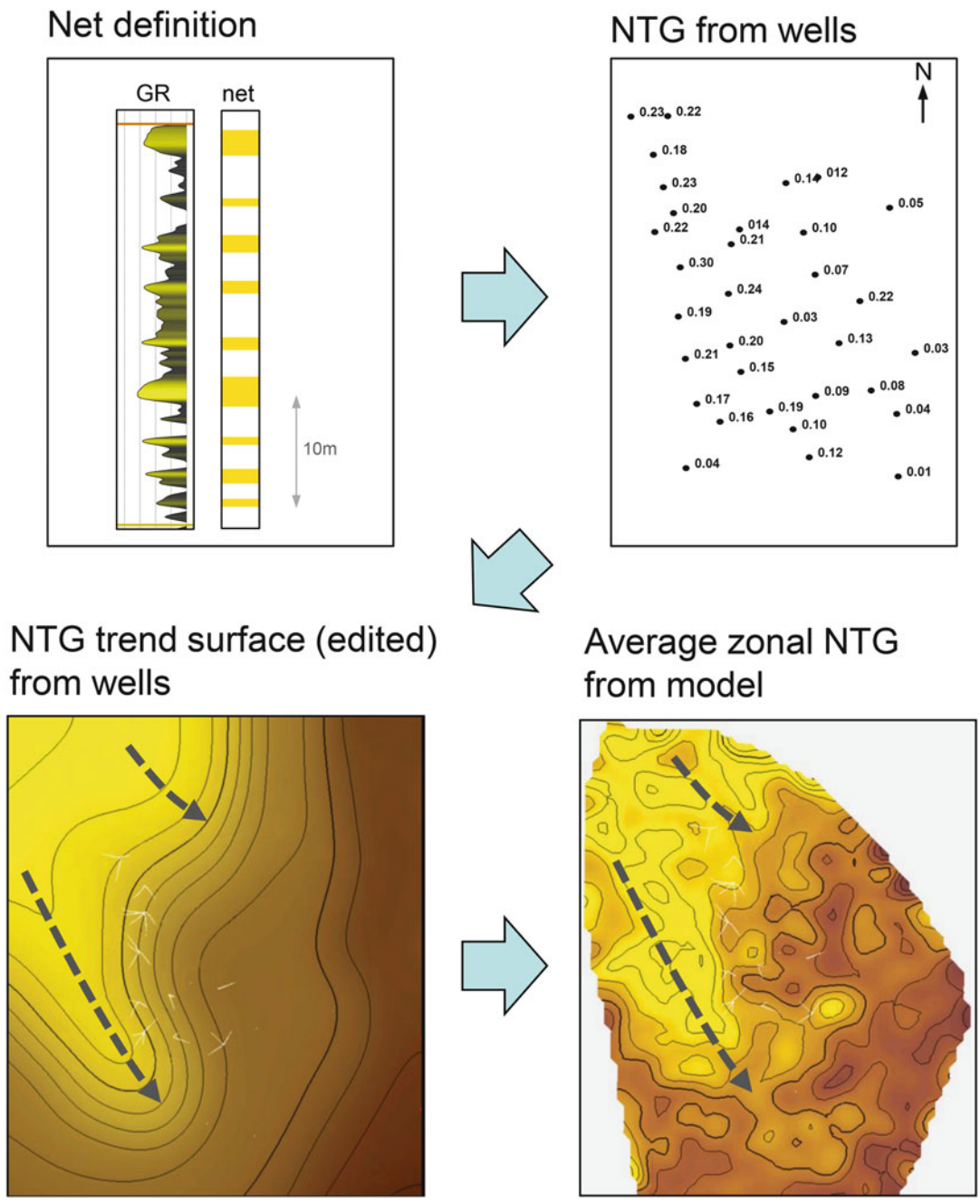

Fig. 2.41 Deterministic application of a horizontal trend

volumes in the trended case are half that calculated for a model with the trends removed, with all other model variables unchanged. Stationarity is overcome and the concept dominates the modelling.

The source of the trend can be an extension of the underlying data, as in the example above, or a less data-independent concept based on a regional model, or a trend surface derived from seismic attributes – the 'soft conditioning' described in Sect. 2.5.

2.7.4.3 3D Probability Volumes

The 3D architecture can be directly conditioned using a 3D volume – a natural extension of the process above. The conditioning volume can be built in a modelling exercise as a combination of

the horizontal/vertical trends described above, or derived from a 3D data source, typically a seismic volume.

Seismic conditioning directly in 3D raises some issues:

1. The volume needs QC. It is generally easier to check simpler data elements, so if the desired trends are separately captured in 2D trend surfaces and vertical proportion curves then combination into a 3D trend volume is not necessary.
2. If conditioning to a 3D seismic volume, the resolution of the model framework needs to be consistent with the intervals the seismic attribute is derived from. For example, if the parameter being conditioned is the sand content within a 25 m thick interval, it must be assumed that the seismic data from which the seismic attribute is derived is also coming from that 25 m interval. This is unlikely to be the case from a simple amplitude extraction and a better approach is to condition from inverted seismic data. The questions to ask are therefore what the seismic inversion process was inverting for (was it indeed the sand content) and, crucially, was the earth model used for the inversion the same one as the reservoir model is being built on?
3. If the criteria for using 3D seismic data (2, above) are met, can a probabilistic seismic inversion be called upon? This is the ideal input to condition to.
4. If the criteria in point 2, above, are not met, the seismic can still be used for soft conditioning, but will be more artefact-free and easier to QC if applied as a 2D trend. The noisier the data, the softer the conditioning will need to be, i.e. the lower the correlation coefficient.

2.7.5 Alternative Rock Modelling Methods – A Comparison

So which algorithm is the one to use? It will be the one that best reflects the starting concept – the architectural sketch – and this may require the application of more than one algorithm, and almost certainly the application of deterministic trends.

To illustrate this, an example is given below, to which alternative algorithms have been applied. The case is taken from a fluvio-deltaic reservoir – the Franken Field – based on a type log with a well-defined conceptual geological model (Fig. 2.42). The main reservoir is the Shelley, which divides into a clearly fluvial Lower Shelley characterised by sheetfloods, and an Upper Shelley, the sedimentology for which is less clear and can be viewed as either a lower coastal plain or a river-dominated delta.

Rock model realisations have been built from element distributions in 19 wells. Cross-sections taken at the same location through the models are illustrated in Figs. 2.43, 2.44 and 2.45 for a 2-, 4- and 7-interval correlation, respectively. The examples within each layering scheme explore object vs. pixel (SIS) modelling and the default model criteria (stationarity maintained) vs. the use of deterministic trends (stationarity overwritten).

The models contrast greatly and the following observations can be made:

1. The more heavily subdivided models are naturally more ‘stripey’. This is partly due to the ‘binning’ of element well picks into zones, which starts to break down stationarity by picking up any systematic vertical organisation of the elements, irrespective of the algorithm chosen and without separate application of vertical trends.
2. The stripey architecture is further enhanced in the 7-zone model because the layering is based on a flooding surface model, the unit boundaries for which are preferentially picked on shales. The unit boundaries are therefore shale-rich by definition and prone to generating correlatable shales if the shale dimension is big enough (for object modelling) or shale variogram range is long enough (for SIS).
3. Across all frameworks, the object-based models are consistently more ‘lumpy’ and the SIS-based models consistently more ‘spotty’, a consequence of the difference between the algorithms described in the sections above.

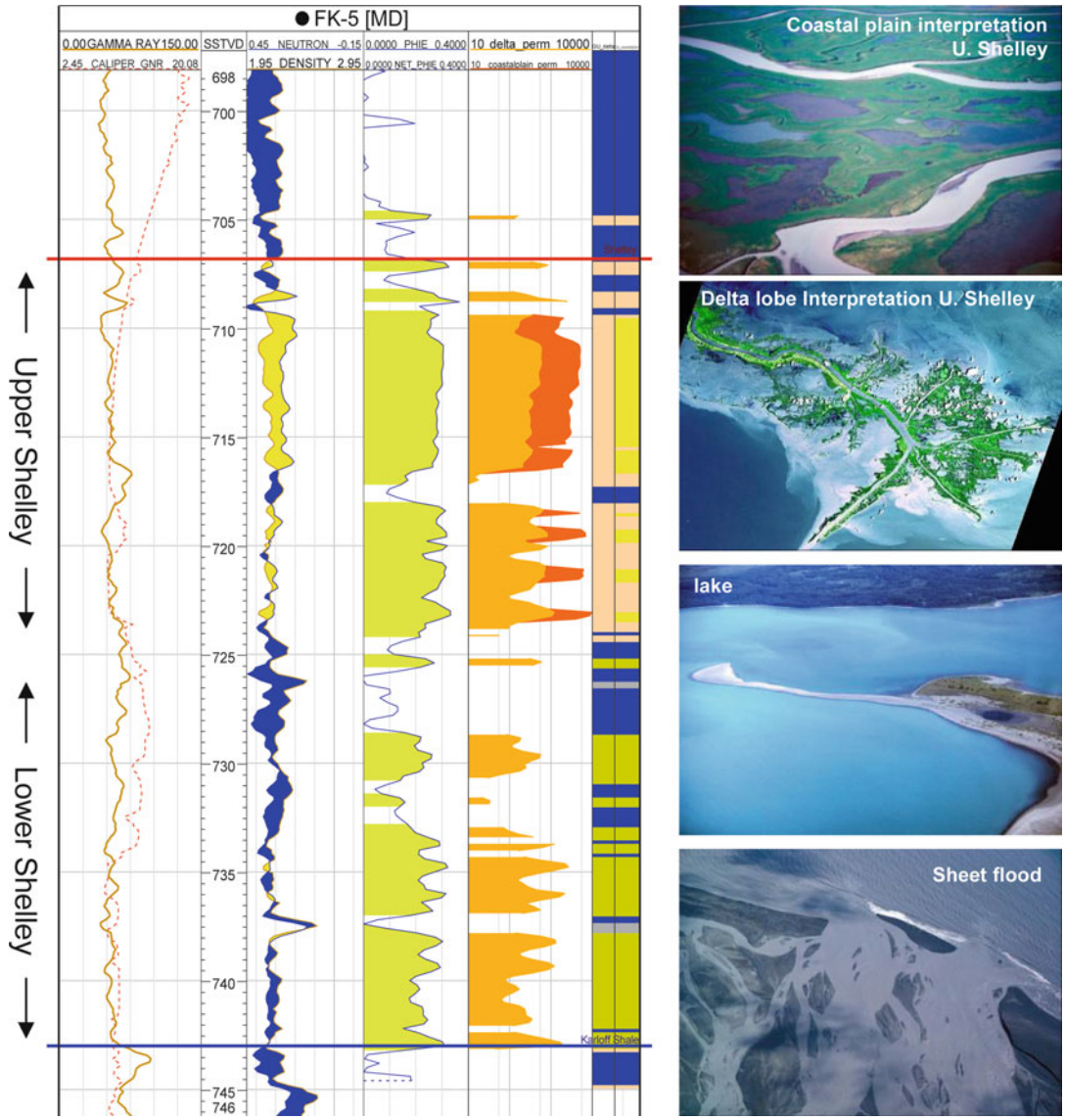

Fig. 2.42 The Franken Field reservoir – type log and proposed depositional environment analogues. The model elements are shown on the *right-hand coloured* logs, one of which is associated with a delta interpretation for the Upper Shelley, the other for an alternative coastal plain model for the Upper Shelley. Sands are marked in *yellow*, muds in *blue*, intermediate lithologies in intermediate colours (Image courtesy of Simon Smith)

4. The untrended object model for the two zone realisation is the one most dominated by stationarity, and looks the least realistic geologically.
5. The addition of deterministic trends, both vertical and lateral, creates more ordered, less random-looking models, as the assumption of stationarity is overridden by the conceptual model.

Any of above models presented in Figs. 2.43, 2.44, and 2.45 could be offered as a 'best guess', and could be supported at least superficially with an appropriate story line. Presenting multiple models using different layering schemes and alternative algorithms also appears thorough and in a peer-review it would be hard to know whether these models are 'good' or 'bad' representations of the reservoir. However, a

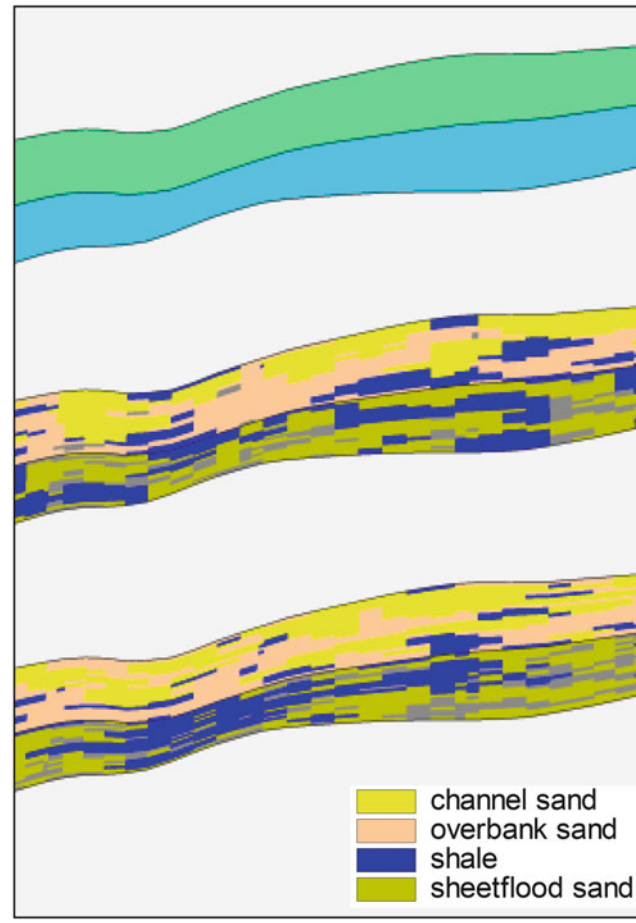

Fig. 2.43 The Franken Field. *Top image*: the two zone subdivision; *middle image*: object model (no trends applied, stationarity maintained); *bottom image*: trended object model

number of the models were made quickly using system defaults and have little substance; stationarity (within zones) is dominant and although the models are statistically valid, they lack an underlying concept and have poor deterministic control. Only the lower models in each Figure take account of the trends associated with the underlying reservoir concept, and it is these which are the superior representations – at least matching the quality of the conceptual interpretation.

The main point to take away from this example is that all the models match the well data and no mechanical modelling errors have been made in their construction, yet the models differ drastically. The comparison reinforces the importance of the underlying reservoir concept as the tool for assessing which of the resulting rock models are acceptable representations of the reservoir.

2.8 Summary

In this chapter we have offered an overview of approaches to rock modelling and reviewed a range of geostatistically-based methods, whilst holding the balance between probability and determinism and the primacy of the underlying concept as the core issues. Reservoir modelling is not simply a process of applying numerical tools to the available dataset – there is always an element of subjective design involved. Overall the rock model must make geological sense and to

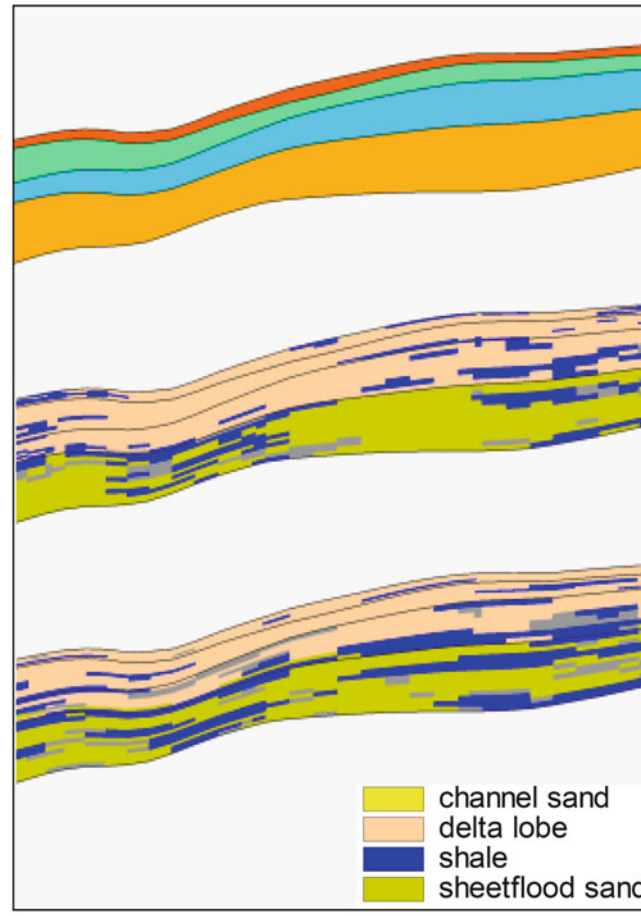

Fig. 2.44 The Franken Field: *Top image*: the four zone subdivision; *middle image*: pixel (SIS) model (no trends applied, stationarity maintained); *bottom image*: trended pixel (SIS) model

summarise this, we offer a brief resume of practical things which can be done to check the quality of the rock model – the QC process.

2.8.1 Sense Checking the Rock Model

(a) Make architectural sketches along depositional strike and dip showing the key features of the conceptual models. During the model build switch the model display to stratigraphic (*simbox)* view to remove the structural deformation. How do the models compare with the sketches?

(b) Watch out for the individual well matches – well by well. These are more useful and diagnostic than the overall 'facies' proportions. Anomalous wells point to weaknesses in the model execution.

(c) Make element proportion maps for each element in each zone and check these against well data and the overall concept. This is an important check on the inter-well probabilistic process.

(d) Check the statistics of the modelled element distribution against that for the well data alone; they should not necessarily be the same, but the differences should be explicable in terms of any applied trends and the spatial location of the wells.

(e) Make net sand isochore maps for each zone without wells posted; imposed trends should be visible and the well locations should not (no bulls-eyes around wells).

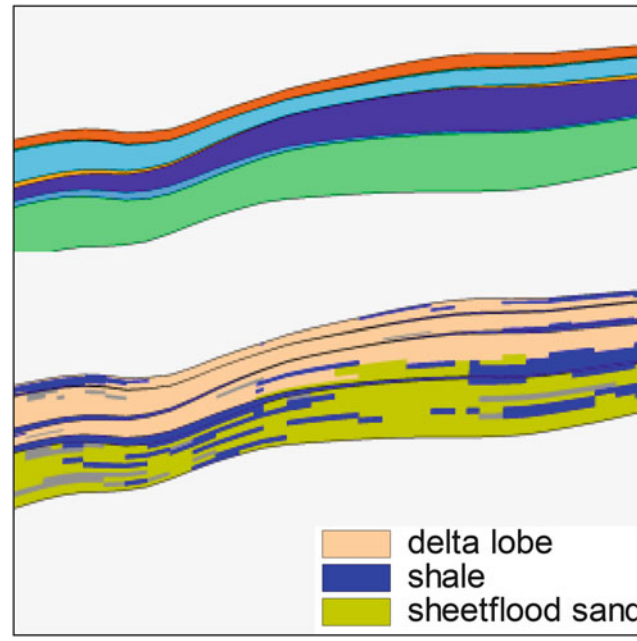

Fig. 2.45 The Franken Field: *Top image*: the seven zone subdivision; *bottom image*: trended SIS model

(f) Make full use of the visualisation tools, especially the ability to scroll through the model vertically, layer by layer, to look for anomalous geometries, e.g. spikes and pinch-outs.

2.8.2 Synopsis – Rock Modelling Guidelines

The first decision to be made is whether or not a rock model is truly required. If rock modelling can add important controls to the desired distribution of reservoir properties, then it is clearly needed. If, however, the desired property distributions can be achieved directly by property modelling, then rock modelling is probably not necessary at all.

If it is decided that a rock model is required, it then needs some thought and design. The use of system default values is unlikely to be successful.

This chapter has attempted to stress the following things:

1. The *model concept* needs to be formed before the modelling begins, otherwise the modeller is 'flying blind'. A simple way of checking your (or someone else's) grasp of the conceptual reservoir model is to make a sketch section of the reservoir, or request a sketch, showing the desired architecture.
2. The model concept needs to be expressed in terms of the chosen *modelling elements*, the selection of which is based on not only a consideration of the heterogeneity, but with a view to the fluid type and production mechanism. Some fluid types are more sensitive to heterogeneity than others; if the fluid molecules do not sense the heterogeneity, there is no need to model it – this is 'Flora's Rule.'
3. Rock models are mixtures of *deterministic* and *probabilistic* inputs. Well data tends to be statistically insufficient, so attempts to extract statistical models from the well data are often not successful. The road to happiness therefore generally lies with strong deterministic control, as determinism is the most direct method of carrying the underlying reservoir concept into the model.
4. To achieve the desired reservoir architecture, the *variogram model* has a leading influence if pixel-based methods are employed. Arguably the *variogram range* is the most important geostatistical input.

5. To get a reasonable representation of the model concept it is generally necessary to impose *trends* (vertical and lateral) on the modelling algorithm, irrespective of the chosen algorithm.
6. Given the above controls on the reservoir model concepts, it is necessary to guide the geostatistical algorithms during a rock model build using an intuitive understanding of the relationship between the underlying reservoir concept and the geostatistical rules which guide the chosen algorithm.
7. It is unlikely that the element proportions in the model will match those seen in the wells – do not expect this to be the case; the data and the model are statistically different – more on this in the next section.

References

Ainsworth RB, Sanlung M, Duivenvoorden STC (1999) Correlation techniques, perforation strategies and recovery factors. An integrated 3-D reservoir modeling study, Sirikit Field, Thailand. Am Assoc Petrol Geol Bull 83(10):1535–1551

Bentley MR, Elliott AA (2008) Modelling flow along fault damage zones in a sandstone reservoir: an unconventional modelling technique using conventional modelling tools in the Douglas Field Irish Sea UK. SPE paper 113958 presented at SPE Europec/EAGE conference and exhibition. Society of Petroleum Engineers (SPE) doi:10.2118/113958-MS

Caers J (2003) History matching under training-image-based geological model constraints. SPE J 8(3):218–226

Caers J (2011) Modeling uncertainty in the earth sciences. Wiley, Hoboken

Campbell CV (1967) Lamina, laminaset, bed, bedset. Sedimentology 8:7–26

Deutsch CV (2002) Geostatistical reservoir modeling. Oxford University Press, Oxford, p 376

Doyen PM (2007) Seismic reservoir characterisation. EAGE Publications, Houten

Dubrule O, Damsleth E (2001) Achievements and challenges in petroleum geostatistics. Petrol Geosci 7:1–7

Fielding CR, Crane RC (1987) An application of statistical modelling to the prediction of hydrocarbon recovery factors in fluvial reservoir sequences. Society of Economic Paleontologists and Mineralogists (SEPM) special publication, vol 39

Haldorsen HH, Damsleth E (1990) Stochastic modelling. J Petrol Technol 42:404–412

Holden L, Hauge R, Skare Ø, Skorstad A (1998) Modeling of fluvial reservoirs with object models. Math Geol 30(5):473–496

Isaaks EH, Srivastava RM (1989) Introduction to applied geostatistics. Oxford University Press, Oxford

Jensen JL, Corbett PWM, Pickup GE, Ringrose PS (1995) Permeability semivariograms, geological structure and flow performance. Math Geol 28(4):419–435

Journel AG, Alabert FG (1990) New method for reservoir mapping. J Petrol Technol 42:212–218

Matheron G (1963) Principles of geostatistics. Econ Geol 58:1246–1266

Strebelle S (2002) Conditional simulation of complex geological structures using multiple-point statistics. Math Geol 34(1):1–21

van de Leemput LEC, Bertram DA, Bentley MR, Gelling R (1996) Full-field reservoir modeling of Central Oman gas-condensate fields. SPE Reserv Eng 11(4):252–259

Van Wagoner JC, Bertram GT (eds) (1995) Sequence stratigraphy of Foreland basin deposits. American Association of Petroleum Geologists (AAPG), AAPG Memoir 64:137–224

Van Wagoner JC, Mitchum RM, Campion KM, Rahmanian VD (1990) Siliciclastic sequence stratigraphy in well logs, cores, and outcrops. AAPG methods in exploration series. American Association of Petroleum Geologists (AAPG), vol 7

Yarus JM, Chambers RL (1994) Stochastic modeling and geostatistics principals, methods, and case studies. AAPG computer applications in geology. American Association of Petroleum Geologists (AAPG), vol 3, p 379

The Property Model

3

Abstract

Now let's say you have a beautiful fit-for-purpose rock model of your reservoir – let's open the box and find out what's inside? All too often the properties used within the geo-model are woefully inadequate.

The aim of this chapter is too ensure the properties of your model are also fit-for-purpose and not, like Pandora's box, full of "all the evils of mankind."

Eros warned her not to open the box once Persephone's beauty was inside[. . .] but as she opened the box Psyche fell unconscious upon the ground. (From The Golden Ass by Apuleius.)

P. Ringrose and M. Bentley, *Reservoir Model Design*, DOI 10.1007/978-94-007-5497-3_3,

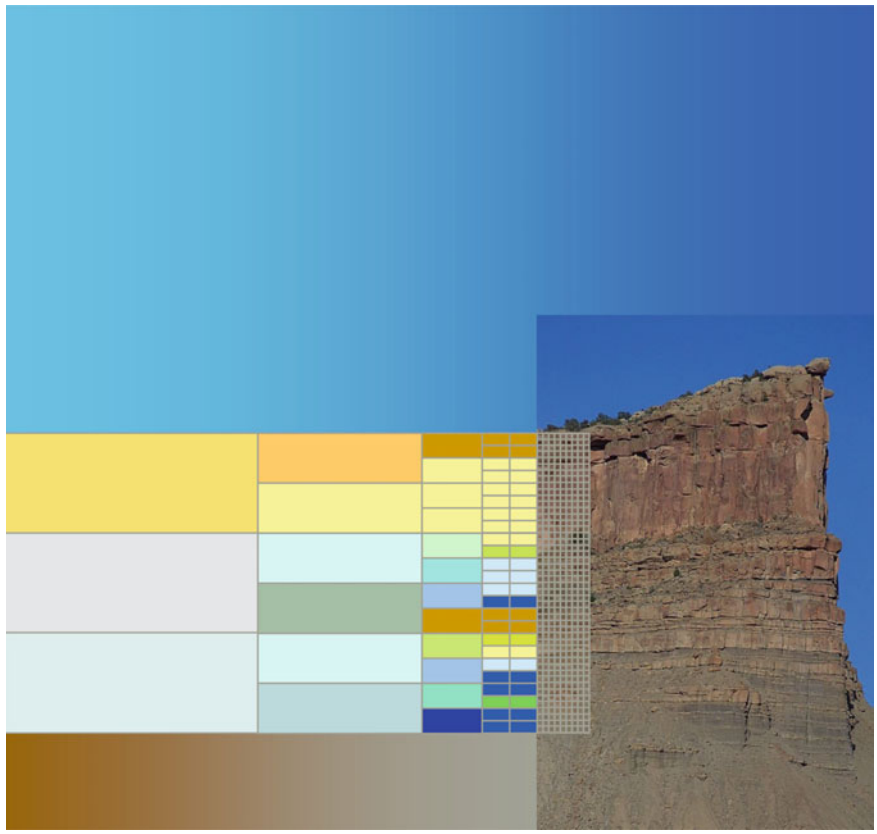

Pixelated rocks

3.1 Which Properties?

First let us recall the purpose of building a reservoir model in the first place. We propose that the overall aim in reservoir model design is:

> *To capture knowledge of the subsurface in a quantitative form in order to evaluate and engineer the reservoir.*

This definition combines knowledge capture, the process of collecting all relevant information, with the engineering objective – the practical outcome of the model (Fig. 3.1). Deciding how to do this is the job of the geo-engineer – a geoscientist with sufficient knowledge of the Earth and the ability to quantify that knowledge in a way that is useful for the engineering decision at hand. A mathematician, physicist or engineer with sufficient knowledge Earth science can make an equally good geo-engineer (Fig. 3.2).

A geological model of a petroleum reservoir is the basis for most reservoir evaluation and engineering decisions. These include (roughly in order of complexity and detail):

- Making estimates of fluid volumes in place,
- Scoping reservoir development plans,
- Defining well targets,
- Designing detailed well plans,
- Optimising fluid recovery (usually for IOR/EOR schemes).

The type of decision involved affects the property modelling approach used. Simple averaging or mapping of properties is more likely to be appropriate for initial volume estimates while advanced modelling with explicit upscaling is mostly employed when designing well plans (Fig. 3.3) or as part of improved reservoir displacement plans or enhanced oil recovery (EOR) strategies.

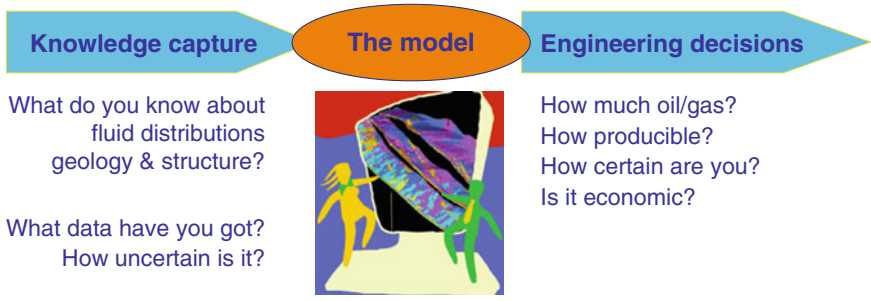

Fig. 3.1 Knowledge capture and the engineering decision

Fig. 3.2 The geo-engineer (Photo, Statoil image archive, © Statoil ASA, reproduced with permission)

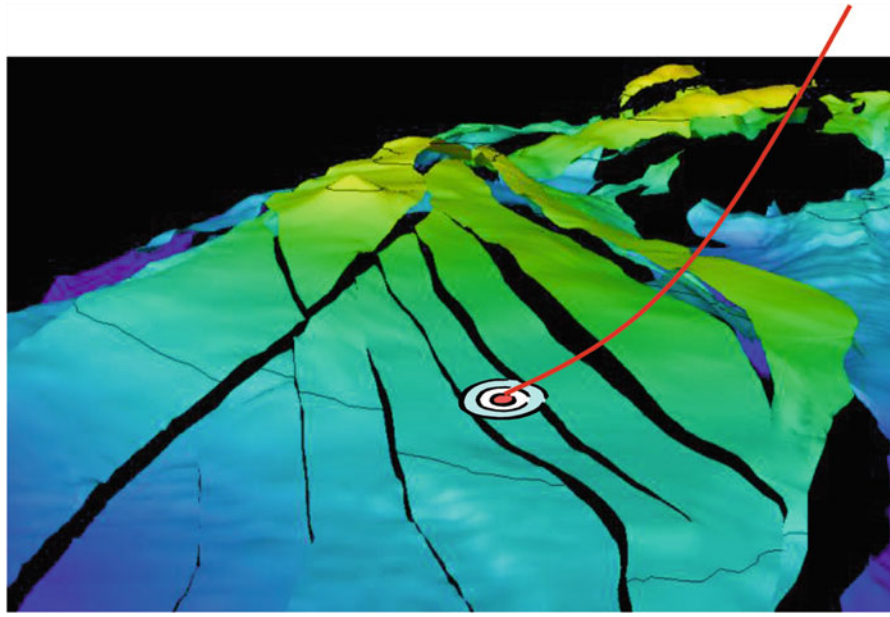

Fig. 3.3 Defining the well target

The next question is which petrophysical properties do we want to model? The focus in this chapter will be on modelling porosity (ϕ) and permeability (k) as these are the essential parameters in the flow equation (Darcy's law). The methods discussed here for handling ϕ and k can also be applied to other properties, such as formation bulk density (ρ_b) or sonic p-wave velocity (v_p), Volume fraction of shale (V_{shale}) or fracture density (F_d), to name but a few. Table 3.1 lists the most commonly modelled rock properties, but the choice should not be limited to these, and indeed a key element of the design should be careful consideration of which properties should or can be usefully represented. Integration of dynamic data with seismic and well data will generally require modelling of several petrophysical properties and their cross correlations.

Permeability is generally the most challenging property to define because it is highly variable in nature and is a tensor property dependent on flow boundary conditions. Permeability is also, in general, a non-additive property, that is:

$$k^{\Delta V} \neq \sum_{1}^{n} k_i^{\partial v} \tag{3.1}$$

In contrast porosity is essentially an additive property:

$$\phi^{\Delta V} = \sum_{1}^{n} \phi_i^{\partial v} \tag{3.2}$$

where ΔV is a large scale volume, δv[n] is the exhaustive set of small scale volumes filling the large-scale volume.

Put in practical terms, if you have defined all the cell porosity values in your reservoir model then the total reservoir porosity is precisely equal to the sum of the cell porosities divided by the number cells (i.e. the average), whereas for permeability this is not the case. We will discuss appropriate use of various permeability averages in following section.

Exercise 3.1

Which methods to use?

Think through the following decision matrix for an oilfield development to decide which approaches are appropriate for which decisions?

Method (for a given reservoir interval)	Choice	Purpose
Conceptual geological sketch of proposed reservoir analogue		Initial fluids-in-place volume estimate
Simple average of porosity, ϕ, permeability, k, and fluid saturation, S_w		Preliminary reserves estimates
2D map of ϕ, k and S_w (e.g. interpolation or kriging between wells)		Reserve estimates for designing top-side facilities (number of wells, platform type)
3D model of ϕ, k and S_w in the reservoir unit (from well data)		Definition of appraisal well drilling plan
3D model of ϕ, k and S_w for each of several model elements (from well data)		Definition of infill or development well drilling plan
3D model of ϕ, k and S_w conditioned to seismic inversion cube (seismic facies)		Submitting detailed well design for final approval
3D model of ϕ, k, S_w and facies conditioned to dynamic data (production pressures and flow rates)		Designing improved oil recovery (IOR) strategy and additional well targets
3D model of ϕ, k, S_w and facies integrating multi-scale static and dynamic data		Implementing enhanced oil recovery (EOR) strategy using an injection blend (e.g. water alternating gas)

Table 3.1 List of properties typically included in geological reservoir models

	Symbol	Property	Units [typical range]
All reservoirs	ϕ	Porosity	Fraction [0, 0.4]
	ϕ_m, ϕ_f	Matrix porosity, Fracture porosity	Fraction [0, 0.4]
	k_h, k_v	Horizontal permeability, vertical permeability	millidarcy, mD [0.001, 10000]
	k_v/k_h	Ratio of vertical to horizontal permeability	millidarcy, mD [10^{-5}, 1]
	V_{shale}, V_{sand}, V_{cement}	Volume fraction (shale, sandstone, cement)	Fraction [0, 1]
	N/G_{sand}, N/G_{res}	Net to gross ratio (sandstone, reservoir)	Fraction [0, 1]
	S_w, S_o, S_g	Fluid Saturation (water, oil, gas)	Fraction [0, 1]
	SAT_{num}	Relative permeability saturation function index	Integer [1, N]
Fractured reservoirs	ϕ_m, ϕ_f	Matrix porosity, Fracture porosity	Fraction [0, 0.4]
	k_f, k_m	Fracture permeability, Matrix permeability	millidarcy, mD [10^{-3}, 10^5]
	F_d	Fracture density	Number per metre, m^{-1} [0.1, 10]
	F_a	Fracture aperture	m [10^{-6}, 10^{-3}]
	C_{mean}	Mean Surface Curvature	2nd derivative [-x>0<+x]
Seismic inversion	ρ_b	Bulk density	g/cc (kg/m^3) [1-2]
	V_p	Seismic velocity (p-wave)	m/s [1400-5000]
	V_p/V_s	Ratio of compression-wave to shear-wave velocity	m/s [700-3000]
	AI_p, AI_s	Acoustic (seismic) Impedance (p-wave, s-wave)	m/s.g/cc (Pa.s/m^3) [6000,14000]
	ϕ_{AVO}	Porosity from AVO inversion	Fraction [0, 0.4]

The final important question to address is: Which reservoir or rock unit do we want to average? There are many related concepts used to define flowing rock intervals – flow units, hydraulic units, geological units or simply "the reservoir". The most succinct term for defining the rock units in reservoir studies is the Hydraulic Flow Unit (HFU), which is defined as representative rock volume with consistent petrophysical properties distinctly different from other rock units. There is thus a direct relationship between flow units and the 'model elements' introduced in the preceding chapter.

Exercise 3.2

Additive properties

Additivity involves a mathematical function in which a property can be expressed as a weighted sum of some independent variable(s). The concept is important to a wide range of statistical methods used in many science disciplines. Additivity has many deeper facets and definitions that are discussed in mathematics and statistical literature.

It is useful to consider a wider selection of petrophysical properties and think through whether they are essentially additive or non-additive (i.e. multiplicative) properties.

What would you conclude about these terms?

- Net-to-gross ratio
- Fluid saturation
- Permeability
- Porosity
- Bulk density
- Formation resistivity
- Seismic velocity, V_p or V_s
- Acoustic Impedance, AI

Abbaszadeh et al. (1996) define the HFU in terms of the Kozeny-Carmen equation to extract Flow Zone Indicators which can be used quantitatively to define specific HFUs from well data. We will return the definition of representative volumes and flow units in Chap. 4 when we look at upscaling, but first we need to understand permeability.

3.2 Understanding Permeability

3.2.1 Darcy's Law

The basic permeability equation is based on the observations and field experience of Henri Darcy (1803–1858) while engineering a pressurized water distribution system in the town of Dijon, France. His equation relates flow rate to the head of water draining through a pile of sand (Fig. 3.4):

$$Q = KA(\Delta H/L) \tag{3.3}$$

where

Q = volume flux of water
K = constant of hydraulic conductivity or coefficient of permeability
A = cross sectional area
ΔH = height of water column
L = length of sand column

From this we can derive the familiar Darcy's Law – a fundamental equation for flow in porous media, based on dimensional analysis and the Navier-Stokes equations for flow in cylindrical pores:

$$u = \frac{-k}{\mu}\nabla(P + \rho g z) \tag{3.4}$$

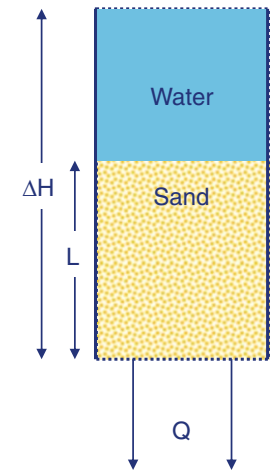

Fig. 3.4 Darcy's experiment

where
u = intrinsic fluid velocity
k = intrinsic permeability
μ = fluid viscosity
∇P = applied pressure gradient
ρgz = pressure gradient due to gravity
∇P (grad P) is the pressure gradient, which can be solved in a cartesian coordinate system as:

$$\nabla P = \frac{dP}{dx} + \frac{dP}{dy} + \frac{dP}{dz} \tag{3.5}$$

The pressure gradient due to gravity is then ρg∇z. For a homogeneous, uniform medium k has a single value, which represents the medium's ability to permit flow (independent of the fluid type). For the general case of a heterogeneous rock medium, k is a tensor property.

Exercise 3.3
Dimensions of permeability

What are the dimensions of permeability? Do a dimensional analysis for Darcy's Law.

For the volumetric flux equation

$$Q = KA(\Delta H/L)$$

The dimensions are

$$\left[L^3T^{-1}\right] = \left[LT^{-1}\right]\ \left[L^2\right]$$

Therefore the SI unit for K is:

$$ms^{-1}$$

Do the same for Darcy's Law:

$$u = -(k/\mu).\nabla(P + \rho gz)$$

The dimensions are

$$[\ \ ] = ([\ \ ]/[\ \ ]).[\ \ ]$$

Therefore the SI unit for k is

$$\_\_\_\_$$

3.2.2 Upscaled Permeability

In general terms, *upscaled permeability* refers to the permeability of a larger volume given some fine scale observations or measurements. The concept is widely used, and abused, and requires some care in its use and application. It is also rather fundamental – if it was a simple thing to estimate the correctly upscaled permeability for a reservoir unit, there would be little value in reservoir modelling (apart from simple volume estimates).

The upscaled (or block) permeability, k_b, is defined as the permeability of an homogeneous block, which under the same pressure boundary conditions will give the same average flows as the heterogeneous region the block is representing (Fig. 3.5). The upscaled block permeability could be estimated, given a fine set of values in a permeability field or model, or it could be measured at the larger scale (e.g. in a well test or core analysis), in which case the fine-scale permeabilities need not be known.

The *effective permeability* is defined strictly in terms of effective medium theory and is an intrinsic large-scale property which is independent of the boundary conditions. The main theoretical conditions for estimation of the effective permeability, k_{eff}, are:

- That the flow is linear and steady state;
- That the medium is statistically homogeneous at the large scale.

When the upscaled domain is large enough, such that these conditions are nearly satisfied, then k_b approaches k_{eff}. The term *equivalent permeability*, is also used (Renard and de Marsily 1997) and refers to a general large-scale permeability which can be applied to a wide range of boundary conditions, to some extent encompassing both k_b and k_{eff}. These terms are often confused or misused, and in this treatment we will refer to the permeability upscaled from a model as the *block permeability*, k_b, and use *effective permeability* as the ideal upscaled permeability we would generally wish to estimate if we could satisfy the necessary conditions. In reservoir modelling we are usually estimating k_b in practice, because we rarely fully satisfy the demands of effective medium theory. However, k_{eff} is an important concept with many constraints that we try to satisfy when estimating the upscaled (block) permeability.

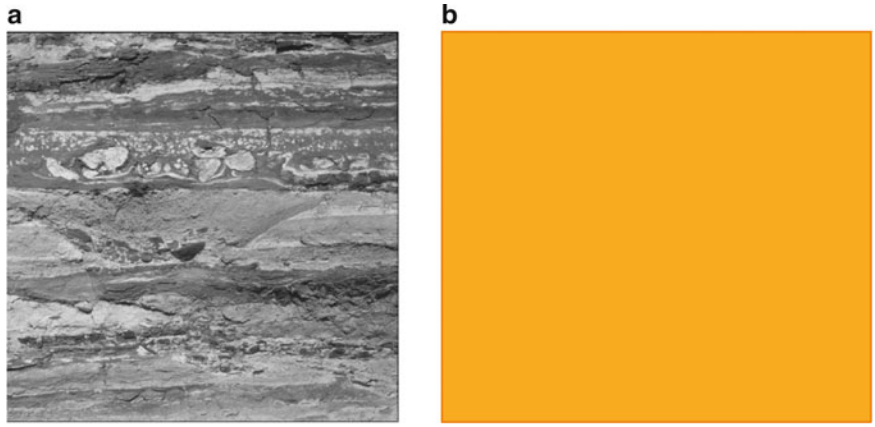

Fig. 3.5 Effective permeability and upscaled block permeability (**a**) Real rock medium has some (unknown) effective permeability. (**b**) Modelled rock medium has an estimated block permeability with the same average flow as the real thing

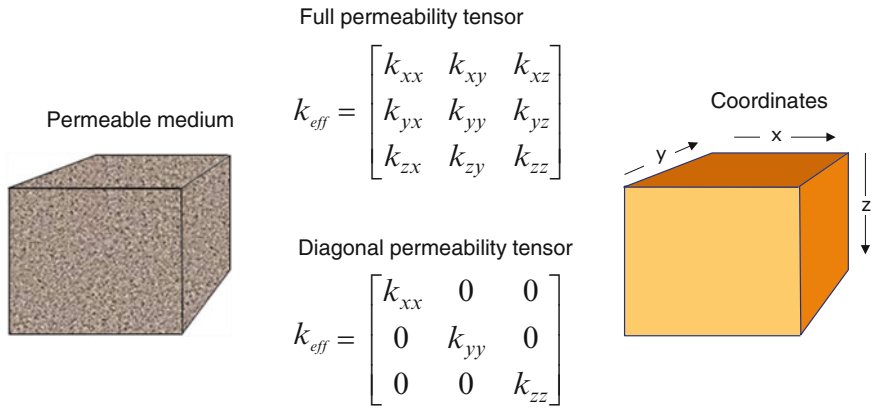

Fig. 3.6 The permeability tensor

Note that in petrophysical analysis, the term 'effective porosity' refers to the porosity of moveable fluids excluding micro-porosity and chemically bound water, while total porosity encompasses all pore types. Although effective porosity and effective permeability both represent properties relevant to, and controlling, macroscopic flow, they are defined on different bases. Effective permeability is essentially a larger scale property requiring statistical homogeneity in the medium, whereas effective porosity is essentially a pore-scale physical attribute. Of course, if both properties are estimated at, or rescaled to, the same appropriate volume, they may correspond and are correctly used together in flow modelling. They should not, however, be automatically associated. For example, in an upscaled heterogeneous volume there could be effective porosity elements (e.g. vuggy pores) which do not contribute to the flow and therefore do not influence the effective permeability.

In general, k_b is a tensor property (Fig. 3.6) where, for example, k_{xy} represents flow in the x direction due to a pressure gradient in the y direction. In practice k_b is commonly assumed to be a diagonal tensor where off-diagonal terms are neglected. A further simplification in many reservoir modelling studies is the assumption that $k_h = k_{xx} = k_{yy}$ and that $k_v = k_{zz}$.

The calculation or estimation of k_b is dependent on the boundary conditions (Fig. 3.7). Note that the assumption of a no-flow or sealed

side boundary condition, forces the result to be a diagonal tensor. This is useful, but may not of course represent reality. Renard and de Marsily (1997) give an excellent review of effective permeability, and Pickup et al. (1994, 1995) give examples of the permeability tensor estimated for a range of realistic sedimentary media.

3.2.3 Permeability Variation in the Subsurface

There is an extensive literature on the measurement of permeability (e.g. Goggin et al. 1988; Hurst and Rosvoll 1991; Ringrose et al. 1999) and its application for reservoir modelling (e.g. Begg et al. 1989; Weber and van Geuns 1990; Corbett et al. 1992). All too often, rather idealised permeability distributions have been assumed in reservoir models, such as a constant value or the average of a few core plug measurements.

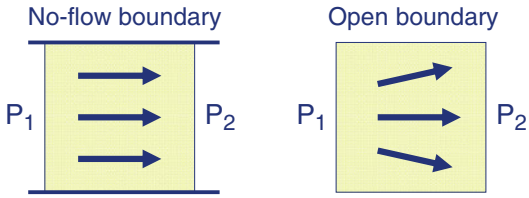

Fig. 3.7 Simple illustration of flow boundary conditions: P1 and P2 are fluid pressures applied at the *left* and *right hand sides* and *arrows* illustrate flow vectors

In reality, the permeability in a rock medium is a highly variable property. In sedimentary basins as a whole we expect variations of at least 10 orders of magnitude (Fig. 3.8), with a general decrease for surface to depth due to compaction and diagenesis. Good sandstone units may have permeabilities typically in the 10–1,000 mD range, but the silt and clay rich units pull the permeability down to around 10^{-3} mD or lower. Deeply buried mudstones forming cap-rocks and seals have permeabilities in the microdarcy to nanodarcy range. Even within a single reservoir unit (not including the shales), permeability may range by at least 5 orders of magnitude. In the example shown in Fig. 3.9 the wide range in observed permeabilities is due both to lithofacies (heterolithic facies tend to be lower than the sand facies) and due to cementation (each facies is highly variable mainly due to the effects of variable degrees of quartz cementation).

3.2.4 Permeability Averages

Due to its highly variable nature, some form of averaging of permeability is generally needed. The question is which average? There are well-known limits for the estimation of k_{eff} in ideal systems. For flow along continuous parallel layers the arithmetic average gives the correct effective permeability, while for flow perpendicular to

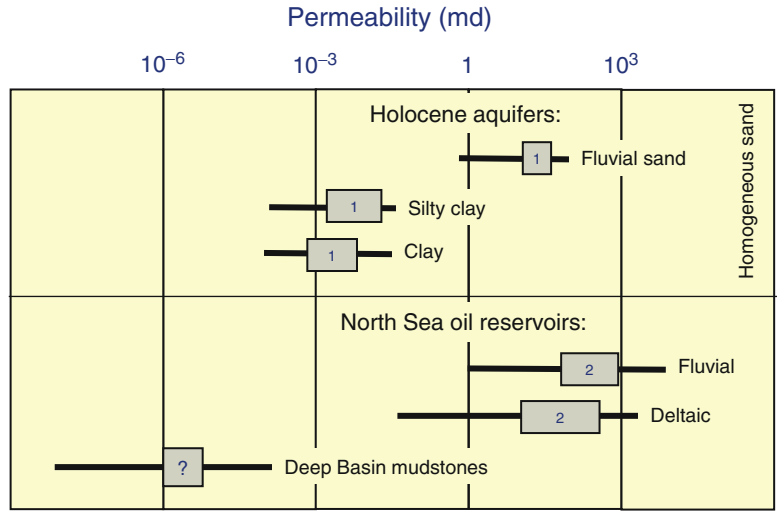

Fig. 3.8 Typical ranges of permeability for near-surface aquifers and North Sea oil reservoirs: *1* = Holocene aquifers (From Bierkins 1996), *2* = Example North Sea datasets (anonymous)

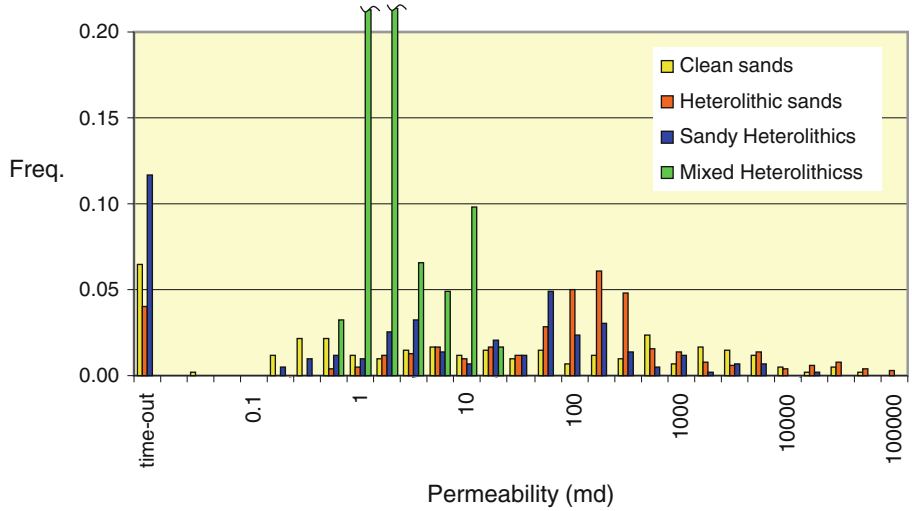

Fig. 3.9 Probe permeameter measurements from a highly variable, deeply-buried, tidal-deltaic reservoir interval (3 m of core) from offshore Norway

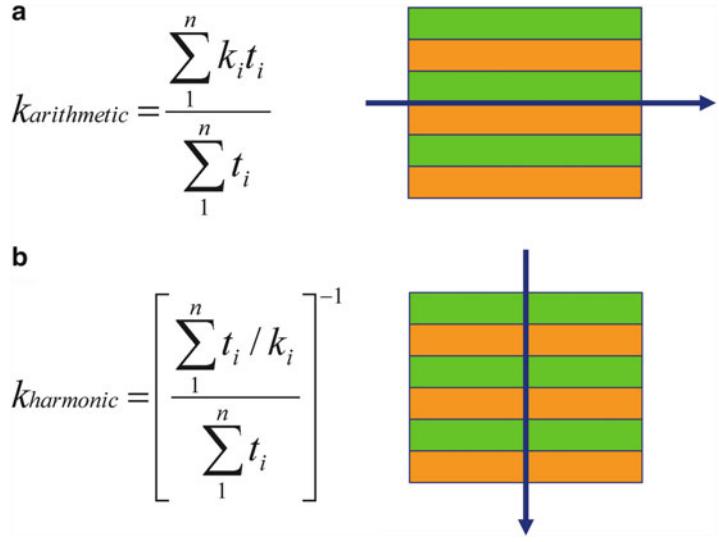

Fig. 3.10 Calculation of effective permeability using averages for ideal layered systems: (**a**) The arithmetic average for flow along continuous parallel layers; (**b**) The harmonic average for flow perpendicular to continuous parallel layers (k_i and t_i are the permeability and thickness of layer i)

continuous parallel layers the harmonic average is the correct solution (Fig. 3.10).

If the layers are in any way discontinuous or variable or the flow is not perfectly parallel or perpendicular to the layers then the true effective permeability will lie in between these averages. This gives us the outer bounds to effective permeability:

$$k_{harmonic} \leq k_{eff} \leq k_{arithmetic}$$

More precise limits to k_{eff} have also been proposed, such as the arithmetic mean of harmonic means of each row of cells parallel to flow (lower bound) and *vice versa* for the upper bound (Cardwell and Parsons 1945). However, for most practical purposes the arithmetic and harmonic means are quite adequate limiting values, especially given that we seldom have an exhaustive set of values to average (the sample problem, discussed in Sect. 3.3 below).

The geometric average is often proposed as a useful or more correct average to use for more variable rock systems. Indeed for flow in a correlated random 2D permeability field with a log-normal distribution and a low variance the effective permeability is equal to the geometric mean:

$$k_{geometric} = \exp\left[\sum_{1}^{n} \ln k_i / n\right] \qquad (3.6)$$

This can be adapted for 3D as long as account is also taken for the variance of the distribution. Gutjahr et al. (1978) showed that for a log-normally distributed permeability field in 3D:

$$k_{eff} = k_{geometric}\left(1 + \sigma^2/6\right) \qquad (3.7)$$

where σ^2 is the variance of ln(k).

Thus in 3D, the theoretical effective permeability is slightly higher than the geometric average, or indeed significantly higher if the variance is large.

An important condition for $k_{eff} \approx k_{geometric}$ is that correlation length, λ, of the permeability variation must be significantly smaller than the size of the averaging volume, L. That is:

$$\lambda_x \lambda_y \lambda_z \ll L_x L_y L_z$$

This relates to the condition of statistical homogeneity. In practice, we have found that λ needs to be at least 5 times smaller than L for $k_b \rightarrow k_{geometric}$ for a log-lognormal permeability field. This implies that the assumption (sometimes made) that $k_{geometric}$ is the 'right' average for a heterogenous reservoir interval is not generally true. Neither does the existence of a log-normal permeability distribution imply that the geometric average is the right average. This is evident in the case of a perfectly layered system with permeability values drawn from a log normal distribution – in such a case $k_{eff} = k_{arithmetic}$.

Averages between the outer-bound limits to k_{eff} can be generalised in terms of the power average (Kendall and Staurt 1977; Journel et al. 1986):

$$k_{power} = \left[\sum k_i^p / n\right]^{1/p} \qquad (3.8)$$

where $p = -1$ corresponds to the harmonic mean, $p \sim 0$ to the geometric mean and $p = 1$ to the arithmetic mean ($p = 0$ is invalid and the geometric mean is calculated using Eq. (3.6)).

For a specific case with some arbitrary heterogeneity structure, a value for p can be found (e.g. by finding a p value which gives best fit to results of numerical simulations). This can be a very useful form of the permeability average. For example, after some detailed work on estimating the permeability of a particular reservoir unit or facies (based on a key well or near-well model) one can derive plausible values for p for general application in the full field reservoir model (e.g. Ringrose et al. 2005). In general, p for k_h will be positive and p for k_v will be negative.

Note that for the general case, when applying averages to numerical models with varying cell sizes, we use volume weighted averages. Thus, the most general form of the permeability estimate using averages is:

$$k_{estimate} = \left[\int k^p dV \Big/ \int dV\right]^{1/p} \langle -1 < p < 1 | \qquad (3.9)$$

where p is estimated or postulated.

3.2.5 Numerical Estimation of Block Permeability

For the general case, where an average permeability cannot be assumed, *a priori,* numerical methods must be used to calculate the block permeability (k_b). This subject has occupied many minds in the fields of petroleum and groundwater engineering and there is a large literature on this subject. The numerical methods used are based on the assumptions of conservation of mass and energy, and generally assume steady-state conditions. The founding father of the subject in the petroleum field is arguably Muskat (1937), while Matheron (1967) founded much of the theory related to estimation of flow properties. De Marsilly (1986) gives an excellent foundation from a groundwater perspective and Renard and de Marsily (1997) give a more recent review on the calculation of equivalent

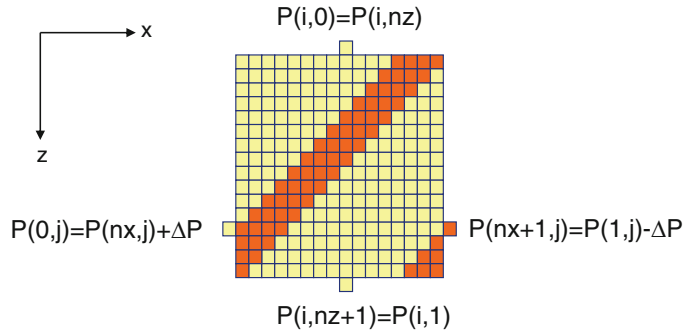

Fig. 3.11 Periodic pressure boundary conditions applied to a periodic permeability field, involving an inclined layer. Example boundary cell pressure conditions are shown

permeability. Some key papers on the calculation of permeability for heterogeneous rock media include White and Horne (1987), Durlofsky (1991) and Pickup et al. (1994).

To illustrate the numerical approach we take an example proposed by Pickup and Sorbie (1996) shown in Fig. 3.11. Assuming a fine-scale grid of permeability values, k_i, we want to calculate the upscaled block permeability tensor, k_b. An assumption on the boundary conditions must be made, and we will assume a period boundary condition (Durlofsky 1991) – where fluids exiting one edge are assumed to enter the opposite edge – and apply this to a periodic permeability field (where the model geometry repeats in all directions). This arrangement of geometry and boundary conditions gives us an exact solution.

First a pressure gradient ΔP is applied to the boundaries in the x direction. For the boundaries parallel to the applied pressure gradient, the periodic condition means that P in cell (i, 0) is set as equal to P in cell (i, nz), where n is the number of cells. A steady-state flow simulation is carried out on the fine-scale grid, and as all the permeabilities are known, it is possible to find the cell pressures and flow values (using matrix computational methods).

We then solve Darcy's Law for each fine-scale block:

$$\vec{u} = -(1/\mu)\underline{\underline{k}}.\nabla P \tag{3.10}$$

where

$\vec{u}$ is the local flow vector

μ is the fluid viscosity

$\underline{\underline{k}}$ is the permeability tensor

ΔP is the pressure gradient

Usually, at the fine scale we assume the local permeability is not a tensor so that only one value of k is required per cell.

We then wish to know the upscaled block permeability for the whole system. This is a relatively simple step once all small scale Darcy equations are known, and involves the following steps:

1. Solve the fine-scale equations to give pressures, P_{ij} for each block.
2. Calculate inter-block flows in the x-direction, using Darcy's Law.
3. Calculate total flow, Q, by summing individual flows between any two planes.
4. Calculate k_b using Darcy's Law applied to the upscaled block.
5. Repeat for the y and z directions.

For the upscaled block this results in a set of terms governing flow in each direction, such that:

$$\begin{aligned} u_x &= -\frac{1}{\mu}\left(k_{xx}\frac{\partial P}{\partial x} + k_{xy}\frac{\partial P}{\partial y} + k_{xz}\frac{\partial P}{\partial z}\right) \\ u_y &= -\frac{1}{\mu}\left(k_{yx}\frac{\partial P}{\partial x} + k_{yy}\frac{\partial P}{\partial y} + k_{yz}\frac{\partial P}{\partial z}\right) \\ u_z &= -\frac{1}{\mu}\left(k_{zx}\frac{\partial P}{\partial x} + k_{zy}\frac{\partial P}{\partial y} + k_{zz}\frac{\partial P}{\partial z}\right) \end{aligned} \tag{3.11}$$

For example, the term k_{zx} is the permeability in the z direction corresponding to the pressure gradient in the x direction. These off-diagonal terms are intuitive when one looks at the permeability field. Take the vertical (x, z) geological model section shown in Fig. 3.12. If the inclined orange layers have lower permeability, then flow applied in the +x direction (to the right) will tend to generate a flux in the –z direction (i.e. upwards). This results

Note to graphics – Ensure grid edges align – redraft if necessary?

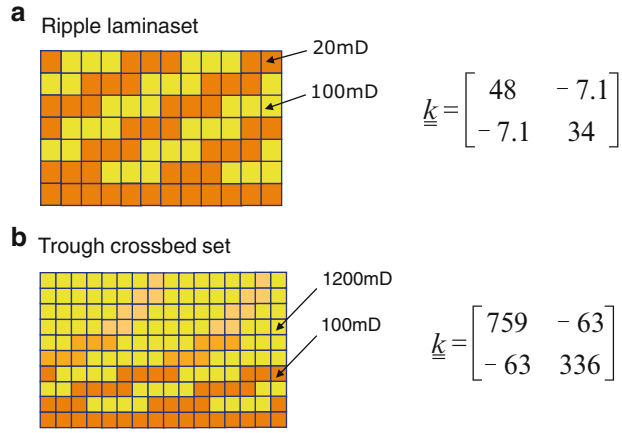

Fig. 3.12 Example tensor permeability matrices calculated for simple 2D models of common sedimentary structures

in a vertical flow and requires a k_{zx} permeability term in the Darcy equation (for a 2D tensor).

Example solutions of permeability tensors for simple geological models are given by Pickup et al. (1994) and illustrated in Fig. 3.12. Ripple laminasets and trough cross-beds are two widespread bedding architectures found in deltaic and fluvial depositional settings – ripple laminasets tend to be 2–4 cm in height while trough cross-bed sets are typically 10–50 cm in height. These simple models are two dimensional and capture typical geometry and permeability variation (measured on outcrop samples) in a section parallel to the depositional current. In both cases, the tensor permeability matrices have relatively large off-diagonal terms, 15 and 8 % of the k_{xx} value, respectively. The negative off-diagonal terms reflect the chosen coordinate system with respect to flow direction (flow left to right with z increasing downwards). Vertical permeability is also significantly lower than the horizontal permeability due to the effects of the continuous low permeability bottomset.

Geological elements like these will tend to fill the volume within a particular reservoir unit, imparting their flow anisotropy and cross-flow tendencies on the overall reservoir unit. Of course, real rock systems will have natural variability in both architecture and petrophysical properties, and our aim is therefore to represent the expected flow behaviour. The effects of geological architecture on flow are frequently neglected – for example, it may be assumed that a Gaussian random field represents the inter-well porosity and permeability architecture. More advanced, geologically-based, flow modelling will, however, allow us to assess the potential effects of geological architecture on flow, and attempt to capture these effects as a set of upscaled block permeability values. Structural architecture in the form of fractures or small faults may also generate pervasive tendencies for strongly tensorial permeability within a rock unit. By aligning grid cells to geological features (faults, dominant fracture orientations, or major bed-set boundaries) the cross-flow terms can be kept to a minimum. However, typically one aligns the grid to the largest-scale geological architecture (e.g. major fault blocks) and so other smaller-scale features inevitably generate some cross-flow.

3.2.6 Permeability in Fractures

Understanding permeability in fractured reservoirs requires some different flow physics – Darcy's law does not apply. Flow within a fracture (Fig. 3.13) is described by Poiseuille's

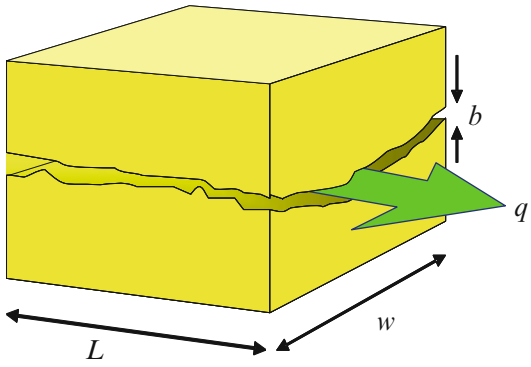

Fig. 3.13 Flow in a fracture

law, which for a parallel-plate geometry gives (Mourzenko et al. 1995):

$$q = \frac{w b^3}{12\mu} \frac{\Delta P}{L} \tag{3.12}$$

where
q is the volumetric flow rate,
w is the fracture width,
b is the fracture aperture,
μ is the fluid viscosity,
ΔP/L is the pressure gradient.

Note that the flow rate is proportional to b^3, and thus highly dependent on fracture aperture. In practice, the flow strongly depends on the stress state and the fracture roughness (Witherspoon et al. 1980), but the underlying concept still holds. To put some values into this simple equation – a 1 mm wide fracture in an impermeable rock matrix would have an effective permeability of around 100 Darcys.

Unfortunately, fracture aperture is not easily measured, and generally has to be inferred from pressure data. This makes fracture systems much harder to model than conventional non-fractured reservoirs.

In practice, there are two general approaches for modelling fracture permeability:

- Implicitly, where we model the overall rock permeability (matrix and fractures) and assume we have captured the "effect of fractures" as an effective permeability.
- Explicitly, where we represent the fractures in a model.

For the explicit case, there are then several options for how this may be done:

1. *Discrete Fracture Network (DFN) models,* where individual fractures with explicit geometry are modelled in a complex network.
2. *Dual permeability models,* where the fracture and matrix permeability are explicitly represented (but fracture geometry is implicitly represented by a shape factor).
3. *Dual porosity models,* where the fracture and matrix porosity are explicitly represented, but the permeability is assumed to occur only in the fractures (and the fracture geometry is implicitly represented by a shape factor).

Fractured reservoir modelling is discussed in detail by Nelson (2001) and covered in most reservoir engineering textbooks, and in Chap. 6 we describe approaches for handling fractured reservoir models. The important thing to keep in mind in the context of understanding permeability, is that fractures behave quite differently (and follow different laws) from the general Darcy-flow concept for flow in permeable (granular) rock media.

3.3 Handling Statistical Data

3.3.1 Introduction

Many misunderstandings about upscaled permeability, or any other reservoir property, are caused by incorrect understanding or use of probability distributions. The treatment of probability distributions is an extensive subject covered in a number of textbooks. Any of the following are suitable for geoscientists and engineers wanting to gain deeper appreciation of statistics and the Earth sciences: Size 1987; Isaaks and Srivastava 1989; Olea 1991; Jensen et al. 2000, and Davis 2003. Here we will identify some of the most important issues related to property modelling, namely:

- Understanding sample versus population statistics;
- Using log-normal and other transforms;
- Use and implications of applying cut-off values.

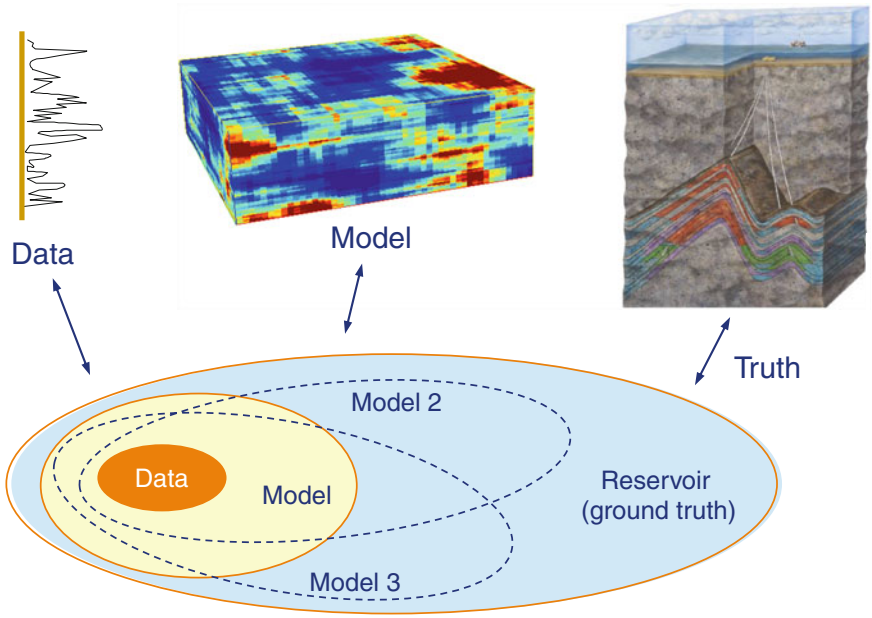

Fig. 3.14 Illustration of the axiom: Data ≠ Model ≠ Truth (Redrawn from Corbett and Jensen 1992, ©EAGE reproduced with kind permission of EAGE Publications B.V., The Netherlands)

Our overall aim in reservoir modelling is to estimate and compare distributions for:

1. The well data (observations);
2. The reservoir model (a hypothesis or postulate);
3. The population (the unknown "true" reservoir properties).

We must always remember not to confuse observations (data) with the model (a hypothesis) and both of these with the "ground truth" (an unknown). This leads us to one of the most important axioms of reservoir modelling:

$$Data \neq Model \neq Truth$$

Of course, we want our models to be consistent with the available data (from wells, seismic, and dynamic data) and we hope they will give us a good approximation of the truth, but too often the reservoir design engineer tries to force an artificial match which leads inevitably to great disappointment. A common mistake is to try to manipulate the data statistics to obtain an apparent match between the model and data. You may have heard versions of the following statements:

- 'We matched the well test permeability (k_h) to the log-derived permeability data by applying a cut-off and using a geometric average.'
- 'The previous models were all wrong, but this one must be right because it matches all the data we have.'

Now statement A sounds good but begs the questions what cut-off was applied and is the geometric average indeed the appropriate average to use? Statement B is clearly arrogant but in fact captures the psychology of every reservoir model builder – we try to do our best with the available data but are reluctant to admit to the errors that must be present. Versions of these statements that would be more consistent with the inequality above might be:

- 'We were able to match the well test permeability (k_h) to within 10 % of the log-derived permeability data by applying the agreed cut-off and using a geometric average, and a power average with $p = 0.3$ gave us an even better match to within 1 %.'
- 'The previous models had several serious errors and weaknesses, but this latest set of three models incorporates the latest data and captures the likely range of subsurface behaviour.'

Figure 3.14 illustrates what the statistical objective of modelling should be. The available

Table 3.2 Statistics for a simple example of estimation of the sand volume fraction, V_s, in a reservoir unit at different stages of well data support

	With 2 wells	With 5 wells	With 30 wells
Mean	38.5	36.2	37.4
σ	4.9	6.6	7.7
SE	3.5	3.0	1.4
C_v	–	0.18	0.21
N_0	–	3	4
N	2	5	30

data is some limited subset of the true subsurface, and the model should extend from the data in order to make estimates of the true subsurface. In terms of set theory:

$$Data \in Model \in Truth$$

Our models should be consistent with that data (in that they encompass it) but should aim to capture a wider range, approaching reality, using both geological concepts and statistical methods. In fact, as we shall see later (in this section and in Sect. 3.4) bias in the data sample and upscaling transforms further complicate this picture whereby the data itself can be misleading.

Table 3.2 illustrates this principle using the simple case of estimating the sand volume fraction, V_s (or N/G_{sand}), at different stages in a field development. We might quickly infer that the 30 well case gives us the most correct estimate and that the earlier 2 and 5 well cases are in error due to limited sample size. In fact, by applying the N-zero statistic (explained below) we can conclude that the 5-well estimate is accurate to within 20 % of the true mean, and that by the 30-well stage we still lie within the range estimated at the 5-well stage. In other words, it is better to proceed with a realistic estimate of the range in V_s from the available data than to assume that the data you have gives the "correct" value. In this case, $V_s = 36\ \% \pm 7\ \%$ constitutes a good model at the 5-well stage in this field development.

3.3.2 Variance and Uncertainty

There are a number of useful measures that can guide the reservoir model practitioner in gaining a realistic impression of the uncertainty involved in using the available data. To put it simply, *variance* refers to the spread of the data you have (in front of you), while *uncertainty* refers to some unknown variability beyond the information at hand. From probability theory we can establish that 'most' values lie close to the mean. What we want to know is 'how close' – or how sure we are about the mean value. The fundamental difficulty here is that the true (population) mean is unknown and we have to employ the theory of confidence intervals to give us an estimate. Confidence limit theory is treated well in most books on statistics; Size (1987) has a good introduction.

Chebyshev's inequality gives us the theoretical basis (and mathematical proof) for quantifying how many values lie within certain limits. For example, for a Gaussian distribution 75 % of the values are within the range of two standard deviations from the mean. Stated simply Chebyshev's theory gives:

$$P(|x - \mu| \geq \kappa\sigma) \leq \frac{1}{\kappa^2} \tag{3.13}$$

where κ is the number of standard deviations.

The *standard error* provides a simple measure of uncertainty. If we have a sample from a population (assuming a normal distribution and statistically independent values), then the standard error of the mean value, $\bar{x}$, is the standard deviation of the sample divided by the square root of the sample size:

$$SE_{\bar{x}} = \frac{\sigma_s}{\sqrt{n}} \tag{3.14}$$

where σ_s is the standard deviation of the sample and n is the sample size.

The standard error can also be used to calculate confidence intervals. For example, the 95 % confidence interval is given by $(\bar{x} \pm SE_{\bar{x}} * 1.96)$.

The *Coefficient of Variation*, C_v, is a normalized measure of the dispersion of a probability distribution, or put simply a normalised standard deviation:

$$C_V = \frac{\sqrt{Var(p)}}{E(p)} \tag{3.15}$$

where Var(p) and E(p) are the variance and expectation of the variable, p.

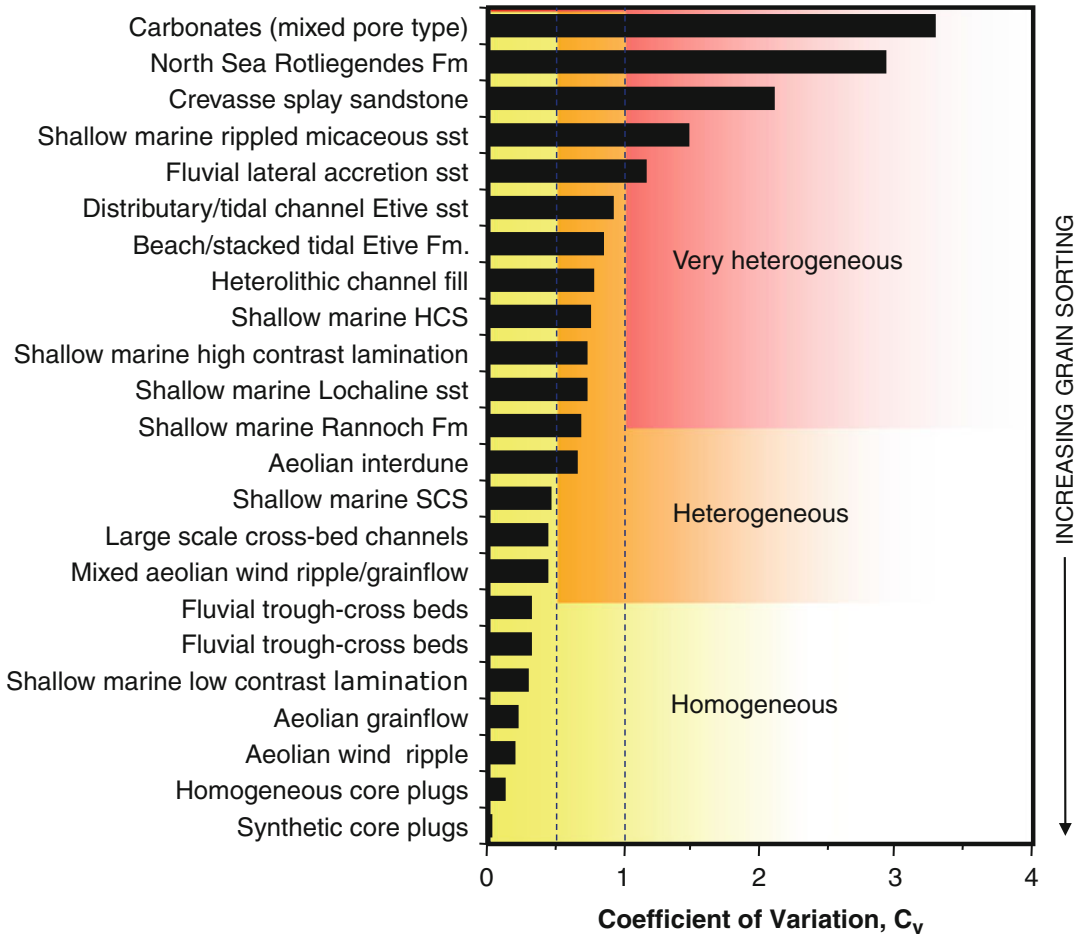

Fig. 3.15 Reservoir heterogeneity for a large range of reservoir and outcrop permeability datasets ranked by the Coefficient of Variation, C_v, (Redrawn from Corbett and Jensen 1992)

The C_v can be estimated from a sample by:

$$C_V \approx \frac{\sigma(p)}{\overline{p}} \tag{3.16}$$

where σ(p) and $\overline{p}$ are the standard deviation and mean of the sample.

Corbett and Jensen (1992) proposed a simple classification of C_v values using a large selection of permeability data from petroleum reservoirs and outcrop analogues (Fig. 3.15):

- $C_v < 0.5$ implies an effectively homogeneous dataset
- $0.5 < C_v < 1$ is termed heterogeneous
- $C_v > 1$ is termed very heterogeneous

The N-zero (N_o) statistic (Hurst and Rosvoll 1991) captures these underlying statistical theories into a practical guideline for deciding how confident one can be given a limited dataset. The N_o statistic indicates the sample number required to estimate the true mean to with a 20 % tolerance (at a 95 % confidence level) as a function of the Coefficient of Variation, C_v:

$$N_o = (10\, C_v)^2 \tag{3.17}$$

If the actual sample number is significantly less than N_o then a clear inference can be made that the sample is insufficient and that the sample statistics must be treated with extreme caution. For practical purposes we can use N_o as rule of thumb to indicate data sufficiency (e.g. Table 3.2). This simple approach assumes a Gaussian distribution and statistical representivity of the sample, so the approach is only intended as a first approximation. More precise estimation of the error associated with

the mean of a given sample dataset can be made using confidence interval theory (e.g. Isaaks and Srivastava 1989; Jensen et al. 2000).

This analysis gives a useful framework for judging how variable your reservoir data really is. Note that more than half the datasets included in Fig. 3.15 are heterogeneous or very heterogenous. Carbonate reservoirs and highly laminated or inter-bedded formations show the highest C_v values. This plot should in no way be considered as definitive for reservoirs for any particular depositional environment. We shall see later (in Chap. 4), that the scale of measurement is a key factor within essentially multi-scale geological reservoir systems. Also keep in mind that your dataset may be too limited to make a good assessment of the true variability – the C_v from a sample dataset is an estimate. Jensen et al. (2000) give a fuller discussion of the application of the C_v measure to petrophysical reservoir data.

3.3.3 The Normal Distribution and Its Transforms

Probability theory is founded in the properties of the Normal (or Gaussian) Distribution. A variable X is a *normal random variable* when the *probability density function* is given by:

$$g(x) = \frac{1}{\sigma\sqrt{2\pi}} e^{-\frac{(x-\mu)^2}{2\sigma^2}} \qquad (3.18)$$

where μ is the mean and σ^2 is the variance.

This bell shaped function is completely determined by the mean and the variance. Carl Friedrich Gauss became associated with the function following his analysis of astronomical data (atmospheric scatter from point light sources), but the function was originally proposed by Abraham de Moivre in 1733 and developed by one of the founders of mathematics, Pierre-Simon de Laplace in his book *Analytical Theory of Probabilities* in 1812. Since that time, a wide range of natural phenomena in the biological and physical sciences have been found to be closely approximated by this distribution – not least measurements in rock media. The function is also fundamental to a wide range of statistical methods and the basis for most geostatistical modelling tools. It is also important to say that many natural phenomena do not conform to the Gaussian distribution – they may, for example, be better approximated by a another function such as the Poisson distribution and in geology have a strong tendency to be more complex and multimodal.

Permeability data is often found to be approximated by a log-normal distribution. A variable X is *log-normally distributed* if its natural logarithmic transform Y is normally distributed with mean μ_Y and standard deviation ${\sigma_Y}^2$. The probability density function for X is given by:

$$f(x) = \frac{1}{\sqrt{2\pi}\sigma_Y x} e^{-\frac{[\ln(x)-\mu_Y]^2}{2\sigma_Y^2}} \quad \text{if } x > 0 \qquad (3.19)$$

The variable statistics, μ_X and ${\sigma_X}^2$ are related to the log transform parameters μ_Y and ${\sigma_Y}^2$ as follows:

$$\mu_X = e^{\mu_Y + 0.5\sigma_Y^2} \qquad (3.20a)$$

$$\sigma_X^2 = \mu_X^2\left(e^{\sigma_Y^2} - 1\right) \qquad (3.20b)$$

This can lead to some confusion, and it is important that the reservoir modelling practitioner keeps close track of which distributions relate to which statistics. For $\sigma = 0$ the mean obeys the simple law of the log transform, $\mu_x = e^{\mu_Y}$, but generally $(\sigma > 0), \mu_x > e^{\mu_Y}$.

Log-normal distributions are appealing and useful because (a) they capture a broad spread of observations in one statistic, and (b) they are easily manipulated using log transforms. However, they also present some difficulties in reservoir modelling:

- They tend to generate excessive distribution tails
- It is tempting to apply them to multi-modal data
- They can cause confusion (e.g. what is the average?)

Note that the correct 'average' for a log-normal distribution of permeability is the geometric average – equivalent to a simple average of ln (k) – but this does not necessarily mean that

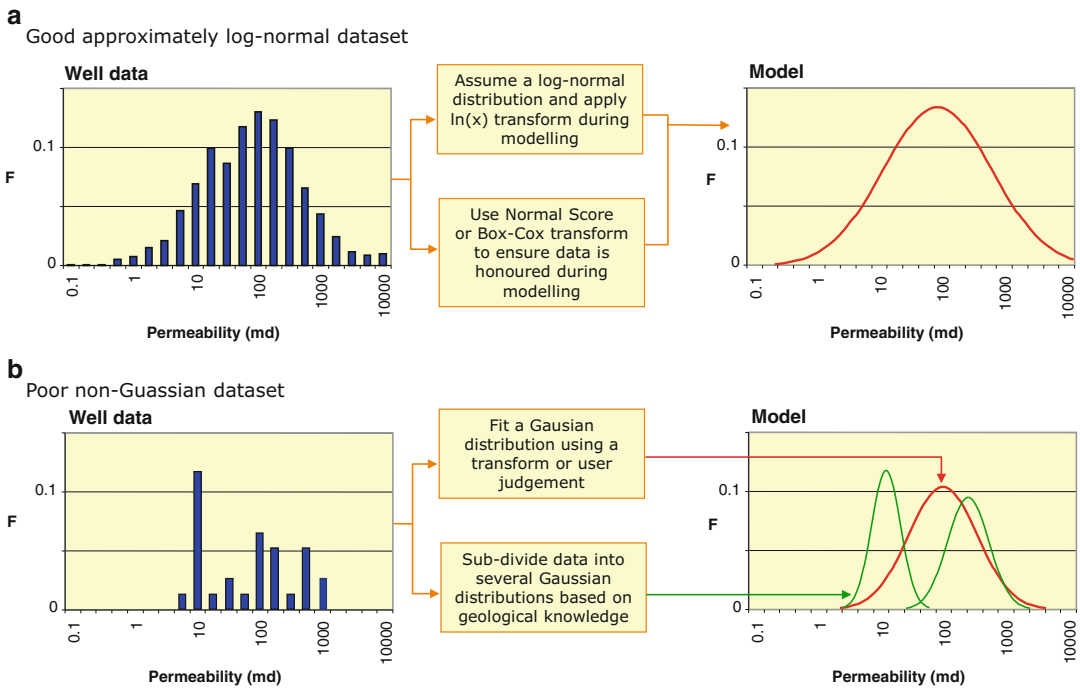

Fig. 3.16 Illustration of data-to-model transforms for (**a**) a well-sampled dataset, and (**b**) a poorly-sampled datasets

this is the "correct" average for flow calculations. In fact, for a layered model with layer values drawn from a log-normal distribution the layer-parallel effective permeability is given by the arithmetic average (see previous section).

There are several useful transforms other than the log-normal transform. The Box–Cox transform (Box and Cox 1964), also known as a power transform, is one of the most versatile and is essentially a generalisation of the log normal transform. It is given by:

$$x^{(\lambda)} = \frac{\left(x^{\lambda} - 1\right)}{\lambda} \quad if\ \lambda \neq 0 \qquad (3.21)$$

$$x^{(\lambda)} = \ln(x) \quad if\ \lambda = 0$$

where the power λ determines the transformed distribution $x^{(\lambda)}$. The square-root transform is given by λ = ½ and for λ = 0 the transform is the log-normal transform.

Another transform widely used in reservoir property modelling is the *normal score transform (NST)* in which an arbitrary distribution is transformed into a normal distribution, using a form of ranking (Deutsch and Journel 1992; Journel and Deutsch 1997). This is done using a cumulative distribution function (cdf) where each point on the cdf is mapped into a standard normal distribution using a transform (the score). There are several ways of doing this but the most common (and simple) is the linear method in which a linear factor is applied to each step (bin) of the cumulative distribution (for a fuller explanation see Soares 2001). This allows any arbitrary distribution to be represented and modelled in a geostatistical process (e.g. Sequential Gaussian Simulation). Following simulation, the results must be back transformed to the original distribution.

These transforms are illustrated graphically in Fig. 3.16. We should add an important note of caution when selecting appropriate transforms in any reservoir modelling exercise. It may be tempting to allow default transforms in a given modelling package (notably the NST) to automatically handle a series of non-Gaussian input data (e.g. Fig. 3.16b). This can be very misleading and essentially assumes that your data cdf's are

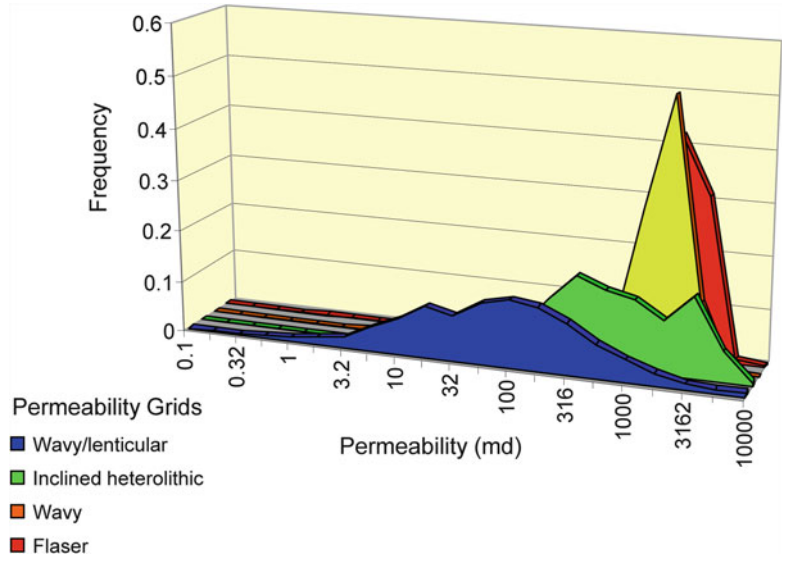

Fig. 3.17 Probe permeability datasets using a 2 mm-spaced measurements on a 10 cm grid of reservoir core slabs from facies in a tidal deltaic reservoir unit

very close to the true population statistics. This is in conflict with the Data ≠ Truth axiom. It is preferable to control and select the transforms being used, and only employ the Normal Score Transform when clearly justified. The selection of the model elements (Chap. 2) is the first step to deconstructing a complex distribution, after which the normal score transform may indeed be applicable: one for each model element.

Two examples of something close to "true" reservoir permeability distributions are shown in Fig. 3.17. Here, exhaustive probe permeability datasets have been assembled using a 2 mm-spaced measurements on a 10 cm grid of reservoir core slabs from facies in a tidal deltaic reservoir unit. In one case, the permeability distribution is close to log-normal, while the others they are clearly not – more root normal or multi-modal.

With more conventional data sets (e.g. core plug sample datasets), we also have the problem of under-sampling to contend with. Figure 3.18 shows three contrasting core plug porosity datasets. The first (a) could be successfully represented by a normal distribution while the second (b) is clearly neither normal nor log-normal. The third (c) is a typical under-sampled dataset where the user needs to infer a 'restored' porosity distribution.

Whatever the nature of the underlying distributions in a reservoir dataset, we should bear in mind an important principle embodied by the *Central Limit Theorem* which can be summarized as follows:

> *The distribution of sample means from a large number of independent random variable usually approximates a normal distribution regardless of the nature of the underlying population distribution functions.*

For example, let us assume we have N wells with permeability data for a given reservoir unit. For each well, we have observed distributions of k which appear to be approximately log-normally distributed (a common observation). However, the distribution of the average well-interval permeability between wells (the mapped parameter) is found to be normally distributed. This is quite consistent, and indeed for a large number of wells this is expected from Central Limit Theory. Similar arguments can apply when upscaling – fine-scale permeability distributions may be quite complex (log-normal or multi-modal) while coarse-scale distributions tend towards being normally distributed. An important constraint for the central limit theorem is that the samples should be statistically independent and reasonably large.

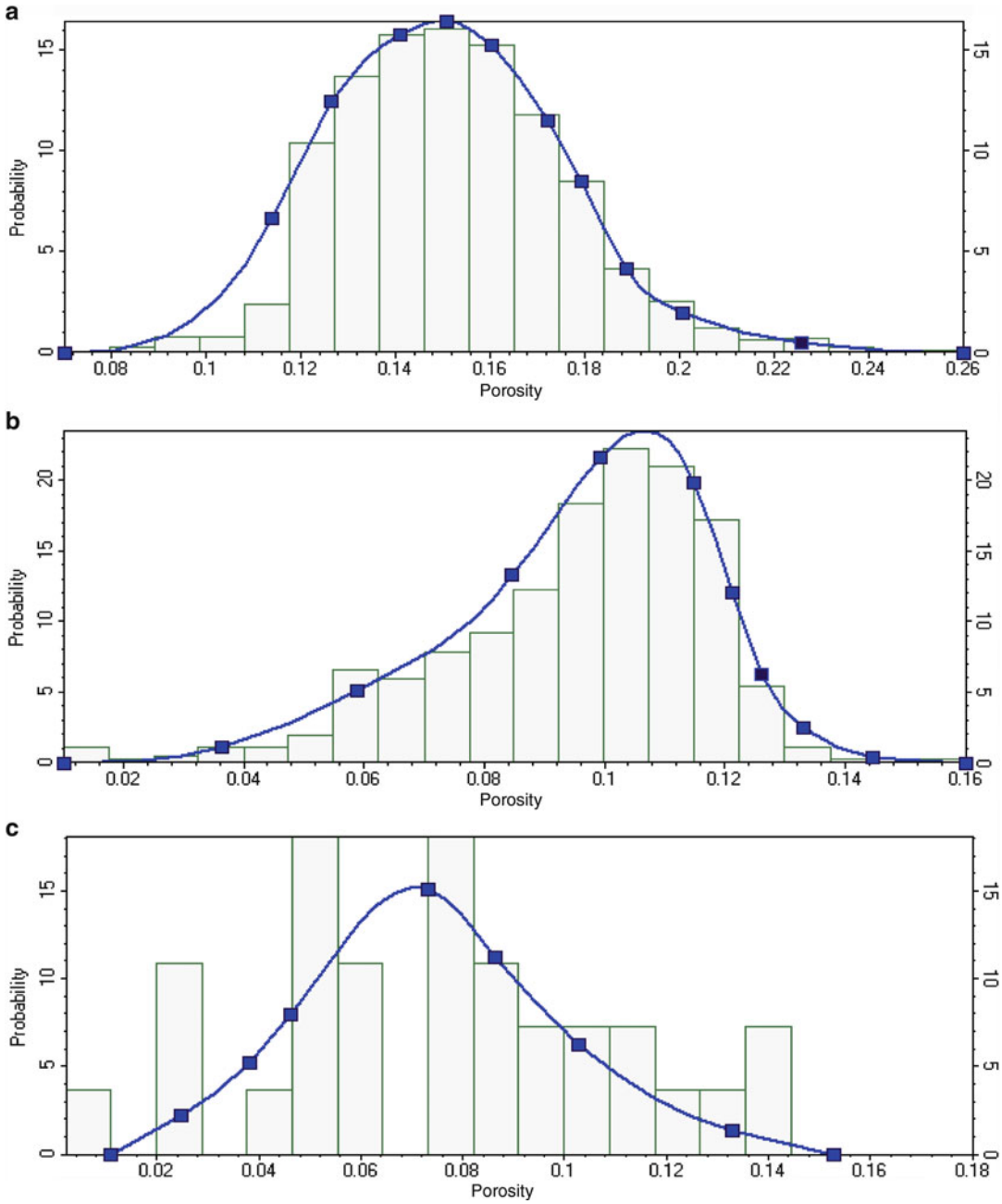

Fig. 3.18 Example sandstone reservoir porosity distributions (*histograms*) and possible model distributions fitted to the data: (**a**) approximately log-normal, (**b**) neither normal nor log-normal, (**c**) under-sampled

3.3.4 Handling ϕ-k Distributions and Cross Plots

Plots of porosity (ϕ) versus permeability (k) are fundamental to the process of reservoir modelling (loosely referred to as poro-perm cross-plots). Porosity represents the available fluid volume and permeability represents the ability of the fluid to flow. In petroleum engineering, porosity is the essential factor determining fluids in place while permeability is the essential factor controlling production and reserves.

(In groundwater hydrology, the terms storativity, a function of the effective aquifer porosity, and the hydraulic conductivity are often used).

Poro-perm cross-plots are used to perform many functions: (a) to compare measured porosity and permeability from core data, (b) to estimate permeability from log-based porosity functions in uncored wells, and (c) to model the distribution of porosity and permeability in the inter-well volume – reservoir property modelling. Good reservoir model design involves careful use of ϕ-k functions while poor handling of this fundamental transform can lead to gross errors. It is generally advisable to regress permeability (the dependent variable) on porosity (as the independent variable).

In general, we often observe permeability data to be log-normally distributed while porosity data is more likely to be normally distributed. This has led to a common practice of plotting porosity versus the log of permeability and finding a best-fit function by linear regression.

Although useful, this assumption has pitfalls:

(a) Theoretical models and well-sampled datasets show that true permeability versus porosity functions depart significantly from a log-linear function. For example, Bryant and Blunt (1992) calculated absolute permeability – using a pore network model – for randomly packed spheres with different degrees of cementation to predict a function (Fig. 3.19) that closely matches numerous measurements of the Fontainebleau sandstone (Bourbie and Zinszner 1985).
(b) Calculations based on an exponential trend line fitted to log-transformed permeability data can lead to serious bias due to a statistical pitfall (Delfiner 2007).
(c) Multiple rock types (model elements) can be grouped inadvertently into a common cross plot which gives a misleading and unrepresentative function.
(d) Sampling errors, including application of cut-offs, lead to false conclusions about the correlation between porosity and permeability.

Delfiner (2007) reviews some of the important pitfalls in the k-ϕ transform process, and in particular recommends using a permeability estimator based on percentiles – Swanson's mean. Swanson's mean permeability, k_{SM}, for a given class of porosity (e.g. 15–20 %) is given by:

$$k_{SM} = 0.3\,X_{10} + 0.4\,X_{50} + 0.3\,X_{90} \qquad (3.22)$$

where, X_{10} is the tenth percentile of the permeability values in the porosity class.

The resulting mean is robust to the log-linear transform and insensitive to the underlying distribution (log-normal or not). The result is a significantly higher k_{mean} than obtained by a simple trend-line fit through the data.

Figure 3.20 illustrates the use of the k-ϕ transform within the Data ≠ Model ≠ Truth paradigm. True pore systems have a non-linear relation between porosity and permeability, depending on the specific mechanical and chemical history of that rock (compaction and diagenesis). We use the Fountainebleau sandstone trend to represent the "true" (but essentially unknown) k-ϕ relationship (Fig. 3.20a). Core data may, or may not, give us a good estimate of true relationship between porosity and permeability, and the

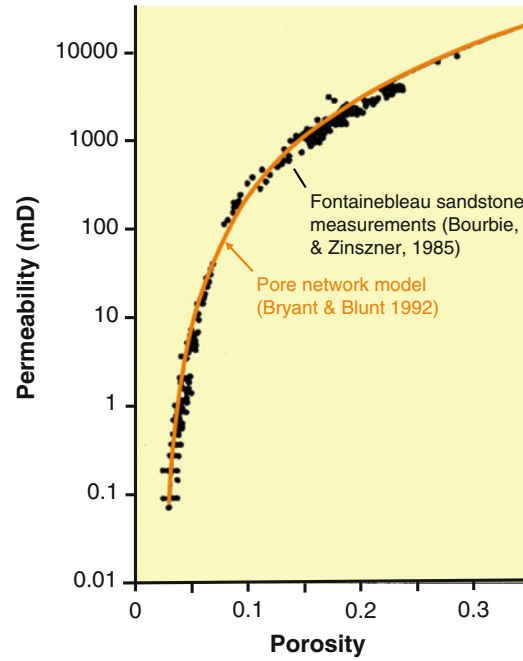

Fig. 3.19 Pore-network model of a porosity-permeability function closely matched to data from the Fontainebleau sandstone

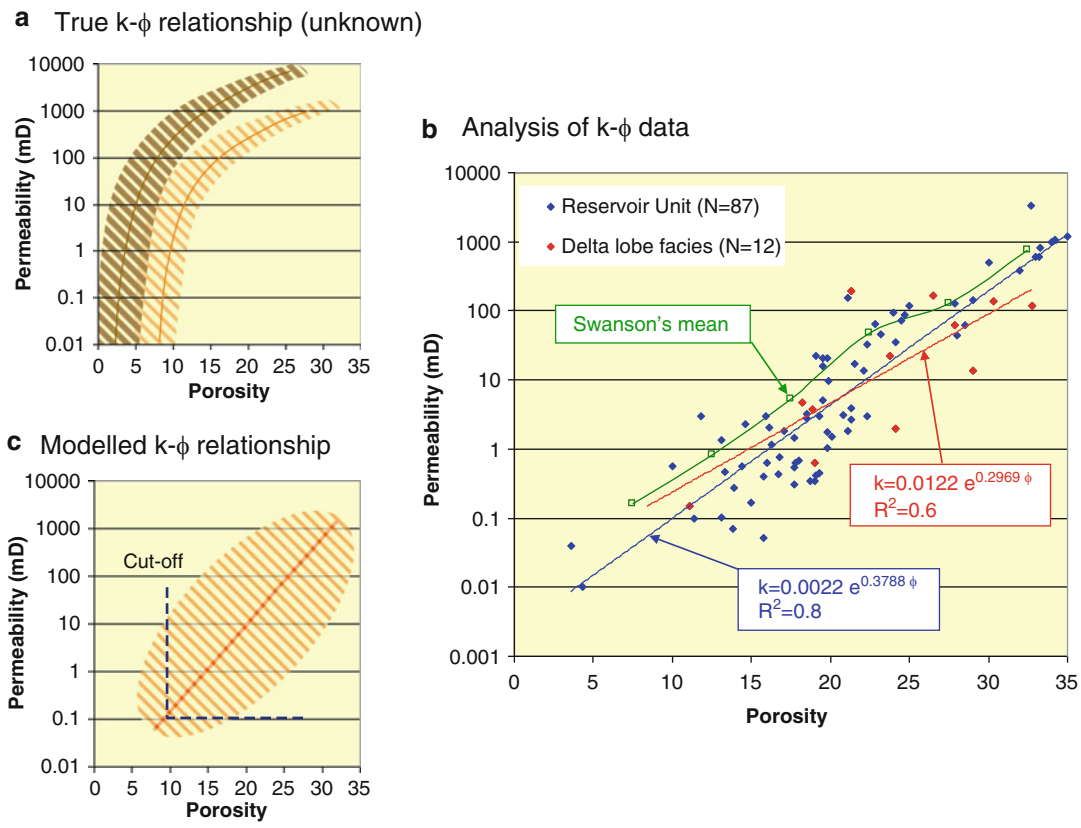

Fig. 3.20 Use of the k-ϕ transform: (**a**) True pore systems exhibit a non-linear relationship with dispersion, (**b**) Data analysis is sensitive to the choice of rock groups and statistical analysis method; (**c**) The model function should be constrained by data and fit-for-purpose

inferred function is strongly dependent on rock grouping and sample size. For example, in Fig. 3.20b, the correlation coefficient (R^2) for a single facies is significantly lower than for the total reservoir unit (due to reduced sample size). Furthermore, for the whole dataset, Swanson's mean gives a higher permeability trend than with a simple exponential fit to the data. The modelled k-ϕ transform (Fig. 3.20c) should be designed to both faithfully represent the data and capture rock trends or populations (that may not be fully represented by the measured data). Upscaling leads to further transformations of the k-ϕ model. In general, we should expect a reduction in variance (therefore improved correlation) in the k-ϕ transform as the length-scale is increased (refer to discussion on variance in Chap. 4).

We have introduced two end member approaches to modelling:

(a) Concept-driven

(b) Data-driven

The concept-driven approach groups the data into a number of distinct model elements, each with their own k-ϕ transform. Simple log transforms and best-fit functions are used to capture trends but k-ϕ cross-correlation is poor and belief in the data support is weak. The process is 'model-driven' and the explicitly modelled rock units capture the complex relationship between porosity and permeability. The data-driven approach assumes a representative dataset and a minimal number of model elements are distinguished (perhaps only one). Care is taken to correctly model the observed k-ϕ transform, using for example a piecewise or percentile-based formula (e.g. Swanson's mean).

The reservoir model is 'data-driven' and the carefully-modelled k-ϕ transform aims to capture the complex relationship between porosity and permeability.

3.3.5 Hydraulic Flow Units

The Hydraulic Flow Unit (HFU) concept offers a useful way of classifying properties on the k-ϕ cross-plot, and can be linked to the definition of model elements in a modelling study. Abbaszadeh et al. (1996) defined HFU's in terms of a modified Kozeny-Carmen equation in which a Flow Zone Indicator, F_{zi}, was used to capture the shape factor and tortuosity terms.

Modifying the Kozeny-Carmen equation gives:

$$0.0314\sqrt{\frac{k}{\emptyset_e}} = \frac{\emptyset_e}{1-\emptyset_e}F_{zi} \qquad (3.23)$$

where k is in mD and ϕ_e is the effective porosity

F_{zi} is a function of the tortuosity, τ, the shape factor, F_s, and the surface area per unit grain volume, S_{gv}:

$$F_{zi} = \frac{1}{\tau\sqrt{F_s}S_{gv}} \qquad (3.24)$$

The F_{zi} term thus gives a formal relationship between k and ø which is related to pore-scale flow physics (laminar flow in a packed bed of spherical particles).

Exercise 3.4

Comparing model distributions to data.

The plot and table below show a comparison of well data with the output of a model realisation designed to represent the data in a geological model. The well data are from a cored well interval identified as a deltaic sandstone facies. The model has used Gaussian statistical modelling to represent the spatial distribution of permeability. The two distributions appear to match quite well – they cover a similar range and have a similar arithmetic mean. However, analysis of the data statistics reveals some strange behaviour – the geometric and harmonic means are quite different.

What is going on here? And is this in fact a good model for the given data?

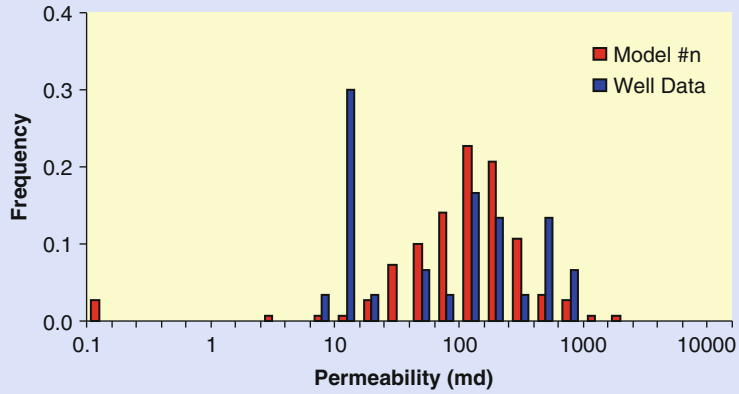

Statistics	Well data	Model #n
Number of data values/cells	30	150
Arithmetic mean	119.9	115.7
Geometric mean	45.9	90.8
Harmonic mean	17.19	0.87

3.4 Modelling Property Distributions

Assuming we have a geological model with certain defined components (zones, model elements), how should we go about distributing properties within those volumes? There are a number of widely used methods. We will first summarize these methods and then discuss the choice of method and input parameters.

The basic input for modelling spatial petrophysical distribution in a given volume requires the following:

- Mean and deviation for each parameter (porosity, permeability, etc.);
- Cross-correlation between properties (e.g. how well does porosity correlate with permeability);
- Spatial correlation of the properties (i.e. how rapidly does the property vary with position in the reservoir);
- Vertical or lateral trends (how does the mean value vary with position):
- Conditioning points (known data values at the wells).

The question is "How should we use these input data sensibly?" Commercial reservoir modelling packages offer a wide range of options, usually based on two or three underlying geostatistical methods (e.g. Hohn 1999; Deutsch 2002). Our purpose is to understand what these methods do and how to use them wisely in building a reservoir model.

3.4.1 Kriging

Kriging is a fundamental spatial estimation technique related to statistical regression. The approach was first developed by Matheron (1967) and named after his student Daniel Krige who first applied the method for estimating average gold grades at the Witwatersrand gold-bearing reef complex in South Africa. To gain a basic appreciation of Kriging, take the simple case of an area we want to map given a few data points, such as wells which intersect the reservoir layer (Fig. 3.21).

We want to estimate a property, Z* at an unmeasured location, o, based on known values of Z_i at locations x_i. Kriging uses an interpolation function:

$$Z^* = \sum_{i=1}^{n} \omega_i Z_i \qquad (3.25)$$

where ω_i are the weights, and employs an *objective function* for minimization of variance.

That is to say a set of weights are found to obtain a minimum expected variance given the available known data points.

The algorithm finds values for ω such that the objective function is honoured. The correlation function ensures gradual changes, and Kriging will tend to give a smooth function which is close to the local mean. Mathematically there are several ways of Kriging, depending on the assumptions made. *Simple Kriging* is mathematically the simplest, but assumes that the mean

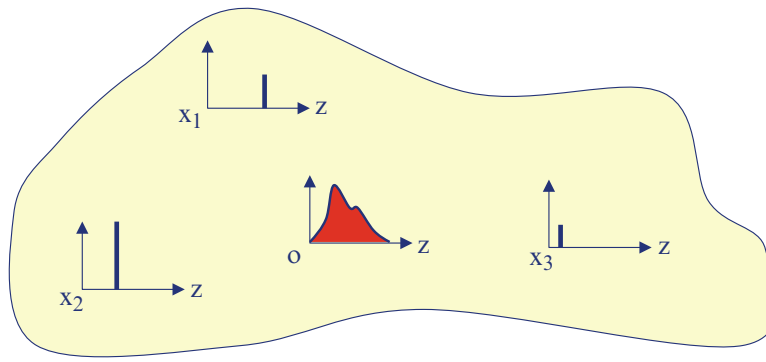

Fig. 3.21 Illustration of the Kriging method

and distribution are known and that they are statistically stationary (i.e. a global mean). *Ordinary Kriging* is more commonly used because it assumes slightly weaker constraints, namely that the mean is unknown but constant (i.e. a local mean) and that the variogram function is known. Fuller discussion of the Kriging method can be found in many textbooks; Jensen et al. (2000) and Leuangthong et al. (2011) give very accessible accounts for non-specialists.

3.4.2 The Variogram

The variogram function describes the expected spatial variation of a property. In Chap. 2 we discussed the ability of the variogram to capture element architecture. Here we employ the same function as a modelling tool to estimate spatial property variations within that architecture. We recall that the semi-variance is half the expected value of the squared differences in values separated by h:

$$\gamma(h) = \frac{1}{2}E\left\{[Z(x+h) - Z(x)]^2\right\} \qquad (3.26)$$

The semi-variogram (Fig. 3.22) has several important features. The lag (h) is the separation between two points. Two adjacent points will tend to be similar and have a γ(h) of close to zero. A positive value at zero lag is known as the nugget. As the lag increases the chance of two points having a similar value decreases, and at some distance a sill is reached where the average difference between two points is large, and in fact close to the variance of the population. The range (equivalent to the correlation length) describes the 'separation distance' at which this occurs. A theoretical semi-variogram has a smooth function rising up towards the variance while measured/observed semi-variogram often has oscillations and complex variations due to, for example, cyclicity in rock architecture.

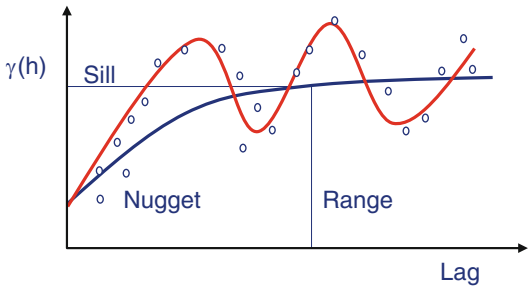

Fig. 3.22 Sketch of the semi-variogram (*blue* = theoretical function; *red* = function through observed data points)

The most common functions for the semi-variogram are spherical, Gaussian and exponential – each giving a different rate of rise towards the sill value (ref. Fig. 2.24). Note that for a specific situation (second order stationarity) the semi-variogram is the inverse of the covariance (de Marsilly 1986, p. 292). Jensen et al. (1995) and Jensen et al. (2000) give a more extensive discussion on the application of the semi-variogram to permeability data in the petroleum reservoirs.

3.4.3 Gaussian Simulation

Gaussian Simulation covers a number of related approaches for estimating reservoir properties away from known points (well observations). The Sequential Gaussian Simulation (SGS) method can be summarized by the following steps (Jensen et al. 2000):

1. Transform the sampled data to be Gaussian;
2. Assign unconditioned cells (inter-well) = conditioned cells (wells);
3. Define a random path to visit each cell;
4. For each cell locate a specified number of conditioning data (the neighbourhood);
5. Perform Kriging in the neighbourhood to determine the local mean and variance (using the variogram as a constraint);
6. Draw a random number to sample the Gaussian distribution (from step 5);
7. Add the new simulated value to the "known" data. Repeat step 4.

Repeating steps 4–7 gives one realisation of a Gaussian random distribution conditioned to known points. Repeating step 3 gives a new realisation. The average of a large number of realisations will approach the kriged result. In this way we can use Gaussian simulation to

give a spatial statistical model of reservoir properties. A good geostatistical model should give a realistic picture of petrophysical structure and variability and can be used for flow simulation and for studies to define drilling targets. However, one realisation is only one possible outcome, and many realisations normally need to be simulated to assess variability and probability of occurrence. To put this in practical terms, a single realisation might be useful to define static heterogeneity for a flow simulation model, but a single realisation would be little value in planning a new well location. For well planning or reserves estimation, the average expectation from many realisations, or a Kriged model, would be a more statistically stable estimate.

Truncated Gaussian Simulation (TGS) is a simple modification of SGS where a particular threshold value of the simulated Gaussian random field is used to identify a rock element or petrophysical property group, such as porosity > X (Fig. 3.23). *Sequential Indicator Simulation* (SIS) uses a similar approach but treats the conditioning data and the probability function as a discrete (binary) variable from the outset (Journel and Alabert 1990). The indicator transform is defined by:

$$i\left(\vec{u};z\right)=\begin{cases}1, & if\ z\left(\vec{u}\right)\le z\\ 0, & if\ not\end{cases} \tag{3.26}$$

where z is the cut-off value for a field of values $\vec{u}$

The field $\vec{u}$ could be derived from, for example, porosity data, the gamma-ray log or seismic impedance. The important decision is the choice of the indicator value. Both these methods are useful for modelling rock elements (Sect. 2.7) as well as for modelling property distributions within elements.

Figure 3.23 illustrates the different methods of Gaussian simulation. The methods can be used in a number of ways, for example to define several nested groups of facies and the properties within them. Gaussian simulation is an essential part of the tool kit for property modelling, and also a key tool for data integration, especially for combining well data with seismic inversion data. Doyen (2007) gives an in-depth account of seismic-based rock property modelling including a detailed description of the application of the SGS and SIS methods to seismic datasets.

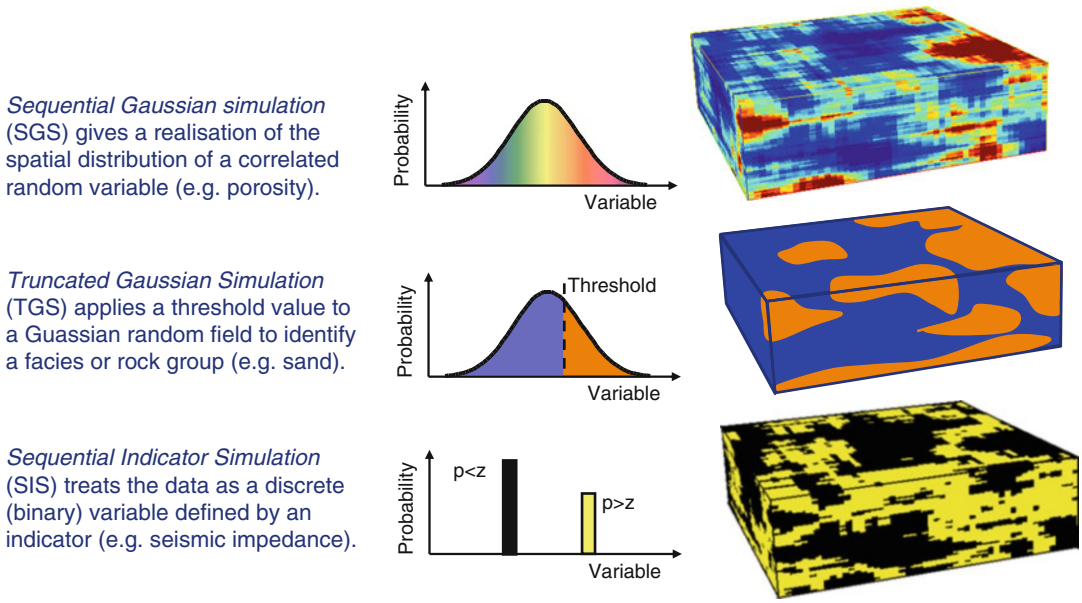

Fig. 3.23 Illustration of the different methods for property modelling using Gaussian simulation

Given that we have a set of recipes for different property modelling methods, how do we combine them to make a good property model? Remember that the mark of a good model is that it is geologically-based and fit for purpose. To illustrate the different approaches to property model design we describe two approaches based on case studies:

- An object-based model of channelized facies based on detailed outcrop data;
- A seismic-based facies model, exploiting good 3D seismic data.

3.4.4 Bayesian Statistics

We have now reviewed the main statistical tools employed in property modelling; however, one important concept is missing. We argued in Chap. 2 that reservoir modelling must find a balance between determinism and probability, and that more determinism is generally desirable. Using Gaussian simulation methods without firm control from the known data is generally unhelpful and dissatisfying. We ideally want geostatistical property models rooted in geological concepts and conditioned to observations (well, seismic and dynamic data), and this is where Bayes comes in. Thomas Bayes (1701–1761) developed a theorem for updating beliefs about the natural world and then later his ideas were developed and formalised by Laplace (in *Théorie analytique des probabilités*, 1812). Subsequently, over the last 50 years Bayesian theory has revolutionized most fields of statistical analysis, not least reservoir modelling.

Bayesian inference derives one uncertain parameter (the posterior probability) from another (the prior probability) via a likelihood function. Bayes' rule states that:

$$P(A|B) = \frac{P(B|A)P(A)}{P(B)} \tag{3.27}$$

where:

P(A|B) is the *posterior* – the probability of A assuming B is observed,

P(A) is the *prior* – the probability of A before B was observed,

P(B|A) is the *likelihood* (of what was actually observed),

P(B) is the underlying evidence (also termed the marginal likelihood).

This comparison of prior and posterior probabilities may at first appear confusing, but is easily explained using a simple example (Exercise 3.5), and fuller discussion can found elsewhere (e.g. Howson and Urbach 1991). The essence of Bayesian estimation is that a probabilistic variable (the posterior) can be estimated given some constraints (the prior). This allows probabilistic models to be constrained by data and observations, even when those data are incomplete or uncertain. This is exactly what probabilistic reservoir models need – a dependence on, or conditioning to, observations. Bayesian methods are used to condition reservoir models to seismic, well data and dynamic data, and are especially valuable for integrating seismic and well data.

Exercise 3.5

Bayes and the cookie jar.

A simple example to illustrate Bayes theory is the "cookie jar" example. There are two cookie jars. One jar has 10 chocolate chip cookies and 30 plain cookies, while the second jar has 20 of each. Fred picks a jar at random, and then picks a cookie at random – he gets a plain one. We all know intuitively he could have picked from either jar, but most likely picked from Jar 1. Use Bayes theory Eq. (3.27) to find probability that Fred picked the cookie from Jar 1.

The answer is 0.6 – but why?

3.4.5 Property Modelling: Object-Based Workflow

Geological modelling using object-based methods was explained in Chap. 2. The geological objects (i.e. model elements such as channels, bar forms, or sheet deposits) need petrophysical properties to be defined. This could be done in a

Table 3.3 Example object dimensions and correlation lengths from the Lajas outcrop model study

Facies	Object length (m)	Object width (m)	Object thickness (m)
Meandering channels	1,000	300	2
Trough cross-bedded cannels	1,000	100	1.5
Mixed tidal flats	500	400	0.5
Correlation lengths for properties within objects	Horizontal correlation length λ_x, λ_y (m)		Vertical correlation length, λ_z (m)
All facies	50–500		0.5–5.0

very simplistic manner – such as the assumption that all channel objects have a constant porosity and permeability – or can be done by "filling" the objects with continuous properties using a Gaussian simulation method. Each model element is assigned the statistical parameters required to define a continuous property field (using Sequential Gaussian Simulation) which applies only to that element. This process can become quite complicated, but allows enormous flexibility and the ability to condition geological reservoir models to different datasets for multiple reservoir zones.

This process is illustrated for an object-based model used for stochastic simulation of permeability for an outcrop model (Brandsæter et al. 2005). A section from the Lajas Formation in Argentina (McIlroy et al. 2005) was modelled due to its value as an analogue to several reservoirs in the Hatenbanken oil and gas province offshore mid Norway. The model is 700 m by 400 m in area and covers about 80 m of stratigraphy – it is thus a very-high resolution model highly constrained by detailed outcrop data. The model illustrates how an object model (based on outcrop data) can be combined with Gaussian simulation of petrophysical properties (based on well data from the Heidrun oilfield offshore Norway). Note that in this case we assign reservoir properties to the outcrop model, whereas normally we would make a reservoir model assuming geological object dimensions derived from outcrop studies.

Table 3.3 summarises some of the dimensions assumed for the geological objects in this model. Object lengths are in the range of 500 m to 1,000 m, with widths slightly smaller, while object thicknesses are in the in 0.5–2 m range. These values have some uncertainty but are relatively well known as they are based on detailed study of the outcrop. However, the correlation lengths, λ_x, λ_y, λ_z, that are required to control property distributions within objects are much less well constrained. In this study, a plausible range of correlation lengths (Table 3.3) was assumed and used as input to a sensitivity analysis. The range was chosen to test the effects of highly-varying or gradually-varying properties within objects (Fig. 3.24). Sensitivity analysis showed that oil production behaviour is very sensitive to this value, alongside the effects of anisotropy and facies model (Brandsæter et al. 2005).

In general, we expect there to be some property variation within geological objects, therefore λ_x, λ_y, λ_z, $<$ object dimension. The question is how much variation? The choice of correlation lengths for property modelling is therefore very uncertain and also rather important for flow modelling. In practice, sensitivity to this parameter needs to be evaluated as part of the model design. The value range should be constrained to any available geological data and to evidence from dynamic data, such as the presence or absence of pressure communication between wells in the same facies or reservoir unit.

A useful guideline is to test the following hypotheses:

(a) Properties are relatively constant within geological objects: $\lambda \approx$ object dimension.
(b) Properties are quite variable within geological objects: $\lambda \approx 1/3$ object dimension.
(c) Properties are highly variable within geological objects: $\lambda \approx 1/10$ object dimension.

Note that the grid size needs to significantly smaller than the correlation length being modelled (e.g. $\lambda \approx 1/10$ object dimension would require a very fine grid).

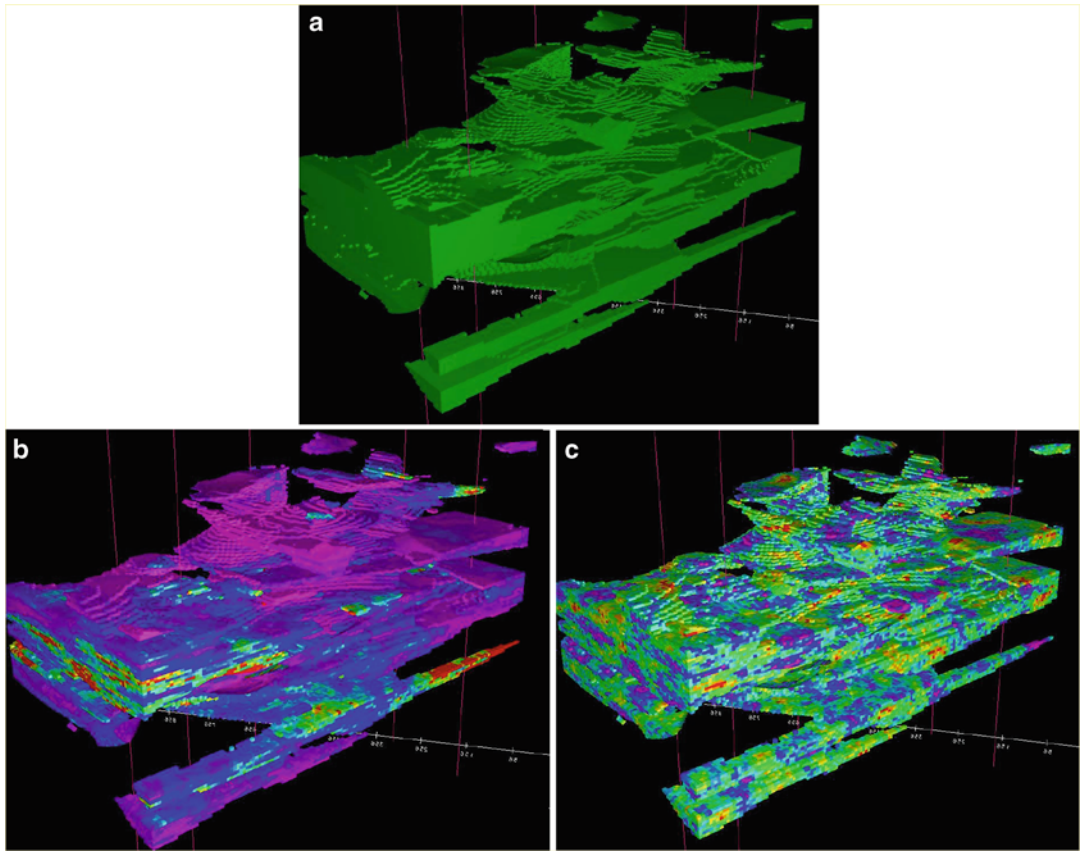

Fig. 3.24 Property model examples from the Lajas tidal delta outcrop model (Brandsæter et al. 2005): (**a**) Modelled tidal channel objects; (**b**) Permeability realisation assuming a short correlation length of 50 m horizontally and 0.5 m vertically; (**c**) Permeability realisation assuming a long correlation length 500 m horizontally and 5 m vertically. *Yellow* and *red* indicate high permeability values while *blue* and *purple* indicate low permeability values

3.4.6 Property Modelling: Seismic-Based Workflow

Seismic imaging has made enormous leaps and bounds in the lasts decades – from simple detection of rock layers that might contain oil or gas to 3D imaging of reservoir units that almost certainly do contain oil and gas (using direct hydrocarbon indicators). In this book we have assumed that seismic imaging is always available in some form to define the reservoir container (e.g. the top reservoir surface and bounding faults). Here we are concerned with the potential for using seismic data to obtain information about the reservoir properties – such as porosity or the spatial distribution of high porosity sandstones.

There are numerous recipes available for obtaining reservoir properties from seismic data (e.g. Doyen 2007). These are all based on the underlying theory of seismology in which reflected or refracted seismic waves are controlled by changes in the density (ρ) and velocity (V_P, V_S) of rock formations. More specifically, seismic imaging is controlled by the acoustic impedance, $AI = \rho V_P$ (for a compressional wave). Zoeppritz, in 1919, determined the set of equations which control the partitioning of

seismic wave energy at a planar interface, and then subsequently many others (notably Shuey 1985) developed approaches for determining rock properties from seismic waves. Because there is a relationship between the reflection coefficient, R, and the angle of incidence, θ, analysis of seismic amplitude variations with offset (AVO) or angle (AVA) allows rock properties of specific rock layers to be estimated.

The simplest form of the AVO equations, known as the Shuey approximation is:

$$R(\theta) = R(0) + G\,sin^2\theta \qquad (3.28)$$

Where R(0) and R(θ) are the reflection coefficients for normal incidence and offset angle θ and G is a function of V_P and V_S, given by:

$$G = \frac{1}{2}\frac{\Delta V_P}{V_P} - 2\frac{V_S^2}{V_P^2}\left(\frac{\Delta\rho}{\rho} + 2\frac{\Delta V_S}{V_S}\right) \qquad (3.29)$$

Subsequently, using empirical correlations, it is then possible to estimate porosity from V_P, V_S and ρ. Assuming that information on rock properties can be gained from seismic data, the next challenge is to find a way of integrating seismic information with well data and the underlying geological concepts. The real challenge here is that well data and seismic data rarely tell the same story – they need to be reconciled. Both seismic data and well data have associated uncertainties. They also sample different volumes with the reservoir – well data needs to be upscaled and seismic data needs to be downscaled (depending on the grid resolution and seismic resolution of the case in hand). This is where the Bayesian method comes into play.

Buland et al. (2003) developed a particularly elegant and effective method for estimating rock properties from AVO data, employing Bayesian inference and the Fourier transform. This approach allows the reservoir modeller to reconcile different scales of data (seismic versus well data, using the Fourier transform) within a robust Bayesian statistical framework: what is the best seismic inversion given the well data – a P(A|B) problem. Nair et al. (2012) have illustrated this workflow for reservoir characterization, combining elastic properties (from seismic) with facies probability parameters (from wells) to condition probabilistic property models.

Having first extracted elastic properties (V_P, V_S and ρ from the seismic AVA data (Fig. 3.25), the challenge is then to relate elastic properties to flow properties.

Since flow properties are essentially estimated from well data (cores and logs), we need to merge (or correlate) the seismic elastic properties with elastic and flow properties at the wells. This is a complicated process. We need a velocity model to convert seismic data from time to depth and we need a way handling the scale

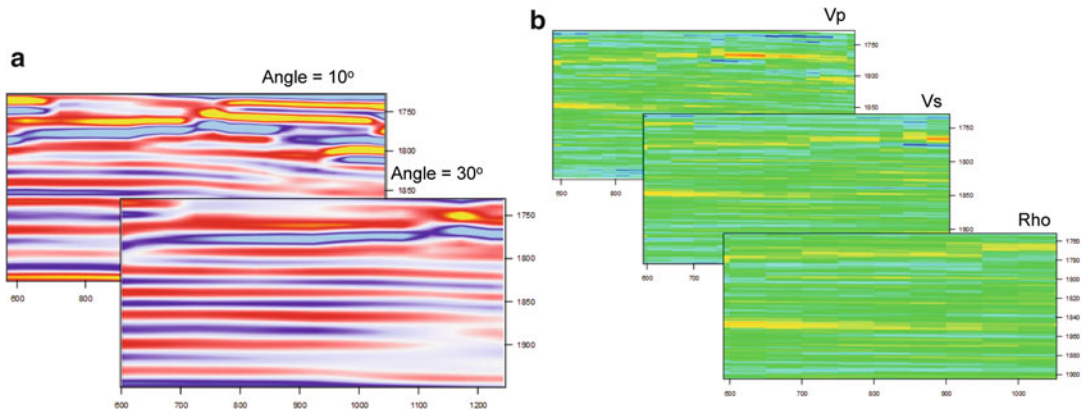

Fig. 3.25 (**a**) Angle stacks and (**b**) corresponding inverted elastic parameters from seismic inversion case study (From Nair et al. 2012) (Redrawn from Nair et al. 2012, ©EAGE reproduced with kind permission of EAGE Publications B.V., The Netherlands)

transition, since well data has high frequency content not present in the seismic data. Using Bayesian reasoning, Buland et al. (2003) and Nair et al. (2012) use the following steps:

(i) Assign the elastic properties from well data as a prior probability model, p(m);
(ii) Treat the seismic AVA data (d) as a likelihood model, p(d|m);
(iii) The Bayesian inversion is then posterior probability model, p(m|d).

To handle the band-limitations of the seismic data a low frequency background model is needed. This is estimated from vertical and lateral trends in the well log data using Kriging to generate a smoothed background model. This background model itself should capture the underlying geological concepts (sand fairways, porosity trends) but is also critical to the seismic inversion. Figure 3.26 shows an example comparison of raw versus inverted V_p logs, an important step in quality control of the process.

The solutions to seismic AVA inversion are non-unique and entail large amounts of data – wavelets and reflection coefficients for each offset angle throughout the volume of interest. By transferring the data into the Fourier domain (the frequency spectrum), Buland et al. (2003) used a fast Fourier transform to handle the seismic covariance matrices and to separate the signal and noise terms. Figure 3.27 compares AI from seismic inversion (the prediction) with two stochastic realisations of simulated AI, incorporating both seismic data and well data. Notice the finer resolution of simulated cases because of inclusion of higher frequency well data with the seismic data in this Bayesian workflow.

The potential for deriving rock properties from seismic data is enormous. The V_p/V_s versus impedance plot (e.g. Fig. 3.28) is widely used as a rock physics template, giving the potential for estimation of facies and flow properties from seismic data. Exactly how successfully this can be done depends on the case at hand and the data quality. We should add a cautionary reminder to seismic inversion enthusiasts – the transform from elastic properties to flow properties is not a simple one, and there are many pitfalls. However, in the hands of an experienced reservoir modeller the Bayesian statistical framework offers a rather elegant way of making that leap from 3D seismic data to predictive flow property models.

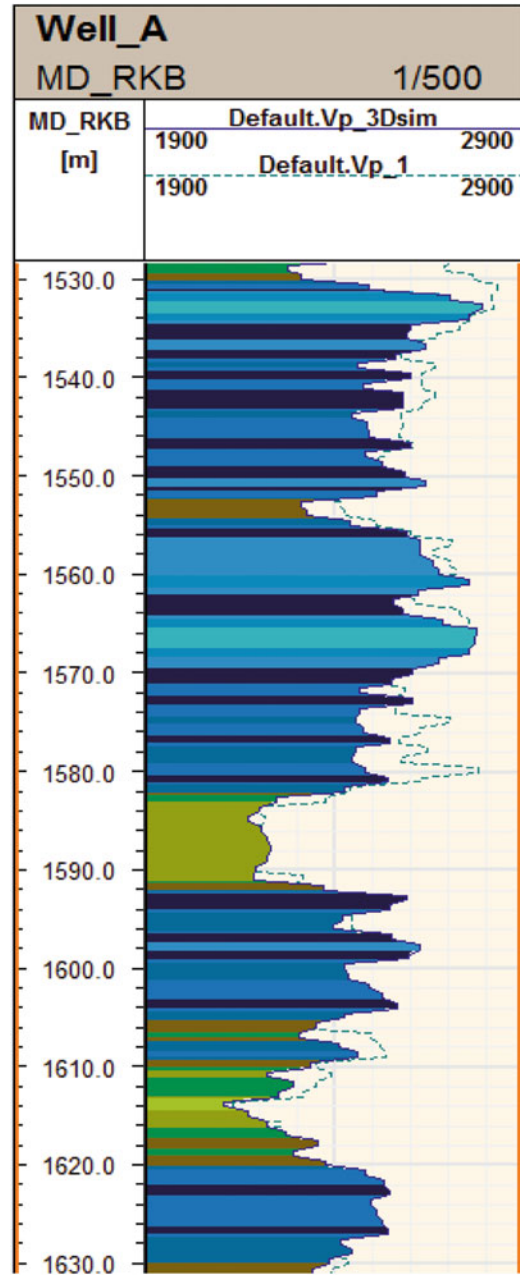

Fig. 3.26 Comparison of raw V_p logs (*dashed lines*) with V_p logs extracted along the well from the inverted 3D seismic data (*continuous lines*), from Nair et al. (2012) (Redrawn from Nair et al. 2012, ©EAGE reproduced with kind permission of EAGE Publications B.V., The Netherlands)

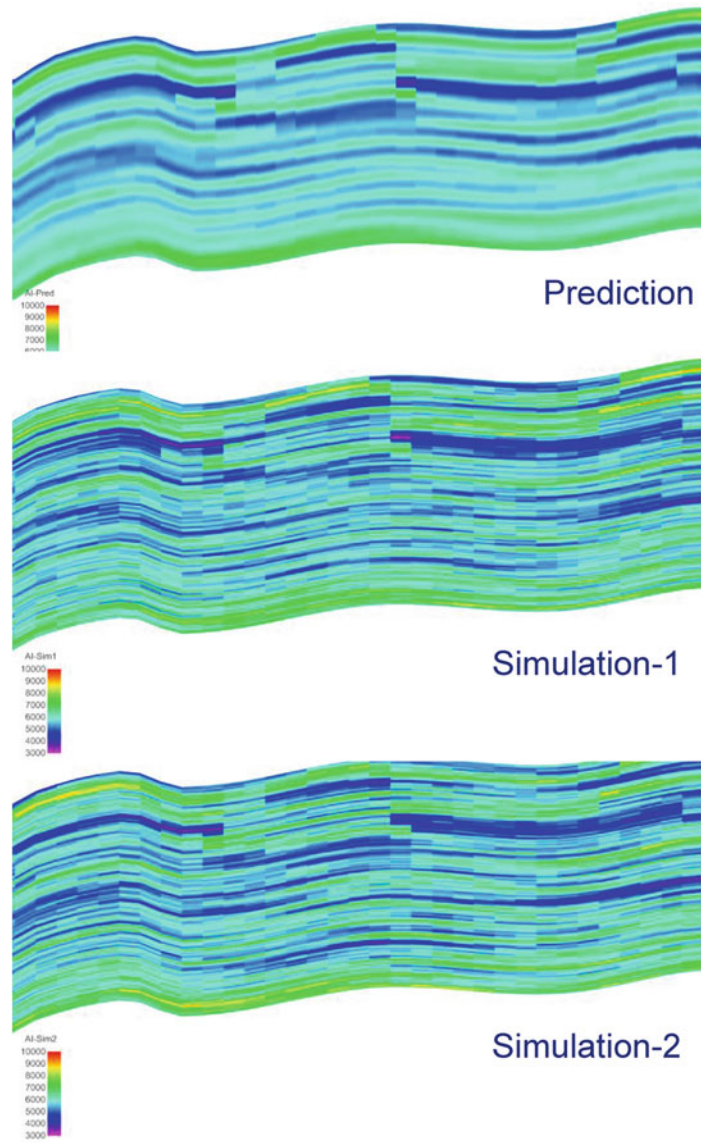

Fig. 3.27 Comparison of AI predicted from seismic inversion with two stochastic simulations integrating both the seismic and the fine-scale well data (From Nair et al. 2012) (Redrawn from Nair et al. 2012, ©EAGE reproduced with kind permission of EAGE Publications B.V., The Netherlands)

3.5 Use of Cut-Offs and N/G Ratios

3.5.1 Introduction

The concept of the net-to-gross ratio (N/G) is widespread in the oil business and consequently reservoir modelling. Unfortunately, the concept is applied in widely differing ways and poor use of the concept can lead to serious errors. In this section, we consider appropriate ways to handle N/G in the context of a typical reservoir modelling work flow and discuss an alternative approach termed total property modelling.

In the simplest case, a clastic reservoir can be divided into a sand and shale components:

$$N/G = Sand\,volume\,fraction\,/\,Gross\,rock\,volume\,(GRV)$$

In most cases rocks have variable sand content and the sands themselves have variable reservoir quality such that:

$$N/G_{resevoir} \neq Sand\,volume\,fraction\,/\,GRV.$$

The term ‘net sand’ is commonly defined with respect to the gamma and porosity logs, as in the

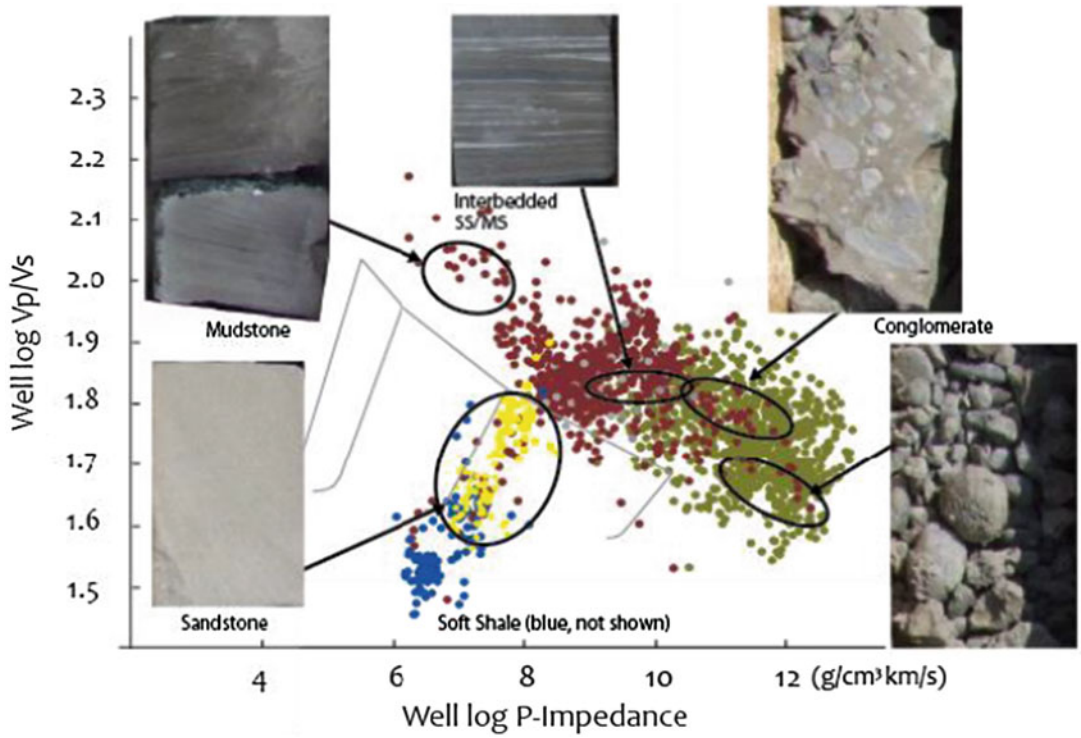

Fig. 3.28 Plot of V_p/V_s versus P-wave Impedance illustrating the separation of facies categories from logs (From Nair et al. 2012) (Redrawn from Nair et al. 2012, ©EAGE reproduced with kind permission of EAGE Publications B.V., The Netherlands)

Table 3.4 Definition of terms used to describe the Net-to-Gross ratio

Term	Definition	Comment
Net sand	A lithologically-clean sedimentary rock	Can only be proved in core but inferred from log data
Net reservoir	Net sand intervals with useful reservoir properties	Usually defined by a log-derived porosity cut-off
Net pay	Net reservoir intervals containing hydrocarbons	Usually defined by a log-derived saturation cut-off
Net-to-gross	A ratio defined explicitly with reference to one of the above, e.g. $N/G_{reservoir}$	$N/G_{sand} \neq N/G_{reservoir}$

logical expression [IF Gamma < X AND Poro > Y THEN NET]. In such a case, 'net sand' has a rather weak and arbitrary association with the geological rock type 'sandstone.' Worthington and Cosentino (2005) discuss this problem at length and show how widely the assumptions vary in definition of net sand or net reservoir. To avoid any further confusion with terminology we adopt their definitions (Table 3.4). Many problems arise from misunderstanding of these basic concepts especially when different disciplines – petrophysics, geoscience and reservoir engineering – assume different definitions.

Another common piece of folklore, often propagated within different parts of the petroleum industry is that oil and gas reservoirs have specific values for permeability cut-off that should be applied: for example the assumption that the cut-off value for an oil reservoir should be 1 mD but 0.1 mD for gas reservoirs. This concept is based in Darcy's law and is best understood in terms of a dynamic cut-off

(Cosentino 2001), in which it is the ratio of permeability, k, to viscosity, μ, that defines the flow potential (the mobility ratio). For example, the following cut-offs are equivalent:

$$\left(\frac{0.01\,md}{0.05\,cp}\right)^{gas} \equiv \left(\frac{1\,md}{5\,cp}\right)^{oil} \qquad (3.30)$$

Worthington and Cosentino (2005) argue that the most consistent way to handle cut-offs is to cross plot porosity versus the k/μ ratio to decide on an appropriate and consistent set of cut off criteria (Fig. 3.29). The cut-off criterion $(k/\mu)_c$ is arbitrary but based on a reservoir engineering decision concerning the flow rate that is economic for the chosen production well concept and the design life of the oil field. It may be the case that later on in the field life the appropriate $(k/\mu)_c$ criterion is revised (to lower values) on account of advances in oil recovery technology and introduction of enhanced oil recovery methods.

Because of these difficulties with terminology and the underlying arbitrary nature of the cut-off assumptions, the key guideline for good reservoir model design is to:

> *Use net-to-gross and cut-off criteria in a consistent way between geological reservoir descriptions, petrophysical interpretations and reservoir flow simulations.*

In the following discussion, we consider two end members of a range of possible approaches – the net-to-gross method and a more general total property modelling approach.

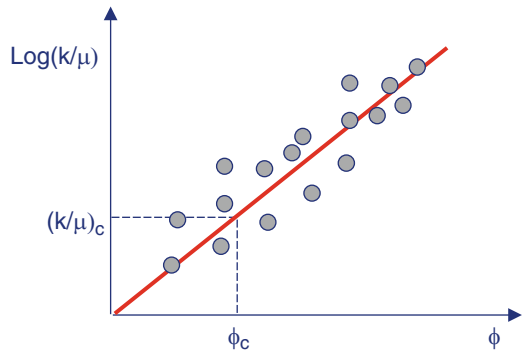

Fig. 3.29 Cross plot of porosity, ø, versus the k/μ ratio to define a consistent set of cut-off criteria, ϕ_c and k_c (Redrawn from Ringrose 2008, ©2008, Society of Petroleum Engineers Inc., reproduced with permission of SPE. Further reproduction prohibited without permission)

3.5.2 The Net-to-Gross Method

From a geological perspective, the ideal case of a reservoir containing clean (high porosity) sandstone set in a background of homogeneous mudstones or shale does not occur in reality. However, for certain cases the pure sand/shale assumption is an acceptable approximation and gives us a useful working model. When using this N/G ratio approach it is important that we define net sand on a geological basis making clear and explicit simplifications. For example, the following statements capture some of the assumptions typically made:

- We assume the fluvial channel facies is 100 % sand (but the facies can contain significant thin shale layers).
- If the net-sand volume fraction in the model grid is within 2 % of the continuous-log net-sand volume fraction, then this is considered as an acceptable error and ignored.
- The estuarine bar facies is given a constant sand volume fraction of 60 % in the model, but in reality it varies between about 40 and 70 %.
- Tightly-cemented sandstones are included with the mudstone volume fraction and are collectively and loosely referred to as "shale".

Having made the geological assumptions clear and explicit, it is important to then proceed to an open discussion (between geologists, petrophysicists, reservoir engineers and the economic decision makers) in order to agree the definition of net reservoir cut-off criteria. For example, a typical decision might be:

- We assume that net reservoir is defined in the well-log data by: IF (Gamma < 40API AND (Poro > 0.05 OR Perm > 0.1 mD) THEN (Interval = $N/G_{reservoir}$)
- After averaging, reservoir modelling and upscaling, the simulation model $N/G_{reservoir}$ may differ from average well-data $N/G_{reservoir}$ by a few percent and will be adjusted to ensure a match.

Hidden within the discussion above is the problem of upscaling. That is, the N/G estimate

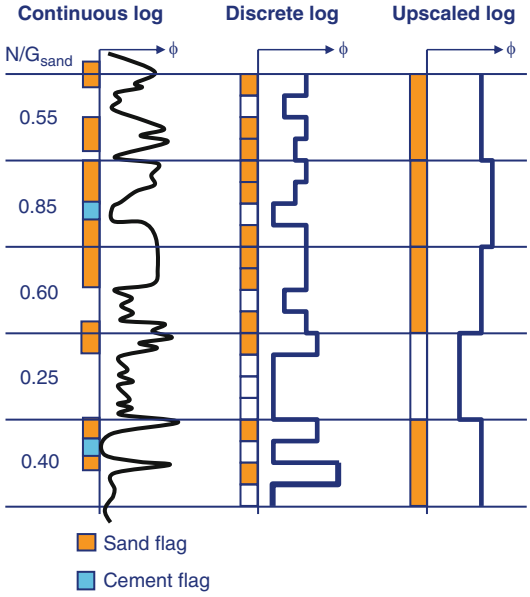

Fig. 3.30 Upscaling of net-sand logs

is likely to change as a function of scale between well data and full-field reservoir simulation model. This is illustrated in Fig. 3.30 for a simplified workflow. There are several important biasing factors which tend to occur in this process:

- Blocked sand intervals are likely to contain non-sand, and the converse (blocking refers to the process of creating a discrete parameter from a higher frequency dataset).
- Upscaling will bias the volume fractions in favour of the majority volume fraction. This is illustrated in Fig. 3.30, where for example in the top layer the N/G_{sand} increases from 0.55 to 0.75 to 1.0 in the transition from continuous log to discrete log to upscaled log.
- Cemented sand is not the same as shale, and will typically be included as part of the shale fraction (unless care is taken to avoid this).
- Since we require net-sand properties we must filter the data accordingly. That is, only the fine-scale net-sand values for k and ϕ are included in the upscaled net-sand values.
- We have to assume something about the non-net sand volume – typically we assume it has zero porosity and some arbitrary low (or zero) value for vertical permeability.

This tendency to introduce bias when upscaling from a fine-scale well-log to the reservoir model can lead to significant errors. Similar blocking errors are introduced for the case of facies modelling (Fig. 3.31) – such that modelled volume fractions of a sandy facies can differ from the well data (due to blocking) in addition to bias related to modelling net sand properties. The errors can be contained by careful tracking of the correct N/G value in the modelling process.

The common assumption in reservoir flow simulation is that the N/G ratio is used to factor down the cell porosity and the horizontal permeability, k_h, in order to derive the correct inter-cell transmissibility. However, no explicit N/G factor is generally applied to the vertical permeability, k_v, as it is assumed that this is independently assigned using a k_v/k_h ratio. This is illustrated in Fig. 3.32. A potential error is to double calculate the N/G effect, where, for example the geologist calculates a total bock permeability of 600 mD and the reservoir engineer then multiplies this again by 0.6 to give $k_x = 360$ mD.

When using the N/G approach the main products from the geological model to the reservoir simulation model are as follows:

(i) Model for spatial distribution of N/G;
(ii) Net sand properties, e.g., ø, k_h, S_w;
(iii) Multi-phase flow functions for net-sand, e.g., $k_{ro}(S_w)$;
(iv) k_v/k_h ratios to be applied to each cell;
(v) Information on stratigraphic barriers and faults.

The N/G ratio approach is widely used and can be consistently and successfully applied through the re-scaling process – from well data to geological model to reservoir-simulation model. However, significant errors can be introduced and care should be taken to ensure that the model correctly represents the underlying assumptions made.

3.5.3 Total Property Modelling

Total Property Modelling refers to an approach where all rock properties are explicitly modelled and where the cut-offs are only applied after modelling (if at all). In this way cut-offs, or net to gross criteria, are not embedded in the process. This

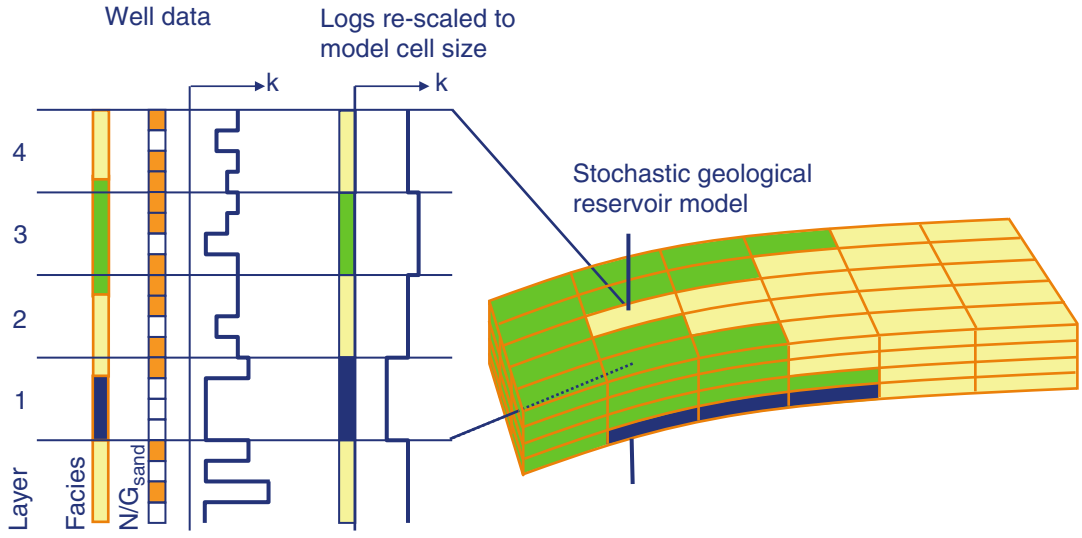

Fig. 3.31 Handling net-sand within a facies model. Block and upscaling can affect both the facies volume fraction and the net-sand volume fraction (Redrawn from Ringrose 2008, ©2008, Society of Petroleum Engineers Inc., reproduced with permission of SPE. Further reproduction prohibited without permission)

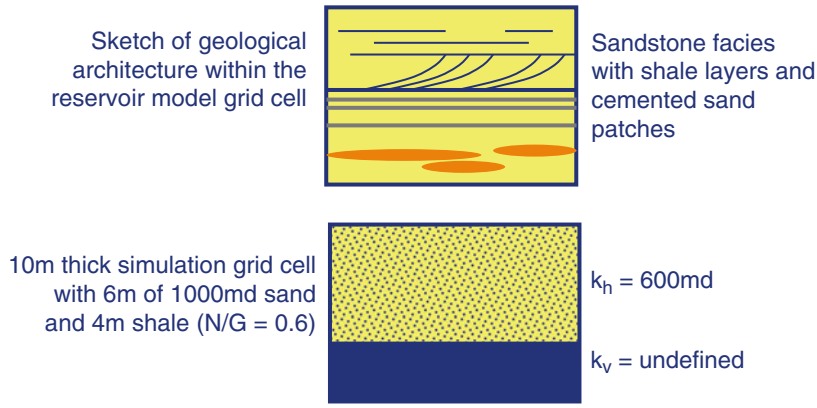

Fig. 3.32 Simple example of a reservoir grid block where the N/G assumption is correctly used to estimate a horizontal block permeability of 600 mD in the case where the net sand has an upscaled permeability of 1000 mD (Redrawn from Ringrose 2008, ©2008, Society of Petroleum Engineers Inc., reproduced with permission of SPE. Further reproduction prohibited without permission)

is a more comprehensive approach and is used in many academic studies where economic cut-off factors (e.g. oil reserves) are not a major concern. This approach is especially appropriate where:

1. Reservoir properties are highly variable or marginal;
2. Cementation is as important as the sand/shale issue;
3. Carbonates comprise the main reservoirs.

The Total Property Modelling (TPM) method is illustrated in Fig. 3.33. Note that net-reservoir is still defined but only after modelling and upscaling. Since shaly or cemented rock units are modelled explicitly alongside better quality sandstones (or carbonates) it is easy to test the effect of assuming different cut-offs – such as "How will an 8 % versus a 10 % porosity cut-off affect the reserves forecast?"

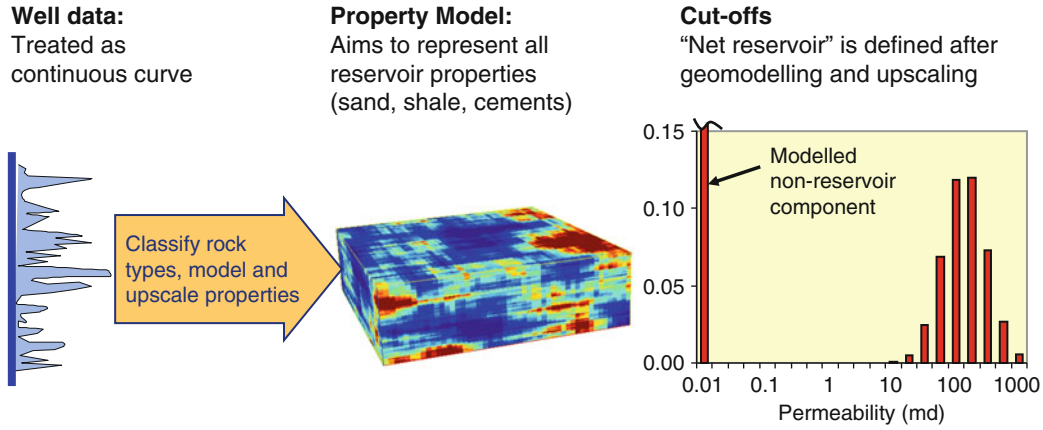

Fig. 3.33 Illustration of the total property modelling approach (Redrawn from Ringrose 2008, ©2008, Society of Petroleum Engineers Inc., reproduced with permission of SPE. Further reproduction prohibited without permission)

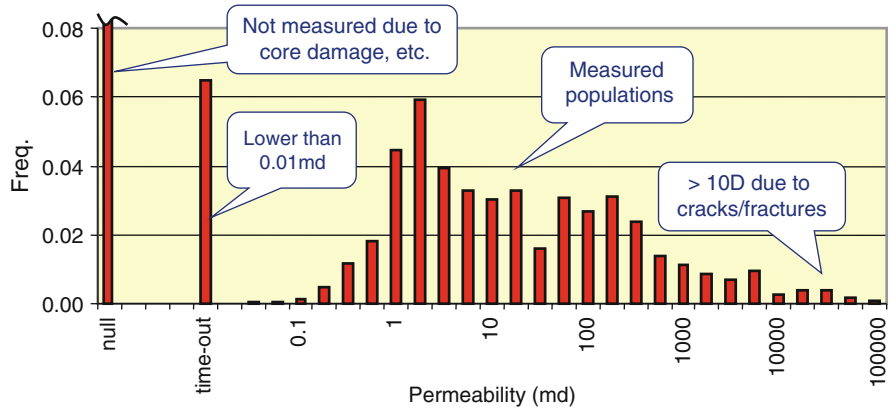

Fig. 3.34 Probe permeability dataset (5 mm-spaced sampling for a 3 m reservoir interval) where permeabilities between 0.01 mD and 10 Darcy have been measured, and where the "lower-than measurable" population has been identified (Redrawn from Ringrose 2008, ©2008, Society of Petroleum Engineers Inc., reproduced with permission of SPE. Further reproduction prohibited without permission)

An important prerequisite for this approach is that the petrophysical data must have been handled appropriately. Net sand concepts are often embedded in petrophysical logging procedures – partly by dint of habit but also because shaly and cemented rock properties are more difficult to measure. Therefore, a major challenge for the total property modelling approach is that property estimation in poor reservoir quality units is difficult or imprecise. However, if it is understood that very low porosity and permeability rock elements will be eventually discounted, it is appropriate to assign a *reasonable guess* to the low-quality reservoir units. This is illustrated by the dataset from a very heterogeneous reservoir unit shown in Fig. 3.34.

Numerical upscaling is generally required when applying the TPM approach (with the N/G approach simple averaging is often assumed). Valid application of numerical upscaling methods requires that a number of criteria are met – related to flow boundary conditions and the statistical validity of the upscaled volume (discussed in Chap. 4). The Total Property

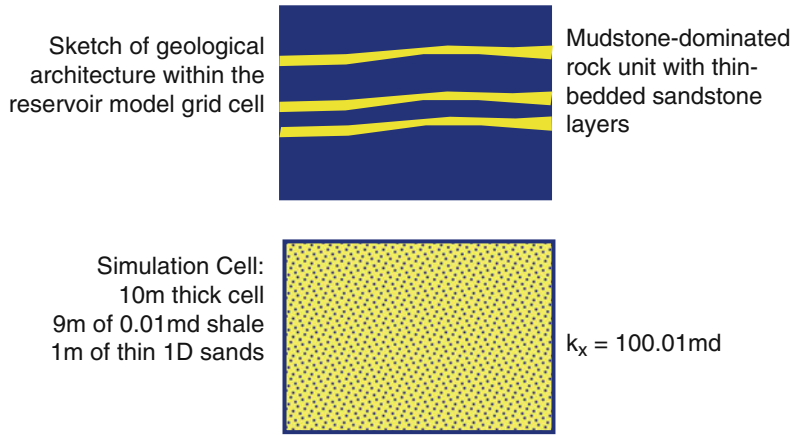

Fig. 3.35 Example of a reservoir grid block modelled using the total property modelling approach. N/G is assumed = 1. Upscaled horizontal block permeability is correctly estimated as 100.1 mD (while the "net sand" method would have assigned the block as non-reservoir)

Modelling approach may often challenge these criteria and can be difficult to apply. However, by using statistical analysis of the rock populations present in the reservoir and careful choice of optimum model length-scales (grid resolution), these problems can be reduced and made tractable.

With the TPM approach, the main products from the geological model to the reservoir simulation model are:

(i) Upscaled porosity and fluid saturation;
(ii) Effective permeabilities for all directions (k_x, k_y, k_z);
(iii) Multi-phase flow functions for the total grid block;
(iv) Information on stratigraphic barriers/faults.

After upscaling, all blocks with upscaled properties less than the chosen cut-off criteria may be declared 'non-reservoir'. An important feature of this approach is that, for example, thin sands will be correctly upscaled where they would have been discounted in the N/G approach (Fig. 3.35).

It is best to illustrate and contrast these approaches by applying them to an example dataset. The example is from a 3 m interval core interval from a deeply buried tidal deltaic reservoir from the Smørbukk Field, offshore Norway (Ringrose 2008). This thin-bedded reservoir interval was characterised using high-resolution-probe permeability data, sampled at 5-mm-intervals, and calibrated to standard core plugs. The thin-bed data set is assumed to give the "ground truth," with lower-than-measurable permeability values set to 0.0001 mD.

Figure 3.36 shows the results of the analyses. For the N/G approach (Fig. 3.36a) the fine-scale data are transformed using a 0.2 m running average (to represent a logging process) and then are blocked to create a 0.5 m discrete log (to represent the gridding process). A N/G_{res} cutoff criterion of 1 mD is assumed, leading to estimates of k_h(net) and N/G_{res} at each upscaling step. At the logging stage the (apparent) kh_{net} = 371 mD and the N/G_{res} is 0.83 and when the blocking filter is applied the k_h (net) = 336 mD and the N/G_{res} is 0.88. These transforms result in significant over-estimation of N/G and underestimation of net horizontal permeability, k_h (net). The upscaled k_h (simulator) is then estimated by k_h (net) × N/G_{res} for each 0.5-m cell value (representing a typical reservoir-simulator procedure). The resulting upscaled k_h (simulator) for the whole interval is 304 mD, which is only slightly higher than the true value (298 mD). However, this apparently satisfactory result hides several errors embedded in the process. The N/G_{res} has been significantly over-estimated while the k_h (net) has been underestimated (errors are shown in Fig. 3.36a). The two errors tend to cancel one another out (but unfortunately two wrongs don't make a right). k_v is also neglected inherently in this procedure and must be estimated independently.

For the TPM approach (Fig. 3.36b), the fine-scale data are transformed directly to the 0.5-m

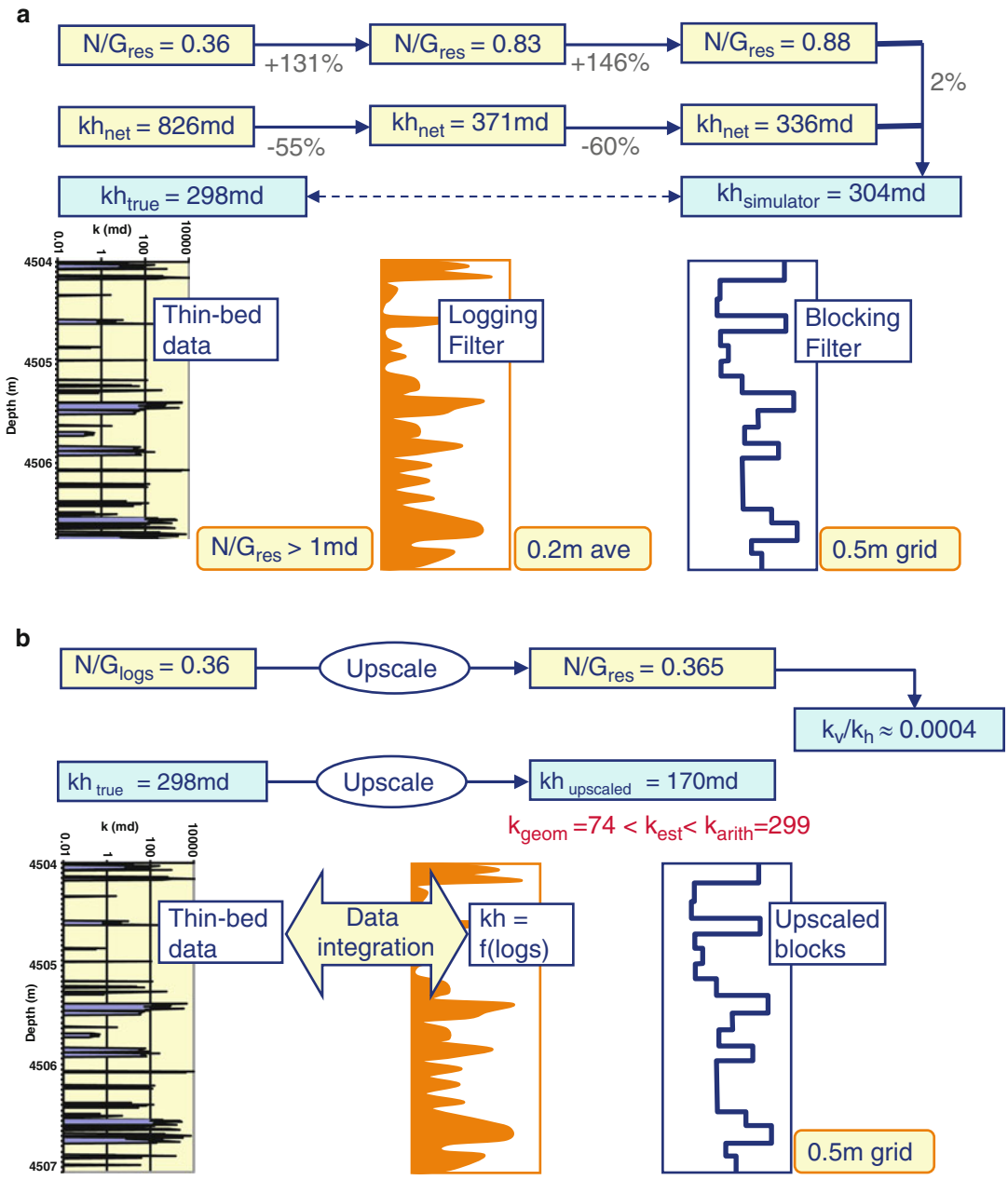

Fig. 3.36 Application of (**a**) the N/G approach and (**b**) the total property modelling approach to an example thin-bed permeability dataset

discrete log by blocking the thin-bed data set (using values for net and non-net reservoir). The discrete-log N/G_{res} estimate is quite accurate, as smoothing has not been applied. Upscaled cell values (k_h and k_v) are then estimated using functions proposed by Ringrose et al. (2003) for permeability in heterolithic bedding systems (described in Sect. 3.6 below). These functions represent the numerical (single-phase) upscaling step in the total-property-modelling workflow. The TPM approach preserves both an accurate estimate for N/G_{res}

and k_h throughout the procedure, and also gives a sound basis for estimation of upscaled k_h and k_v. The upscaled k_h (170 mD for the whole interval) is significantly lower than the arithmetic average k_h because of the effects of sandstone connectivity and the presence of shales and mudstone layers. A degree of validation that we have derived a "reasonable estimate" for k_h is found in the observation that k_h lies in the range $k_{geometric}$ to $k_{arithmetic}$ (Fig. 3.36b).

The main challenges of the Total Property Modelling approach are:

1. The approach requires some form of explicit upscaling, and upscaling always has some associated errors;
2. Where only log data are available (i.e. in the absence of fine-scale core data) some form of indirect estimate of the fine-scale sand/mud ratios and rock properties is needed, and this inevitably introduces additional random error in the estimation of N/G_{res}.

However, for challenging, heterogeneous or low-permeability reservoirs, these (generally minor) errors are preferable to the errors associated with the inappropriate simplifications of the N/G approach.

In summary then, the widely used N/G approach is simpler to apply and can be justified for relatively good-quality reservoirs or situations where quick estimates are warranted. The method tends to embed errors in the process of re-scaling from well data to reservoir model, and care should be taken to minimise and record these errors. The TPM approach is generally more demanding but aims to minimize the (inherent) upscaling errors by making estimates of the effective flow properties of the rock units concerned. N/G ratios can be calculated at any stage in the TPM modelling workflow.

3.6 Vertical Permeability and Barriers

3.6.1 Introduction to k_v/k_h

The ratio of vertical to horizontal permeability, k_v/k_h, is an important, but often neglected, reservoir modelling property. Too often, especially when using the net-sand modelling method, a value for the k_v/k_h ratio is assumed at the last minute with little basis in reality. Figure 3.37 captures a typical "history" for this parameter; neglected or assumed = 1 in the early stages then rapidly drops after unexpected barriers are encountered and finally rises again to a more plausible value late in the field life.

The problem of vertical permeability is also further confounded because it is very difficult to measure. Routine core plug analysis usually gives some estimate of core-plug scale k_v/k_h but these data can be misleading due to severe under sampling or biased sampling (discussed by Corbett and Jensen 1992).

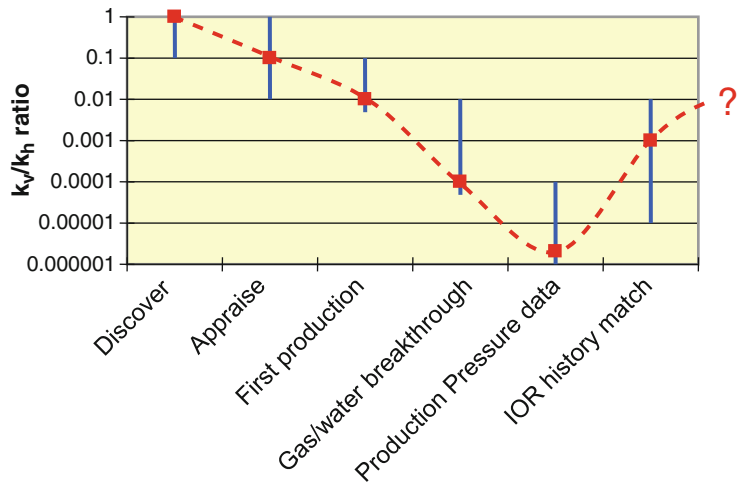

Fig. 3.37 Typical "history" of the k_v/k_h ratio

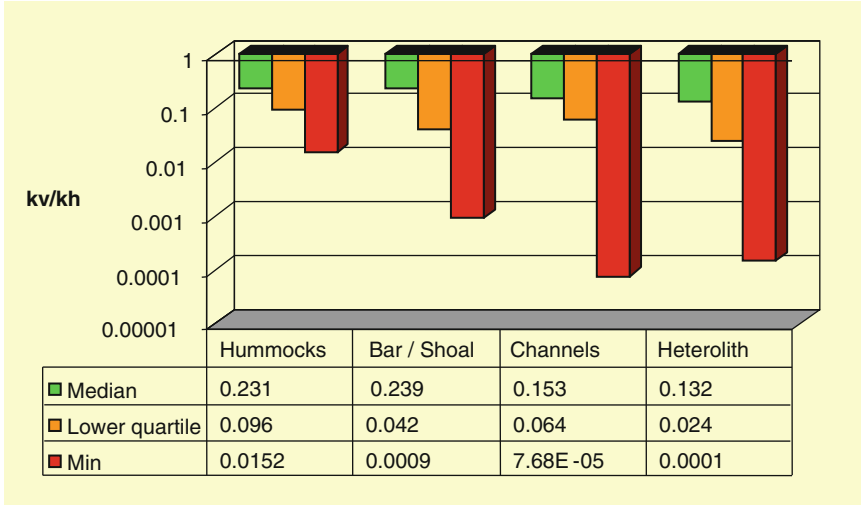

	Hummocks	Bar / Shoal	Channels	Heterolith
Median	0.231	0.239	0.153	0.132
Lower quartile	0.096	0.042	0.064	0.024
Min	0.0152	0.0009	7.68E -05	0.0001

Fig. 3.38 Statistics of measured k_v/k_h ratios from core plug pairs from an example reservoir interval

Figure 3.38 illustrates some typical core-plug anisotropy data. For this example we know from production data that the mean value is far too high (due to under sampling) and in fact the minimum observed plug k_v/k_h ratio gives a more realistic indication of the true values at the reservoir scale.

A frequent problem with modelling or estimating permeability anisotropy is confusion between (or mixing the effects of) thin barriers and rock fabric anisotropy. The following two sections consider these two aspects separately.

3.6.2 Modelling Thin Barriers

Large extensive barriers are best handled explicitly in the geological reservoir model:

- Fault transmissibilities can be mapped onto to cell boundaries;
- Extensive shales and cemented layers can be modelled as objects and then transformed to transmissibility multipliers onto to cell boundaries.

Some packages allow simulation of sub-seismic faults as effective permeability reduction factors within grid cells (see for example Manzocchi et al. 2002, or Lescoffit and Townsend 2005). Some modelling packages offer the option to assign a sealing barrier between specified layers. For the more general situation, the geo-modeller needs to stochastically simulate barriers and ensure they are applied in the simulation model. Pervasive discontinuous thin shales and cements may also be modelled as cell-value reduction factors (an effective k_v/k_h multiplier).

Figure 3.39 shows and example of barrier modelling for calcite cements in an example reservoir. The fine-scale barriers are first modelled as geological objects and then assigned as vertical transmissibility values using single-phase upscaling.

Before plunging into stochastic barrier modelling, it is important to consider using well established empirical relationships that may save a lot of time. Several previous studies have considered the effects of random shales on a sandstone reservoir. Begg et al. (1989) proposed a general estimator for the effective vertical permeability, k_{ve}, for a sandstone medium containing thin, discontinuous, impermeable mudstones, based on effective medium theory and geometry of ideal streamlines. They proposed:

$$k_{VE} = \frac{k_x(1 - V_m)}{(a_z + fd)^2} \tag{3.30}$$

where

V_m is the volume fraction of mudstone

a_z is given by $(k_{sv}/k_{sh})^{1/2}$

k_{sh} and k_{sv} are the horizontal and vertical permeability of the sandstone

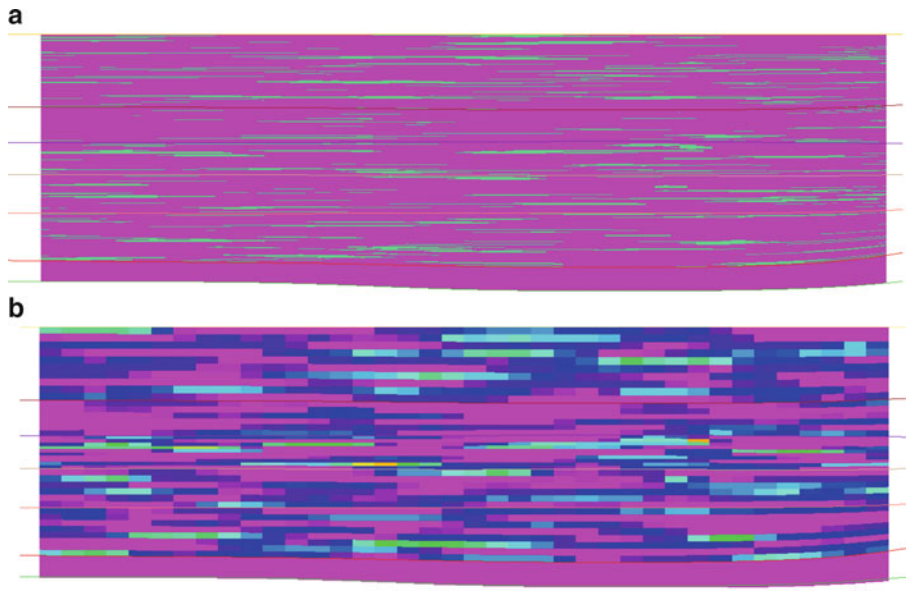

Fig. 3.39 Example modelling of randomly distributed calcite cement barriers in an example reservoir (Reservoir is c. 80 m thick) (**a**) Fine-scale model of calcite barriers. (**b**) Upscaled k_v as vertical transmissibility multipliers (Modified from Ringrose et al. 2005, Petrol Geoscience, Volume 11, © Geological Society of London [2005])

f is the barrier frequency
d is a mudstone dimension
(d = $L_m/2$ for a 2D system with mean mudstone length, L_m).

This method is valid for low mudstone volume fractions and assumes thin, uncorrelated, impermeable, discontinuous mudstone layers.

Desbarats (1987) estimated effective permeability for a complete range of mudstone volume fractions in 2D and 3D, using statistical models with spatial covariance and a range of anisotropies. For strongly stratified media, the effective horizontal permeability, k_{he}, was found to approach the arithmetic mean, while k_{ve} was found to be closer to the geometric mean. Deutsch (1989) proposed using both power-average and percolation models to approximate k_{he} and k_{ve} for a binary permeability sandstone–mudstone model on a regular 3D grid, and showed how both the averaging power and the percolation exponents vary with the anisotropy ratio.

Whatever the chosen method, it is important to separate out the effects of thin barriers (or faults) from the more general rock permeability anisotropy (discussed below).

3.6.3 Modelling of Permeability Anisotropy

Using advances in small-scale geological modelling, it is now possible to accurately estimate k_v/k_h ratios for sandstone units. Ringrose et al (2003, 2005) and Nordahl et al (2005) have developed this approach for some common bedding types found in tidal deltaic sandstone reservoirs (i.e. flaser, wavy and lenticular bedding). Their method gives a basis for general estimation for facies-specific k_v/k_h ratios. Example results are shown in Figs. 3.40 and 3.41.

The method takes the following steps:

1. Perform a large number of bedding simulations to understand the relationship between k_{sand}, k_{mud} and V_{mud} (simulations are unconditioned to well data and can be done rapidly).
2. Input values for the small-scale models are the typical values derived from measured core permeabilities.
3. A curve is fitted to the simulations to estimate the k_v or k_v/k_h ratio as a function of other modelled parameters: e.g. k_h, V_{mud}, or ø.

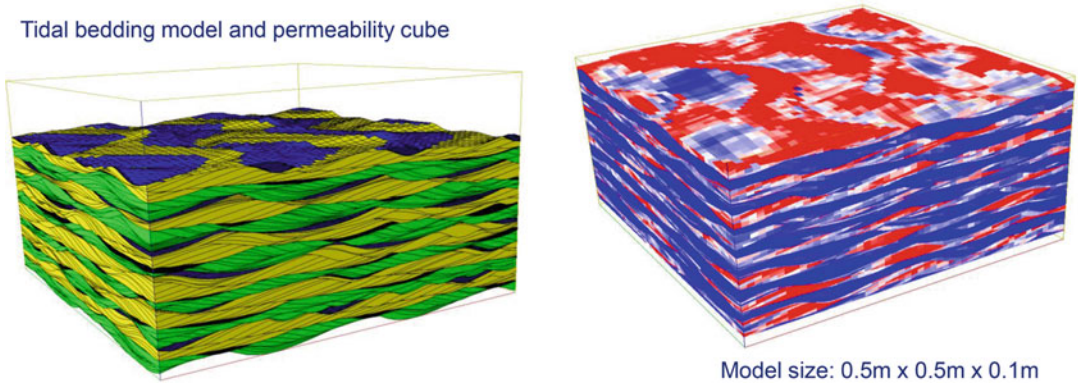

Fig. 3.40 Example model of heterolithic flaser bedding (*left*) with corresponding permeability model (*right*). Note the bi-directional sand lamina sets (*green* and *yellow* laminae) and the partially preserved mud drapes (*dark tones*). Higher permeabilities indicated by *hot colours* (Modified from Ringrose et al. 2005 Petrol Geoscience, Volume 11, © Geological Society of London [2005])

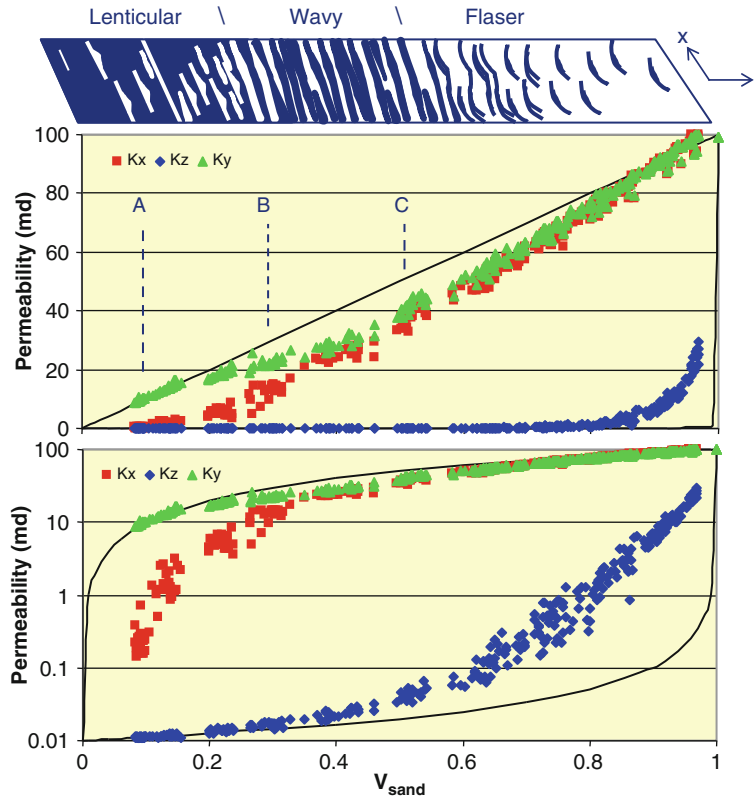

Fig. 3.41 Results of sub-metre-scale simulation of heterolithic bedding in tidal deltaic reservoirs. Effective permeability simulation results are for the constant petrophysical properties case (i.e. sandstone and mudstone have constant permeability). Observed effective permeability is compared to bedding styles and the critical points *A*, *B* and *C*. *A* is the percolation threshold for k_x, and *C* is the percolation threshold for k_z, while *B* is the theoretical percolation threshold for a simple 3D system. Thin lines are the arithmetic and harmonic averages

The following function was found to capture the characteristic vertical permeability of this system (Ringrose et al. 2003):

$$k_v = k_{sand}\left(\frac{k_{mud}}{k_{sand}}\right)^{\frac{V_m}{V_{mc}}} \tag{3.31}$$

where V_{mc} is the critical mudstone volume fraction (or percolation threshold).

This formula is essentially a re-scaled geometric average constrained by the percolation threshold. This is consistent with the previous findings by Desberats (1987) and Deutsch (1989) who observed that the geometric average was close to simulated k_v for random shale systems, and also noted percolation behaviour in such systems. This equation captures the percolation behaviour (the percolation threshold is estimated for the geometry of a specific depositional system or facies), while still employing a general average function that can be easily applied in reservoir simulation.

The method has been applied to a full-field study by Elfenbein et al. (2005) and compared to well-test estimates of anisotropy (Table 3.5). The comparison showed a very good match in the Garn 4 Unit but a poorer match in the Garn 1–3 Units. This can be explained by the fact that the lower Garn 1–3 Units have abundant calcite cements (which were modelled in the larger-scale full-field geomodel), illustrating the importance of understanding both the thin large-scale barriers and the inherent sandstone anisotropy (related to the facies and bedding architecture).

3.7 Saturation Modelling

3.7.1 Capillary Pressure

An important interface between the static and dynamic models is the definition of initial water saturation. There are numerous approaches to this problem, and in many challenging situations analysis and modelling of fluid saturations requires specialist knowledge in the petrophysics and reservoir engineering disciplines. Here we introduce the important underlying concepts that will enable the initial saturation model to be linked to the geological model and its uncertainties.

The initial saturation model is usually based on the assumption of capillary equilibrium with saturations defined by the capillary pressure curve. We recall the basic definition for capillary pressure:

$$\begin{aligned} P_c &= P_{\text{non-wetting phase}} \\ &\quad - P_{\text{wetting-phase}}[P_c = f(S)] \end{aligned} \tag{3.32}$$

The most basic form for this equation is given by:

$$P_c = AS_{wn}{}^{-b}\sqrt{\phi/k} \tag{3.33}$$

That is, capillary pressure is a function of the wetting phase saturation and the rock properties, summarized by ϕ and k. The exponent b is related to the pore size distribution of the rock. Note the use of the normalised water saturation:

$$S_{wn} = (S_w - S_{wi})/(S_{wor} - S_{wi}) \tag{3.34}$$

Table 3.5 Comparison of simulated kv/kh ratios with well test estimates from the case study by Elfenbein et al. (2005)

Reservoir unit	Modelled k_v/k_h: Geometric average of simulation model	Modelled k_v/k_h: Geometric average of well test volume	Well test k_v/k_h: Analytical estimate	Comments
			Tyrihans South, well test in well 6407/1-2	
Garn 4	0.031	0.043	<0.05	Test of Garn 4 interval
Garn 3	0.11			Producing interval uncertain
Garn 2	0.22			Complex two-phase flow
Garn 1	0.11			
			Tyrihans North, well test in well 6407/1-3	
Garn 4	0.025			
Garn 3	0.123	0.19	0.055	Test of Garn 1 to 3 interval
Garn 2	0.24			Analytical gas cap
Garn 1	0.12			Partial penetration model

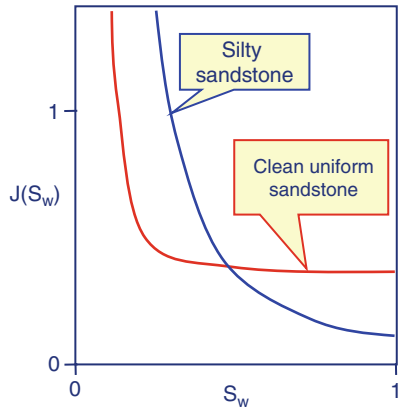

Fig. 3.42 Example capillary pressure J-functions

We can expand the P_c equation to include the fluid properties:

$$P_c(S_w) = \sigma \cos\theta J(S_w)\sqrt{\phi/k} \qquad (3.35)$$

where
σ = interfacial tension
θ = interfacial contact angle
$J(S_w)$ = Leverett J-junction.

Rearranging this we obtain the J-function:

$$J(S_w) = \frac{P_c(S_w)}{\sigma \cos\theta}\left(\frac{k}{\phi}\right)^{1/2} \qquad (3.36)$$

Figure 3.42 shows two example J-functions for contrasting rock types.

To put this more simply, we could measure and model any number of capillary pressure curves, $P_c = f(S)$. However, the J-function method allows a number of similar functions to be normalized with respect to the rock and fluid properties and plotted with a single common curve.

3.7.2 Saturation Height Functions

There are a number of ways of plotting the $P_c = f(S)$ function to indicate how saturation varies with height in the reservoir. The following equation is a general form of the P_c equation, including all the key rock and fluid terms.

$$S_{wn}{}^{-b} = \frac{(\rho_w - \rho_o)gh}{\sigma \cos\theta}\left(\frac{k}{\phi}\right)^{1/2} \qquad (3.37)$$

Here P_c is defined by the fluid buoyancy term, $\Delta(\rho)gh$, where h is the height above the free water level. This equation gives a useful basis for forward modelling water saturation, given some known rock and fluid properties.

For practical purposes we often want to estimate the S_w function from well log data. There are again several approaches to this (Worthington 2001 gives a review), but the simplest is the power law function which has the same form as the J-function:

$$S_w = C.h^d \qquad (3.38)$$

A significant issue in reservoir modelling is how the apparent (and true) saturation height function is affected by averaging of well data and/or upscaling of the fine-scale geological model data.

To illustrate these effects in the reservoir model, we take a simple case. We must first define the *free water level* (FWL) – the fluid water interface in the absence of rock pores, i.e. resulting only from fluid forces (buoyancy and hydrodynamic pressure gradients). The effect of rock pores is to introduce another factor (capillary forces) on the oil-water distribution, so that the oil-water contact is different from the free water level.

A simple model for this behaviour is given by the following saturation-height function:

$$S_w = S_{wi} + (1 - S_{wi})\left[0.1h\sqrt{k/\phi}\right]^{-2/3} \qquad (3.39)$$

Figure 3.43 shows example curves, based on this function, and illustrates how at least 10 m variation in oil-water contact can occur due to changes in pore throat size. In general, for a high porosity/permeability rock OWC $\approx$ FWL. However, for low permeability or heterogeneous reservoirs the fluid contact will vary considerably as a function of rock properties, and OWC $\neq$ FWL.

Further difficulties in interpretation of these functions come with upscaling or averaging saturations from heterogeneous systems. For example, suppose you had a thinly-bedded reservoir comprising alternating rock types 2 and 4 (Fig. 3.43), then the average saturation-height

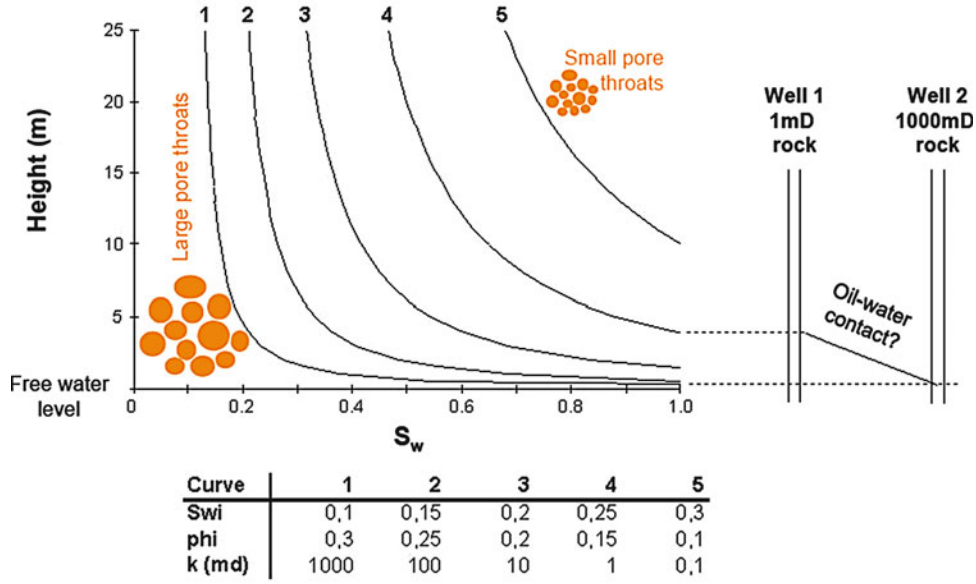

Fig. 3.43 Example saturation-height functions for the listed input parameters, illustrating how an apparent change in oil-water contact may be caused by rock property variations between wells

Table 3.6 Selected examples of tilted oil-water contacts

Field, Location	Tilt of OWC (m/km)	References
South Glenrock, Wy. USA	<95	Dahlberg (1995)
Norman Wells, NWT, Canada	75	Dahlberg (1995)
Tin-Fouye, Algeria	10	Dahlberg (1995)
Weyburn, Sask., Canada	10	Dahlberg (1995)
Kraka, North Sea (Denmark)	10	Thomasen and Jacobsen (1994)
Billings Nose, N.Da., USA	5	Berg et al. (1994)
Knutson, N.Da., USA	3	Berg et al. (1994)

function (detected by a logging tool) would be close to curve 3. That is, the average S_w corresponds to the average k/ϕ. However, if the thin beds were composed of an unknown random mix of rocks types 1, 2, 3, 4 and 5 then it would clearly be very difficult to infer the correct relationship between S_w, k and ϕ.

3.7.3 Tilted Oil-Water Contacts

Depending on which part of the world the petroleum geologist is working, tilted oil-water contacts are either part of accepted or disputed folk law. In parts of the Middle East, North Africa and North America, there are numerous well-documented examples. These represent continental basins with appreciable levels of topographically driven groundwater flow, or hydrodynamic gradients. Dahlberg (1995) provides a fairly comprehensive study of the evidence for, and interpretation of, tilted oil water contacts. Berg et al. (1994) give good documentation of some examples from Dakota, USA. In the offshore continental shelf petroleum provinces, such as offshore NW Europe the cases are fewer, but still evident. Table 3.6 lists a range of examples.

Here, we are concerned with the implications that tilted hydrocarbon-water contacts might

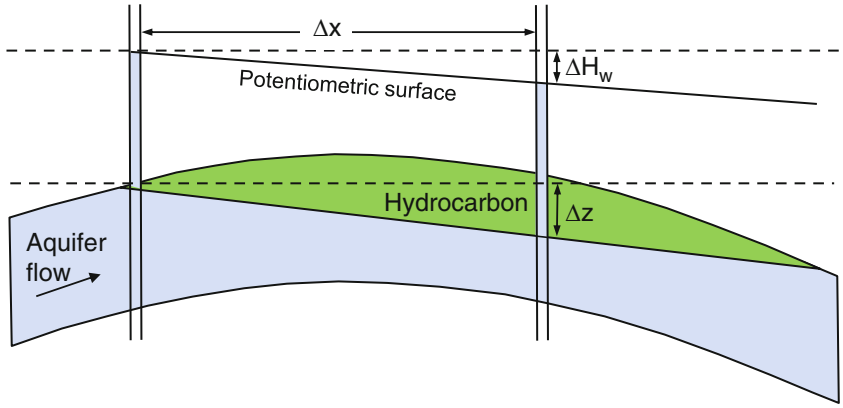

Fig. 3.44 Terms defining a tilted oil-water contact (Redrawn from Dahlberg 1995 (Fig. 12.5), Springer-Verlag, New York, with kind permission from Springer Science and Business Media B.V.)

have for a dynamic modelling of petroleum accumulations. For simplicity we mainly consider oil-water contacts, but the theory applies to any hydrocarbon: gas, condensate or oil. The main principle governing this phenomenon is potentiometric head. If an aquifer contains flowing water driven by some pressure gradient (Fig. 3.44), then this pressure gradient causes a slope in the petroleum-water interface of any accumulation within that aquifer, defined by Hubbert (1953) as:

$$\Delta z/\Delta x \approx (\rho_w/\rho_w - \rho_o).(\Delta H_w/\Delta x) \quad (3.40)$$

where

$\rho_w - \rho_o$ = density of water and petroleum

$\Delta z/\Delta x$ = slope of the hydrocarbon-water interface

$\Delta H_w/\Delta x$ = potentiometric surface in aquifer

The greater the difference in fluid density (i.e. the lighter the petroleum), the smaller the tilt of the fluid contact. It is important to differentiate the free-water level (FWL) from the oil-water contact (OWC). Where the capillary pressures are significant (due to small pores), the difference between FWL and OWC can be significant (Fig. 3.43). In Eq. (3.40), the $\Delta z/\Delta x$ term relates to the FWL (and only approximately to the OWC). A more comprehensive treatment of this topic is given by Muggeridge and Mahmode (2012), who include the terms for the effective permeability in the aquifer, k_{aq}, and reservoir, k_{res}, to derive a relationship between the hydrocarbon-water interface and the hydrodynamic pressure gradient in terms of steady-state flow:

$$(\Delta z/\Delta x) = \left(k_{res}/k_{aq}\Delta\rho g\right).(\Delta H_w/\Delta x) \quad (3.41)$$

As can be seen from Table 3.6, the actual value of the tilted oil-water contact can be quite small (most documented examples are around 10 m/km), so that uncertainties in detection become important. There are many situations which can give an apparent tilt in oil-water contact, including:

- Undetected faults (usually the first explanation to be proposed) or stratigraphic boundaries;
- Variations in reservoir properties – systematic changes in pore throat size across a field can lead to a variation in the oil-water contact of 5 m or more (Fig. 3.43);
- Misinterpretation of paleo-oil-water contacts (marked by residual oil stains or tar mats) as present-day contacts;
- Errors in deviation data for well trajectories.

Thus, proof of the presence of a tilted oil-water contact requires either multiple well data explained by a common inclined surface (Fig. 3.45) or multiple data types explained

coherently in terms of a common hydrodynamic model (as in the Kraka field example discussed below). Possible hydrodynamic aquifer influence on a static (i.e. passive) petroleum accumulation must also be considered alongside the concepts of a dynamic petroleum accumulation (e.g. ongoing migration or leakage) or pressure transients in the aquifer.

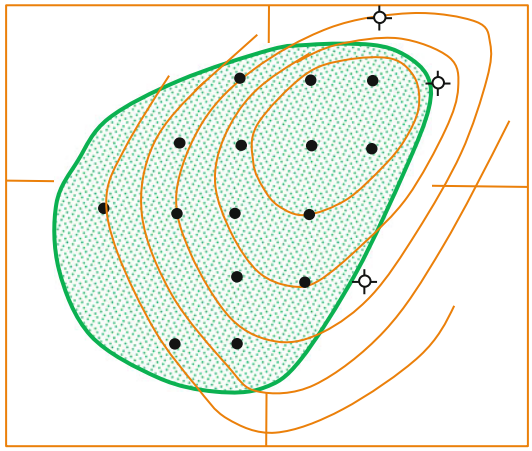

Fig. 3.45 Map of the Cairo Pool oilfield, Arkansas showing a hydrodynamic offset of an oil accumulation (After Dahlberg 1995). Contours are 20 foot intervals; *black dots* = wells with oil in the reservoir interval, *open circles* = wells with water in the reservoir interval (Redrawn from Dahlberg 1995 (Fig. 12.5), Springer-Verlag, New York, with kind permission from Springer Science and Business Media B.V.)

3.7.3.1 Kraka Field Example

This small chalk reservoir in the Danish sector of the North Sea provides an interesting account of the phenomenon of tilted oil-water contacts and their interpretation. The subtle nature of the tilt and the use of multiple data sources to confirm an initially doubtful interpretation are very informative. A study of the field by Jørgensen and Andersen (1991) included some initial observations on a tilted oil-water contact, and a tentative argument that it was due to tectonic tilting during the Tertiary. A subsequent study by Thomasen and Jacobsen (1994), give a detailed description and a more thorough basis for interpretation a 0.6° dip in both free water level and oil-water contact (Fig. 3.46).

Their main observations were:

- Repeat Formation Tester (RFT) data from three wells indicated a free-water level (interpreted from the change in slope of water and oil zones) falling by about 70 m over a 2 km distance (Fig. 3.47).
- Due to the heterogeneous and fractured nature of the chalk reservoir zone, logs from seven wells show highly variable saturations (Fig. 3.48). These were interpreted by best-fit capillary pressure saturation functions. Difficulties in fitting a function assuming a horizontal free-water level were resolved by fitting functions to individual wells and then identifying the implied tilt in free water level.

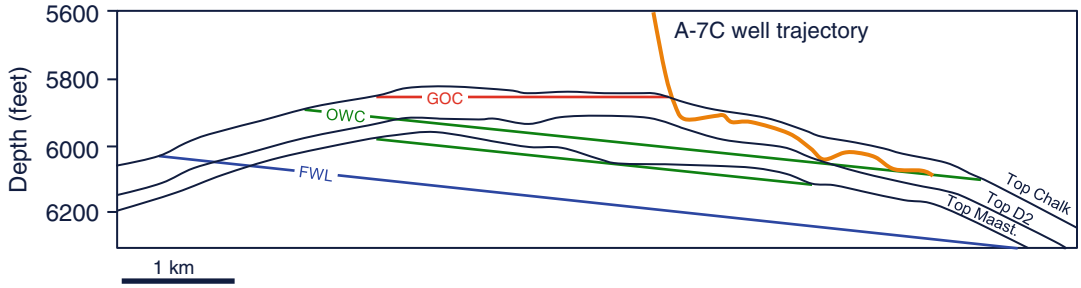

Fig. 3.46 Cross-section through the Kraka field (From Thomasen and Jacobsen 1994) showing interpreted fluid contacts and horizontal well to exploit down-dip reserves (Redrawn from Thomasen and Jacobsen 1994, ©1994, Society of Petroleum Engineers Inc., reproduced with permission of SPE. Further reproduction prohibited without permission)

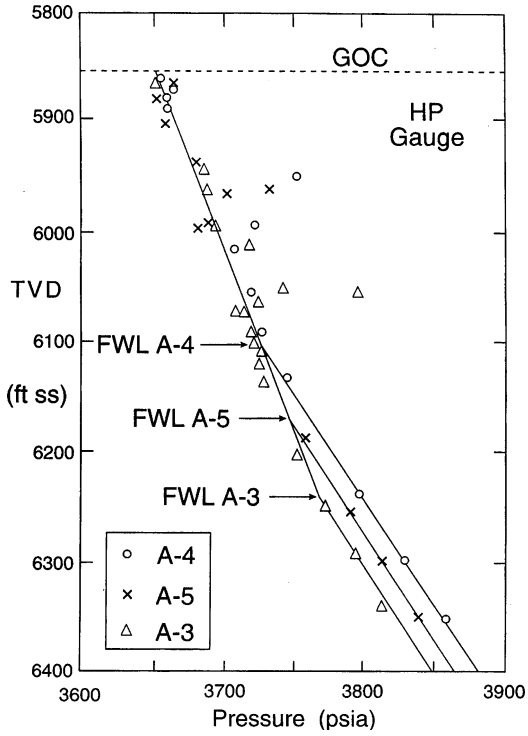

Fig. 3.47 RFT data for three wells for the Kraka field (From Thomasen and Jacobsen 1994) (Redrawn from Thomasen and Jacobsen 1994, ©1994, Society of Petroleum Engineers Inc., reproduced with permission of SPE. Further reproduction prohibited without permission)

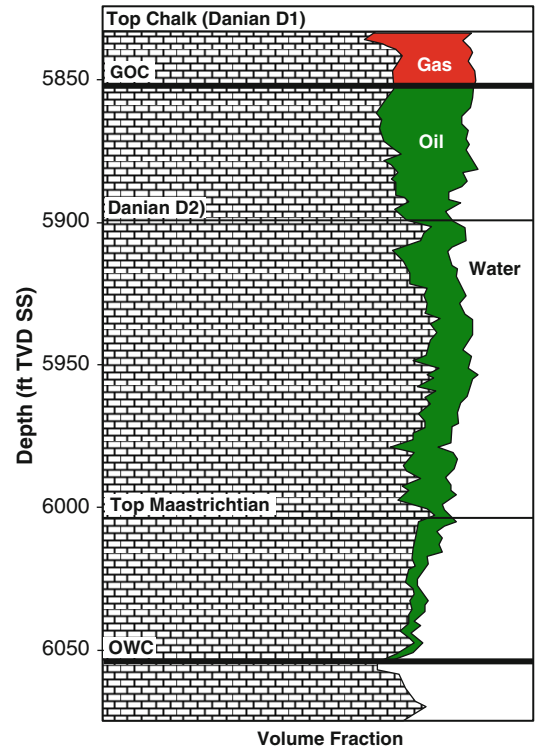

Fig. 3.48 Type log for the Kraka field illustrating the variable oil saturations and the thick transition zone (Redrawn from Thomasen and Jacobsen 1994, ©1994, Society of Petroleum Engineers Inc., reproduced with permission of SPE. Further reproduction prohibited without permission)

The slope of the free-water level inferred from this was found to be close to the RFT pressure data model.

- An intra-reservoir seismic reflection interpreted as the matrix oil-water contact was mapped around the field and extrapolated to its intersection with top reservoir, and was again found to be in good agreement with the saturation model.
- The orientation of the inferred hydrodynamic gradient (towards the SE) was found to be in agreement with regional gradients from inter-field pressure variations.

This integrated interpretation had a significant economic benefit in terms of the appropriate placement of horizontal wells in the thicker part of the accumulation, and in the estimation of inter-well permeability in this fairly marginal field development.

3.8 Summary

We have covered a range of issues related to petrophysical property modelling of oil and gas reservoirs. The theoretical principles that underlie the modelling "buttons" and workflows in geological reservoir modelling packages have been discussed along with many of the practical issues that govern the choice of parameters.

To summarise this chapter, we offer a check list of key questions to ask before proceeding with your property modelling task:

1. Have you agreed with your colleagues across disciplines (geoscience, petrophysics and reservoir engineering):
   - The key geological issues you need to address – rock heterogeneity, sedimentary barriers, faults, etc.

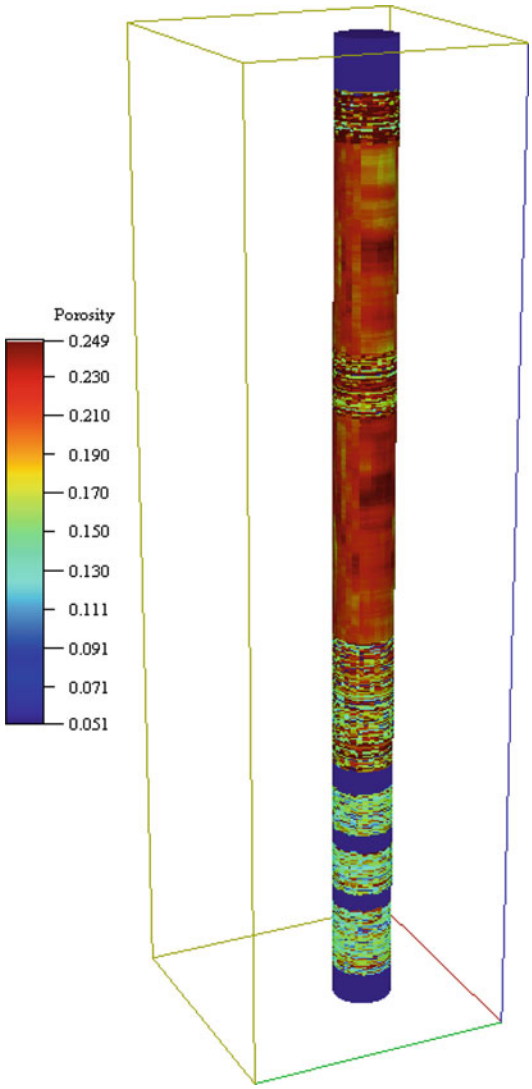

Fig. 3.49 Near-wellbore porosity model (1 m^2 × 10 m)

- A consistent method for handling net-to-gross (N/G) and cut-off values?

2. Is your petrophysical data representative of the rock unit (sampling problems, tails of distributions), and if not how will you address that uncertainty?
3. Have you used appropriate averaging and/or upscaling methods?
4. Is the model output consistent with data input? Compare the statistics of input and output distributions. The variance may be as important as the mean.
5. Have you run sensitivities to check important assumptions?
6. Have you considered the effects of possible un-detected flow barriers in the system?

A final word about the future of property modelling – if we are looking for fit-for-purpose models for interpreting petrophysical well data, then we are probably talking about high-resolution near-wellbore models (Fig. 3.49). These models could be very detailed or could be just a simple equation. Either way they need to be focussed on the scale of rock property variation – the subject of the next chapter.

References

Abbaszadeh M, Fujii H, Fujimoto F (1996) Permeability prediction by hydraulic flow units – theory and applications. SPE Form Eval 11(4):263–271

Begg SH, Carter RR, Dranfield P (1989) Assigning effective values to simulator gridblock parameters for heterogeneous reservoirs. SPE Reserv Eng 1989:455–463

Berg RR, DeMis WD, Mitsdarffer AR (1994) Hydrodynamic effects on Mission Canyon (Mississippian) oil accumulations, Billings Nose area, North Dakota. AAPG Bull 78(4):501–518

Bierkins MFP (1996) Modeling hydraulic conductivity of a complex confining layer at various spatial scales. Water Resour Res 32(8):2369–2382

Bourbie T, Zinszner B (1985) Hydraulic and acoustic properties as a function of porosity in Fontainebleau sandstone. J Geophys Res 90(B13):11524–11532

Box GEP, Cox DR (1964) An analysis of transformations. J R Stat Soc Series B: 211–243, discussion 244–252

Brandsæter I, McIlroy D, Lia O, Ringrose PS (2005) Reservoir modelling of the Lajas outcrop (Argentina) to constrain tidal reservoirs of the Haltenbanken (Norway). Petrol Geosci 11:37–46

Bryant S, Blunt MJ (1992) Prediction of relative permeability in simple porous media. Phys Rev A 46:2004–2011

Buland A, Kolbjornsen O, Omre H (2003) Rapid spatially coupled AVO inversion in the fourier domain. Geophysics 68(1):824–836

Cardwell WT, Parsons RL (1945) Average permeabilities of heterogeneous oil sands. Trans Am Inst Mining Met Pet Eng 160:34–42

Corbett PWM, Jensen JL (1992) Estimating the mean permeability: how many measurements do you need? First Break 10:89–94

Corbett PWM, Ringrose PS, Jensen JL, Sorbie KS (1992) Laminated clastic reservoirs: the interplay of capillary pressure and sedimentary architecture. SPE paper 24699, presented at the SPE annual technical conference, Washington, DC

Cosentino L (2001) Integrated reservoir studies. Editions Technip, Paris, 310 pp
Dahlberg EC (1995) Applied hydrodynamics in petroleum exploration, 2nd edn. Springer, New York
Davis JC (2003) Statistics and data analysis in geology, 3rd edn. Wiley, New York, 638 pp
de Marsilly G (1986) Quantitative hydrogeology. Academic, San Diego
Delfiner P (2007) Three statistical pitfalls of phi-k transforms. SPE Reserv Eval Eng 10:609–617
Desberats AJ (1987) Numerical estimation of effective permeability in sand-shale formations. Water Resour Res 23(2):273–286
Deutsch C (1989) Calculating effective absolute permeability in sandstone/shale sequences. SPE Form Eval 4:343–348
Deutsch CV (2002) Geostatistical reservoir modeling. Oxford University Press, Oxford, 376 pp
Deutsch CV, Journel AG (1992) Geostatistical software library and user's guide, vol 1996. Oxford University Press, New York
Doyen PM (2007) Seismic reservoir characterisation. EAGE Publications, Houten
Durlofsky LJ (1991) Numerical calculations of equivalent grid block permeability tensors for heterogeneous porous media. Water Resour Res 27(5):699–708
Elfenbein C, Husby Ø, Ringrose PS (2005) Geologically-based estimation of kv/kh ratios: an example from the Garn Formation, Tyrihans Field, Mid-Norway. In: Dore AG, Vining B (eds) Petroleum geology: North-West Europe and global perspectives. Proceedings of the 6th petroleum geology conference. The Geological Society, London
Goggin DJ, Chandler MA, Kocurek G, Lake LW (1988) Patterns of permeability variation in eolian deposits: page sandstone (Jurassic), N.E. Arizona. SPE Form Eval 3(2):297–306
Gutjahr AL, Gelhar LW, Bakr AA, MacMillan JR (1978) Stochastic analysis of spatial variability in subsurface flows 2. Evaluation and application. Water Resour Res 14(5):953–959
Hohn ME (1999) Geostatistics and petroleum geology, 2nd edn. Kluwer, Dordrecht
Howson C, Urbach P (1991) Bayesian reasoning in science. Nature 350:371–374
Hubbert MK (1953) Entrapment of petroleum under hydrodynamic conditions. AAPG Bull 37(8):1954–2026
Hurst A, Rosvoll KJ (1991) Permeability variations in sandstones and their relationship to sedimentary structures. In: Lake LW, Carroll HB Jr, Wesson TC (eds) Reservoir characterisation II. Academic, San Diego, pp 166–196
Isaaks EH, Srivastava RM (1989) Introduction to applied geostatistics. Oxford University Press, Oxford
Jensen JL, Corbett PWM, Pickup GE, Ringrose PS (1995) Permeability semivariograms, geological structure and flow performance. Math Geol 28(4):419–435
Jensen JL, Lake LW, Corbett PWM, Goggin DJ (2000) Statistics for petroleum engineers and geoscientists, 2nd edn. Elsevier, Amsterdam
Jørgensen LN, Andersen PM (1991) Integrated study of the Kraka Field. SPE paper 23082, presented at the offshore Europe conference, Aberdeen, 3–6 Sept 1991
Journel AG, Alabert FG (1990) New method for reservoir mapping. J Petrol Technol 42.02:212–218
Journel AG, Deutsch CV (1997) Rank order geostatistics: a proposal for a unique coding and common processing of diverse data. Geostat Wollongong 96:174–187
Journel AG, Deutsch CV, Desbarats AJ (1986) Power averaging for block effective permeability. SPE paper 15128, presented at SPE California regional meeting, Oakland, California, 2–4 April
Kendall M, Staurt A (1977) The advanced theory of statistics, vol. 1: distribution theory, 4th edn. Macmillan, New York
Lescoffit G, Townsend C (2005) Quantifying the impact of fault modeling parameters on production forecasting for clastic reservoirs. In: Evaluating fault and cap rock seals, AAPG special volume Hedberg series, no. 2. American Association of Petroleum Geologists, Tulsa, pp 137–149
Leuangthong O, Khan KD, Deutsch CV (2011) Solved problems in geostatistics. Wiley, New York
Manzocchi T, Heath AE, Walsh JJ, Childs C (2002) The representation of two-phase fault-rock properties in flow simulation models. Petrol Geosci 8:119–132
Matheron G (1967) Éléments pour une théorie des milieux poreux. Masson and Cie, Paris
McIlroy D, Flint S, Howell JA, Timms N (2005) Sedimentology of the tide-dominated Jurassic Lajas Formation, Neuquen Basin, Argentina. Geol Soc Lond Spec Publ 252:83–107
Mourzenko VV, Thovert JF, Adler PM (1995) Permeability of a single fracture; validity of the Reynolds equation. J de Phys II 5(3):465–482
Muggeridge A, Mahmode H (2012) Hydrodynamic aquifer or reservoir compartmentalization? AAPG Bull 96 (2):315–336
Muskat M (1937) The flow of homogeneous fluids through porous media. McGraw-Hill, New York (Reprinted by the SPE and Springer 1982)
Nair KN, Kolbjørnsen O, Skorstad A (2012) Seismic inversion and its applications in reservoir characterization. First Break 30:83–86
Nelson RA (2001) Geologic analysis of naturally fractured reservoirs, 2nd edn. Butterworth-Heinemann, Boston
Nordahl K, Ringrose PS, Wen R (2005) Petrophysical characterisation of a heterolithic tidal reservoir interval using a process-based modelling tool. Petrol Geosci 11:17–28
Olea RA (ed) (1991) Geostatistical glossary and multilingual dictionary, IAMG studies in mathematical geology no. 3. Oxford University Press, Oxford
Pickup GE, Sorbie KS (1996) The scaleup of two-phase flow in porous media using phase permeability tensors. SPE J 1:369–381
Pickup GE, Ringrose PS, Jensen JL, Sorbie KS (1994) Permeability tensors for sedimentary structures. Math Geol 26:227–250

Pickup GE, Ringrose PS, Corbett PWM, Jensen JL, Sorbie KS (1995) Geology, geometry and effective flow. Petrol Geosci 1:37–42

Renard P, de Marsily G (1997) Calculating equivalent permeability: a review. Adv Water Resour 20:253–278

Ringrose PS (2008) Total-property modeling: dispelling the net-to-gross myth. SPE Reserv Eval Eng 11:866–873

Ringrose PS, Pickup GE, Jensen JL, Forrester M (1999) The Ardross reservoir gridblock analogue: sedimentology, statistical representivity and flow upscaling. In: Schatzinger R, Jordan J (eds) Reservoir characterization – recent advances, AAPG memoir no. 71., pp 265–276

Ringrose PS, Skjetne E, Elfeinbein C (2003) Permeability estimation functions based on forward modeling of sedimentary heterogeneity. SPE 84275, presented at the SPE annual conference, Denver, CO, USA, 5–8 Oct 2003

Ringrose PS, Nordahl K, Wen R (2005) Vertical permeability estimation in heterolithic tidal deltaic sandstones. Petrol Geosci 11:29–36

Shuey RT (1985) A simplification of the Zoeppritz equations. Geophysics 50(4):609–614

Size WB (ed) (1987) Use and abuse of statistical methods in the earth sciences, IAMG studies in mathematical geology, no. 1. Oxford University Press, Oxford

Soares A (2001) Direct sequential simulation and cosimulation. Math Geol 33(8):911–926

Thomasen JB, Jacobsen NL (1994) Dipping fluid contacts in the Kraka Field, Danish North Sea. SPE paper 28435, presented at the 69th SPE annual technical conference and exhibition, New Orleans, LA, USA, 25–28 Sept 1994

Weber KJ, van Geuns LC (1990) Framework for constructing clastic reservoir simulation models. J Petrol Tech 42:1248–1297

White CD, Horne RN (1987) Computing absolute transmissibility in the presence of fine-scale heterogeneity. SPE paper 16011, presented at the 9th SPE symposium of reservoir simulation, San Antonio, TX, 1–4 Feb 1987

Witherspoon PA, Wang JSY, Iwai K, Gale JE (1980) Validity of cubic law for fluid flow in a deformable rock fracture. Water Resour Res 16(6):1016–1024

Worthington PF (2001) Scale effects on the application of saturation-height functions to reservoir petrofacies units. SPE Reserv Eval Eng 4(5):430–436

Worthington PF, Cosentino L (2005) The role of cut-offs in integrated reservoir studies (SPE paper 84387). SPE Reserv Eval Eng 8(4):276–290

Upscaling Flow Properties

4

Abstract

To upscale flow properties means to estimate large-scale flow behaviour from smaller-scale measurements. Typically, we start with a few measurements of rock samples (lengthscale ~3 cm) and some records of flow rates and pressures in test wells (~100 m). Our challenge is to estimate how the whole reservoir will flow (~1 km).

Flow properties of rocks vary enormously over a wide range of length-scales, and estimating upscaled flow properties can be quite a challenge. Unfortunately, many reservoir modellers choose to overlook this problem and blindly hope that a few measurements will correctly represent the whole reservoir. The aim of this chapter is to help make intelligent estimates of large-scale flow properties. In the words of Albert Einstein:

> *Two things are infinite: the universe and human stupidity; and I'm not sure about the universe.*

P. Ringrose and M. Bentley, *Reservoir Model Design*, DOI 10.1007/978-94-007-5497-3_4,

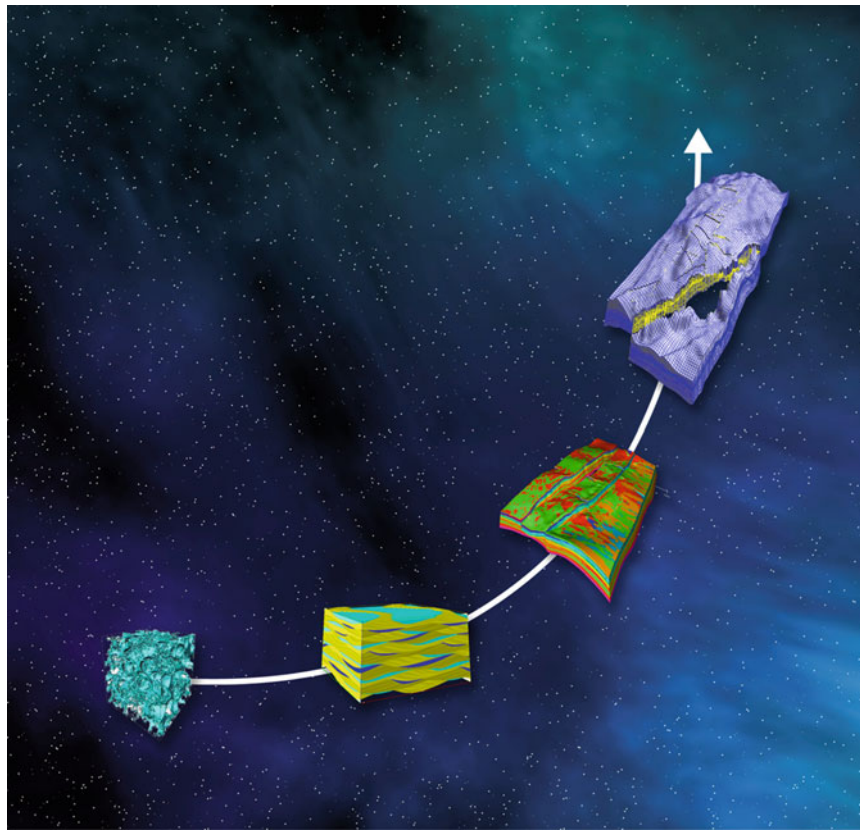

Upscaling – from pore to field, and beyond . . .

4.1 Multi-scale Flow Modelling

This chapter concerns the implementation of multi-scale flow modelling for oil and gas reservoir studies. *Multi-scale flow modelling* is defined here as any method which attempts to explicitly represent the flow properties at more-than-one scale within a reservoir. We may, for example, have (a) an estimate of flow properties around a single well in a specific flow unit (or reservoir interval) and (b) a *rationale* for using this estimate to calculate the flow properties in the whole reservoir. This *rationale* could simply be some multiplication factors transforming the single-well flow property to the reservoir scale, or might involve a 3-dimensional array (or grid) of values drawn from statistical population (which includes the single-well flow property).

In multi-scale geological modelling, the essence is that geological concepts are used to make the transition from smaller-scale measurements to larger-scale estimates (models) of reservoir properties or behaviour (Fig. 4.1). Geological modelling in itself is an art form requiring some intimate knowledge of the geological system – typically involving Picasso-type geologists (Fig. 4.2) with an interest in detail. For upscaling we require representative geological models in which the geological elements (e.g. layers of sandstone, siltstone, mudstone and limestone) are represented as properties relevant for fluid modelling – porosity, permeability, capillary pressure functions, etc.

This process inevitably involves some simplification of the intricate variability of rock architecture, as we aim to group the rock elements into

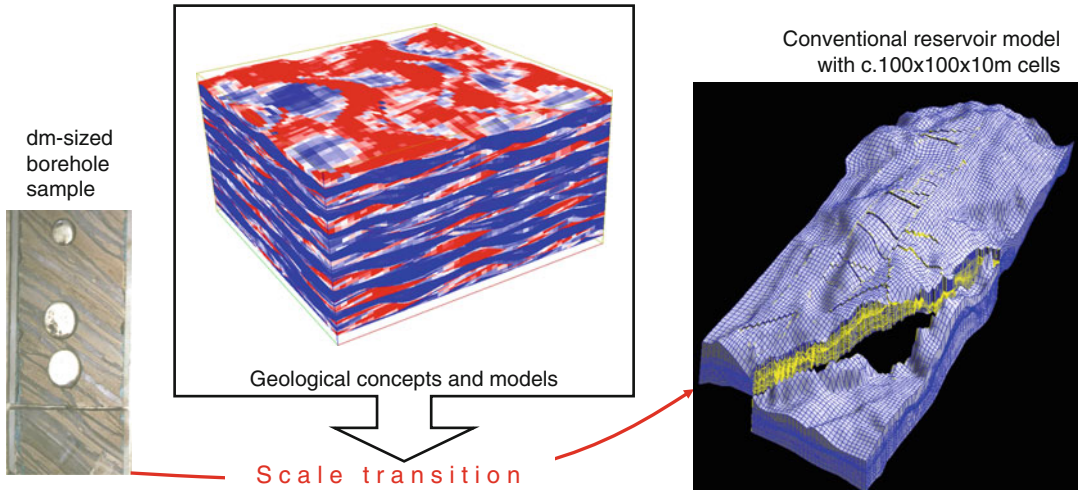

Fig. 4.1 Scale transition in reservoir modelling and the role of geological concepts

Fig. 4.2 The art of geological modelling: "Picasso-type geologists" aim to represent fine detail in their art work while "Rothko-type geologists" aim to capture only the representative flow units as essential colours (Pablo Picasso, Violins and Grapes, oil on canvas (1912) and Mark Rothko, *No. 10,* 1950. Oil on canvas, 229.2 × 146.4 cm, reproduced with permission DIGITAL IMAGE © The Museum of Modern Art/Scala, Florence)

flow units with similar properties. In the art analogy this process is more like the work of Mark Rothko, where broad bands of colour capture the essence of the object or concept being described (Fig. 4.2).

The process of transferring information between scales is referred to as *upscaling* or, more generally, re-scaling. Upscaling involves some form of numerical or analytical method for estimating effective or equivalent flow

properties at a larger scale given some set of finer scale rock properties. Upscaling methods for single and multiphase flow are reviewed in detail by Renard and de Marsily (1997), Barker and Thibeau (1997), Ekran and Aasen (2000) and Pickup et al. (2005). We will review the methods involved and establish the principles which guide the flow upscaling process. The term *downscaling* has also been used (Doyen 2007) to mean the process by which smaller-scale properties are estimated from a larger–scale property. This is most commonly done in the context of seismic data where, for example, a porosity value estimated from seismic impedance is used to constrain the porosity values of thin layers below the resolution of the seismic wavelet. In more general terms, if we know all the fine-scale properties then the upscaled property can be estimated uniquely. Conversely, if we know only the large-scale property value then there are many alternative fine-scale property models that could be consistent with the upscaled property.

We will develop the argument that upscaling is essential in reservoir modelling – whether implicit or explicit. There is no such thing as the *correct* value for the permeability of a given hydraulic flow unit. The relevant permeability value depends on length-scale, the boundary conditions and flow process. Efforts to define the diagnostic characteristics for hydraulic flow units (HFU) (e.g. Abbaszadeh et al. 1996) provide valuable approaches to petrophysical data analysis, but HFUs should always be related to a representative elementary volume (REV). As we will show it is not always simple to define the REV, and when flow process are brought into play different REVs may apply to different flow processes. Hydraulic flow units are themselves multi-scale.

The framework we will use for upscaling involves a series of steps where smaller-scale models are nested within larger scale models. These steps essentially involve models or concepts at the pore-scale, geological concepts and models at the field-scale and reservoir simulations (Fig. 4.3).

The factors involved in these scale transitions are enormous; certainly around 10^9 as we go from the rock pore to the full-field reservoir model (Table 4.1), and important scale markers involved in reservoir modelling are best illustrated on a logarithmic scale (Fig. 4.4). Despite these large scale transitions, most flow processes average out the local variations – so that what we are looking for is the correct average flow behaviour at the larger scales. How we do this is the rationale for this chapter.

Flow simulation of detailed reservoir models is a fairly demanding exercise, involving many mathematical tools for creating and handling flow grids and calculating the flows and pressures between the grid cells. The mathematics of flow simulation is beyond the scope of this book, and will be treated only in an introductory sense. Mallet (2008) gives a recent review of the processes involved in the creation of numerical rock models and their use in flow simulation. King and Mansfield (1999) also give a fairly comprehensive discussion of flow simulation of geological reservoir models, in terms of managing and handling the grid and associated flow terms (transmissibility factors). In this chapter, we will take as our starting point the existence of a numerical rock model, created by some set of recipes in a geological modelling toolkit, and will focus on the methods involved for performing multi-scale upscaling. Before we do that we need to introduce, or recapitulate, some of the basic theory for multiphase fluid flow.

4.2 Multi-phase Flow

4.2.1 Two-Phase Flow Equations

In Chap. 3 we introduced the concept of permeability and the theoretical basis for estimating effective permeability using averages and numerical recipes. This introduced us to upscaling for single-phase flow properties. Here we extend this by looking at two-phase flow and the upscaling of multi-phase flow properties.

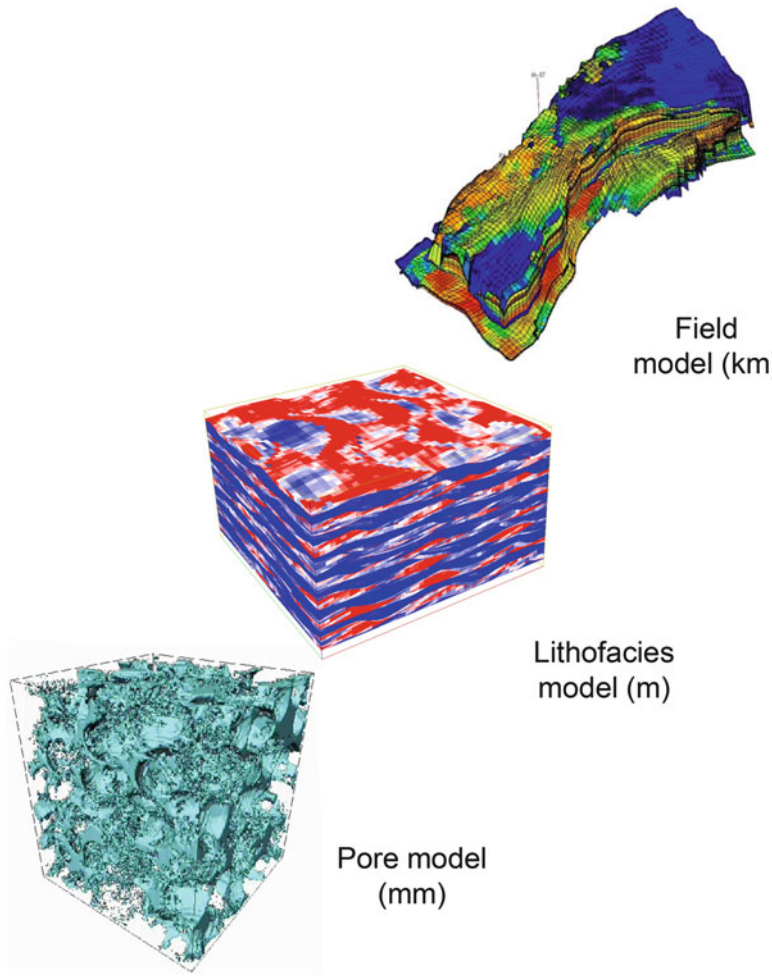

Fig. 4.3 Reservoir models at different scales (Statoil image archives, © Statoil ASA, reproduced with permission)

Table 4.1 Typical dimensions for important volumes used in multi-scale reservoir modelling

	X (m)	Y(m)	Z(m)	Volume (m^3)	Cubic root (m)	Fraction of reservoir volume
Pore-scale model	5×10^{-5}	50×10^{-5}	50×10^{-5}	1.25×10^{-13}	0.00005	0.00000005
Core plug sample	0.025	0.025	0.025	0.000031	0.031	0.00003
Well test volume	400	300	10	1,200,000	106	0.1
Reservoir model	8,000	4,000	40	1,280,000,000	1,086	1

For a fuller treatment of multi-phase flow theory applied to oil and gas reservoir systems refer to reservoir engineering textbooks (e.g. Chierici 1994; Dake 2001; Towler 2002). A more geologically-based introduction to multi-phase flow in structured sedimentary media is given by Ringrose et al. (1993) and Ringrose and Corbett (1994).

The first essential concept in multiphase flow is the principal of mass balance. Any fluid which flows into a grid cell (mass accumulation) over a particular interval of time must be equal to the mass of fluids which have flowed out. This principle may be rather trivial for single phase flow, but becomes more critical for multiphase flow, where different fluids may have different

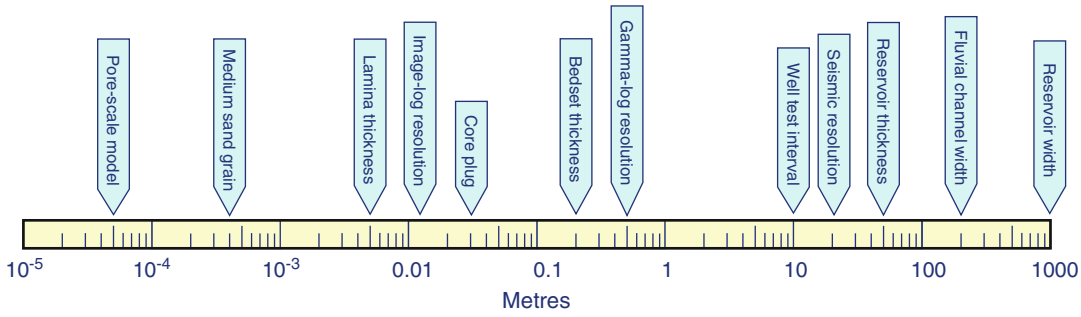

Fig. 4.4 Important length scales involved in reservoir modelling

densities, viscosities, and permeabilities. What goes in must be balanced by what comes out, and for a complex set of flow equations the zero-sum constraint for each grid cell is essential.

Fluid flow in porous media is represented by Darcy's Law (Sect. 4.3.2) which relates the fluid velocity, u, to the pressure gradient and two terms representing the rock and the fluid:

$$u = -\underline{\mathbf{k}}/\mu.\nabla(P + \rho gz) \tag{4.1}$$

The pressure term comprises an imposed pressure gradient, $\nabla(P)$, and a pressure gradient due to gravity, $\nabla(\rho gz)$. In Cartesian coordinates the gradient of pressure, ∇P, is resolved as:

$$\nabla P = \frac{dP}{dx} + \frac{dP}{dy} + \frac{dP}{dz} \tag{4.2}$$

The rock (or the permeable medium) is represented by the permeability tensor, $\underline{\mathbf{k}}$, and fluid by the viscosity, μ.

When two or more fluid phases are flowing, it becomes necessary to introduce terms for the density, viscosity and permeability of each phase and for the interfacial forces (both fluid-fluid and fluid-solid). For two-phase immiscible flow (oil and water), the two-phase Darcy equation and the capillary pressure equation are used:

$$u_o = -\underline{\mathbf{k}}k_{ro}/\mu_o.\nabla(P_o + \rho_o gz) \tag{4.3}$$

$$u_w = -\underline{\mathbf{k}}k_{rw}/\mu_w.\nabla(P_w + \rho_w gz) \tag{4.4}$$

$$P_c = P_o - P_w \tag{4.5}$$

where:

o and w refer to the oil and water phases,

k_{rw} and k_{ro} are the relative permeabilities of each phase,

μ and ρ are fluid viscosity and density,

P_c is the capillary pressure,

∇P_o is the gradient of pressure for the oil phase

This set of equations is non-linear as the k_{rw}, k_{ro} and P_c terms are all functions of phase saturation, S_w, which is itself controlled by the flow rates. Thus, in order to solve these equations for a given set of initial and boundary conditions, numerical codes (reservoir simulators) are used, in which saturation-dependent functions for k_{rw}, k_{ro} and P_c are given as input, and an iterative numerical recipe is used to estimate saturation and pressure. Figure 4.5 shows a typical set of oil-water relative permeability curves with the endpoint terminology.

Note that the total fluid mobility is <1 (mobility is the permeability/viscosity ratio for the flowing phase). That is, the permeability of a rock containing more than one phase is significantly lower than a rock with only one phase. Clearly the fluid viscosity is a key factor but the fluid-fluid interactions also play a role. The functions are drawn between 'endpoints,' which are a mathematical convenience, but are also based on physical phenomena – the point at which the flow rate of one phase becomes insignificant. However, the endpoint values themselves are not physically fixed. For example, there exists a measurable irreducible water saturation, but its precise value depends on many things (e.g. oil phase pressure or temperature). Many of the problems and errors in upscaling

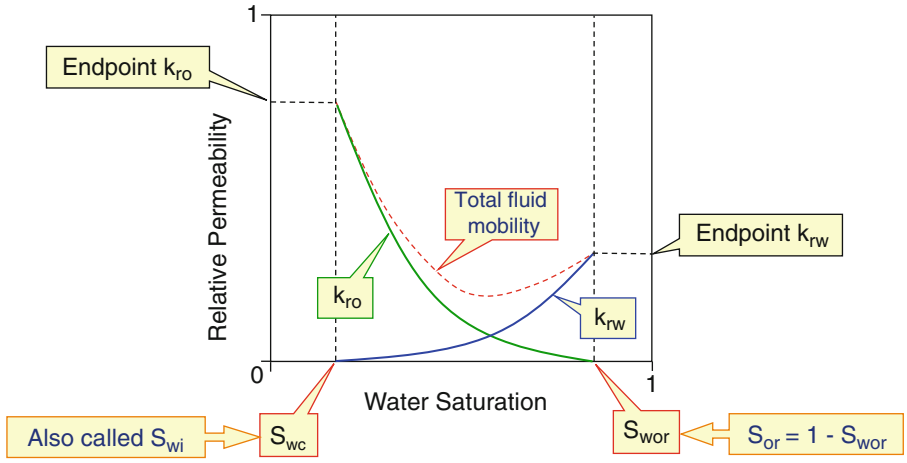

Fig. 4.5 Example oil-water relative permeability functions

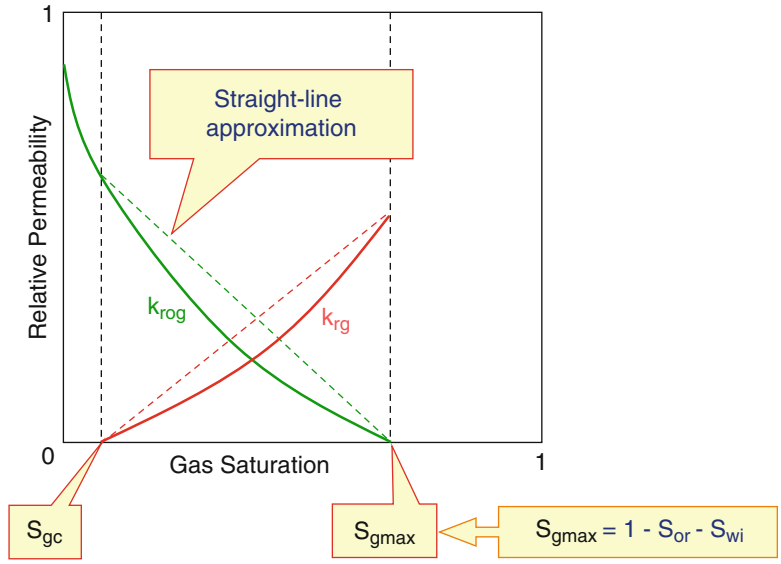

Fig. 4.6 Example gas-oil relative permeability functions

arise from poor treatment or understanding of these endpoints.

The most common functions used for relative permeability are the Corey exponent functions:

$$k_{ro} = A(1 - S_{wn})^x \tag{4.6}$$

$$k_{rw} = B(S_{wn})^y \tag{4.7}$$

where S_{wn} is the normalized saturation:

$$S_{wn} = (S_w - S_{wc})/(S_{wor} - S_{wc}) \tag{4.8}$$

Typical values for a water-wet light oil might be:

$$k_{ro} = 0.85(1 - S_{wn})^3 \text{ and } k_{rw} = 0.3(S_{wn})^3 \tag{4.9}$$

A similar set of functions can be used to describe a gas-oil system (Fig. 4.6), where the functions are bounded by the critical gas saturation, S_{gc}, and the maximum gas saturation, S_{gmax}. However, gas-oil relative permeability curves tend to have less curvature (lower Corey exponents) and sometimes straight-line functions

are assumed, implying perfect mixing or a fully-miscible gas-oil system.

These functions describe the flows and pressures for multi-phase flow. The third equation required to completely define a two-phase flow system is the capillary pressure equation. For the general case (any fluid pair):

$$P_c = P_{\text{non-wetting phase}} - P_{\text{wetting-phase}} \quad [P_c = f(S)] \qquad (4.10)$$

Capillary pressure, P_c, is a function of phase saturation, and must be defined by a set of functions. The capillary pressure curve is a summary of fluid-fluid interactions, and for any element of rock gives the average phase pressures for all the fluid-fluid contacts within the porous medium at a given saturation. For an individual pore, P_c can be related to measurable geometries (curvatures) and forces (interfacial tension), and defined theoretically – but for a real porous medium it is an average property. Figure 4.7 shows some example measured Pc curves, based on mercury intrusion experiments (Neasham 1977).

The slope of the P_c curve is related to the pore size distribution. More uniform pore-size distributions have a fairly flat function (as for the 1,000 mD curve in Fig. 4.7), while highly variable pore size distributions have a gradually rising function (as with the 50 mD curve in Fig. 4.7). The capillary entry pressure is a function of the largest accessible pore. Different P_c curves are followed for drainage (oil invasion) and imbibition (waterflood) processes.

We summarise our introduction by noting that the complexities of multi-phase flow boil down to a set of rules governing how two or more phases interact in the porous medium. Figure 4.8 shows an example micro-model (an artificial etched-glass pore space network) in which fluid phase distributions can be visualised. Even for this comparatively simple pore space, the number and nature of the fluid-fluid and fluid-solid interfaces is bewildering. What determines whether gas, oil or water will invade the next available pore as the pressure in one phase changes?

One response – the modelling approach – is that good answers to this problem are found in mathematical modelling of pore networks (e.g. McDougall and Sorbie 1995; Blunt 1997; Øren and Bakke 2003; Behbahani and Blunt 2005).

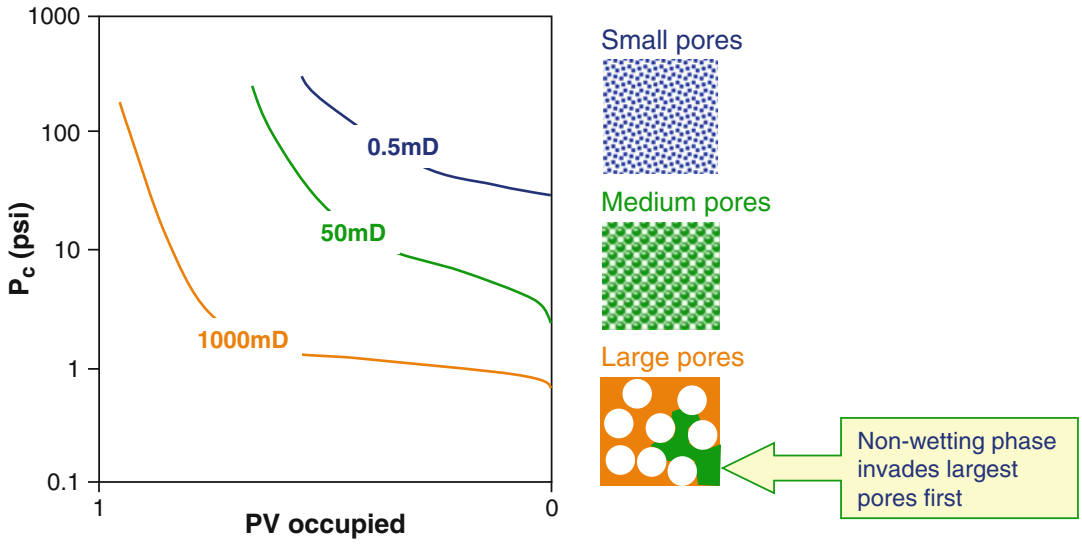

Fig. 4.7 Example capillary pressure functions: capillary drainage curves based on mercury intrusion experiments measuring the non-wetting phase pressure required to invade a certain pore volume (PV)

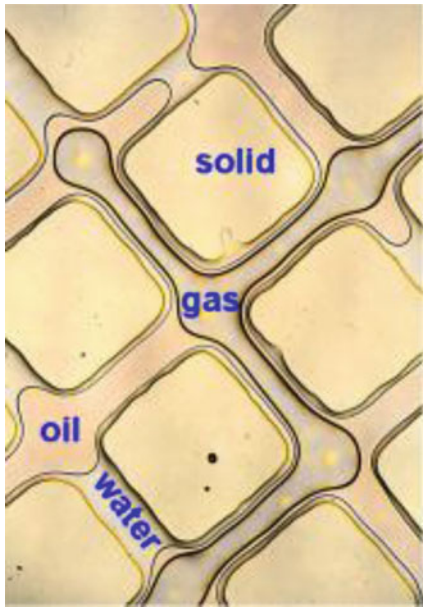

Fig. 4.8 Example micro-model, where fluid distributions are visualised within an artificial laboratory pore-space (Statoil archive image of micromodel experiment conducted at Heriot Watt University)

Another response – the laboratory approach – is that you need to measure the multiphase flow behaviour in real rock samples at true reservoir conditions (pressures and temperatures). In reality, you need both measurements and modelling to obtain a good appreciation of the "rules" governing multiphase flow. Our concern here is to understand how to handle and upscale these functions within the reservoir model.

4.2.2 Two-Phase Steady-State Upscaling Methods

Multiphase flow upscaling, involves the process of calculating the large-scale multiphase flows given a known distribution of the small-scale petrophysical properties and flow functions. There are many methods for doing this, but it is useful to differentiate two:

1. Dynamic methods
2. Steady-state methods

Fuller discussions of these methods are found in, for example, Barker and Thibeau (1997), Ekran and Aasen (2000), Pickup et al. (2005).

Reservoir simulators generally perform *dynamic* multi-phase flow simulations – that is, the pressures and saturations are allowed to vary with position and time in the simulation grid. The Kyte and Berry (1975) upscaling method is the most well-known dynamic two-phase upscaling method, but there have been many alternatives proposed, such as Stone's (1991) method and Todd and Longstaff (1972) for miscible gas. The strength of the dynamic methods is that they attempt to capture the '*true*' flow behaviour for a given set of boundary conditions. Their principle weaknesses are that they can be difficult and time-consuming to calculate and can be plagued by numerical errors.

In contrast, the steady-state methods are easier to calculate and understand and represent ideal multi-phase flow behaviour. There are three steady-state end-member assumptions:

- *Viscous limit* (VL): The assumption that the flow is steady state at a given, constant fractional flow. Capillary pressure is assumed to be zero.
- *Capillary equilibrium* (CE): The assumption that the saturations are completely controlled by capillary pressure. Applied pressure gradients are assumed to be zero or negligible.
- *Gravity-Capillary equilibrium* (GCE): Similar to CE, except that in addition the saturations are also controlled by the effect of gravity on the fluid density difference. Note that GCE is similar to the vertical equilibrium (VE) assumption also applied in reservoir simulation (Coats et al. 1971), except that VE assumes negligible capillary pressure.

The viscous limit assumption is similar to a steady-state core flood experiment which is sometimes used in core analysis of multi-phase flow (referred to as special core analysis, or SCAL). Here, a known and constant fraction of oil and water is injected into the sample (let us say 20 % oil and 80 % water) and the permeability for each phase is calculated from the pressure drop and flow rate for that phase. The procedure

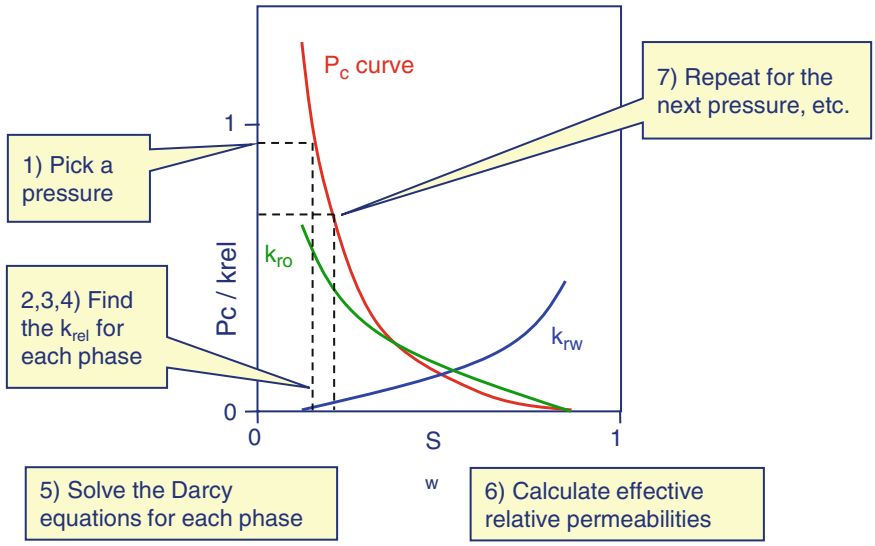

Fig. 4.9 Illustration of the capillary equilibrium steady-state upscaling method

is then repeated for a different fractional flow, and so on. It is assumed that capillary pressure and gravity have no effect. The method can be assumed to apply for a Darcy-flow-dominated two-phase flow system. The method is considered to be valid at larger length-scales, where capillary forces can generally be neglected (e.g. for model grid cell sizes greater than about 1 m vertically).

For the capillary equilibrium steady state assumption it is the Darcy flow effects that are neglected and all fluxes are deemed to be controlled by the capillary pressure curve. For a given pressure, the saturation is known from the P_c curve and the local phase permeability is then determined from the relative permeability curves. The calculation is then repeated for each chosen decrement of pressure until the saturation range is covered (Fig. 4.9). The method is considered to be valid at smaller length-scales, where capillary forces are likely to dominate (e.g. at length-scales less than about 0.2 m). There is also a rate-dependence for viscous and capillary forces – higher flow rates favour viscous forces while lower flow rates favour capillary forces. Note that layering in sedimentary rock media is often at the mm to cm scale

Fig. 4.10 SEM image of laminae in an aeolian sandstone (Image courtesy of British Gas)

(Fig. 4.10), and therefore capillary forces are likely to be important at this length-scale.

The gravity-capillary equilibrium method uses the same principle as the CE method except that vertical pressure gradient is also

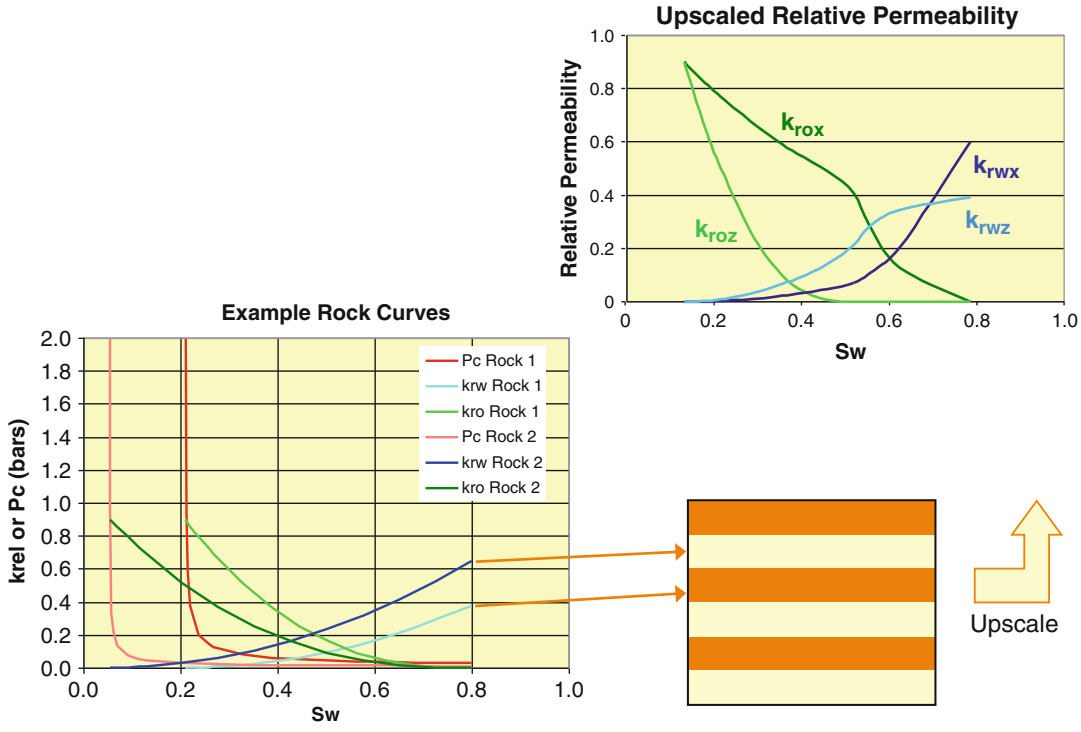

Fig. 4.11 Capillary equilibrium steady-state upscaling method applied to a simple layered model

applied resulting in a vertical trend in the saturation at any chosen pressure reference. The GCE solution should tend towards the CE solution as the length-scale becomes increasingly small.

All three steady-state methods involve a series of independent single-phase flow calculations and therefore can employ a standard single-phase pressure solver algorithm. The methods can therefore be rapidly executed on standard computers.

The capillary equilibrium method can be easily calculated for a simple case, as illustrated in Figure 4.11 by an example set input functions for a regular layered model. Upscaled relative permeability curves for this simple case can be calculated analytically (using a spreadsheet or calculator). The method uses the following steps (refer to Fig. 4.9):

1. Chose a value for pressure, P_{c1};
2. Find the corresponding saturation value, S_{w1};
3. Determine the relative permeability for oil and water for each rock type, k_{ro1}, k_{rw1}, k_{ro2}, k_{rw2};
4. Find the phase permeabilities, e.g. $k_{o1} = k_1 * k_{ro1}$;
5. Calculate the upscaled permeability for each direction and for each phase using the arithmetic and harmonic averages;
6. Invert back to upscaled relative permeability, e.g. $k_{ro1} = k_{o1}/k_{upscaled}$ (once again the arithmetic and harmonic averages are used to obtain the upscaled absolute permeability);
7. Repeat for next value pressure, P_{c2}.

Note that the upscaled curves are highly anisotropic, and in fact sometimes lie outside the range of the input curves. This is because of the effects of capillary forces – specifically capillary trapping when flowing across layers. Capillary forces result in preferential imbibition of water (the wetting phase) into the lower permeability layers, making flow of oil (the non-wetting phase) into these low permeability layers even more difficult.

These somewhat non-intuitive effects of capillary pressure in laminated rocks can be demonstrated experimentally (Fig. 4.12). In the case of two-phase flow across layers in a water-wet

laminated rock – a cross-bedded aeolian sandstone (Fig. 4.10), oil becomes trapped in the high permeability layers upstream of low permeability layers due to water imbibition into the lower permeability layers (Huang et al. 1995).

The chosen flow rate for this experiment was at typical reservoir waterflood rate (around 0.1 m/day). This trapped oil can be mobilised either by reducing the capillary pressure (e.g. by modifying the interfacial tension by use of surfactant chemicals) or by increasing the flow rate, and thereby the viscous forces. Alternatively, a modified flow strategy favouring flow along the rock layers (parallel to bedding) would result in less capillary trapping and a more efficient waterflood. In the more general case, where the rock has variable wettability the effects of capillary/viscous interactions become more complex (e.g. McDougall and Sorbie 1995; Huang et al. 1996; Behbahani and Blunt 2005).

Exercise 4.1

Permeability upscaling for a simple layered model.

The simple repetitive layered model shown in Fig. 4.11 can be used to illustrate single and multi-phase permeability upscaling using the "back of the envelope" maths. We assume the two layers are regular and of equal thickness. Rock type 1 has a permeability of 100md and rock type 2 has a permeability of 1,000md.

(a) Calculate the upscaled horizontal and vertical single-phase permeability using averaging.

(b) Calculate selected values for the upscaled two-phase relative permeability curves, assuming steady-state capillary equilibrium conditions. Use the flow functions shown in Fig. 4.11, as tabulated below, with water saturation, S_w; relative permeability to water, krw; relative permeability to oil, krow; capillary pressure, P_c (bars). Choose P_c values of 0.05 and 0.3 (shown in bold).

Table for rock type 1 (100 mD)				Table for rock type 2 (1,000 mD)			
Sw	krw	krow	Pc	Sw	krw	krow	Pc
0.2092	0.0	0.9	10.0	0.05432	0.0	0.9	10.0
0.209791	0.0000004	0.897752	2.744926	0.055066	0.0	0.897752	0.976926
0.212154	0.000009	0.888792	0.938248	0.058048	0.000016	0.888792	0.333925
0.215108	0.000038	0.877668	0.590923	**0.059**	**0.000023**	**0.887**	**0.3**
0.221016	0.000151	0.855673	0.372172	0.061777	0.000065	0.877668	0.210311
0.226	**0.0003**	**0.839**	**0.3**	0.069234	0.000259	0.855673	0.132457
0.238740	0.000943	0.791683	0.201984	0.091604	0.001618	0.791683	0.071887
0.256464	0.002413	0.730655	0.147628	0.113974	0.004141	0.730655	0.052541
0.26828	0.003771	0.691590	0.127213	**0.119**	**0.005**	**0.718**	**0.05**
0.32736	0.015084	0.515190	0.080120	0.128888	0.006471	0.691590	0.045275
0.38644	0.033939	0.368967	0.061135	0.203456	0.025884	0.515190	0.028515
0.44552	0.060336	0.250969	0.050461	0.278024	0.058239	0.368967	0.021758
0.449	**0.062**	**0.245**	**0.05**	0.352592	0.103536	0.250969	0.017959
0.5046	0.094275	0.159099	0.043483	0.42716	0.161775	0.159099	0.015476
0.56368	0.135756	0.091074	0.038504	0.501728	0.232956	0.091074	0.013704
0.62276	0.184779	0.044366	0.034742	0.576296	0.317079	0.044366	0.012365
0.68184	0.241344	0.016099	0.031781	0.650864	0.414144	0.016100	0.011311
0.74092	0.305451	0.002846	0.029380	0.725432	0.524151	0.002846	0.010456
0.8	0.3771	0.000000	0.027386	0.8	0.6471	0.000000	0.009747

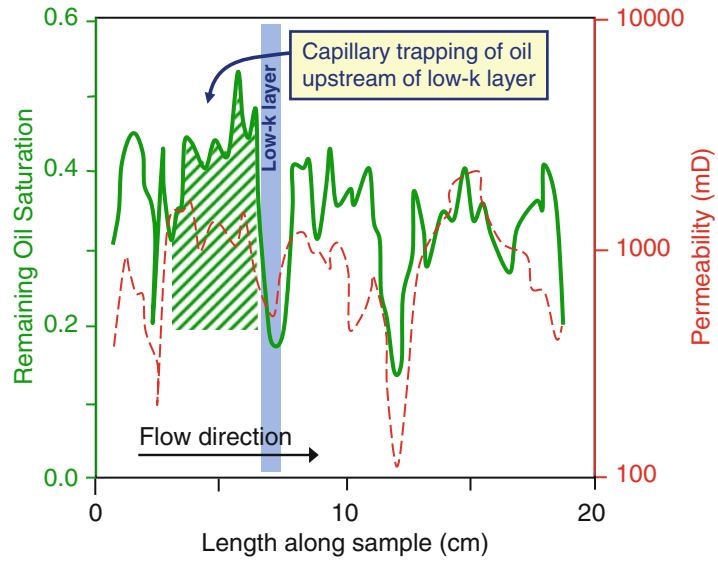

Fig. 4.12 Summary of a waterflood experiment across a laminated water-wet rock sample (Redrawn from Huang et al. 1995, ©1995, Society of Petroleum Engineers Inc., reproduced with permission of SPE. Further reproduction prohibited without permission)

4.2.3 Heterogeneity and Fluid Forces

It is important to relate these multi-phase fluid flow processes to the heterogeneity being modelled. This is a fairly complex issue, and fundamental to what reservoir model design is all about. As a way in to this topic we use the *balance of forces* concept to give us a framework for understanding which scales most affect a particular flow process. For example, we know that capillary forces are likely to be important for rocks with strong permeability variations at the small scale (less than 20 cm scale is a good rule of thumb).

Figure 4.13 shows a simple sketch of the end-members of the fluid force system. We have three end members: gravity-, viscous- and capillary-dominated. Reality will lie somewhere within the triangle, but appreciation of the end-member systems is useful to understand the expected flow-heterogeneity interactions. Note, that for the same rock system the flow behaviour will be completely different for a gravity-dominated, viscous-dominated or capillary-dominated flow regime. The least intuitive is the capillary-dominated case where water (for a water-wet system) imbibes preferentially into the lower permeability layers.

To treat this issue more formally, we use scaling group theory (Rapoport 1955; Li and Lake 1995; Li et al. 1996; Dengen et al. 1997) to understand the balance of forces. The viscous/capillary ratio and the gravity/capillary ratio are two of a number of dimensionless scaling group ratios that can be determined to represent the balance of fluid forces. For example, for an oil-water system we can define the following force ratios:

$$\frac{Viscous}{Capillary} = \frac{u_x \Delta x \mu_o}{k_x (dP_c/dS)} \tag{4.11}$$

$$\frac{Gravity}{Capillary} = \frac{\Delta\rho\, g\, \Delta z}{(dP_c/dS)} \tag{4.12}$$

where,

Δx, Δz are system dimensions,

u_x is fluid velocity,

μ_o is the oil viscosity,

k_x is the permeability in the x direction,

(dP_c/dS) is the slope of the capillary pressure function,

$\Delta\rho$ is the fluid density difference and g is the constant due to gravity.

The viscous/capillary ratio is essentially a ratio of Darcy's law with a capillary pressure

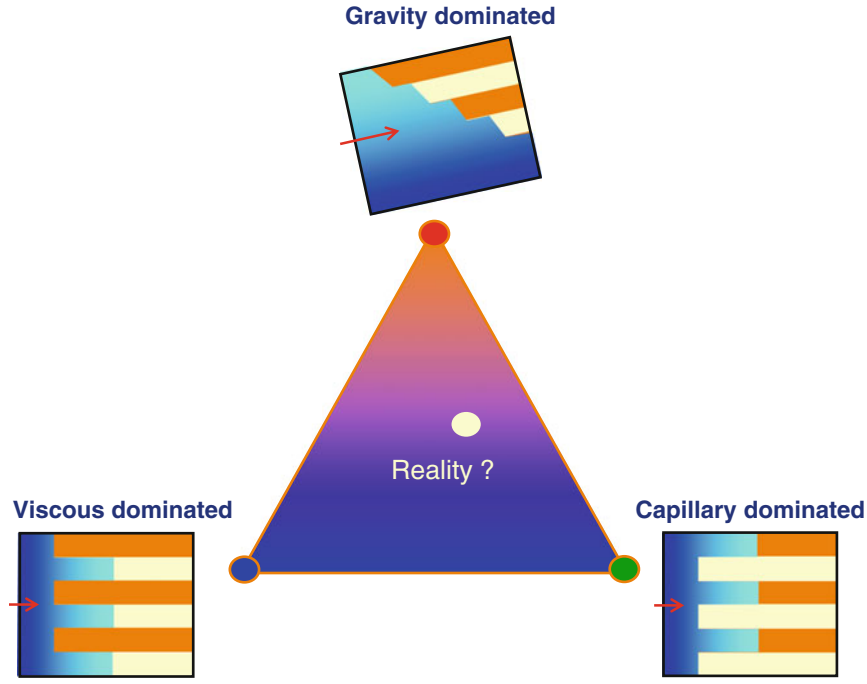

Fig. 4.13 The fluid forces triangle with sketches to illustrate how a water-flood would behave for a layered rock (*yellow* = high permeability layers)

gradient term, while the gravity/capillary ratio is the buoyancy term against the capillary pressure gradient. Δx and Δz represent the physical length scales – essentially the size of the model in the x and z directions. There are several different forms of derivation of these ratios depending on the physical assumptions and the mathematical approach, but the form given above should allow the practitioner to gain an appreciation of the factors involved. It is important that a consistent set of units are used to ensure the ratios remain dimensionless.

For example, a calculation to determine when capillary/heterogeneity interactions are important can be made by studying the ratio of capillary to viscous forces. Figure 4.14 shows a reference well pair assuming 1 km well spacing and a 150 psi pressure drawdown at the producing well. We are interested in the balance of forces and a rock unit within the reservoir, represented by alternating permeability layers with a spacing of Δx. Figure 4.15 shows the result of the analysis of the viscous/capillary

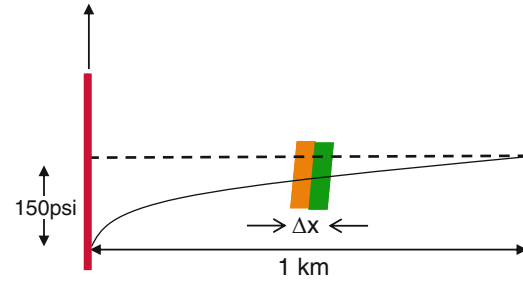

Fig. 4.14 Sketch of pressure drawdown between an injection and production well pair for water-flooding an oil reservoir

ratio for different layer contrasts and heterogeneity length-scales (Ringrose et al. 1996).

If the layering in a reservoir occurs at the >10 m scale then viscous forces tend to dominate (or the Viscous/Capillary ratio must be very low for capillary forces to be significant at this scale). However, if the layers are in the mm-to-cm range then capillary forces are much more likely to be important (or the Viscous/Capillary ratio must be

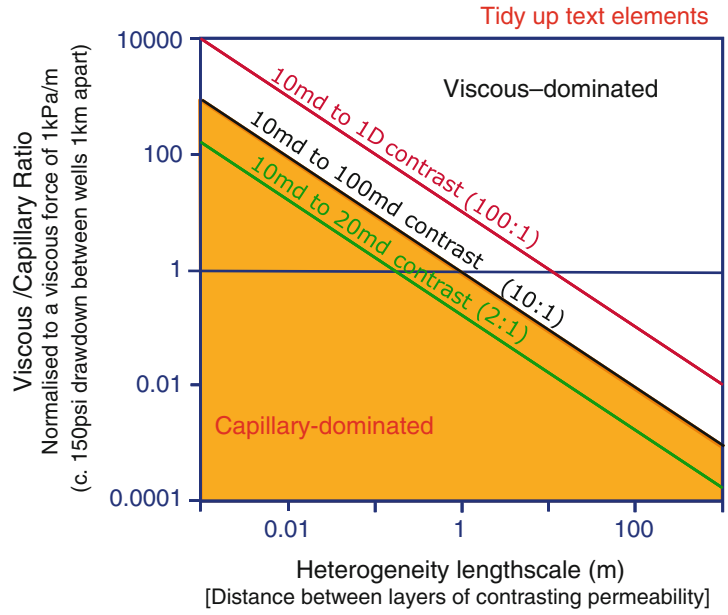

Fig. 4.15 Example calculation of the viscous/capillary ratio for a layered system as a function of length scale, for selected permeability contrasts (Redrawn from Ringrose et al. 1996, ©1996, Society of Petroleum Engineers Inc., reproduced with permission of SPE. Further reproduction prohibited without permission)

very high to override capillary effects). Note, however, that the pressure gradients will vary as a function of spatial position and time and so in fact the Viscous/Capillary ratio will vary – viscous forces will be high close to the wells and lower in the inter-well region.

An important and related concept is the capillary number, most commonly defined as:

$$C_a = \frac{\mu q}{\gamma} \tag{4.13}$$

where μ is the viscosity, q is the flow rate and γ is the interfacial tension.

This is a simpler ratio of the viscous force to the surface tension at the fluid-fluid interface. Capillary numbers around 10^{-4} or lower are generally deemed to be capillary-dominated.

4.3 Multi-scale Geological Modelling Concepts

4.3.1 Geology and Scale

The importance of multiple scales of heterogeneity for petroleum reservoir engineering has been recognised for some time. Haldorsen and Lake (1984) and Haldorsen (1986) proposed four conceptual scales associated with averaging properties in porous rock media:

- Microscopic (pore-scale);
- Macroscopic (representative elementary volume above the pore scale);
- Megascopic (the scale of geological heterogeneity and or reservoir grid blocks);
- Gigascopic (the regional or total reservoir scale).

Weber (1986) showed how common sedimentary structures including lamination, clay drapes and cross-bedding affect reservoir flow properties and Weber and van Geuns (1990) proposed a framework for constructing geologically-based reservoir models for different depositional environments. Corbett et al. (1992) and Ringrose et al. (1993) argued that multi-scale modelling of water-oil flows in sandstones should be based on a hierarchy of sedimentary architectures, with smaller scale heterogeneities being especially important for capillary-dominated flow processes (see Sect. 2.3.2.2 for an introduction to hierarchy). Campbell (1967) established a basic hierarchy of sedimentary features related to fairly universal processes of

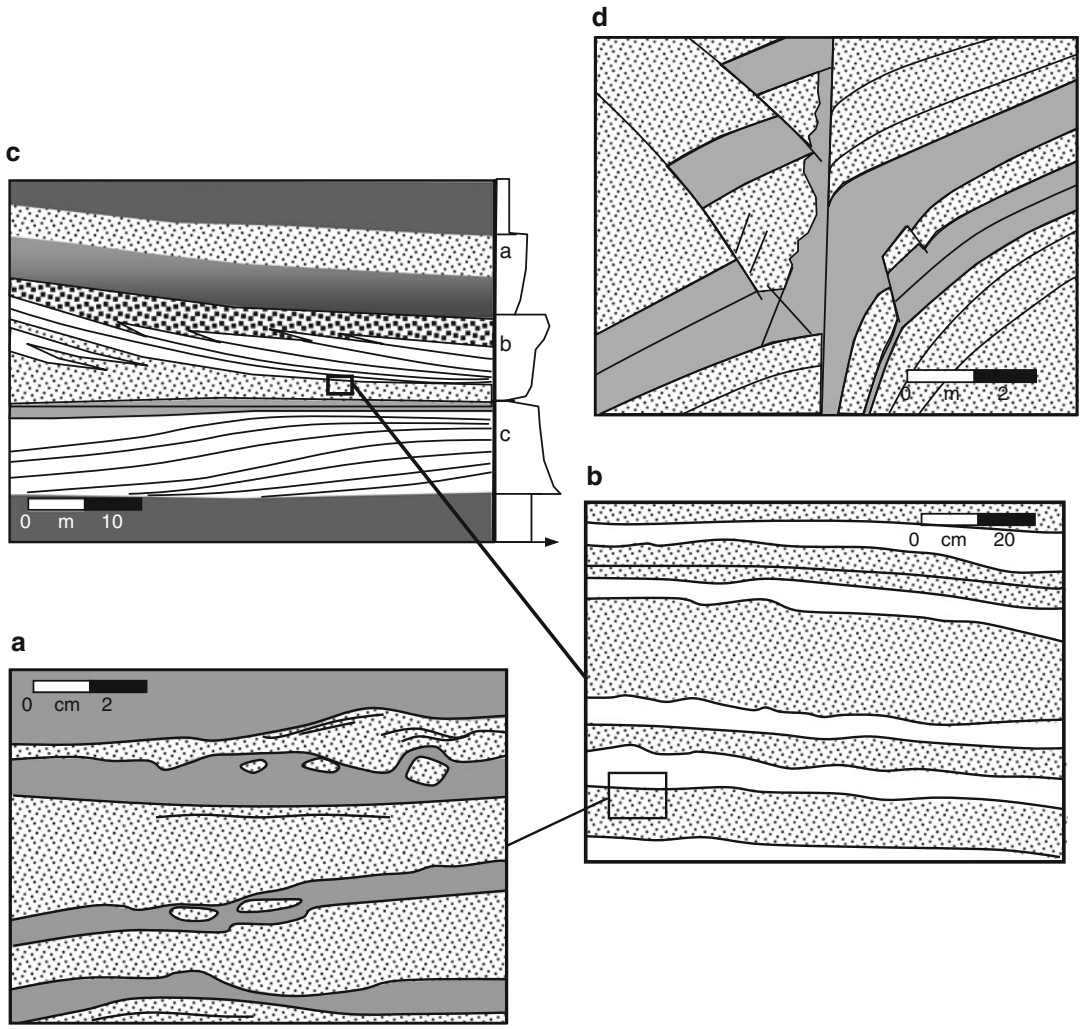

Fig. 4.16 Field outcrop sketches illustrating multi-scale reservoir architecture
(**a**) Sandstone and siltstone lamina-sets from a weakly-bioturbated heterolithic sandstone
(**b**) Sandy and muddy bed-sets in a tidal deltaic lithofacies
(**c**) Prograding sedimentary sequences from a channelized tidal delta
(**d**) Fault deformation fabric around a normal fault through an inter-bedded sandstone and silty clay sequence (Redrawn from Ringrose et al. 2008, The Geological Society, London, Special Publications 309 © Geological Society of London [2008])

deposition, namely lamina, laminasets, beds and bedsets. Miall (1985) showed how the range of sedimentary bedforms can be defined by a series of bounding surfaces from a 1st order surface bounding the laminaset to 4th (and higher) order surfaces bounding, for example, composite point-bars in fluvial systems.

Figure 4.16 illustrates the geological hierarchy for a heterolithic sandstone reservoir. Lamina-scale, lithofacies-scale and sequence-stratigraphic scale elements can be identified. In addition to the importance of correctly describing the sedimentary length scales, structural (Fig. 4.16d) and diagenetic processes act to modify the primary depositional fabric.

At the most elemental level we are interested in the pore scale (Fig. 4.17) – the rock pores that contain fluids and determine the multi-phase flow

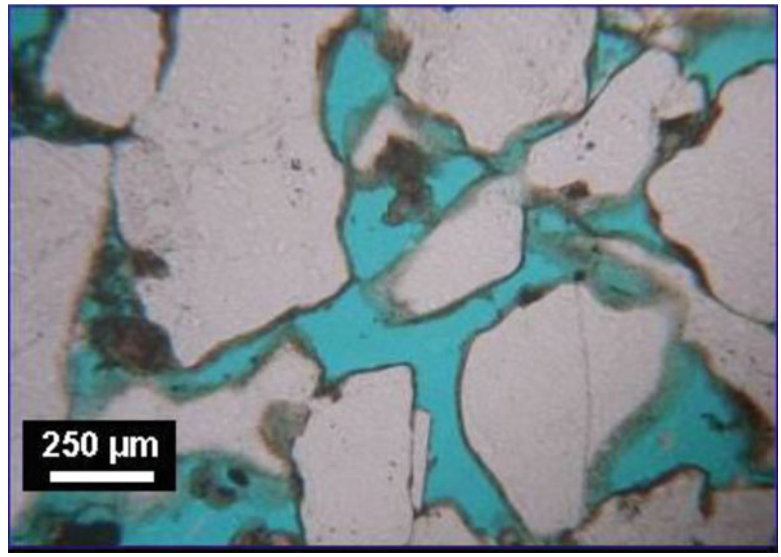

Fig. 4.17 The pore scale – example thin section of pores in a sandstone reservoir (Statoil image archive, © Statoil ASA, reproduced with permission)

behaviour. Numerical modelling at the pore scale has been widely used to better understand permeability, relative permeability and capillary pressure behaviour for representative pore systems (e.g. Bryant and Blunt 1992; Bryant et al. 1993; McDougall and Sorbie 1995; Bakke and Øren 1997; Øren and Bakke 2003). Most laboratory analysis of rock samples is devoted to measuring pore-scale properties – resistivity, acoustic velocity, porosity, permeability, and relative permeability. Pore-scale modelling allows these measured flow properties to be related to fundamental rock properties such as grain size, grain sorting and mineralogy. However, the application of pore-scale measurements and models in larger-scale reservoir models requires *a framework for assigning pore-scale properties* to the geological concept. We do this by assigning flow properties to lamina-scale, lithofacies-scale or stratigraphic-scale models. This can be done quite loosely, with weak assumptions, or systematically within a multi-scale upscaling hierarchy.

Statistical methods for representing the spatial architecture of geological systems were covered in Chap. 2. What concerns us here is how we integrate geological models within a multi-scale hierarchy. This may require a re-evaluation of the scales of models needed to address different scale transitions.

Pixed-based modelling approaches (e.g. SGS, SIS) can be applied at pretty-much any scale, whereas object-based modelling approaches will tend to have very clear associations with pre-defined length scales. In both cases the model grid resolution needs to be fine enough to explicitly capture the heterogeneity being represented in the model. Process-based modelling methods (e.g. Rubin 1987; Wen et al. 1998; Ringrose et al. 2003) are particularly appropriate for capturing the effects of small-scale geological architecture within a multi-scale modelling framework.

In the following sections we look at some key questions the reservoir modelling practitioner will need to address in building multi-scale reservoir models:

1. How many scales to model and upscale?
2. Which scales to focus on?
3. How to best construct model grids?
4. Which heterogeneities matter most?

4.3.2 How Many Scales to Model and Upscale?

Despite the inherent complexities of sedimentary systems, dominant scales and scale transitions can be identified (Fig. 4.18). These dominant scales

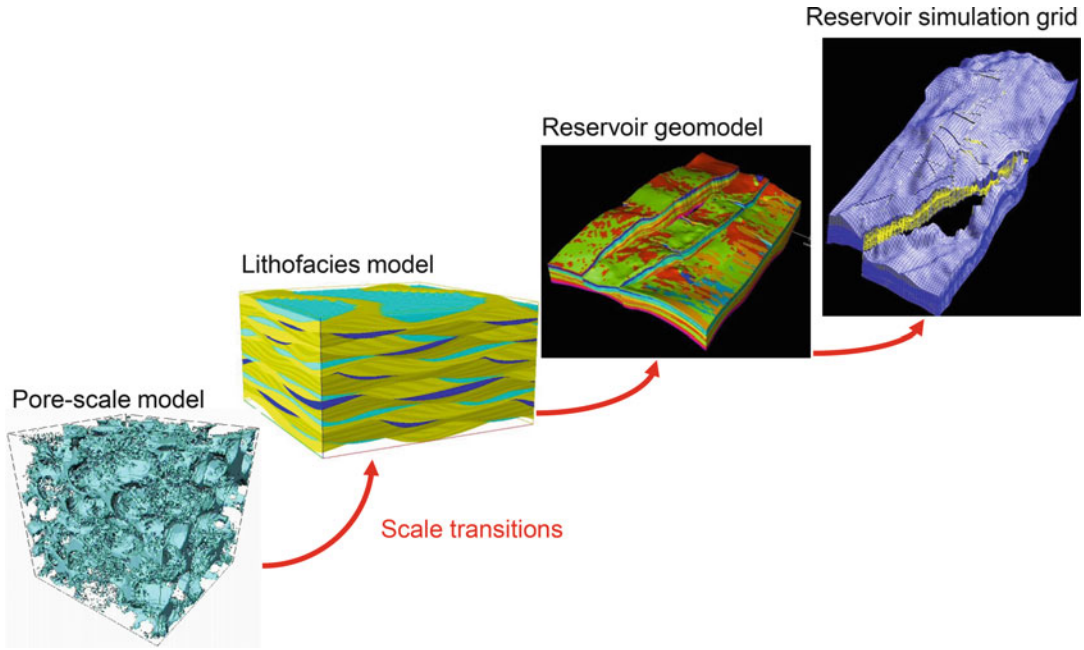

Fig. 4.18 Examples of geologically-based reservoir simulation models at four scales
(**a**) Model of pore space used as the basis for multi-phase pore network models (50 μm cube);
(**b**) Model of lamina-sets within a tidal bedding facies (dimensions 0.05 m × 0.3 m × 0.3 m);
(**c**) Facies architecture model from a sector of the Heidrun field showing patterns of tidal channel and bars (dimensions 80 m × 1 km × 3 km);
(**d**) Reservoir simulation grid for part of the Heidrun field illustrating grid cells displaced by faults in true structural position (dimensions 200 m × 3 km × 5 km)
(Statoil image archives, © Statoil ASA, reproduced with permission)

are based both on the nature of rock heterogeneity and the principles which govern macroscopic flow properties. In this discussion, we assume four scales – pore, lithofacies, geomodel and reservoir. This gives us three scale transitions:

1. *Pore to lithofacies*. Where a set of pore-scale models is applied to models of lithofacies architecture to infer representative or typical flow behaviour for that architectural element. The lithofacies is a basic concept in the description of sedimentary rocks and presumes an entity that can be recognised routinely. The lamina is the smallest sedimentary unit, at which fairly constant grain deposition processes can be associated with a macroscopic porous medium. The lithofacies comprises some recognisable association of laminae and lamina sets. In certain cases, where variation between laminae is small, pore-scale models could be applied directly to the lamina-set or bed-set scales.
2. *Lithofacies to geomodel*. Where a larger-scale geological concept (e.g. a sequence stratigraphic model, a structural model or a diagenetic model) postulates the spatial arrangement of lithofacies elements. Here, the geomodel is taken to mean a geologically-based model of the reservoir, typically resolved at the sequence or zone scale.
3. *Geomodel to reservoir simulator*. This stage may often only be required due to computational limitations, but may also be important to ensure good transformation of a geological model into 3-dimensional grid optimised for flow simulation (e.g. within the constraints of finite-difference multiphase flow simulation). This third step is routinely taken by practitioners, whereas steps 1 and 2 tend to be neglected.

Features related to structural deformation (faults, fractures and folds) occur at a wide range of scales (Walsh et al. 1991; Yielding et al. 1992) and do not naturally fall into a

step-wise upscaling scheme. Structural features are typically incorporated at the geomodel scale. However, effects of smaller scale faults may also be incorporated as effective properties (as transmissibility multipliers) using upscaling approaches. The incorporation of fault transmissibility into reservoir simulators is considered thoroughly by Manzocchi et al (2002). Conductive fractures may also affect sandstone reservoirs, and are often the dominant factor in carbonate reservoirs. Approaches for multi-scale modelling of fractured reservoirs have also been developed (e.g. Bourbiaux et al. 2002) and will be developed further in Chap. 6.

Historical focus over the last few decades has been on including increasingly more detail into the geomodel, with only one upscaling step being explicitly performed. Full-field geomodels are typically in the size range of 1–10 million cells with horizontal cell sizes of 50–100 m and vertical cell sizes of order 1–10 m. Multi-scale modelling allows for better flow unit characterization and improved performance predictions (e.g. Pickup et al. 2000; Scheiling et al. 2002). There are also examples where a large number of grid cells are applied to sector or near-well models reducing cell sizes to the dm-scale. Upscaling of the near-well region requires methods to specifically address radial flow geometry (e.g. Durlofsky et al. 2000).

Recent focus on explicit small-scale lithofacies modelling includes the use of million cell models with mm to cm size cells (e.g. Ringrose et al. 2003; Nordahl et al 2005). Numerical pore-scale modelling employs a similar number of network nodes at the pore scale (e.g. Øren and Bakke 2003). Model resolution is always limited by the available computing power, and although continued efficiencies and memory gains are expected in the future, the use of available numerical discretisation at several scales within a hierarchy is preferred to efforts to apply the highest possible resolution at one of the scales (typically the geomodel). There is also an argument that advances in seismic imaging coupled with computing power will enable direct geological modelling at the seismic resolution scale. However, even when this is possible, seismic-based lithology prediction (using seismic inversion) will require smaller-scale modelling of the petrophysical properties within the seismically resolved element (see Chap. 2).

Upscaling methods impose further limitations on the value and utility of models within a multi-scale framework. In conventional upscaling – from a geological model to a reservoir simulation grid – there are various approaches used. These cover a range which can be classed in terms of the degree of simplification/complexity:

1. *Averaging of well data directly into the flow simulation grid:* This approach essentially ignores explicit upscaling and neglects all aspects of smaller scale structure and flows. The approach is fast and simple and may be useful for quick assessment of expected reservoir flows and mass balance. It may also be adequate for very homogeneous and highly permeable rock sequences.
2. *Single-phase upscaling only in Δz:* This commonly applied approach assumes a simulation grid designed with the same Δx, the Δy as the geological grid. The approach is often used where complex structural architecture provides very tight constraints to design of the flow modelling grid. Upscaling essentially comprises use of averaging methods but ensures a degree of representation of thin layering or barriers. Also, where seismic data gives a good basis for the geological model in the horizontal dimensions, vertical upscaling of fine-scale layering to the reservoir simulator scale is typically required.
3. *Single-phase upscaling in Δx Δy and Δz:* With this approach multi-scale effective flow properties are explicitly estimated and the upscaling tools are widely available (diagonal tensor or full-tensor methods). Multiphase flow effects are however neglected.
4. *Multi-phase upscaling in Δx Δy and Δz:* This approach represents an attempt to calculate effective multiphase flow properties in larger scale models. The approach has been used rather too seldom due to demands of time and resources. However, the development of steady-state solutions to multiphase flow upscaling problems (Smith 1991; Ekran and Aasen 2000; Pickup and Stephen 2000) has led to wider use in field studies (e.g. Pickup et al 2000; Kløv et al 2003).

These four degrees of upscaling complexity help define the number and dimensions of models required. The number of scales modelled is typically related to the complexity and precision of answer sought. Improved oil recovery (IOR) strategies and reservoir drainage optimisation studies are often the reason for starting a multi-scale approach. A minimum requirement for any reservoir model is that the assumptions used for smaller scale processes (pore scale, lithofacies scale) are explicitly stated.

For example, a typical set of assumptions commonly used might be:

> *We assume that two special core analysis measurements represent all pore-scale physical flow processes and that all effects of geological architecture are adequately summarised by the arithmetic average of the well data.*

Assumptions like these are rarely stated (although often implicitly assumed). More ideally, some form of explicit modelling at each scale should be performed using 3D multiphase upscaling methods. At a minimum, it is recommended to explicitly define pore-scale and geological-scale models, and to determine a rationale for associating the pore-scale with the geological scale, as in the example shown in Fig. 4.18.

4.3.3 Which Scales to Focus On? (The REV)

Geological systems present us with variability at nearly every scale (Fig. 4.19). To some extent they are fractal (Turcotte 1992), showing similar variability at all scales. However, geological systems are more accurately described as *multi-fractal* – showing some scale-independent similarities – but dominated by process-controlled scale-dependent features (e.g. Ringrose 1994). However you describe them, geological systems are complex, and we need an approach for simplifying that complexity and focussing on the important features and length-scales.

The Representative Elementary Volume (REV) concept (Bear 1972) provides the essential framework for understanding measurement scales and geological variability. This concept is fundamental to the analysis of flow in permeable media – without a representative pore space we cannot measure a representative flow property

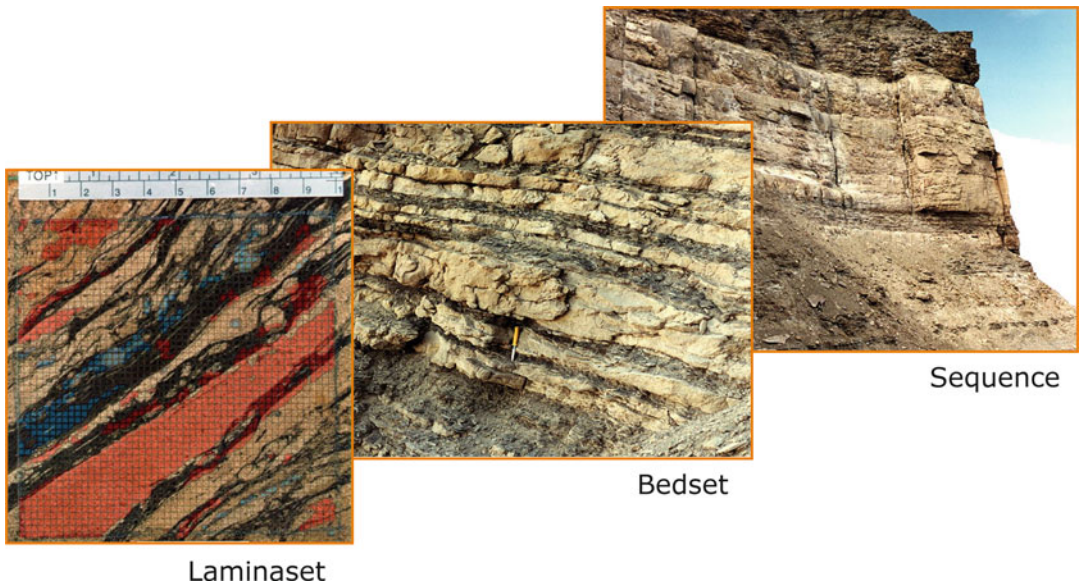

Fig. 4.19 Multi-scale variability in a heterolithic (tidal delta) sandstone system: Laminaset scale: Core photograph with measured permeability (*Red* indicates >1 Darcy); Bedset scale: interbedded sandy and muddy bedsets (hammer for scale); Sequence-stratigraphic scale: Sand-dominated para-sequence between mudstone units (Photos A. Martinius/Statoil © Statoil ASA, reproduced with permission)

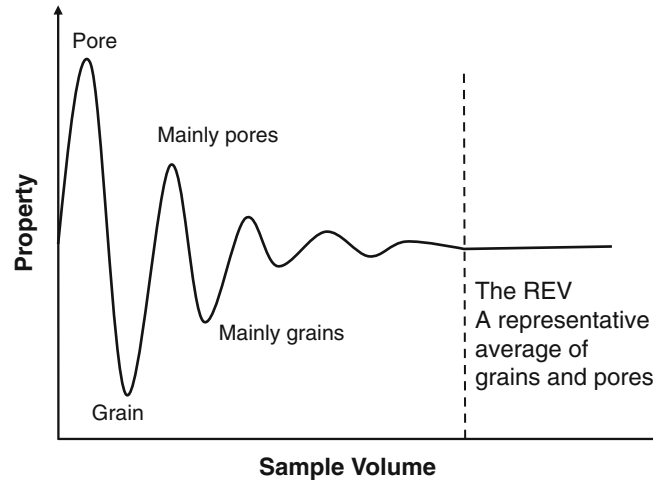

Fig. 4.20 The Representative Elementary Volume (REV) concept, after Bear 1972

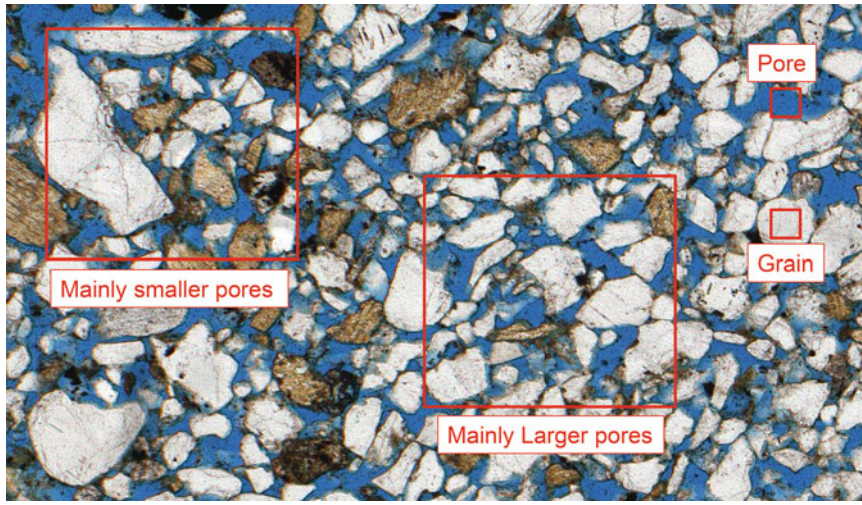

Fig. 4.21 The pore-scale REV illustrated for an example thin section (The whole image is assumed to be the pore-scale REV) (Photo K. Nordahl/Statoil © Statoil ASA, reproduced with permission)

nor treat the medium as a continuum in terms of the physics of flow. The original concept (Fig. 4.20) refers to the scale at which pore-scale fluctuations in flow properties approach a constant value both as a function of changing scale and position in the porous medium, such that a statistically valid macroscopic flow property can be defined, as illustrated in Fig. 4.21.

The pore-scale REV is thus an essential assumption for all reservoir flow properties. However, rock media have several such scales where smaller-scale variations approach a more constant value. It is therefore necessary to develop a multi-scale approach to the REV concept. It is not at first clear how many averaging length-scales exist in a rock medium, or indeed if a REV can be established at the scale necessary for reservoir flow simulation. Despite the challenges, some degree of representativity of estimated flow properties is necessary for flow modelling within geological media, and a multi-scale REV framework is required.

Several workers (e.g. Jackson et al. 2003; Nordahl et al. 2005) have shown that an REV can be established at the lithofacies scale – e.g. at around a length-scale of 0.3 m for tidal

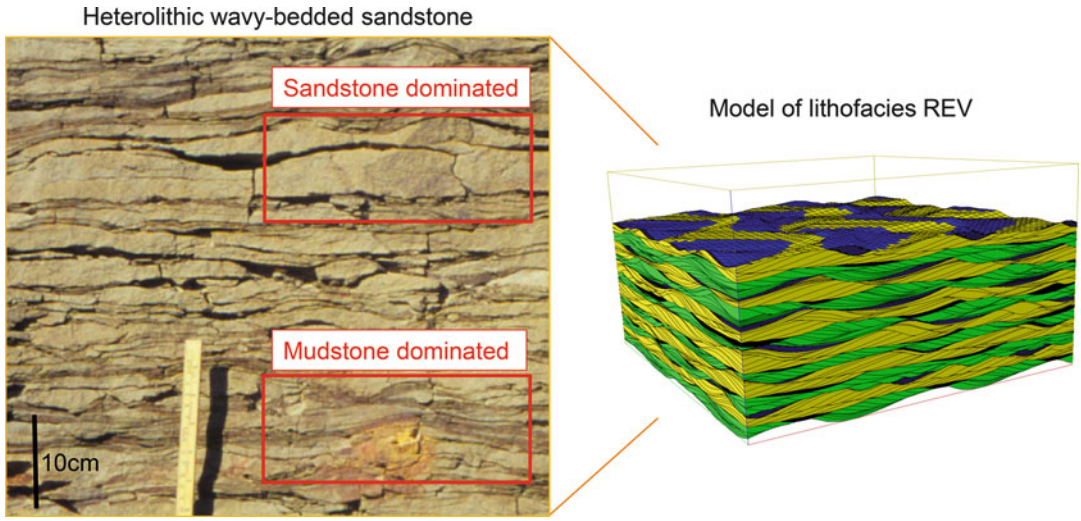

Fig. 4.22 The lithofacies REV illustrated for an example heterolithic sandstone (Photo K. Nordahl/Statoil © Statoil ASA, reproduced with permission)

heterolithic bedding (Fig. 4.22). In fact, the concept of representivity is inherent in the definition of a lithofacies, a recognisable and mappable subdivision of a stratigraphic unit. The same logic follows at larger geological scales, such as the parasequence, the facies association or the sequence stratigraphic unit. Recognisable and continuous geological units are identified and defined by the sedimentologist, and the reservoir modeller then seeks to use these units to define the reservoir modelling elements (*cf* Chap. 2.4).

As a general observation, core plug data is often not sampled at the REV scale and therefore tends to show a wide scatter in measured values, while wire-line log data is often closer to a natural REV in the reservoir system. The true REV – if it can be established – is determined by the geology and not the measurement device. However, wire-line log data usually needs laboratory core data for calibration, which presents us with a dilemma – how should we integrate different scales of measurement?

Nordahl et al. (2005) performed a detailed assessment of the REV for porosity and permeability in a heterolithic sandstone reservoir unit (Fig. 4.23). This example illustrates how apparently conflicting datasets from core plug and wireline measurements can in fact be reconciled within the REV concept. The average and spread of the two datasets differ – the core plugs at a smaller scale record high degree of variability while the wireline data provides a more averaged result at a larger scale. Both sets of data can be integrated into a petrophysical model at the lithofacies REV. Nordahl and Ringrose (2008) extended this concept to propose a multi-scale REV framework (Fig. 4.24), whereby the natural averaging length scales of the geological system can be compared with the various measurement length scales.

Whatever the true nature of rock variability, it is a common mistake to assume that the averaging inherent in any measurement method (e.g. electrical logs or seismic wave inversion) relates directly to the averaging scales in the rock medium. For example, samples from core are often at an inappropriate scale for determining representativity (Corbett and Jensen 1992; Nordahl et al. 2005). At larger scales, inversion of reservoir properties from seismic can be difficult or erroneous due to thin-bed tuning effects. Instead of assuming that any particular measurement gives us an appropriate average, it is much better to relate the measurement to the inherent averaging length scales in the rock system.

So how do we handle the REV concept in practice? The key issue is to find the length-scale (determined by the geology) where the

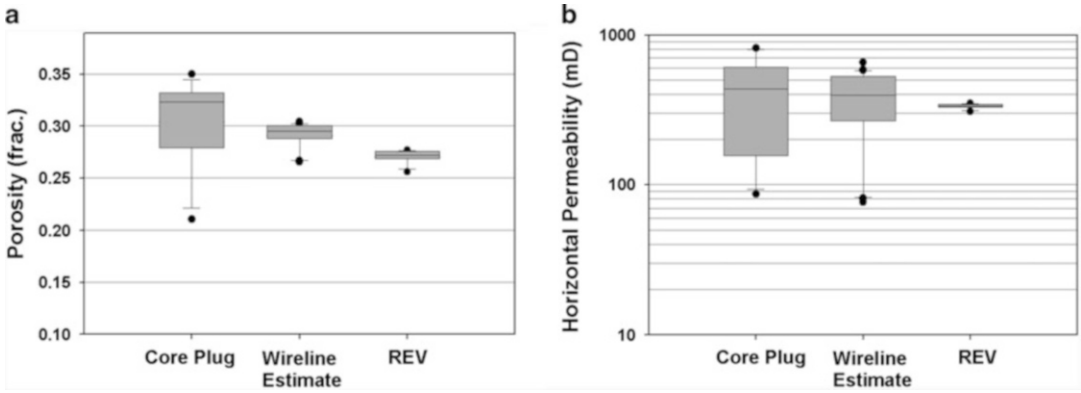

Fig. 4.23 Assessment of the lithofacies REV, from Nordahl et al. (2005). Comparison of porosity (**a**) and horizontal permeability (**b**) estimated or measured from different sources and sample volumes. The lower and upper limits of the box indicate the 25th and the 75th percentile while the whiskers represent the 10th and the 90th percentile. The *solid line* is the median and the *black dots* are the outliers. The values at the REV are measured on the bedding model at a representative scale (With the distribution based on ten realisations) (Redrawn from Nordahl et al. 2005, Petrol Geoscience, v. 11 © Geological Society of London [2005])

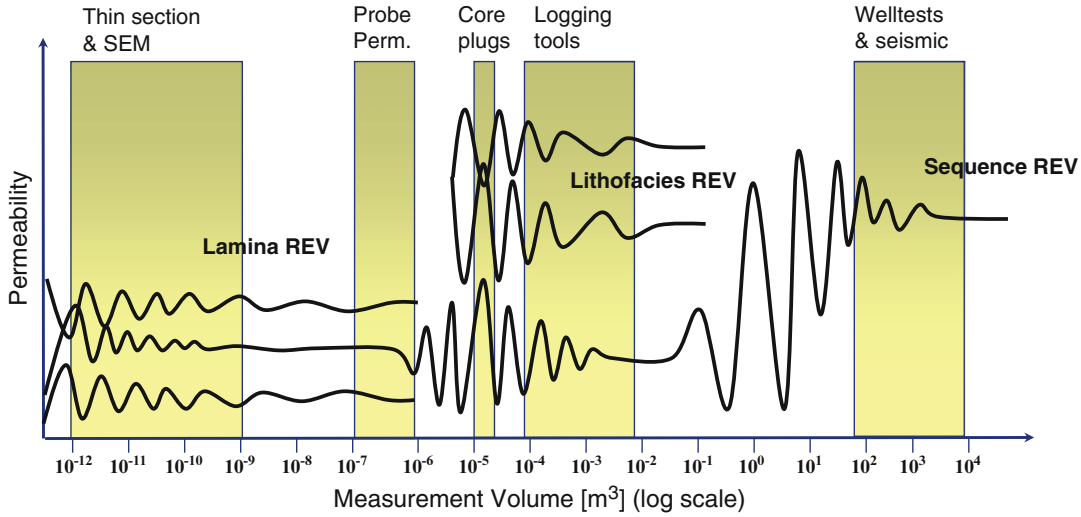

Fig. 4.24 Sketch illustrating multiple scales of REV within a geological framework and the relationship to scales of measurement (Adapted from Nordahl and Ringrose 2008)

measurement or model gives a representative average of the smaller-scale natural variations (Fig. 4.25). At the pore-scale this volume is typically around a few mm^3. For heterogeneous rock systems the REV is of the order of m^3. The challenge is to find the representative volumes for the reservoir system in the subsurface.

4.3.4 Handling Variance as a Function of Scale

Typical practice in petroleum reservoir studies is to assume that an average measured property for any rock unit is valid and that small-scale variability can be ignored. Put more simply, we often assume that the average log-property

Fig. 4.25 Rock sculpture by Andrew Goldsworthy (NW Highlands of Scotland) elegantly capturing the concept of the REV

response for a well through a reservoir interval is the 'right average.' A statistician will know that an arbitrary sample is rarely an accurate representation of the truth. Valid statistical treatment of sample data is an extensive subject treated thoroughly in textbooks on statistics in the Earth Sciences – e.g. Size (1987), Davis (2003), Isaaks and Srivastava (1989) and Jensen et al. (2000).

The challenges involved in correctly inferring permeability from well data are illustrated here using an example well dataset (Fig. 4.26, Table 4.2). This 30 m cored-well interval is from a tidal deltaic reservoir unit with heterolithic lithofacies and moderate to highly variable petrophysical properties (the same well dataset is discussed in detail by Nordahl et al. (2005)).

Table 4.2 compares the permeability statistics for different types of data from this well:

(a) High resolution probe permeameter data;
(b) Core plug data;
(c) A continuous wireline-log based estimator of permeability for the whole interval;
(d) A blocked permeability log as might be typically used in reservoir modelling.

Statistics for ln(k) are shown as the population distributions are approximately log normal. It is well known that the sample variance should reduce as sample scale is increased. Therefore, the reduction in variance between datasets (c) and (d) – core data to reservoir model – is expected. It is, however, a common mistake in multi-scale reservoir modelling for an inappropriate variance to be applied in a larger scale model, e.g. if core plug variance was used directly to represent the upscaled geomodel variance.

Comparison of datasets (a) and (b) reveals another form of variance that is commonly ignored. The probe permeameter grid (2 mm spaced data over a 10 cm × 10 cm core area) shows a variance of 0.38 [ln(k)]. The core plug dataset for the corresponding lithofacies interval (estuarine bar), has σ^2 ln(k) = 0.99, which represents variance at the lithofacies scale. However, blocking of the probe permeameter data at the core plug scale shows a variance reduction factor of 0.79 up to the core plug scale (column 2 in Table 4.2). Thus, in this dataset (where high resolution measurements are available) we know that a significant degree of variance is missing

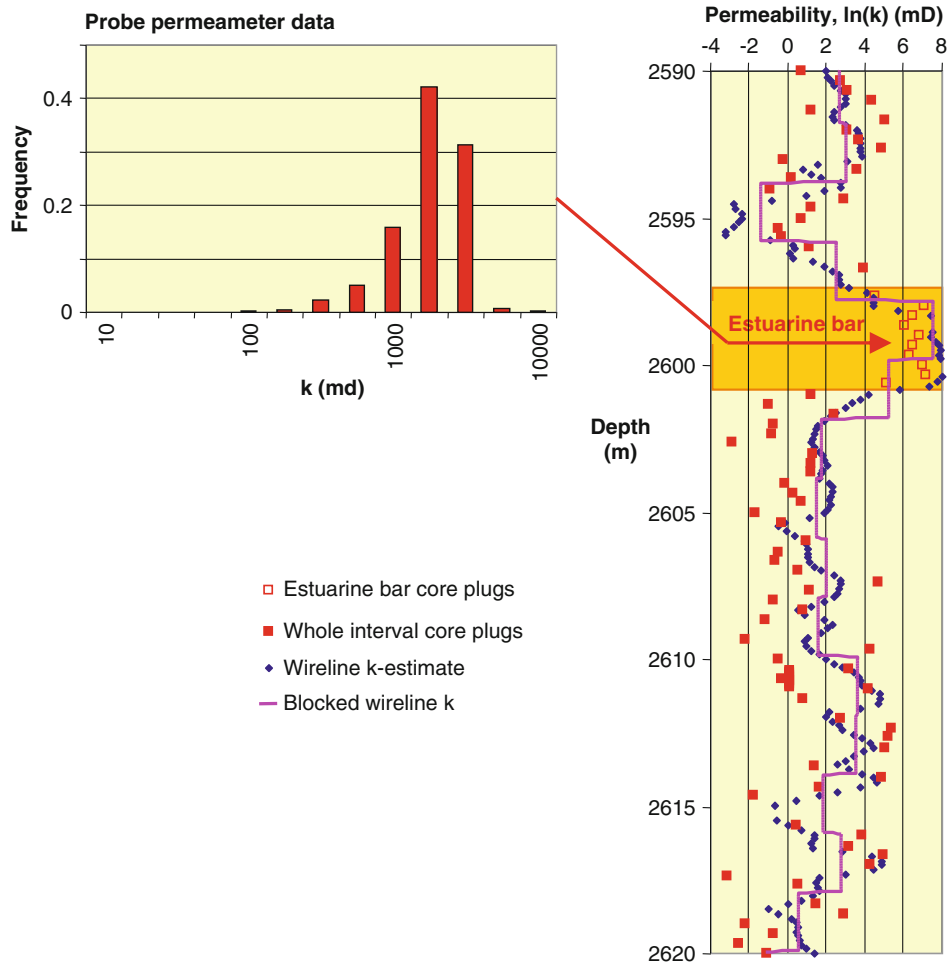

Fig. 4.26 Example dataset from a tidal deltaic flow unit illustrating treatment of permeability data used in reservoir modelling (Redrawn from Ringrose et al. 2008, The Geological Society, London, Special Publications 309 © Geological Society of London [2008])

Table 4.2 Variance analysis of example permeability dataset

	Estuarine bar lithofacies			Whole interval (flow unit)		
	(a) Probe-k data	(b) Probe data upscaled to plug scale	(c) Core plug data	(d) Core plug data	(e) Wireline-k estimate	(f) Blocked well data
Scale of data	10 × 10 cm; 2 mm spaced data	2 × 2 cm squares of 2 mm-spaced data	c.15–30 cm spaced core plugs	c.15–30 cm spaced plugs	15 cm digital log	2 m blocking
N =	2,584	25	11	85	204	16
Mean ln(k)	7.14	7.14	6.39	1.73	2.32	2.17
σ^2 ln(k)	0.38	0.30	0.99	8.44	5.94	4.80
Variance adjustment factor, *f*	–	0.79	–	–	–	0.81

from the datasets conventionally used in reservoir modelling.

Improved treatment of variance in reservoir modelling is clearly needed and presents us with a significant challenge. The statistical basis for treating population variance as a function of sample support volume is well established with the concept of *Dispersion Variance* (Isaaks and Srivastava 1989), where:

$$\underset{\text{Total variance}}{\sigma^2(a,c)} = \underset{\text{Variance within blocks}}{\sigma^2(a,b)} + \underset{\text{Variance between blocks}}{\sigma^2(b,c)} \quad (4.14)$$

where a, b and c represent different sample supports (in this case, a = point values, b = block values and c = total model domain).

The variance adjustment factor, *f*, is defined as the ratio of block variance to point variance and can be used to estimate the correct variance to be applied to a blocked dataset. For the example dataset (Table 4.2, Fig. 4.26) the variance adjustment factor is around 0.8 for both scale adjustment steps.

With additive properties, such as porosity, treatment of variance in multi-scale datasets is relatively straightforward. However, it is much more of a challenge with permeability data as flow boundary conditions are an essential aspect of estimating an upscaled permeability value (see Chap. 3). Multi-scale geological modelling is an attempt to represent smaller scale structure and variability as an upscaled block permeability value. In this process, the principles guiding appropriate flow upscaling are essential. However, improved treatment of variance is also critical. There is, for example, little point rigorously upscaling a core plug sample dataset if it is known that that dataset is a poor representation of the true population variance.

The best approach to this rather complex problem, is to review the available data within a multi-scale REV framework (Fig. 4.24). If the dataset is sampled at a scale close to the corresponding REV, then it can be considered as fairly reliable and representative data. If however, the dataset is clearly not sampled at the REV (and is in fact recording a highly variable property) then care is needed to handle and upscale the data in order to derive an appropriate average. Assuming that we have datasets which can be related to the REV's in the rock system, we can then use the same multi-scale framework to guide the modelling length scales. Reservoir model grid-cell dimensions should ideally be determined by the REV lengthscales. Explicit spatial variations in the model (at scales larger than the grid cell) are then focussed on representing property variations that cannot be captured by averages. To put this concept in its simplest form consider the following modelling steps and assumptions:

1. *From pore scale to lithofacies scale:* Pore-scale models (or measurements) are made at the pore-scale REV and then spatial variation at the lithofacies scale is modelled (using deterministic/probabilistic methods) to estimate rock properties at the lithofacies-scale REV.
2. *From lithofacies scale to geomodel scale.* Lithofacies-scale models (or measurements) are made at the lithofacies-scale REV and then spatial variation at the geological architecture scale is modelled (using deterministic/probabilistic methods) to estimate reservoir properties at the scale of the geological-unit REV (equivalent to geological model elements).
3. *From geomodel to full-field reservoir simulator.* Representative geological model elements are modelled at the full-field reservoir simulator scale to estimate dynamic flow behaviour based on reservoir properties that have been correctly upscaled and are (arguably) representative.

There is no doubt that multi-scale modelling within a multi-scale REV framework is a challenging process, but it is nevertheless much preferred to 'throwing in' some weakly-correlated random noise into an arbitrary reservoir grid and hoping for a reasonable outcome. The essence of good reservoir model design is that it is based on some sound geological concepts, an appreciation of flow physics, and a multi-scale approach to determining statistically representative properties.

Every reservoir system is somewhat unique, so the best way to apply this approach method is try it out on real cases. Some of these are illustrated in the following sections, but consider trying Exercise 4.2 for your own case study.

Exercise 4.2
Find the REVs for your reservoir?

Use your own knowledge a particular geological reservoir system or outcrop to sketch on the most likely scales of high variability and low variability (the REV) – similar to Fig. 4.21 – using the sketch below. Note that the horizontal axis is given as a vertical length scale (dz, across bedding) to make volume estimation easier.

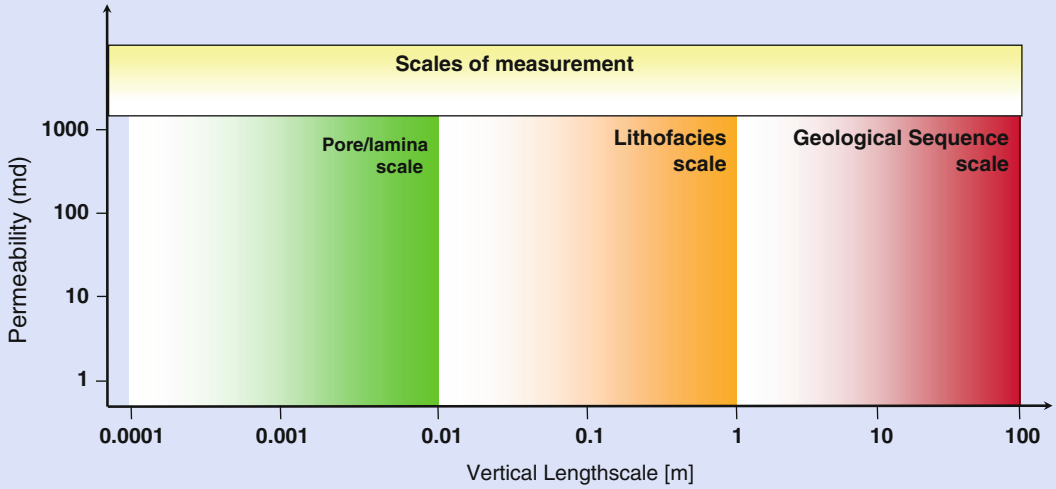

4.3.5 Construction of Geomodel and Simulator Grids

The choice of grid and grid-cell dimensions is clearly important. Upscaled permeability, the balance of fluid forces, and reservoir property variance are all intimately connected with the model length-scale. The construction of three dimensional geological models from seismic and well data remains a relatively time consuming task requiring considerable manual work both in construction of the structural framework and, not least, in construction of the grid for property modelling (Fig. 4.27).

Problems especially arise due to complex fault block geometries including reverse faults and Y-faults (Y-shaped intersections in the vertical plane). Difficulties relate partly to the mapping of horizons into the fault planes for construction of consistent fault throws across faults. Currently, most commercial gridding software is not capable of automatically producing adequate 3D grids for realistic fault architectures, and significant manual work is necessary. Upscaling procedures for regular Cartesian grids are well established, but the same operation in realistically complex grids is much more challenging.

The construction of 3D grids suitable for reservoir simulation is also non-trivial and requires significant manual editing. There are several reasons for this:

- The grid resolution in the geologic model and the simulation models are different, leading to missing cells or miss fitting cells in the simulation model. The consequences are overestimation of pore volumes, possibly wrong communication across faults, and difficult numerical calculations due to a number small or "artificial" grid cells.
- The handling of Y-shaped faults using corner point grid geometries (now widely used in black oil simulators) is difficult. Similarly, the use of vertically stair-stepped faults

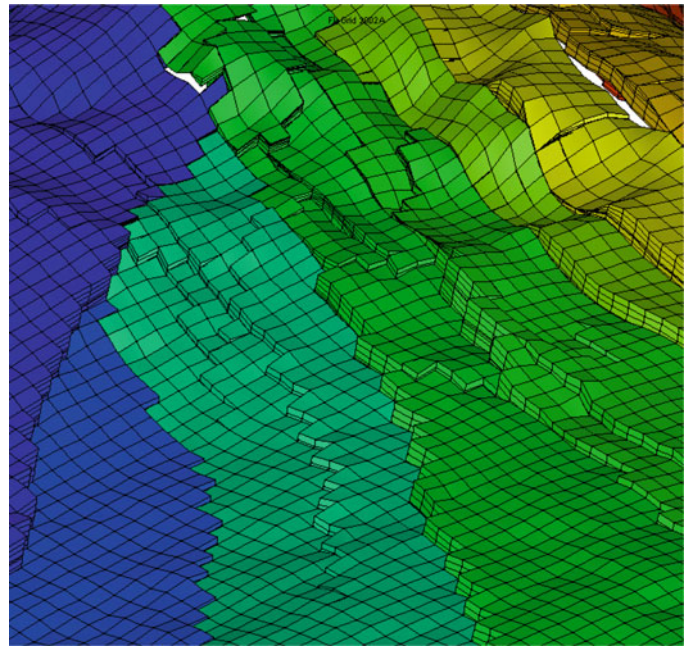

Fig. 4.27 Example reservoir model grid (Heidrun Field fault segments, colour coded by reservoir segment) (Statoil image archives, © Statoil ASA, reproduced with permission)

improves the grid quality and flexibility, but does not solve the whole problem. When using grids with stair-step faults special attention must be paid to estimation of fault seal and fault transmissibility. There is generally insufficient information in the grid itself for these calculations, and the calculation of fault transmissibility must be calculated based on information from the conceptual geological model.

- The handling of dipping reverse faults using stair-step geometry in a corner point grid requires a higher total number of layers than required for an un-faulted model.
- Regions with fault spacing smaller than the simulation grid spacing give problems for appropriate calculation of fault throw and zone to zone communication. Gridding implies that smaller-scale geomodel faults are merged and a cumulated fault throw is used in the simulation model. This is not generally possible with currently available gridding tools, and an effective fault transmissibility, including non-neighbour connections, must be calculated based on information from the geomodel, i.e. using the actual geometry containing all the merged faults.
- Flow simulation accuracy depends on the grid quality, and the commonly used numerical discretisation schemes in commercial simulators have acceptable accuracy only for 'near' orthogonal grids. Orthogonal grids do not comply easily with complex fault structures, and most often compromises are made between honouring geology and keeping "near orthogonal" grids.

Figure 4.28 illustrates how some of these problems have been addressed in oilfield studies (Ringrose et al. 2008). After detailed manual grid construction including stair-step faults to handle Y-faults, smaller faults are added directly into the flow simulation grid. However, some gridding problems cannot be fully resolved using the constraints of corner point simulation grids and optimal, consistent and automated grid generation based on realistic geomodels is a challenge. The use of unstructured grids reduces some of the gridding problems, but robust, reliable and cost efficient numerical flow solution methods for these unstructured grids are not generally available. Improved and consistent solutions for construction of structured grids and associated transmissibilities have been proposed (e.g. Manzocchi et al 2002; Tchelepi et al.

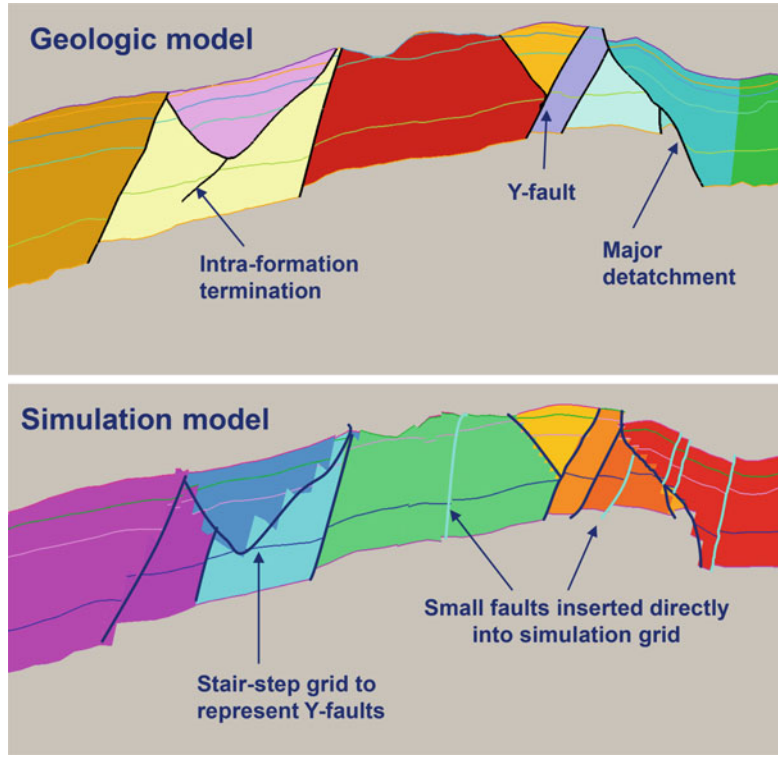

Fig. 4.28 Illustration of the transfer of a structural geological model to a reservoir simulation grid (Redrawn from Ringrose et al. 2008, The Geological Society, London, Special Publications 309 © Geological Society of London [2008])

2005) and flow simulation on faulted grids remains a challenge.

4.3.6 Which Heterogeneities Matter?

There are a number of published studies in which the importance of different multi-scale geological factors on reservoir performance have been assessed. Table 4.3 summarizes the findings of a selection of such studies in which a formalised experimental design with statistical analysis of significance has been employed. The table shows only the main factors identified in these studies (for full details refer to sources). What is clear from this work is that several scales of heterogeneity are important for each reservoir type. While one can conclude that stratigraphic sequence position is the most important factor in a shallow marine depositional setting or that vertical permeability is the most important factors in tidal deltaic setting, each case study shows that both larger and smaller-scale factors are generally significant. This is a clear argument in favour of explicit multi-scale reservoir modelling.

Furthermore, in the studies where the effects of structural heterogeneity were assessed, both structural and sedimentary features were found to be significant. That is to say, structural features and uncertainties cannot be neglected and are fully coupled with stratigraphic factors.

Another approach to this question is to consider how the fluid forces will interact with the heterogeneity in terms of the REV (Fig. 4.29). Pore and lamina-scale variations have the strongest effect on capillary-dominated fluid processes while the sequence stratigraphic (or facies association) scale most affects flow processes in the viscous-dominated regime. Gravity operates at all scales, but gravity-fluid effects are most important at the larger scales, where significant fluid segregation occurs. That is, when both capillary forces and applied pressure gradients fail to compete effectively against gravity stabilisation of the fluids involved.

Several projects have demonstrated the economic value of multi-scale modelling in the

Table 4.3 Summary of selected studies comparing multi-scale factors on petroleum reservoir performance

	Shallow Marine[a]	Faulted Shallow Marine[b]	Fluvial[c]	Tidal Deltaic[d]	Fault modelling[e]
Sequence model	V	V			V
Sand fraction	S	S	V	S	n/a
Sandbody geometry			S	S	n/a
Vertical permeability	S	S		V	n/a
Small-scale heterogeneity			S	S	n/a
Fault pattern	n/a	S	n/a	n/a	S
Fault seal	n/a	S	n/a	n/a	S

V Most significant factor, *S* Significant factor, *n/a* not assessed
[a]Kjønsvik et al. (1994)
[b]England and Townsend (1998)
[c]Jones et al. (1993)
[d]Brandsæter et al. (2001a)
[e]Lescoffit and Townsend (2005)

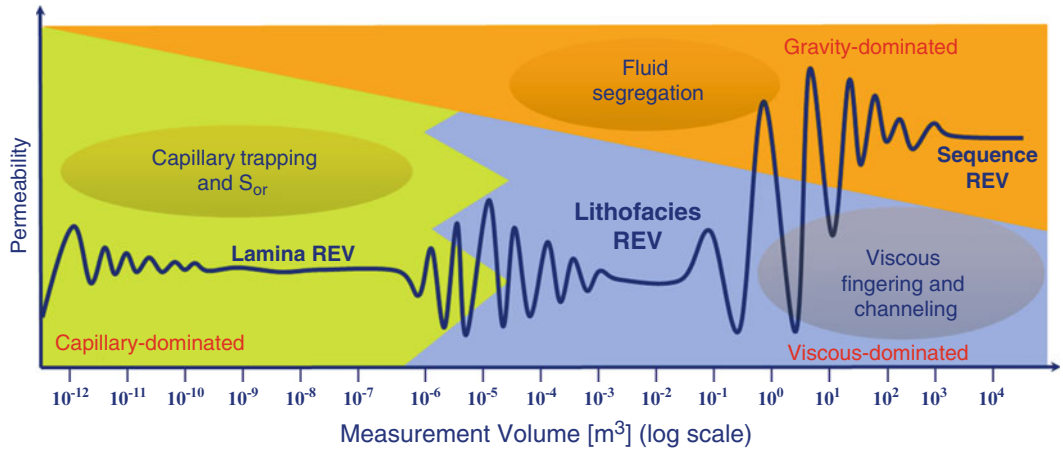

Fig. 4.29 Sketch illustrating the expected dominant fluid forces with respect to the important heterogeneity length-scales

context of oilfield developments. An ambitious study of the structurally complex Gullfaks field (Jacobsen et al 2000) demonstrated that 25 million-cell geological grid (incorporating structural and stratigraphic architecture) could be upscaled for flow simulation and resulted in a significantly improved history match. Both stratigraphic barriers and faults were key factors in achieving improved pressure matches to historic well data. This model was also used for assessment of IOR using CO_2 flooding.

Multi-scale upscaling has also been used to assess complex reservoir displacement processes, including gas injection in thin-bedded reservoirs (Fig. 4.30) (Pickup et al 2000; Brandsæter et al. 2001b, 2005), water-alternating-gas (WAG) injection on the Veslefrikk Field (Kløv et al 2003), and depressurization on the Statfjord field (Theting et al 2005). These studies typically show of the order of 10–20 % difference in oilfield recovery factors when advanced multi-scale effects are implemented, compared with conventional single-scale reservoir simulation studies. For example, Figure 4.31 shows the effect of one-step and two-step upscaling for the gas injection case study (illustrated in Fig. 4.30). The coarse-grid case without upscaling gives a forecasting error of over 10 % when compared to the fine-grid reference case, while the coarse-grid case with two-step upscaling gives a result very close to the fine-grid reference case.

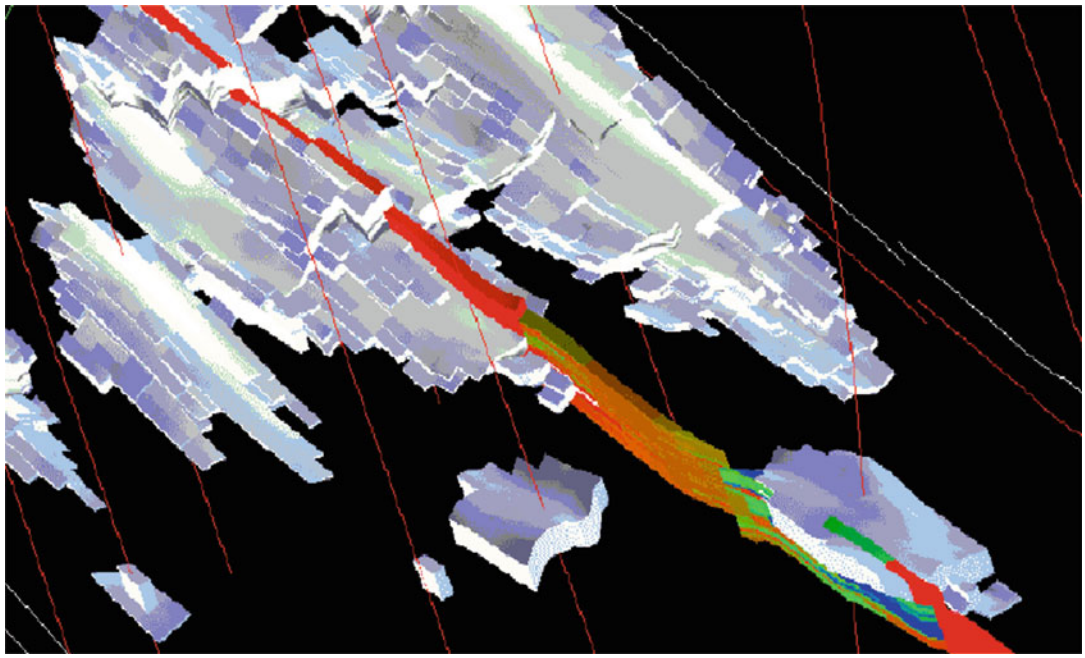

Fig. 4.30 Gas injection patterns in a thin-bedded tidal reservoir modelled using a multi-scale method and incorporating the effects of faults in the reservoir simulation model (From a study by Brandsæter et al 2001b)

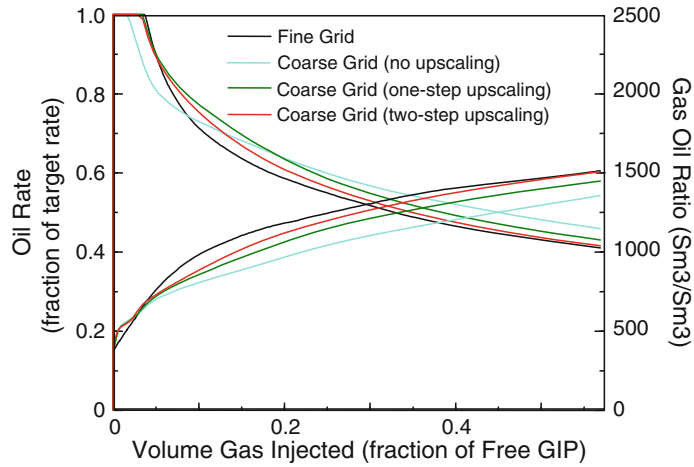

Fig. 4.31 Effect of multi-scale upscaling on estimates of oil rate and GOR for the gas injection case study shown in Fig. 4.30 (Redrawn from Pickup et al. 2000, ©2000, Society of Petroleum Engineers Inc., reproduced with permission of SPE. Further reproduction prohibited without permission)

4.4 The Way Forward

4.4.1 Potential and Pitfalls

Multi-scale reservoir modelling has moved from a conceptual phase, with method development on idealised problems, into a practical phase, with more routine implementation on real reservoir cases. The modelling methods have achieved sufficient speed and reliability for routine implementation (generally using steady-state methods on near-orthogonal corner-point grid systems). However, a number of challenges remain which require further developments of methods and modelling tools. In particular:

- Multi-scale modelling within a realistic structural geological grid is still a major challenge;

- Handling of variance from multiple-scale datasets is frequently incorrect;
- The tool-set for upscaling is still incomplete and far from integrated; for example multiphase flow, gridding and fault seal are generally treated in separate software packages and require a degree of manual data-file conversion.

Software tool developments will undoubtedly steadily resolve these challenges, but what ultimately is the goal? We suggest the overall target of reservoir modelling is multi-scale (pore-to-field) modelling and data integration. The level of detail involved depends very much on the task at hand. Some problems are essentially pore-scale – e.g. will a different fluid displacement mechanism such as CO_2 injection make a difference to ultimate oil recovery? Other problems are essentially large-scale – e.g. does this gas field have sufficient volumes to justify a billion dollar investment? Nevertheless, executing either of these projects in detail will require a multi-scale analysis.

4.4.2 Pore-to-Field Workflow

There are many ways for defining a series of explicit steps from the pore scale to the full-field scale. The following summarises a typical geologically-based workflow within a multi-scale design framework. We define four dominant length scales:

- Pore scale: μm-cm scale
- Lithofacies scale: cm-m scale
- Geomodel (facies architecture) scale: 10 m–10 km scale
- Reservoir simulator scale (typically some coarsening up of the full-field reservoir geomodel): 100 m–10 km scale.

These scales are based both on the nature of rock heterogeneity and the principles for establishing macroscopic flow properties. These four scales give three transitions:

1. Pore to lithofacies
2. Lithofacies to geomodel
3. Geomodel to reservoir simulator.

At each scale we define flow properties for each cell (or pore) in the model and then use a numerical upscaling method to determine the upscaled flow property. The upscaled flow property is then used as input in the next scale up. A realistic illustration of this workflow for the pore to lithofacies scale is shown in Figure 4.32. Here we assume we can define two different pore/rock types (e.g. coarse well sorted sand and fine-grained sand).

Flow functions for each rock type are defined either from Special Core Analysis (SCAL) or from pore network modelling, or preferably both. Secondly, we assume we have a selection of different facies models: e.g. trough cross bedded sandstone (as in Fig. 4.32). These models should correspond to the selection of modelling elements described in Chapter 2.4. For each lithofacies element, pore-scale properties are assigned to each lamina (or bed). Upscaling is performed to calculate the lithofacies-scale flow properties (absolute and relative permeabilities for each flow direction). These flow properties are then assigned to each cell in the geomodel, with further upscaling to the reservoir simulator, if necessary.

For most cases, to make this explicit pore-to-field upscaling computationally feasible, we use steady-state approximations to multi-phase flow (e.g. capillary limit and viscous limit methods). These steady-state approximations have been reviewed and discussed by for example Ekran and Aasen (2000) and Pickup and Stephen (2000). Published examples of the pore to lithofacies to full-field multi-scale workflow include Pickup et al. (2000), Theting et al. (2005) and Rustad et al. (2008).

4.4.3 Essentials of Multi-scale Reservoir Modelling

We conclude this chapter with a check-list of essential questions that need to be asked for any reservoir flow-modelling problem.

1. Have you identified the main reservoir elements that impact on flow?
   - *Hint:* Use the HFU concept of petrophysically distinct units

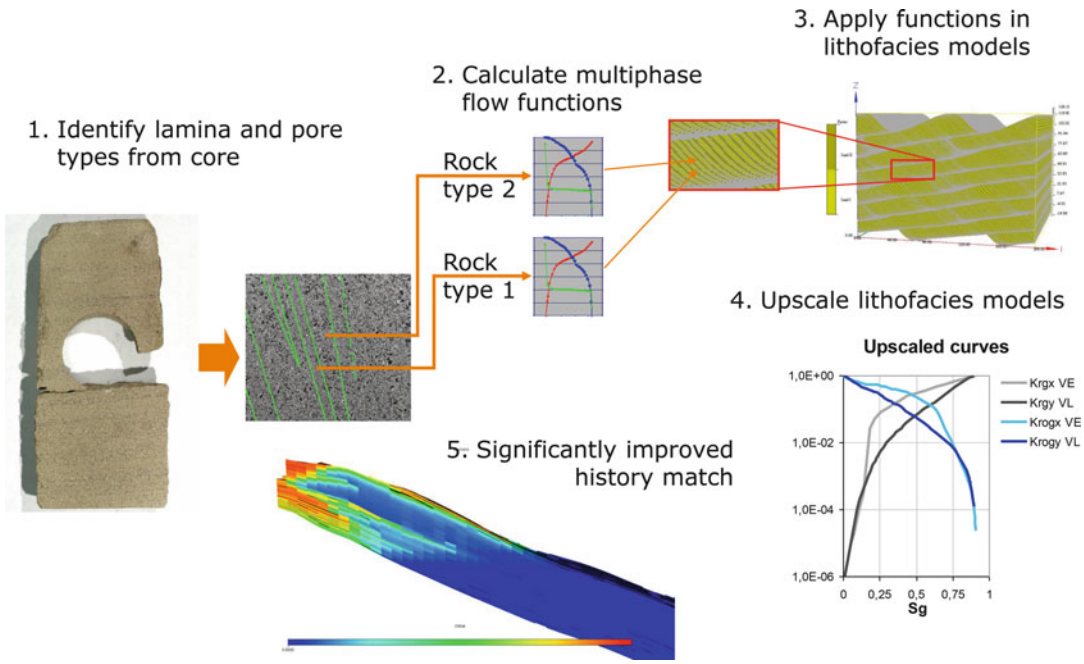

Fig. 4.32 Pore to lithofacies modelling workflow (Photos K. Nordahl & A. Rustad/Statoil © Statoil ASA, reproduced with permission)

2. Are your rock properties estimated at the REV?
   - *Hint:* Try to relate your model length scales (grid sizes) to the natural rock architecture length scales using the multi-scale REV sketch.
3. What length scale has the largest influence on the flow process?
   - *Hint:* Some flow processes ignore small-scale variations while other flow processes may be are strongly controlled by them. Use Flora's rule (Fig. 2.15).
4. Are your flow forecasts based on single-phase or multi-phase flow equations using *representative* rock properties and *appropriate* fluid properties.
   - *Hint:* What really controls your flow process – $k_{effective}$, $k_{fracture}$, $k_{relative}$, k_v or P_c.

Are you reasonably happy with your assumptions? Press 'execute' on the simulator and review the outcomes.

References

Abbaszadeh M, Fujii H, Fujimoto F (1996) Permeability prediction by hydraulic flow units – theory and applications. SPE Form Eval 11(4):263–271

Bakke S, Øren P-E (1997) 3-D pore-scale modelling of sandstones and flow simulations in pore networks. SPE J 2:136–149

Barker JW, Thibeau S (1997) A critical review of the use of pseudo relative permeabilities for upscaling. SPE Reserv Eng 12(5):138–143

Bear J (1972) Dynamics of fluids in porous media. Elsevier, New York

Behbahani H, Blunt MJ (2005) Analysis of imbibition in mixed-wet rocks using pore-scale modeling. SPE J 10(4):466–474

Blunt MJ (1997) Effects of heterogeneity and wetting on relative permeability using pore level modeling. SPE J 2(1):70–87

Bourbiaux B, Basquet R, Cacas M-C, Daniel J-M, Sarda S (2002) An integrated workflow to account for multi-scale fractures in reservoir simulation models: implementation and benefits. SPE paper 78489 presented at Abu Dhabi international petroleum exhibition and

conference, Abu Dhabi, United Arab Emirates, 13–16 October
Brandsæter I, Wist HT, Næss A, Li O, Arntzen OJ, Ringrose P, Martinius AW, Lerdahl TR (2001a) Ranking of stochastic realizations of complex tidal reservoirs using streamline simulation criteria. Pet Geosci 7:53–63
Brandsæter I, Ringrose PS, Townsend CT Omdal S (2001b) Integrated modelling of geological heterogeneity and fluid displacement: Smørbukk gas-condensate field, Offshore Mid-Norway. SPE paper 66391 presented at the SPE reservoir simulation symposium, Houston, TX, 11–14 Feb 2001
Brandsæter I, McIlroy D, Lia O, Ringrose PS (2005) Reservoir modelling of the Lajas outcrop (Argentina) to constrain tidal reservoirs of the Haltenbanken (Norway). Pet Geosci 11:37–46
Bryant S, Blunt MJ (1992) Prediction of relative permeability in simple porous media. Phys Rev A 46:2004–2011
Bryant S, King PR, Mellor DW (1993) Network model evaluation of permeability and spatial correlation in a real random sphere packing. Transp Porous Media 11:53–70
Campbell CV (1967) Lamina, laminaset, bed, bedset. Sedimentology 8:7–26
Chierici GL (1994) Principles of petroleum reservoir engineering, vol 1 & 2. Springer, Berlin
Coats KH, Dempsey JR, Henderson JH (1971) The use of vertical equilibrium in two-dimensional simulation of three-dimensional reservoir performance. Soc Petrol Eng J 11(01):63–71
Corbett PWM, Jensen JL (1992) Estimating the mean permeability: how many measurements do you need? First Break 10:89–94
Corbett PWM, Ringrose PS, Jensen JL, Sorbie KS (1992) Laminated clastic reservoirs: the interplay of capillary pressure and sedimentary architecture. SPE paper 24699, presented at the SPE annual technical conference, Washington, DC
Dake LP (2001) The practice of reservoir engineering (Rev edn). Elsevier, Amsterdam
Davis JC (2003) Statistics and data analysis in geology, 3rd edn. Wiley, New York, 638 pages
Dengen Z, Fayers FJ, Orr FM Jr (1997) Scaling of multiphase flow in simple heterogeneous porous media. SPE Reserv Eng 12(3):173–178
Doyen PM (2007) Seismic reservoir characterisation. EAGE Publications, Houten
Durlofsky LJ, Milliken WJ, Bernath A (2000) Scaleup in the near-well region. SPE J 5(1):110–117
Ekran S, Aasen JO (2000) Steady-state upscaling. Transp Porous Media 41(3):245–262
England WA, Townsend C (1998) The effects of faulting on production form a shallow marine reservoir – a study of the relative importance of fault parameters. Soc Petrol Eng. doi:10.2118/49023-MS
Haldorsen HH (1986) Simulator parameter assignment and the problem of scale in reservoir engineering. In: Lake LW, Caroll HB (eds) Reservoir characterization. Academic, Orlando, pp 293–340
Haldorsen HH, Lake LW (1984) A new approach to shale management in field-scale models. Soc Petrol Eng J 24:447–457
Huang Y, Ringrose PS, Sorbie KS (1995) Capillary trapping mechanisms in water-wet laminated rock. SPE Reserv Eng 10:287–292
Huang Y, Ringrose PS, Sorbie KS, Larter SR (1996) The effects of heterogeneity and wettability on oil recovery from laminated sedimentary. SPE J 1(4):451–461
Isaaks EH, Srivastava RM (1989) Introduction to applied geostatistics. Oxford University Press, New York
Jackson MD, Muggeridge AH, Yoshida S, Johnson HD (2003) Upscaling permeability measurements within complex heterolithic tidal sandstones. Math Geol 35(5):499–519
Jacobsen T, Agustsson H, Alvestad J, Digranes P, Kaas I, Opdal S-T (2000) Modelling and identification of remaining reserves in the Gullfaks field. Paper SPE 65412 presented at the SPE European petroleum conference, Paris, France, 24–25 October
Jensen JL, Lake LW, Corbett PWM, Goggin DJ (2000) Statistics for petroleum engineers and geoscientists, 2nd edn. Elsevier, Amsterdam
Jones A, Doyle J, Jacobsen T, Kjønsvik D (1993) Which sub-seismic heterogeneities influence waterflood performance? A case study of a low net-to-gross fluvial reservoir. In: De Haan HJ (ed) New developments in improved oil recovery, vol 84, Geological Society special publication. Geological Society, London, pp 5–18
King MJ, Mansfield M (1999) Flow simulation of geologic models. SPE Reserv Eval Eng 2(4):351–367
Kjønsvik D, Doyle J, Jacobsen T, Jones A (1994) The effect of sedimentary heterogeneities on production from a shallow marine reservoir – what really matters?. SPE paper 28445 presented at the European petroleum conference, London, 25–27 Oct 1994
Kløv T, Øren P-E, Stensen JÅ, Lerdahl TR, Berge LI, Bakke S, Boassen T, Virnovsky G (2003) SPE paper 84549 presented at the SPE annual technical conference and exhibition, Denver, CO, USA, 5–8 October
Kyte JR, Berry DW (1975) New pseudofunctions to control numerical dispersion. SPE J 15:276–296
Lescoffit G, Townsend C (2005) Quantifying the impact of fault modeling parameters on production forecasting for clastic reservoirs. In: Evaluating fault and cap rock seals, vol 2, AAPG special volume Hedberg series. AAPG, Tulsa, pp 137–149
Li D, Lake LW (1995) Scaling fluid flow through heterogeneous permeable media. SPE Adv Technol Ser 3(1):188–197
Li D, Cullick AS, Lake LW (1996) Scaleup of reservoir-model relative permeability with a global method. SPE Reserv Eng 11(3):149–157
Mallet JL (2008) Numerical earth models. European Association of Geoscientists and Engineers, Houten, p 147
Manzocchi T, Heath AE, Walsh JJ, Childs C (2002) The representation of two-phase fault-rock properties in flow simulation models. Pet Geosci 8:119–132
McDougall SR, Sorbie KS (1995) The impact of wettability on waterflooding: pore-scale simulation. SPE Reserv Eng 10(3):208–213

Miall AD (1985) Architectural-element analysis: a new method of facies analysis applied to fluivial deposits. Earth-Sci Rev 22:261–308

Neasham JW (1977) The morphology of dispersed clay in sandstone reservoirs and its effect on sandstone shaliness, pore space and fluid flow properties. SPE paper 6858 presented at the SPE annual technical conference and exhibition, Denver, CO, 9–12 Oct 1977

Nordahl K, Ringrose PS (2008) Identifying the representative elementary volume for permeability in heterolithic deposits using numerical rock models. Math Geosci 40(7):753–771

Nordahl K, Ringrose PS, Wen R (2005) Petrophysical characterisation of a heterolithic tidal reservoir interval using a process-based modelling tool. Pet Geosci 11:17–28

Øren P-E, Bakke S (2003) Process-based reconstruction of sandstones and prediction of transport properties. Transp Porous Media 12(48):1–32

Pickup GE, Stephen KS (2000) An assessment of steady-state scale-up for small-scale geological models. Pet Geosci 6:203–210

Pickup GE, Ringrose PS, Sharif A (2000) Steady-state upscaling: from lamina-scale to full-field model. SPE J 5:208–217

Pickup GE, Stephen KD, Zhang M, Ma J, Clark JD (2005) Multi-stage upscaling: selection of suitable methods. Transp Porous Media 58:119–216

Rapoport LA (1955) Scaling laws for use in design and operation of water-oil flow models. Am Inst Min Metallur Petrol Eng Trans 204:143–150

Renard P, de Marsily G (1997) Calculating equivalent permeability: a review. Adv Water Resour 20:253–278

Ringrose PS (1994) Structural and lithological controls on coastline profiles in Fife, Eastern Britain. Terra Nova 6:251–254

Ringrose PS, Corbett PWM (1994) Controls on two-phase fluid flow in heterogeneous sandstones. In: Parnell J (ed) Geofluids: origin, migration and evolution of fluids in sedimentary basins, vol 78, Geological Society special publication. Geological Society, London, pp 141–150

Ringrose PS, Sorbie KS, Corbett PWM, Jensen JL (1993) Immiscible flow behaviour in laminated and cross-bedded sandstones. J Petrol Sci Eng 9:103–124

Ringrose PS, Jensen JL, Sorbie KS (1996) Use of geology in the interpretation of core-scale relative permeability data. SPE Form Eval 11(03):171–176

Ringrose PS, Skjetne E, Elfeinbein C (2003) Permeability estimation functions based on forward modeling of sedimentary heterogeneity. SPE 84275, Presented at the SPE annual conference, Denver, USA, 5–8 Oct 2003

Ringrose PS, Martinius AW, Alvestad J (2008) Multiscale geological reservoir modelling in practice. In: Robinson A et al (eds) The future of geological modelling in hydrocarbon development, vol 309, Geological Society special publications. Geological Society, London, pp 123–134

Rubin DM (1987) Cross-bedding, bedforms and palaeocurrents, vol 1, Concepts in sedimentology and palaeontology. Society of Economic Paleontologists and Mineralogists Special Publication, Tulsa

Rustad AB, Theting TG, Held RJ (2008) Pore-scale estimation, upscaling and uncertainty modelling for multiphase properties. SPE paper 113005, presented at the 2008 SPE/DOE improved oil recovery symposium, Tulsa, OK, UK, 19–23 Apr 2008

Scheiling MH, Thompson RD, Siefert D (2002) Multiscale reservoir description models for performance prediction in the Kuparuk River Field, North Slope of Alaska. SPE paper 76753 presented at the SPE Western Regional/AAPG Pacific Section Joint Meeting, Anchorage, Alaska, 20–22 May

Size WB (ed) (1987) Use and abuse of statistical methods in the earth sciences, IAMG studies in mathematical geology, no. 1. Oxford University Press, Oxford

Smith EH (1991) The influence of small-scale heterogeneity on average relative permeability. In: Lake LW et al (eds) Reservoir characterisation II. Academic Press, San Diego

Stone HL (1991) Rigorous black oil pseudo functions. SPE paper 21207, presented at the SPE symposium on reservoir simulation, Anaheim, CA, 17–20 Feb 1991

Tchelepi HA, Jenny P, Lee C, Wolfsteiner C (2005) An adaptive multiscale finite volume simulator for heterogeneous reservoirs. SPE paper 93395 presented at the SPE reservoir simulation symposium, The Woodlands, Texas, 31 January–2 February

Theting TG, Rustad AB, Lerdahl TR, Stensen JÅ, Boassen T, Øren P-E, Bakke S, Ringrose P (2005) Pore-to-field multi-phase upscaling for a depressurization process. Presented at the 13th European symposium on improved oil recovery, Budapest, Hungary, 25–27 Apr 2005

Todd MR, Longstaff WJ (1972) The development, testing, and application of a numerical simulator for predicting miscible flood performance. J Petrol Technol 1972:874–882

Towler BF (2002) Fundamental principles of reservoir engineering, vol 8, SPE textbook series. Henry L. Doherty Memorial Fund of AIME, Society of Petroleum Engineers, Richardson

Turcotte DL (1992) Fractals and chaos in geology and geophysics. Cambridge University Press, Cambridge

Walsh J, Watterson J, Yielding G (1991) The importance of small-scale faulting in regional extension. Nature 351:391–393

Weber KJ (1986) How heterogeneity affects oil recovery. In: Lake LW, Carroll HB (eds) Reservoir characterisation. Academic, Orlando, pp 487–544

Weber KJ, van Geuns LC (1990) Framework for constructing clastic reservoir simulation models. J Pet Technol 42:1248–1297

Wen R, Martinius AW, Næss A, Ringrose PS (1998) Three-dimensional simulation of small-scale heterogeneity in tidal deposits – a process-based stochastic method. In: Buccianti A et al (eds) Proceedings of the 4th annual conference of the international association of mathematical geology, Naples, pp 129–134

Yielding G, Walsh J, Watterson J (1992) The prediction of small-scale faulting in reservoirs. First Break 10(12):449–460

Handling Model Uncertainty

5

Abstract

The preceding chapters have highlighted a number of ways in which a reservoir model can go right or wrong.

Nothing, however, compares in magnitude with the mishandling of uncertainty. An incorrect saturation model, for example, can easily give a volumetric error of 10 % and perhaps even 50 %. A flawed geological concept could be much worse. Mishandling of uncertainty, however, can result in the whole modelling and simulation effort becoming worthless.

The cause of this is occasionally misuse of software, more commonly it is due to the limitations of our datasets, but primarily it is our behaviour and our design choices which are at fault.

Our aim is to place our models within a framework that can overcome data limitations and personal bias and give us a useful way of quantifying forecast uncertainty.

P. Ringrose and M. Bentley, *Reservoir Model Design*, DOI 10.1007/978-94-007-5497-3_5,

Did you expect to see the trees?

5.1 The Issue

5.1.1 Modelling for Comfort

In Chap. 1 we identified the tendency for modelling studies to become a panacea for decision making – modelling for comfort rather than analytical rigour. It is certainly often the case that reservoir modelling is used to hide uncertainty rather than illustrate it. We have a natural tendency to determine a best guess – the anchoring heuristic of Kahneman and Tverky (1974) – and the management process in many companies often inadvertently encourages the guesswork.

However, in a situation of dramatic undersampling the guess is often wrong and influenced unconsciously by behavioural biases of the individuals or teams involved (summarised in Kahneman 2011). Best-guess models therefore tend to be misleading and their role is reduced to one of providing comfort to support a business decision, one which has perhaps already been made. In this case we are indeed simply 'modelling for comfort', a low value activity, rather than taking the opportunity to use modelling to identify a significant business risk.

5.1.2 Modelling to Illustrate Uncertainty

Useful modelling can be expressed as 'reasonable forecasting.' A convenient metaphor for this is our ability to predict the image on a picture from a small number of sample points.

We illustrate this, graphically, using sampled selections (Fig. 5.1) from a landscape photograph (the chapter cover image). A routine modelling workflow would lead us to analyse and characterise each sample point: the process of reservoir characterisation. Data-led modelling with no underlying concept and no application of trends

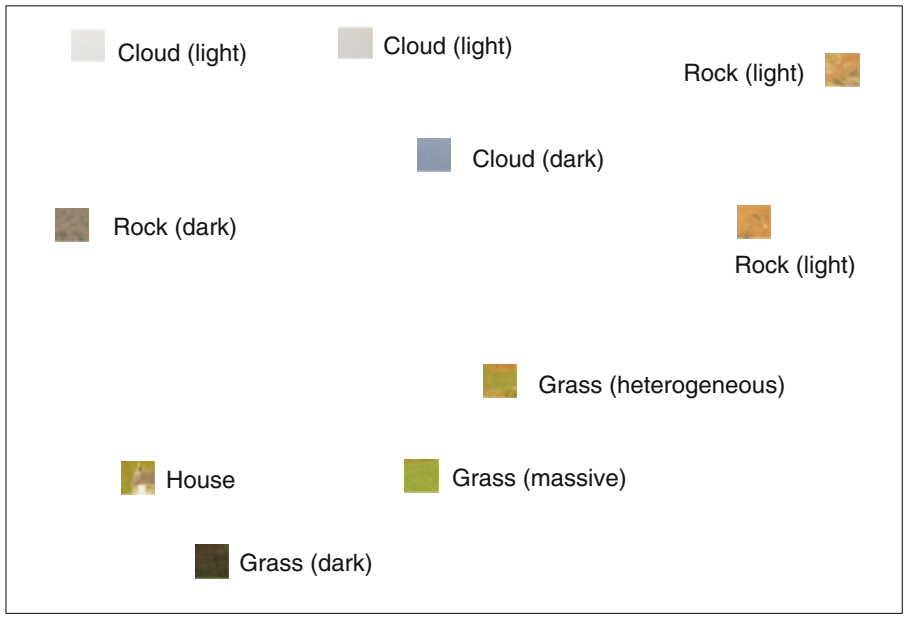

Fig. 5.1 An undersampled picture – our task is to determine the image

could produce the stochastic result shown in Fig. 5.2. This representation is statistically consistent with the underlying data, and would pass a simple QC test comparing frequency of occurrences in the data and in the model, yet the result is clearly meaningless.

Application of logical deterministic trends to the modelling process, as described in Chap. 2, would make a better representation, one which would at least fit an underlying landscape concept: the sky is more likely to be at the top, the grass at the bottom (Fig. 5.3). Furthermore, there is an anisotropy ratio we can use so that we can predict better spatial correlation laterally (the sky is more likely to extend across much of the image, rather than up and down). If the texture from this trend-based approach is deemed unrepresentative of landscapes, an object-based alternative may be preferred (Fig. 5.4). Grass is accordingly arranged in clusters, broadly elliptical, as are sky colours (clouds) and the rocky areas are arranged into 'hills', anchored around the data points they were observed in. A rough representation is beginning to take shape.

The model representations in Figs. 5.2, 5.3, and 5.4 each adhere to the same element proportions, and in this sense all 'match' the data, although with strongly contrasting textures. Assuming we then proceeded to add "colours" for petrophysical properties (Chap. 3) and rescale the image for flow simulation (Chap. 4), these images would produce strongly contrasting fluid-flow forecasts.

Using these different images as possible alternative realisations could be one way of exploring uncertainty, but we argue this would be a poor route to follow. Reference to the actual image (Fig. 5.5) reveals a familiar theme:

$$data \neq model \neq truth$$

Even though most aspects of the image were sampled, and the applied deterministic trends were reasonable, there are significant errors in the representation – object modelling of the sky was inappropriate, hierarchical organisation was missed, and even some aspects of the characterisation (grass vs. rocks) were oversimplified. There are also some modelling elements missing, most noticeably: *there were no trees*. Rearranging the data and detailed analysis of the original samples does not reveal the

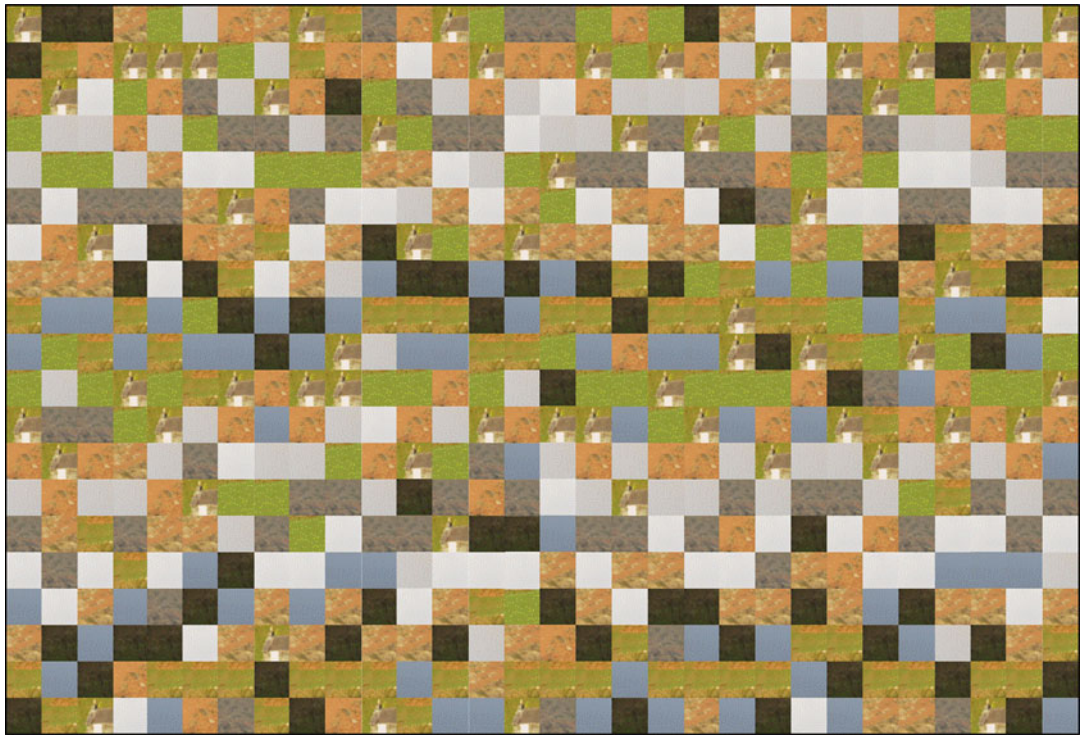

Fig. 5.2 Stochastic model representation of the data in Fig. 5.1, assuming stationarity

Fig. 5.3 Overlay of deterministic trends on the stochastic model in Fig. 5.2, overcoming stationarity

Fig. 5.4 Object model alternative to Fig. 5.3, maintaining deterministic trends and embracing a loose alignment of lozenge shapes

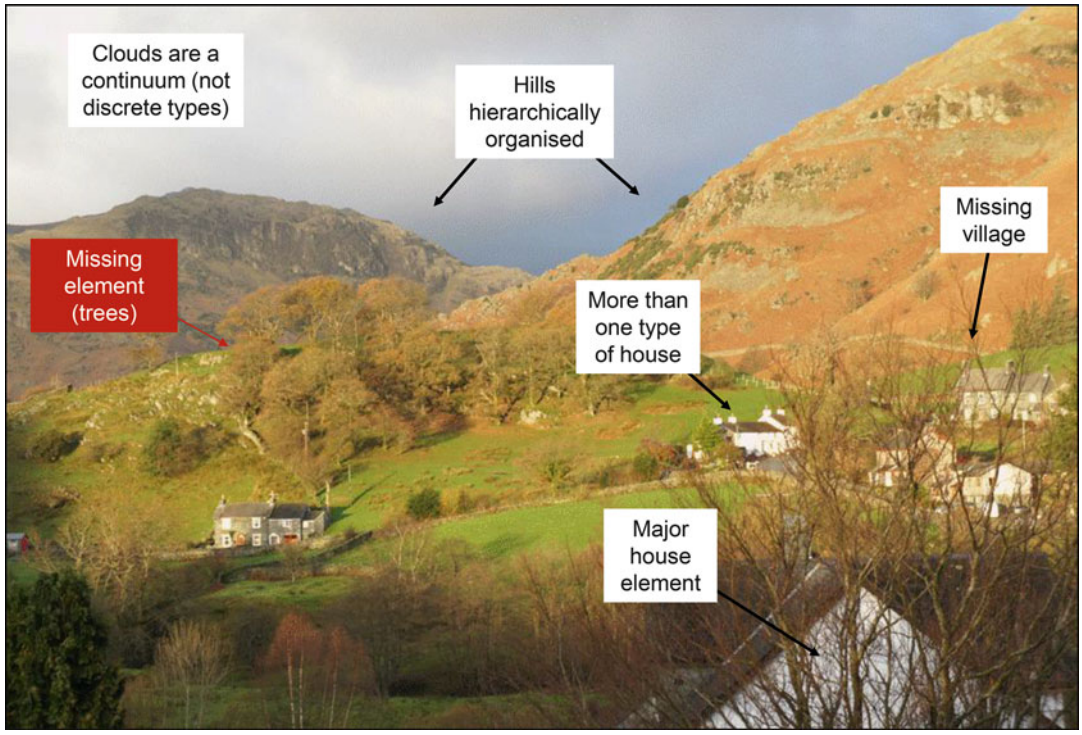

Fig. 5.5 Reality: the data set was unable to detect key missing elements, therefore these elements are also absent from the simple probabilistic model, even with a useful deterministic trend imposed

missing elements. On reflection, we can see that the aim of reproducing the statistical content of the sample dataset brings with it a major flaw in all the models.

Could the missing elements in Fig. 5.5 have been foreseen, given that they were absent in the data sample? We would argue yes, to a large extent. From the data set it is possible to establish a concept of hilly countryside in a temperate climate – the 'expert judgement' of Kahneman and Klein (2009). Having established this, there are in fact certain aspects which are consistent with the concept but not actually seen by the sample data. However, these can be anticipated. Ask yourself:

- Could there be more than one type of house? *Yes*.
- Could there be a small village? *Yes*.
- Is there a structure to the clouds? *Yes*.
- Are the hills logically arranged, ones with greater contrast in the foreground? *Yes*
- Could there be trees?

Taking the issue of trees specifically, these are highly likely to be present, given the underlying concept (grass and hills in a temperate climate). They are also likely to be under-sampled.

The parallels with reservoir modelling are hopefully clear: we need to use concepts to honour the data but work beyond it to include missing elements. If these elements are important to the field development (e.g. open natural fractures, discontinuous but high permeability layers, cemented areas, sealing sub-seismic faults, thin shales) then the presence or absence of these features becomes the important uncertainty. We should always ask ourselves: "could there be trees?"

5.2 Differing Approaches

Abandoning the route of modelling for comfort and embarking on the harder but more interesting and ultimately more useful route of modelling to illustrate uncertainty, we need a workflow (see Caers 2011, for a summary of statistical methodologies). This chapter will review alternative approaches to uncertainty handling, and lead to a general recommendation for scenario-based approaches, along the way also distinguishing different flavours of 'scenario'.

Scenario-based modelling became a popular means of managing sub-surface uncertainty during the 1990s, although opinions differ widely on the nature of the 'scenarios' – particularly with reference to the relative roles of determinism and probability. In the context of reservoir modelling, a scenario is defined here as *a possible real-world outcome* and is one of several possible outcomes (Bentley and Smith 2008).

The idea of alternative, discrete scenarios followed on logically from the emergence of integrated reservoir modelling tools (e.g. Cosentino 2001; Towler 2002), which emphasised the use of 3D static reservoir modelling, ideally fed from 3D seismic data and leading to 3D dynamic reservoir simulation, generally on a full-field scale.

Appreciating the numerous uncertainties involved in constructing such field models, the desire for multiple modelling naturally arises. Although not universal (see discussion in Dubrule and Damsleth 2001), the application of multiple stochastic modelling techniques is now widespread, with the alternative models described variously as 'runs', 'cases', 'realisations' or 'scenarios'.

The different terminologies are more than semantic. The notion of multiple modelling has been explored differently by different workers, the essential variable being the balance between deterministic and probabilistic inputs. Using "multiple realisations" may sound more routed in statistical theory than using some alternative "model runs" – but is it? These concepts are best related to differing approaches to the application of geostatistical algorithms, and to differing ideas on the role of the probabilistic component (Fig. 5.6).

The contrasting approaches to uncertainty handling broadly fall into three groups:

Rationalist approaches, in which a preferred model is chosen as a base case (Fig. 5.7). The model is either run as a technical best guess, or with a range of uncertainty added

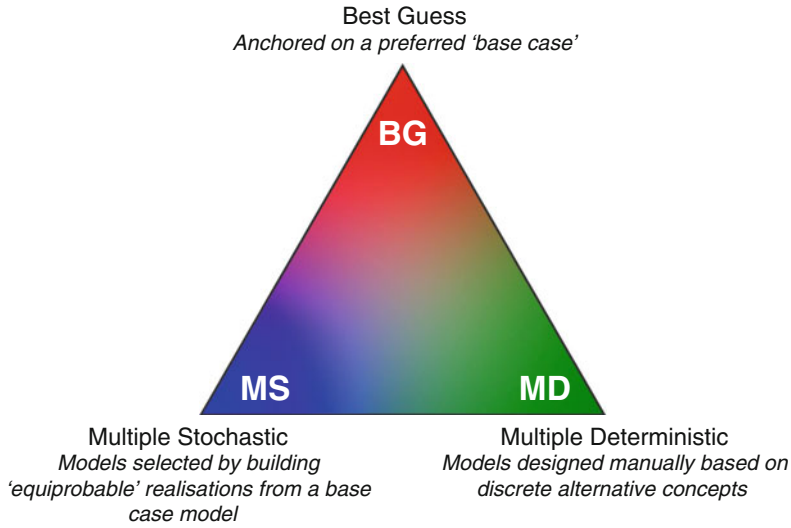

Fig. 5.6 Alternative approaches to uncertainty handling

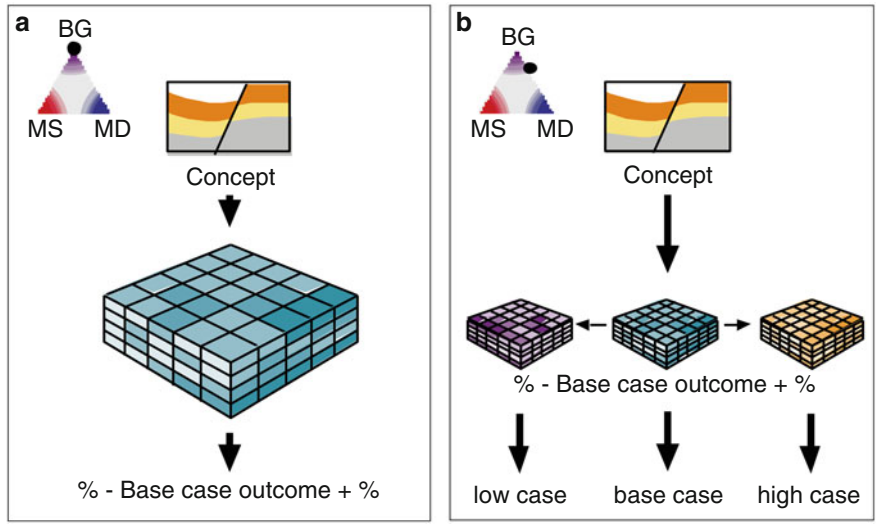

Fig. 5.7 Base case–dominated, rationalist approaches (Redrawn from Bentley and Smith 2008, The Geological Society, London, Special Publications 309 © Geological Society of London [2008])

to that guess. This may be either a percentage factor in terms of the model output (e.g. ±20 % of the base case volumes in-place) or separate low and high cases flanking the base case. This approach can be viewed as 'traditional' determinism.

Multiple stochastic approaches, in which a large number of models are probabilistically generated by geostatistical simulation (Fig. 5.8). The deterministic input lies in the choice of the boundary conditions for the simulations, such as assumed correlation lengths. Yarus and Chambers (1994) give several examples of this approach, and the options and choices are reviewed by Caers (2011).

Multiple deterministic approaches, which avoid making a single best-guess or choosing a preferred base-case model (Fig. 5.9). In this approach a smaller number of models

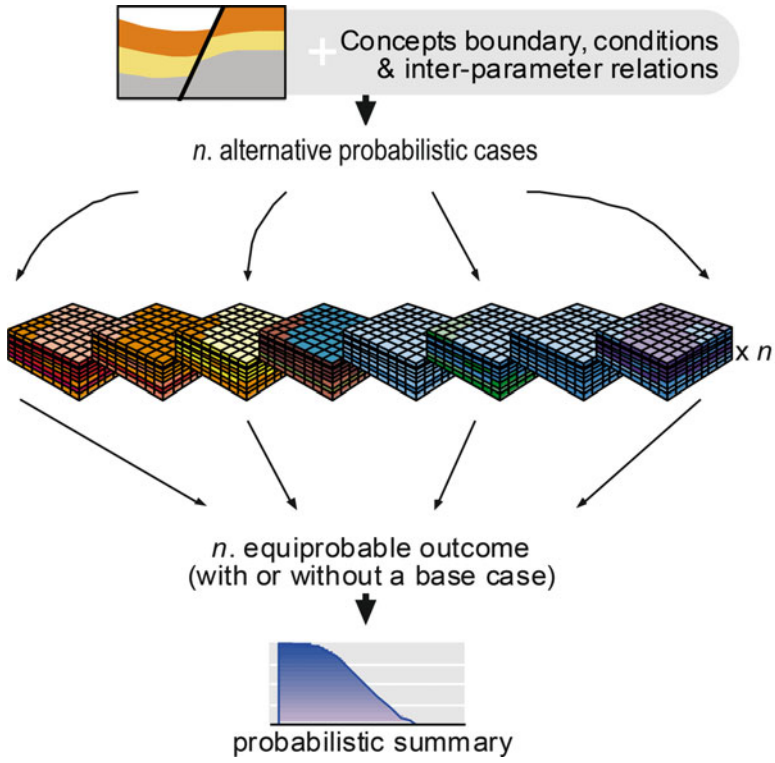

Fig. 5.8 Multiple stochastic approaches (Redrawn from Bentley and Smith 2008, The Geological Society, London, Special Publications 309 © Geological Society of London [2008])

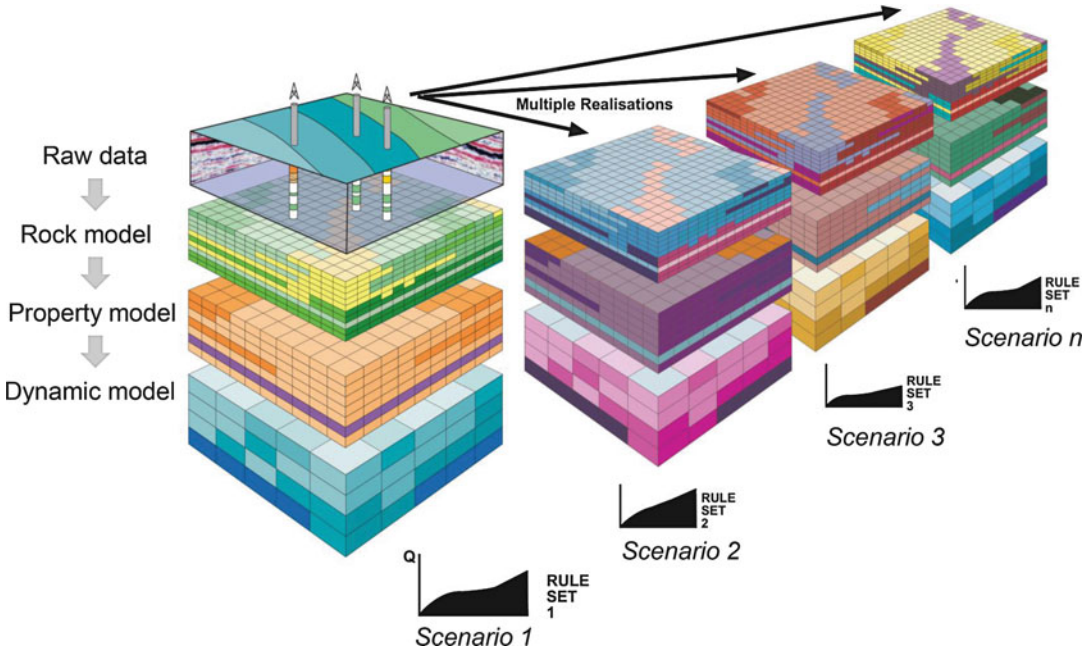

Fig. 5.9 Multiple-deterministic, 'scenario-based' approach

are built, each one reflecting a complete real-world outcome following an explicitly-defined reservoir concept. Geostatistical simulation may be applied in the building of the 3D model but the *selection* of the model realisations is made manually (or mathematically) rather than by statistical simulation (e.g. van de Leemput et al. 1996).

Each of the above approaches have been referred to as 'scenario modelling' by different reservoir modellers. The argument we develop here is that although all three approaches have some application in subsurface modelling, multiple-deterministic scenario-building is the preferred route in most circumstances.

In order to make this case, we need to recall the underlying philosophy of uncertainty handling and give a definition for 'scenario modelling'.

5.3 Anchoring

5.3.1 The Limits of Rationalism

The rationalist approach, described above as the 'best-guess' method, is effectively simple forecasting – and puts faith in the ability of an individual or team to make a reasonably precise judgement. If presented as the best judgement of a group of professional experts then this appears reasonable. The weak point is that the best guess is only reliable when the system being described is well ordered and well understood, to the point of being highly predictable (Mintzberg 1990). It must be assumed that enough data is available from past activities to predict a future outcome with confidence, and this applies equally to production forecasting, exploration risking, volumetrics or well prognoses. Although this is rarely the case in the subsurface, except perhaps for fields with a large (100+) number of regularly spaced wells, there is a strong tendency for individuals or teams (or managers) to desire a best guess, and to subsequently place too much confidence in that guess (Baddeley et al. 2004).

It is often stated that for mature fields, a simple, rationalist approach may suffice because uncertainty has reduced through the field life cycle. This is a fallacy. Although, the *magnitude* of the initial development uncertainties tends to decrease with time, we generally find that as the field life cycle progresses new, more subtle, uncertainties arise and these now drive the decision making. For example, in the landscape image in Fig. 5.5, 100 samples would significantly improve the ability to describe the image, but this is still insufficient to specify the location of an unsampled house. The impact of uncertainties in terms of their ability to erode value may, in fact, be as great near the end of the field life as at the beginning.

Despite this, rationalist, base-case modelling remains common across the industry. In a review of 90 modelling studies conducted by the authors and colleagues across many companies, field modelling was based on a single, best-guess model in 36 % of the cases (Smith et al. 2005). This was the case, despite a bias in the sampling from the authors' own studies, which tended to be scenario-based. Excluding the cases where the model design was made by the authors, the proportion of base case-only models rose to 60 %.

5.3.2 Anchoring and the Limits of Geostatistics

The process of selecting a best guess in spite of wide uncertainty is referred to as 'anchoring', and is a well-understood cognitive behaviour (Kahneman and Tverky 1974). Once anchored, the adjustment away from the initial best guess is too limited as the outcome is overly influenced by the anchor point.

This often also occurs in statistical approaches to uncertainty handling, as these tend to be anchored in the available data and may therefore make the same rational starting assumption as the simple forecast, although adding ranges around a 'most probable' prediction (see examples in Chellingsworth et al. 2011).

Geostatistical simulation allows definition of ranges for variables, followed by rigorous

sampling and combination of parameters to yield a range of results, which can be interpreted probabilistically. If the input data can be specified accurately, and if the combination process maintains a realistic relationship between all variables, the outcome may be reasonable. In practice, however, input data is imperfectly defined and the 'reasonableness' of the automated combination of variables is hard to verify. Statistical rigour is applied to data sets which are not necessarily statistically significant and an apparently exhaustive analysis may have been conducted on insufficient data.

The validity of the outcome may also be weakened by centre-weighting of the input data to variable-by-variable best-guesses, which creates an inevitability that the 'most likely' probabilistic outcome will be close to the initial best guess (Wynn and Stephens 2013). The geostatistical simulation itself is thus 'anchored'.

It is therefore argued that the application of geostatistical simulation does not in itself compensate for a natural tendency towards a rationalist best guess – it often tends to simply reflect it. The crucial step is to select a workflow which removes the opportunity for anchoring on a best guess; and this is what scenario modelling, as defined here, attempts to achieve.

5.4 Scenarios Defined

The definition of 'scenario' adopted here follows that described by van der Heijden (1996), who discussed the use of scenarios in the context of corporate strategic planning and defined scenarios as *a set of reasonably plausible, but structurally different futures*.

Alternative scenarios are not incrementally different models based on slight changes in continuous input data (as with multiple probabilistic models), but models which are *structurally* distinct based on some defined design criteria. Translated to oil and gas field development, a 'scenario' is therefore a plausible development outcome, and the 'scenario-based approach' to reservoir modelling is defined as:

> *the building of multiple, deterministically-driven models of plausible development outcomes*

Each scenario is a complete and internally consistent static/dynamic subsurface realisation with an associated plan tailored to optimise its development. In an individual subsurface scenario, there is clear linkage between technical detail in a model, and an ultimate commercial outcome; a change in any element of the model prompts a quantitative change in the outcome and the dependency between *all* parameters in the chain (between the changed element and the outcome) is unbroken.

This contrasts with many probabilistic simulations, in which model design parameters are statistically sampled and cross-multiplied, and in which dependencies between variables are either lost, or collapsed into correlation coefficients.

The scenario approach therefore places a strong emphasis on deterministic representation of a subsurface concept: geological, geophysical, petrophysical and dynamic. Without a clearly defined concept of the subsurface – clear in the sense that a geoscientist could represent it as a simple sketch – the modelling cannot progress meaningfully. We have used the mantra: *if you can sketch it, you can model it*. Geostatistical simulation may be a key tool required to build an individual scenario but the design of the scenarios is determined directly by the modeller. Multiple models are based on multiple, deterministic designs. This distinguishes the workflows for scenario modelling, as defined here, from multiple stochastic modelling which tends to be based on statistical sampling from a single initial design. Note that multiple stochastic modelling is a powerful tool for understanding reservoir model ranges and outcomes; it is simply not sufficient to fully explore subsurface uncertainties from poorly sampled reservoirs.

Scenario-based approaches place an emphasis on listing and ranking of uncertainties, from which a suite of scenarios will be built, with no attempt being made to select a best guess case up-front.

5.5 The Uncertainty List

The key to success in scenario modelling lies in deriving an appropriate list of key uncertainties, a matter of experience and judgement. However, there is a strong tendency to conceptualise key uncertainties for at least the static reservoir models in terms of the parameters of the STOIIP equation, *i.e.* when asked to define the key uncertainties in the field, modellers will often quote parameters such as 'porosity' or 'net sand' as key factors. If the model-build progresses with these as the key uncertainties to alter, this will most likely be represented as a range for a continuous variable, anchored around a best guess.

A better approach is to question why 'porosity' or 'net sand count' are considered significant uncertainties. It will either emerge that the uncertainty is not that significant or, if it is, then it relates to some underlying root cause, such as heterogeneous diagenesis, or some local facies control which has not been extracted from the data analysis.

For example, in Fig. 5.10 a PDF of net-to-gross is shown. A superficial approach to model uncertainty would involve taking the PDF, inputting it to a geostatistical algorithm and allowing sampling of the spread to account for the uncertainty. As the data in the figure illustrates, this would be misleading, because the range is reflecting mixed geological concepts. The real need is to understand the facies distribution, and isolate the facies-based factors (in this case the proportion of different channel types), and then establish whether this ratio is known within reasonable bounds. If not known, the uncertainty can be represented by building contrasting, but realistic, depositional models (the basis for two scenarios) in which these elements are specifically contrasted. The uncertainty in the net-to-gross parameter within each scenario is a second-order issue to the geological uncertainty.

In defining key uncertainties, the need is therefore to chase the source of the uncertainty to the underlying causative factor – 'root cause analysis' – and model the conceptual range of uncertainty of that factor with discrete cases, rather than simply input a data distribution for a higher level parameter such as net-to-gross.

5.6 Applications

5.6.1 Greenfield Case

The application of scenario modelling has been most successfully reported for cases involving new or 'greenfield' reservoir studies.

One of the first published examples was that of van de Leemput et al. (1996), who described an application of scenario-based modelling in the context of an LNG field development. Once sufficient proven volumes were established to support the scheme, the commercial structure of the project focussed attention on the issue of the associated capital expenditure (CAPEX). CAPEX therefore became the prime quantitative outcome of the modelling exercise, driven largely by well numbers and the requirements for, and timing of, gas compression facilities.

The model scenarios were driven by a selection of principal uncertainties, summarised in Fig. 5.11. Six static and five dynamic uncertainties were drawn up, based on the judgement of the project team and input from peers. Maintaining the uncertainty list became a continuing process, iterating with new well data from appraisal drilling, and the changing views of the group.

For the field development plan itself, the uncertainty list generated 22 discrete scenarios, each of which was matched to the small amount of production data, then individually tailored to optimise the development outcome over the life of the LNG scheme. The outcomes, in term of impact on project cost (CAPEX), are shown in Fig. 5.11.

A key learning outcome from this exercise was that a list of 11 uncertainties was unnecessarily long to generate the ultimate result, although convenient for satisfying concerns of stakeholders. The effect of statistical dominance meant that the range was not driven by all

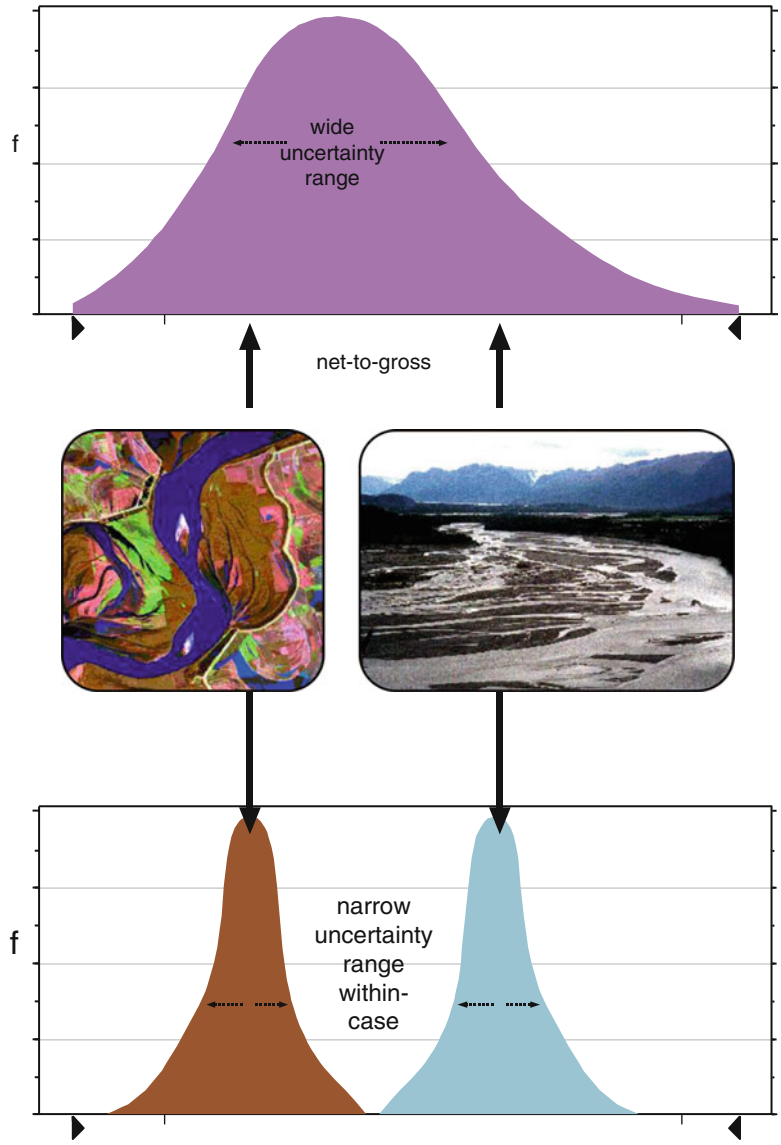

Fig. 5.10 Root-cause analysis: defining the underlying causative uncertainty (Redrawn from Bentley and Smith 2008, The Geological Society, London, Special Publications 309 © Geological Society of London [2008])

11 uncertainties, but by 2 or 3 key uncertainties to which the scheme was particularly sensitive.

Contrary to the expectations of geoscientists, gross rock volume on the structures was not a key development issue, even though the fields were large and each had only two or three well penetrations at the time of the field development plan (FDP) submission. The key issue was the potential enhancements of well deliverability offered by massive hydraulic fracturing – not a factor typically at the heart of reservoir modelling studies. The majority of the issues normally addressed by modelling: sand body geometries, relative permeabilities, aquifer size *etc*., were certainly poorly understood, but could be shown to have no significant impact on the field development decision. In hindsight, the dominant issues were foreseeable without modelling.

In the light of the above, continued post-FDP modelling became more focussed, with a smaller number of scenarios fleshing out the dominant issues only. Tertiary issues were effectively treated as constants.

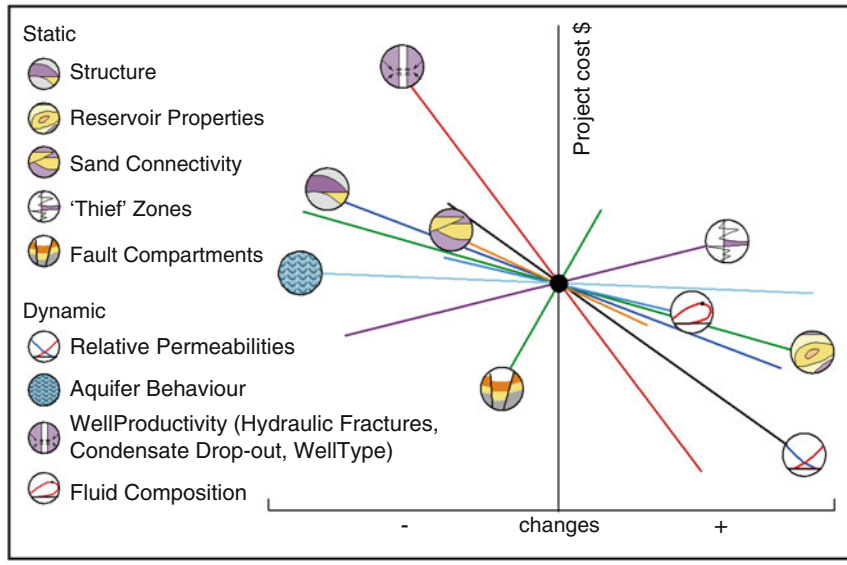

Fig. 5.11 Application of deterministic scenarios to a green field case: forecasting costs (Redrawn from Bentley and Smith 2008, The Geological Society, London, Special Publications 309 © Geological Society of London [2008])

The above example was conducted without selecting a 'base case' model. A development scheme was ultimately selected, but this was based on a range of outcomes defined by the subsurface team.

Scenario modelling for greenfields has been conducted many times since the publication of this example. In the experience of the authors, the early learnings described in the case above have held true, notably:

- Large numbers of scenarios are not required to capture the range of uncertainty;
- The main uncertainties can generally be drawn up through cross-discipline discussion prior to modelling – if not these can be established by running quick sensitivities;
- This list should be checked and iterated as the modelling progresses;
- The dominant uncertainties on a development project do not always include the issue of seismically driven gross rock volume, even at the pre-development phase;
- It is not necessary to select a base case model.

5.6.2 Brownfield Case

Two published examples are summarised here which illustrate the extension of scenario modelling to mature, or 'brownfield', reservoir cases.

The first concerns the case of the Sirikit Field in Thailand (Bentley and Woodhead 1998). The requirement was to review the field mid-life and evaluate the potential benefit of introducing water injection to the field. At that point the field had been on production for 15 years, with 80 wells producing from a stacked interval of partially-connected sands. The required outcome was a quantification of the economic benefit of water injection, to which a scenario–based approach was to be applied.

The uncertainty list is summarised in Fig. 5.12. The static uncertainties were used to generate the suite of static reservoir models for input to simulation. In contrast to the greenfield cases, where production data is limited, the dynamic uncertainties were used as the history

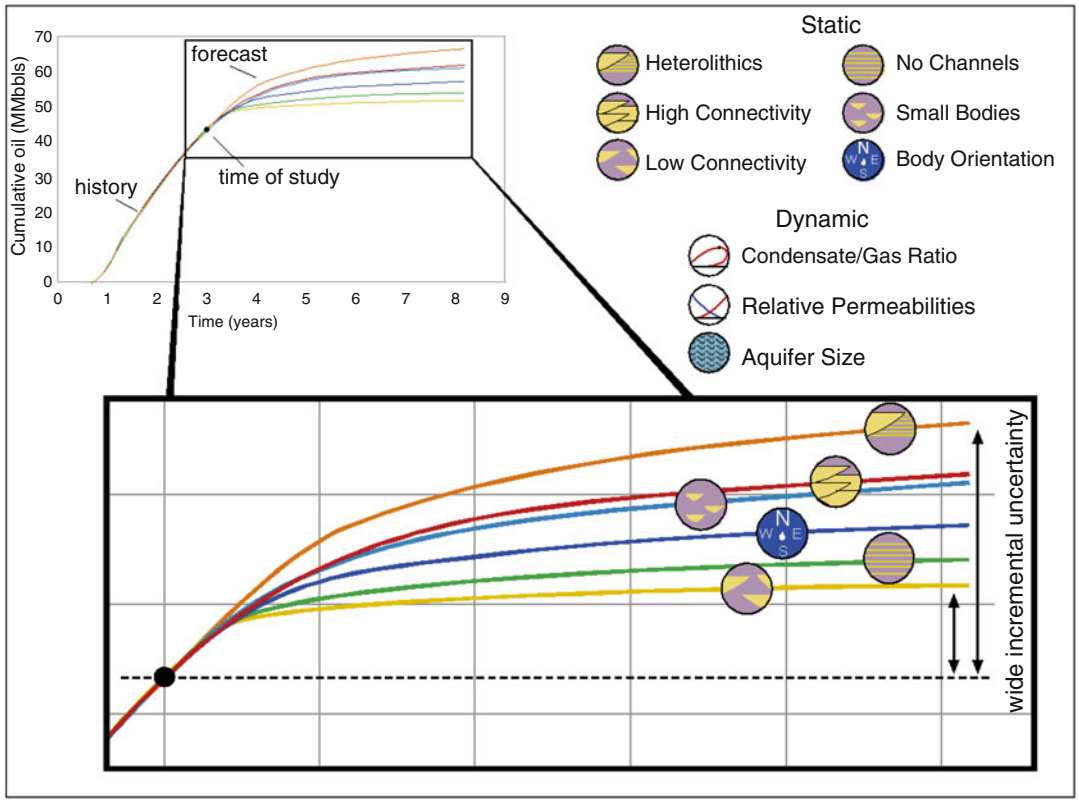

Fig. 5.12 Application of deterministic scenarios to a brownfield case: forecasting production (Redrawn from Bentley and Smith 2008, The Geological Society, London, Special Publications 309 © Geological Society of London [2008])

matching tools – the permissible parameter ranges for those uncertainties being established *before* the matching began.

A compiled production forecast for the 'no further drilling case' is shown in Fig. 5.12. The difference between that spread of outcomes and the spread from a parallel set of outcomes which included water injection, was used to quantify the value of the injection decision. Of interest here is the nature of that spread. Although all models gave reasonable matches to history, the incremental difference between the forecasts was larger than that expected by the team. It was hoped that some of the static uncertainties would simply be ruled out by the matching process. Ultimately none were, despite 80 wells and 15 years of production history.

The outlier cases were reasonable model representations of the subsurface, none of the scenarios was strongly preferred over any other, and all were plausible. A base case was not chosen.

The outcome makes a strong statement about the non-uniqueness of simulation model matches. If a base case model had been rationalised based on preferred guesses, any of the seven scenarios could feasibly have been chosen – only by chance would the eventual median model have been selected.

The Sirikit case also confirmed that multiple deterministic modelling was achievable in reasonable study times – scaled sector models were used to ease the handling of production data (see Bentley and Woodhead 1998). The workflow yielded a surprisingly wide range of model forecasts.

Fig. 5.13 summarises an application of scenario modelling to a producing field with 4D seismic, which generated additional insights into the use of scenarios. The case is from the

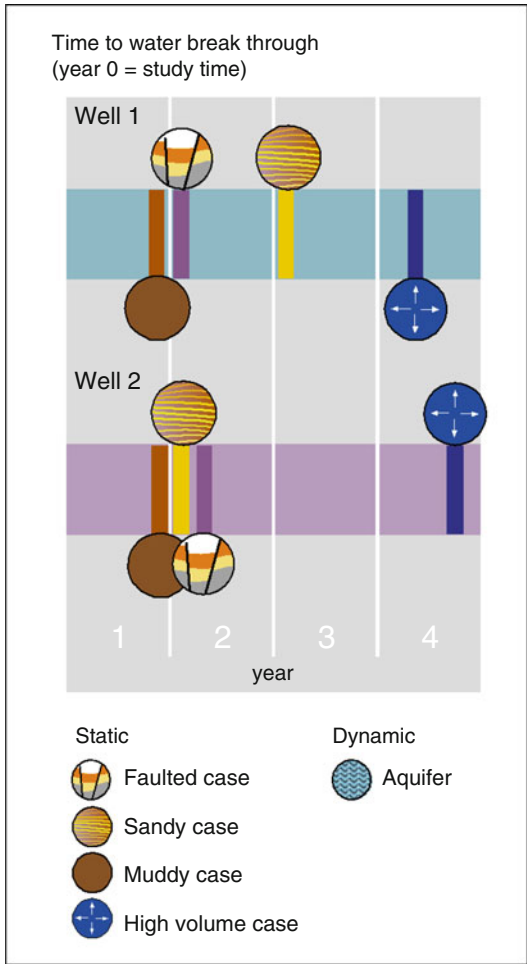

Fig. 5.13 Application of deterministic scenarios to a brownfield case: forecasting water breakthrough (Redrawn from Bentley and Smith 2008, The Geological Society, London, Special Publications 309 © Geological Society of London [2008])

Gannet B Field in the Central North Sea (Bentley and Hartung 2001; Kloosterman et al. 2003).

The issue to model in the Gannet B case was the risk and timing of potential water breakthrough in one of the field's two gas producers, and placing value on the possible contingent activities post-breakthrough. As with the cases above, the study started with a listing and qualitative ranking of principal uncertainties in a cross-discipline forum. Unlike the previous cases, it proved not to be possible to match all static reservoir models with history. The lowest volume realisation would not match. The model outcome – a range of water-cut breakthrough times – is illustrated in Fig. 5.13.

The Gannet B study offered some additional insights into mature field scenario modelling:

- Although the truism is offered that multiple models can match production data (there is no uniqueness to history matches), the converse is not necessarily true – everything cannot always be matched;
- The above is more likely to be true in smaller fields, where physical field limitations constrain possible scenarios;
- In the specific case of Gannet B, the principal matching tool was 4D seismic data (not well production data), and it was the seismic which was the matching target for the multiple model scenarios;
- A base case selection from the quantified range in water breakthrough times would have been highly misleading; "between 9 months and 4 years" was the answer to the question based on the available data. Making a median guess would have simply hidden the risk.

5.7 Scenario Modelling – Benefits

The scenario-based approach as defined here offers specific advantages over base case modelling and multiple probabilistic modelling:

Determinism: the dominance of the underlying conceptual reservoir model, which is deterministically applied via the model design. Although the models may use any required level of geostatistical simulation to re-create the desired reservoir concept, the geostatistical algorithms are not used to select the cases to be run, nor to quantify the uncertainty ranges in the model outcomes.

Lack of anchoring: the approach is not built on the selection of a base case, or best guess. Qualitatively, the natural tendency to underestimate uncertainties is less prone to occur if a best guess is not required – the focus lies instead on an exploration of the range.

Dependence: direct dependence between parameters is maintained through the modelling process; a contrast between two model

realisations is fed through directly to two quantitative scenarios, which allow the significance of the uncertainty to be evaluated.

Transparency: although the models may be internally complex, the workflow is simple, and feeds directly off the uncertainty list, which may be no more complex than a short list of the key issues which drive the decision at hand. If the key issues which could cause a project to fail are identified on that list, the model process will evaluate the outcome in the result range. The focus is therefore not on the intricacies of the model build (which can be reviewed by an expert, as required), but on the uncertainty list, which is transparent to all interested parties.

5.8 Multiple Model Handling

It is generally assumed that more effort will be required to manage multiple models than a single model, particularly when brownfield sites require multiple history matching. However, this is not necessarily the case – it all comes down to a choice of workflow.

Multiple model handling in greenfield sites is not necessarily a time-consuming process. Figure 5.14a illustrates results from a study involving discrete development scenarios. These were manually constructed from permutations of 6 underlying static models and dynamic uncertainties in fluid distribution and composition. This was an exhaustive approach in which all combinations of key uncertainties were assessed. The final result could have been achieved with a smaller number of scenarios, but the full set was run simply because it was not particularly time-consuming (the whole study ran over roughly 5 man weeks, including static and dynamic modelling). The case illustrates the efficacy of multiple static/dynamic modelling in greenfields, even when the compilation of runs is manual. Figure 5.14b shows the results of a more recent study (Chellingsworth, et al. 2011) in which 124 STOIIP-related cases were efficiently analysed using a workflow-manager algorithm.

This issue is more pressing for brownfield sites, although the cases described above from the Sirikit and Gannet fields illustrate that workflows for multiple model handling in mature fields can be practical. This challenge is also being improved further by the emergence of a new breed of automatic history matching tools which achieve model results according to input guidelines which can be deterministically controlled.

It is thus suggested that the running of multiple models is not a barrier to scenario modelling, even in fields with long production histories. Once the conceptual scenarios have been clearly defined, it often emerges that complex models are not required. Fit-for-purpose models also come with a significant time-saving.

Cross-company reviews by the authors indicate that model-building exercises which are particularly lengthy are typically those where a very large, detailed, base-case model is under construction. History matching is often pursued to a level of precision disproportionate to the accuracy of the static reservoir model it is based on. By contrast, multiple modelling

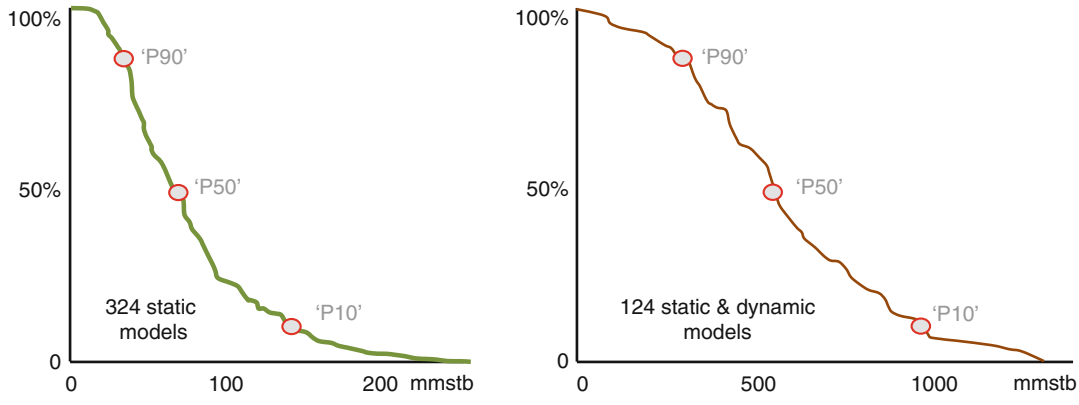

Fig. 5.14 Multiple deterministic cases for STOIIP (*left*) and ultimate recovery (*right*)

exercises tend to be more focussed and, paradoxically, tend to be quicker to execute than the very large, very detailed base-case model builds.

5.9 Linking Deterministic Models with Probabilistic Reporting

The next question is how to link multiple-deterministic scenarios with a probabilistic framework? Ultimately we wish to know how likely an outcome is. In reservoir modelling, probability is most commonly summarised as the percentiles of the cumulative probability distribution – P90, P50, and P10, where P90 is the value (e.g. reserves) which has a 90 % probability of being exceeded, and P50 is the median of the distribution. With multiple-deterministic scenarios, as each scenario is qualitatively defined, the link to statistical descriptions of the model outcome (*e.g.* P90, P50 and P10) can be qualitative (e.g. a visual ranking of outcomes) or formalised in a more quantitative manner.

An important development has been the merging of deterministically-defined scenario models with probabilistic reporting using a collection of approaches broadly described as 'experimental design'. This methodology offers a way of generating probabilistic distributions of hydrocarbons in place or reserves from a limited number of deterministic scenarios, and of relating individual scenarios to specific positions on the cumulative probability function (or 'S' curve). In turn, this provides a rationale for selecting specific models for screening development options.

Experimental design is a well-established technique in the physical and engineering sciences where it has been used for several decades (*e.g.* Box and Hunter 1957). It has more recently become popular in reservoir modelling and simulation (*e.g.* Egeland et al. 1992; Yeten et al. 2005; Li and Friedman 2005) and offers a methodology for planning experiments so as to extract the maximum amount of information about a system using the minimum number of experimental runs. In subsurface modelling, this can be achieved by making a series of reservoir models which combine uncertainties in ways specified by a theoretical template or design.

The type of design depends on the purpose of the study and on the degree of interaction between the variables. A simple approach is the Plackett-Burmann formulation. This design assumes that there are no interactions between the variables and that a relatively small number of experiments are sufficient to approximate the behaviour of the system. More elaborate designs, for example D-optimal or Box-Behnken (e.g. Alessio et al. 2005; Cheong and Gupta 2005; Peng and Gupta 2005), attempt to analyse different orders of interaction between the uncertainties and require a significantly greater number of experiments. The value of elaboration in the design needs to be assessed – *more is not always better* – and depends on the model purpose, but the principles described below apply generally.

A key aspect of experimental design is that the uncertainties can be expressed as end-members. The emphasis on making a base case or a best guess for any variable is reduced, and can be removed.

The combination of Plackett-Burmann experimental design with the scenario-based approach is illustrated by the case below from a mature field re-development plan involving multiple-deterministic scenario-based reservoir modelling and simulation (Bentley and Smith 2008). The purpose of the modelling was to build a series of history-matched models that could be used as screening tools for a field development.

As with all scenario-based approaches, the workflow started with a listing of the uncertainties (Fig. 5.15), presumed in this case to be:

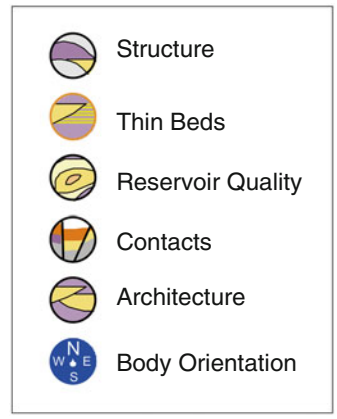

Fig. 5.15 Experimental design case: uncertainty list

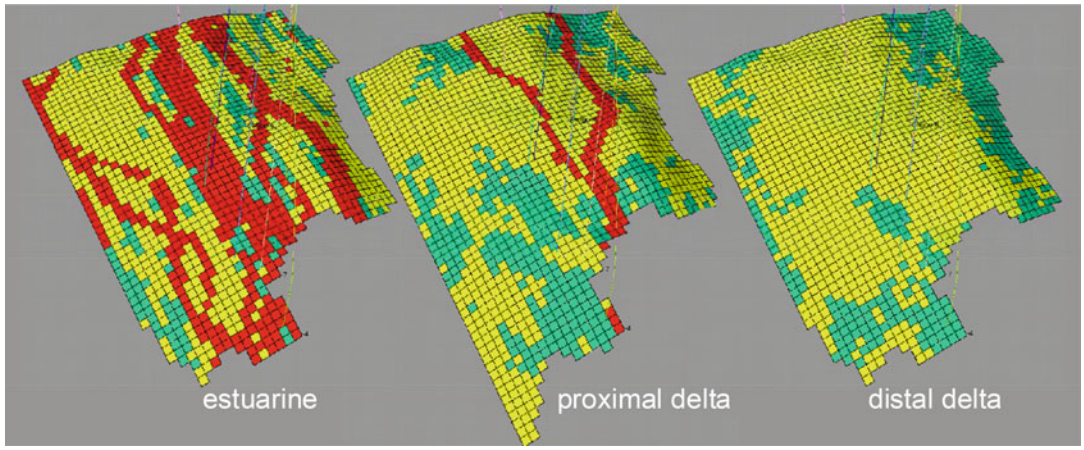

Fig. 5.16 Alternative reservoir architectures (Images courtesy of Simon Smith) (Redrawn from Bentley and Smith 2008, The Geological Society, London, Special Publications 309 © Geological Society of London [2008])

Realisation	Structure	Quality	Contacts	Architecture	Thin beds	Orientation	Response
1	-1	1	1	1	-1	1	1178
2	-1	-1	1	1	1	-1	380
3	-1	-1	-1	-1	-1	-1	109
4	1	-1	1	1	-1	1	1105
5	-1	-1	-1	1	1	1	402
6	1	-1	1	-1	-1	-1	1078
7	1	1	-1	1	1	-1	1176
8	1	-1	-1	-1	1	1	1090
9	-1	1	-1	-1	-1	1	870
0	-1	1	1	-1	1	-1	932
11	1	1	-1	1	-1	-1	1201
12	1	1	1	-1	1	1	1245
13	0	0	0	0	0	0	956
14	1	1	1	1	1	1	1656

Fig. 5.17 Plackett-Burmann matrix showing high/low combinations of model uncertainties and the resulting response (resource volumes in Bscf)

1. *Top reservoir structure;* caused by poor quality seismic and ambiguous depth conversion. This was modelled using alternative structural cases capturing plausible end-members.
2. *Thin-beds;* the contribution of intervals of thin-bedded heterolithics was uncertain as these intervals had not been produced or tested in isolation. This uncertainty was modelled by generating alternative net-to-gross logs.
3. *Reservoir architecture;* uncertainty in the interpretation of the depositional model was expressed using three conceptual models: tidal estuarine, proximal tidal-influenced delta and distal tidal-influenced delta models (Fig. 5.16). A model was built for each, with no preferred case.
4. *Sand quality;* this is an uncertainty simply because of the limited number of wells and was handled by defining alternative cases for facies proportions, the range guided by the best and worst sand quality seen in wells.
5. *Reservoir orientation;* modelled using alternative orientations of the palaeodip.
6. *Fluid contacts;* modelled using plausible end-members for fluid contacts.

These six uncertainties were combined using a 12-run Plackett-Burmann design. The way in which the uncertainties were combined is shown

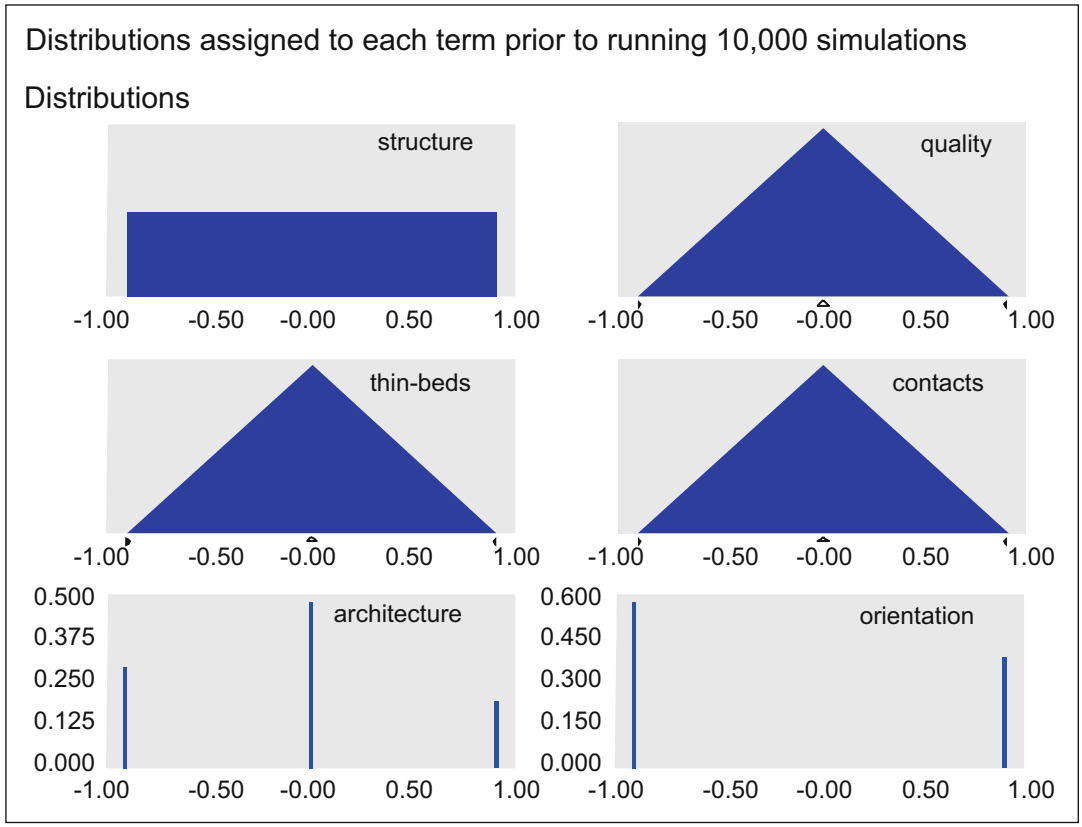

Fig. 5.18 Parameter ranges and distribution shapes for each uncertainty

in the matrix in Fig. 5.17, in which the high case scenario is represented by +1, the low case by −1 and a mid case by 0. In this case two additional runs were added, one using all the mid points and one using all the low values. Neither of these two cases is strictly necessary but can be useful to help understand the relationship between the uncertainties and the ultimate modelled outcome.

The 14 models were built and the resource volume (the 'response') determined for each reservoir. A linear least-squares function was derived from the results, capturing the relationship between the response and the individual uncertainties. The relative impact of the individual uncertainties on the resource volumes is captured by a co-efficient specific to the impact of each uncertainty.

The next step in the workflow is to consider the likelihood of each uncertainty occurring in between the defined end-member cases, that is, in between the '1' and the '−1'. This relates back to the underlying conceptual model, and requires the definition of a parameter distribution function (e.g. uniform, Gaussian, triangular). The distribution shapes selected for each uncertainty in this case are shown in Fig. 5.18. For variables where the value can be anywhere between the 1 and −1 end members, a uniform distribution is appropriate, for those with a central tendency a normal distribution is preferred (simplified as a triangular distribution) and for some variables only discrete alternative possibilities were chosen.

Once the design is set up, and assuming the independence of the chosen variables is still valid, the distributions can then be sampled by standard Monte-Carlo analysis to generate a probabilistic distribution. The existing suite of models can then be mapped onto a probabilistic, or S-curve, distribution (Fig. 5.19).

There are three distinct advantages to using this workflow. Firstly, it makes a link between

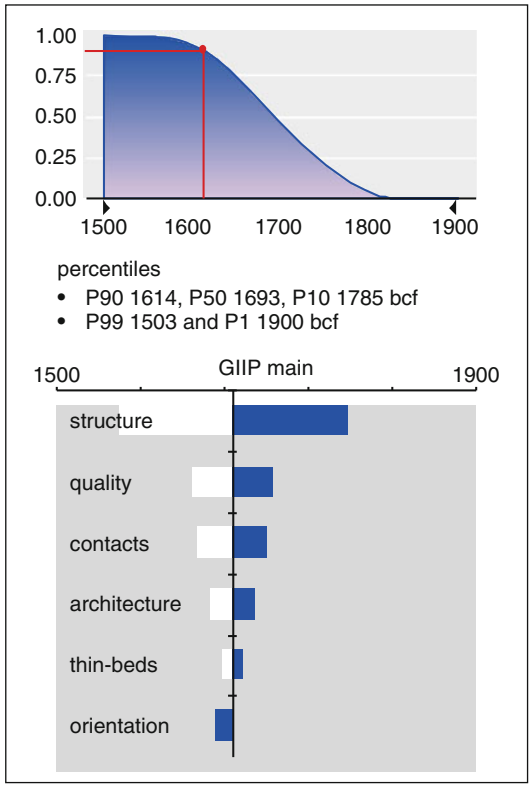

Fig. 5.19 Probabilistic volumes from Monte Carlo simulation of the experimental design formulation

probabilistic reporting and discrete multiple-deterministic models. This can be used to provide a rationale for selecting models for simulation. For example, P90, P50 and P10 models can be identified from this analysis and it may emerge that models reasonably close to these probability thresholds were built as part of the initial experimental design. Alternatively, the comparison may show that new models need to be built. This is easier to do now that the impact of the different uncertainties has been quantified, and is an improvement on an arbitrary assumption that a high case model, for example, represents the P10 case. Secondly, the workflow focuses on the end-members and on capturing the range of input variables, avoiding the need to anchor erroneously on a best guess. Finally, the approach provides a way of quantifying the impact of the different uncertainties via tornado diagrams or simple spider plots, which can in turn be used to steer further data gathering in a field.

Moreover, having conducted an experimental design, it may emerge that the P50 outcome is significantly different from the previously assumed initial 'best guess.' That is, this uncertainty modelling approach can help compensate for the biases that the user, or subsurface team, started with.

5.10 Scenarios and Uncertainty-Handling

Scenario-based approaches offer an improvement over base-case modelling, as results from the latter are anchored around best guess assumptions. Best guesses are invariably misleading because data from the subsurface is generally insufficient to be directly predictive. Scenarios are defined here as 'multiple, deterministically-driven models of plausible development outcomes', and are preferred to multiple stochastic modelling alone, the application of which is limited by the same data insufficiency which limits base case modelling. Each scenario is a plausible development future based on a specific concept of the subsurface, the development planning response to which can be optimised.

The application of geostatistical techniques, and conditional simulation algorithms in particular, is wholly supported as a means of completing a realistic subsurface model – usually by infilling a strongly deterministic model framework. Multiple stochastic modelling can also be useful to explore sensitivities around an individual deterministic scenario. Deterministic design of each over-arching scenario, however, is preferred because of transparency, relative simplicity and because each scenario can be validated as a realistic subsurface outcome.

Scenario-based modelling is readily applicable to greenfield sites but, as the examples shown here confirm, is also practical for mature, brownfield sites, where multiple history matching may be required at the simulation stage.

The key to success is the formulation of the uncertainty list. If the issues which could cause the business decision to fail are identified, then the modelling workflow will capture this and the decision risk can be mitigated. If the issue is

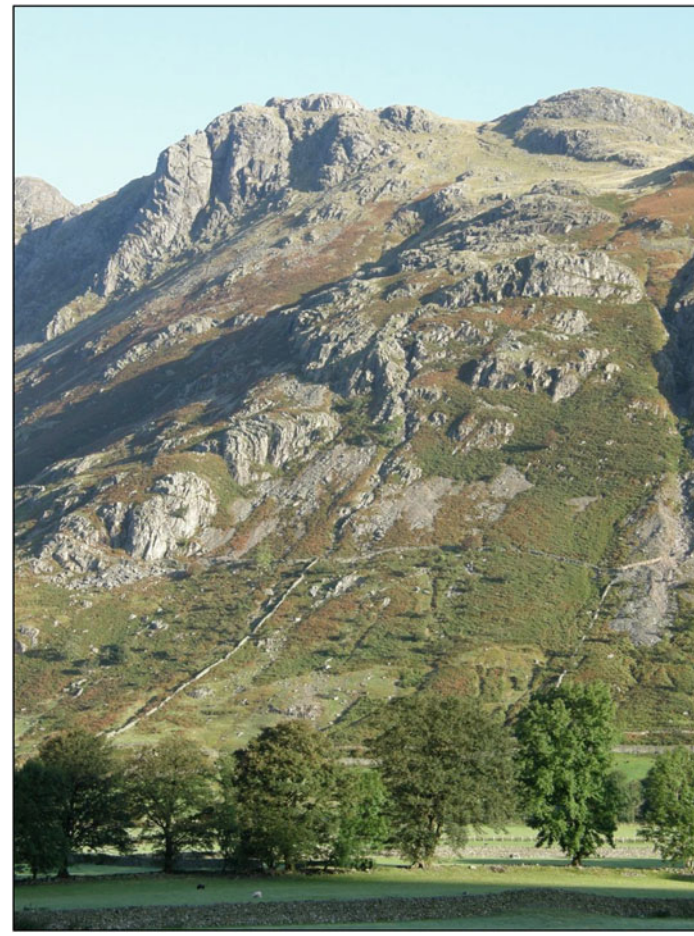

Fig. 5.20 Did you anticipate the trees?

missed, no amount of modelling of any kind can compensate. The list is therefore central, including the identification of issues not explicit in the current data set, but which can be anticipated with thought. Remember, there may be trees (Fig. 5.20).

References

Alessio L, Bourdon L, Coca S (2005) Experimental design as a framework for multiple realisation history matching: F6 further development studies. SPE 93164 presented at SPE Asia Pacific Oil and Gas conference and exhibition, Jakarta, 5–7 Apr 2005

Baddeley MC, Curtis A, Wood R (2004) An introduction to prior information derived from probabilistic judgements: elicitation of knowledge, cognitive bias and herding. In: Curtis A, Wood R (eds) Geological prior information. Informing science and engineering, The Geological Society special publications, 239. The Geological Society, London, pp 15–27

Bentley MR, Hartung M (2001) A 4D surprise at Gannet B. EAGE annual technical conference, Amsterdam (extended abstract)

Bentley M, Smith S (2008) Scenario-based reservoir modelling: the need for more determinism and less anchoring. In: Robinson A et al (eds) The future of geological modelling in hydrocarbon development, The Geological Society special publications, 309. The Geological Society, London, pp 145–159

Bentley MR, Woodhead TJ (1998) Uncertainty handling through scenario-based reservoir modelling. SPE paper 39717 presented at the SPE Asia Pacific conference on Integrated Modelling for Asset Management, 23–24 Mar 1998, Kuala Lumpur

Box GEP, Hunter JS (1957) Multifactor experimental designs for exploring response surfaces. Ann Math Stat 28:195–241

Caers J (2011) Modeling uncertainty in the earth sciences. Wiley (published online)

Chellingsworth L, Kane P (2013) Expectation analysis in the assessment of volume ranges in appraisal and development – a case study (abstract). Presented at the Geological Society conference on Capturing Uncertainty in Geomodels – Best Practices and Pitfalls, Aberdeen, 11–12 Dec 2013. The Geological Society, London

Chellingsworth L, Bentley M, Kane P, Milne K, Rowbotham P (2011) Human limitations on hydrocarbon resource estimates – why we make mistakes in data rooms. First Break 29(4):49–57

Cheong YP, Gupta R (2005) Experimental design and analysis methods for assessing volumetric uncertainties. SPE J 10(3):324–335

Cosentino L (2001) Integrated reservoir studies. Editions Technip, Paris, 310 p

Dubrule O, Damsleth E (2001) Achievements and challenges in petroleum geostatistics. Petroleum Geosci 7:S53–S64

Egeland T, Hatlebakk E, Holden L, Larsen EA (1992) Designing better decisions. SPE paper 24275 presented at SPE European Petroleum Computer conference, Stavanger, 25–27 May 1992.

Kahneman D (2011) Thinking fast and slow. Farrar, Straus and Giroux, New York, 499 p

Kahneman D, Klein G (2009) Conditions for intuitive expertise: a failure to disagree. Am Psycol 64:515–526

Kahneman D, Tverky A (1974) Judgement under uncertainty: heuristics and biases. Science 185:1124–1131

Kloosterman HJ, Kelly RS, Stammeijer J, Hartung M, van Waarde J, Chajecki C (2003) Successful application of time-lapse seismic data in Shell Expro's Gannet Fields, Central North Sea, UKCS. Petroleum Geosci 9:25–34

Li B, Friedman F (2005) Novel multiple resolutions design of experiment/response surface methodology for uncertainty analysis of reservoir simulation forecasts. SPE paper 92853, SPE Reservoir Simulation symposium, 31 Jan–2 Feb, The Woodlands, 2005

Mintzberg H (1990) The design school, reconsidering the basic premises of strategic management. Strateg Manage J 6:171–195

Peng CY, Gupta R (2005) Experimental design and analysis methods in multiple deterministic modelling for quantifying hydrocarbon in place probability distribution curve. SPE paper 87002 presented at SPE Asia Pacific conference on Integrated Modelling for Asset Management, Kuala Lumpur, 29–30 Mar 2004

Smith S, Bentley MR, Southwood DA, Wynn TJ, Spence A (2005) Why reservoir models so often disappoint – some lessons learned. Petroleum Studies Group meeting, Geological Society, London. Abstract.

Towler BF (2002) Fundamental principles of reservoir engineering, vol 8, SPE textbook series. Henry L. Doherty Memorial Fund of AIME, Society of Petroleum Engineers, Richardson

van de Leemput LEC, Bertram D, Bentley MR, Gelling R (1996) Full-field reservoir modeling of Central Oman gas/condensate fields. SPE Reservoir Eng 11(4):252–259

van der Heijden K (1996) Scenarios: the art of strategic conversation. Wiley, New York, 305pp

Wynn T, Stephens E (2013) Data constraints on reservoir concepts and model design (abstract). Presented at the Geological Society conference on Capturing Uncertainty in Geomodels – Best Practices and Pitfalls, Aberdeen, 11–12 Dec 2013

Yarus JM, Chambers RL (1994) Stochastic modeling and geostatistics principals, methods, and case studies. AAPG Comput Appl Geol 3:379

Yeten B, Castellini A, Guyaguler B, Chen WH (2005) A comparison study on experimental design and response surface methodologies. SPE 93347, SPE Reservoir Simulation symposium, The Woodlands, 31 Jan–2 Feb 2005

Reservoir Model Types

6

Abstract

Every reservoir is in some way unique.

There are nevertheless generic issues pertinent to certain reservoir types and, in terms of model design, these are the issues which inevitably require attention.

We don't aim to cover all possible reservoir types but we do hope to indicate trains of thought which we have found fruitful. Along the way, we can elicit distinctions between models for clastic and carbonate reservoirs and some courses of action to take if the reservoir turns out to be fractured.

If all reservoirs were just tanks of sand, this task would be trivial. In practice, geology and fluid dynamics combine in complex and intriguing but ultimately understandable ways. Adapting a line from Leo Tolstoy's Anna Karenina:

> *Homogeneous reservoirs are all alike; every heterogeneous reservoir is heterogeneous in its own way.*

P. Ringrose and M. Bentley, *Reservoir Model Design*, DOI 10.1007/978-94-007-5497-3_6,

Fault damage zone within aeolian sandstones, Moray Coast, Scotland

There are many ways one could classify different types of reservoirs, such as siliciclastic, carbonate and fractured reservoirs. We have chosen to group sandstone reservoirs by common depositional settings, namely:

- Aeolian reservoirs
- Fluvial reservoirs
- Tidal-deltaic reservoirs
- Shallow-marine reservoirs
- Deep-marine reservoirs

We then go on to consider carbonate and structurally-controlled reservoirs as two further types. In practice, many carbonate reservoir systems may contain siliciclastic units, and both sandstone and carbonate reservoirs may be significantly influenced by the presence of faults and fractures.

The main issue is to identify the key characteristics of the reservoir under consideration as a starting point for the reservoir model design which will be unique to that reservoir.

6.1 Aeolian Reservoirs

Aeolian depositional environments are one of a number of 'siliciclastic' sedimentary systems. Siliciclastics are silicate- (typically quartz-) dominated, clastic, sedimentary rocks, or put more simply, sediments predominantly composed of sand grains. We often use the term *clastic* as an abbreviation (slightly incorrectly as clastics may also be carbonates) but their main feature is the predominance of quartz sand grains, the size of which varies enormously, from mudstones (grains of a few μm in diameter) to coarse-grained sands (mm sized) to conglomerates (cm-sized grains). Contrasting siliciclastic systems will be reviewed in the following five sections, starting with the most quartz-rich: the aeolian (wind-blown) sand systems.

Aeolian systems typically produce high net-to-gross (or at least high sand fraction) reservoir

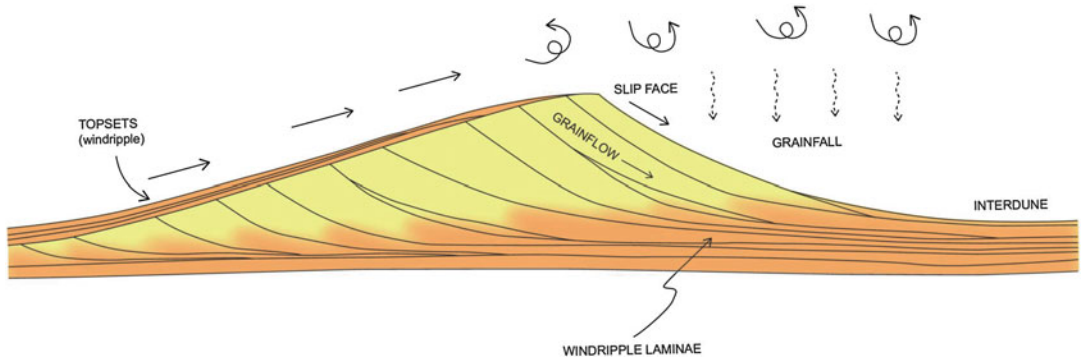

Fig. 6.1 Typical elements of aeolian systems

systems with blocky responses on open hole logs. Consequently, there is a tendency to treat them as 'sand tanks', a tendency encouraged by well-behaved porosity-permeability relationships derived from the excellent sorting capability of the wind.

The risk is therefore that aeolian systems can be over-simplified, particularly because important heterogeneities are often found at a scale below log resolution. The highly laminated nature of aeolian strata and the strong permeability contrasts between some of these strata are belied by relatively benign standard log responses.

Aeolian systems are, however, very well organised with distinct generic bedform types, and thus lend themselves well to modelling, and multi-scale modelling in particular. The highly laminated heterogeneity is typically well organised and therefore within reach of geologically-based modelling tools.

6.1.1 Elements

The component model elements of aeolian systems are well understood. Fryberger (1990a) describes aeolian systems in terms of four main facies: dune, interdune, sandsheet and sabkha, within which four principal types of bedding recur:

- grainflow strata, resulting from avalanche down the steep side of dunes,
- grainfall strata, dropped from airborne transport,
- wind ripple laminations, a product of saltation, and
- adhesion strata, resulting from drifting sands adhering to damp surfaces.

The aeolian bedding types usually have dune morphologies and have predictable reservoir property contrasts (Weber 1987, Fig. 6.1). As a rule of thumb, dune systems offer the best quality reservoirs, and it is the well-sorted, mostly coarse-grained grainflow beds on the slip faces of the dunes which typically carry the highest permeabilities within the dunes (Heward 1991).

Figure 6.2 shows some typical k/ϕ relationships for these elements; with grain flow sands on the slip face offering an order of magnitude uplift in permeability for any given porosity class.

6.1.2 Effective Properties

The effective properties of some elements of aeolian systems are captured well by standard log and core measurements; however, for other elements, especially the different lamina types, this is predictably not the case, and a consideration of the multi-scale REVs for aeolian systems distinguishes the elements which require more attention. The excellent exposure of the dune system shown in Fig. 6.3 reveals many heterogeneities, which can be summarised in terms of permeability length scales and a hierarchical arrangement of REVs, as shown in Fig. 6.4.

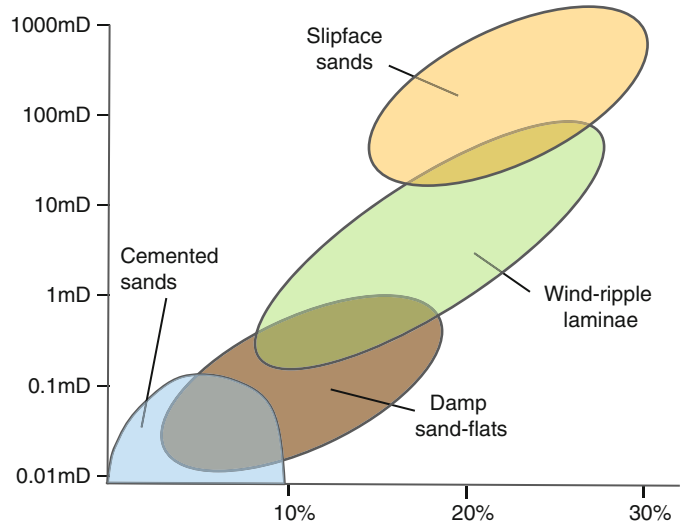

Fig. 6.2 Typical petrophysical contrasts within aeolian systems

Fig. 6.3 Dune core exposed at Clashach Cove, Moray Firth, Scotland

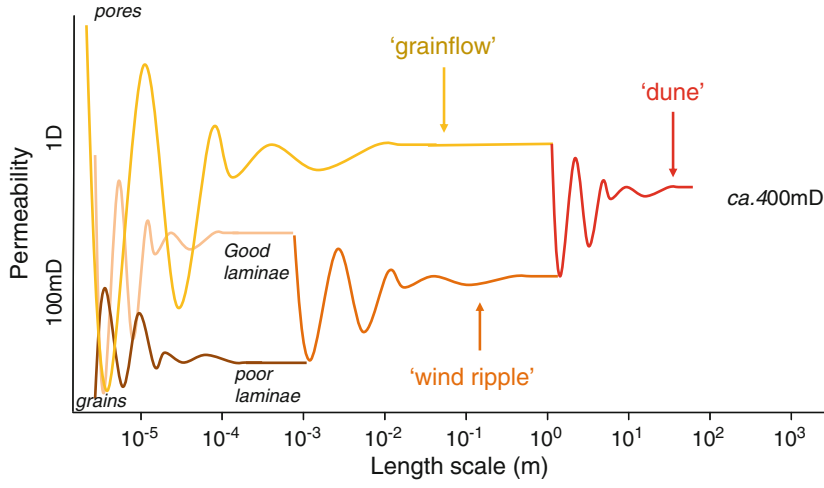

Fig. 6.4 Permeability length scales for the Clashach outcrop (Fig. 6.3)

Fig. 6.5 Components of the dune system; *top photo*: grainflow bedsets; *middle photo*: wind-ripple bedsets; *bottom photo*: permeability contrasts between wind-ripple laminae emphasised by weathering. The *red boxes* approximate REVs for each element

The REV summary in Fig. 6.4 is derived from observations such as those in Fig. 6.5, which shows the contrast between thicker grainflow beds and the fine laminations of the wind-ripple strata. The values used to build the REV plot are based on mini-permeameter data, calibrated against core data from an analogue oil-field over comparable lithologies.

The more blocky, homogeneous grainflow beds achieve an REV at a relatively fine scale, and this would be measured reasonably well by core plugs. Log data would offer a good measure of average

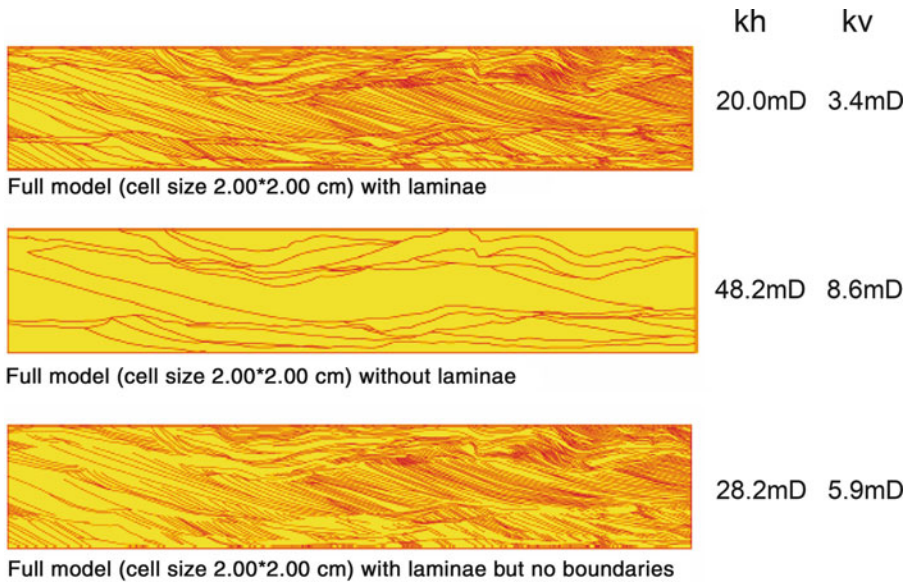

Fig. 6.6 Effective permeability in aeolian laminae. Assuming: no-flow boundaries, 3 cm wind ripple laminae (0.6 mD) and 60 mD grainflow bedsets; bounding surface 6 cm thick. (Pickup and Hern 2002) (Redrawn from Pickup and Hern 2002, reproduced with kind permission from Springer Science+Business Media B.V)

porosity on the metre-scale, which could be calibrated against core plug data, and the orderly k/ϕ relationship from core plug data (e.g. Fig. 6.2) would lead to a reasonable estimate of the effective permeability of the interval.

The wind ripple bed sets are more heterogeneous and a larger sample volume is required to derive an effective average property. At the lamina scale, permeability is highly variable. Crucially, this occurs on a scale slightly smaller than the core-plug, core plugs neither representing the permeability of the coarse-grained laminae, nor giving a representative average of good and poor laminae. Log data will measure a reasonable average porosity over both good and bad laminae, but not necessarily the same average as would be measured from core plugs. Put another way, the scale of the measurement does not coincide with the scale of the relevant REVs.

Small-scale modelling could be used to provide a better range of estimates of the effective permeability as a function of scale for wind ripple intervals.

Model-based handling of aeolian laminae is comparable to the handling of thin bed heterolithics (described in the tidal deltaic and deep-water sections), the main difference being the more predictable form of the well-organised aeolian bed sets. The effective properties of fine scale heterogeneity have, for example, been explored using small-scale models by Pickup and Hern (2002), who show how the effective permeability of an interval varies depending on the presence or absence of laminae and the baffling effect of bounding surfaces (Fig. 6.6).

The effective permeability of small-scale aeolian architecture can therefore usually be quantified, and the main question for reservoir modelling is how the REVs are architecturally organised on a larger scale. This is less predictable and two principal issues recur when modelling aeolian architecture:

1. How do the aeolian elements stack on a well-spacing scale, and
2. Does the resulting pattern impart a large-scale effective anisotropy on a producing reservoir?

6.1.3 Stacking

Strongly contrasting dune architectures are reported for linear, barchan and star dunes, with stacking patterns governed by the hierarchical arrangement of bounding surfaces (e.g. Fig. 6.7).

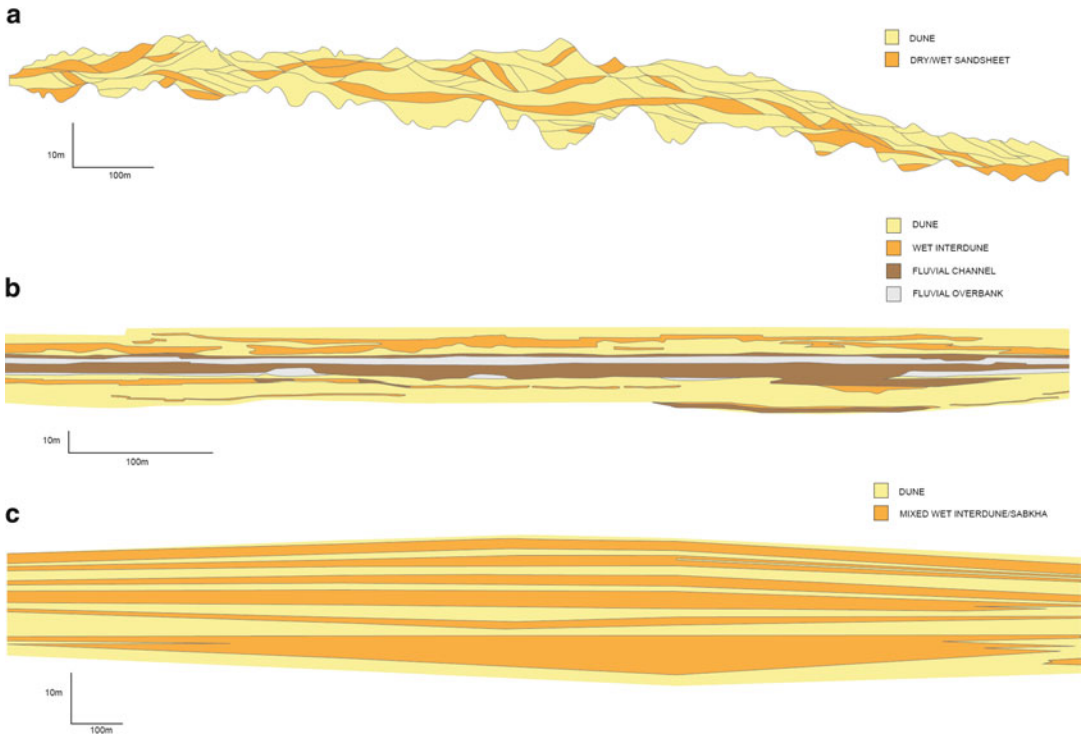

Fig. 6.7 Contrasting dune architectures: (**a**) dry aeolian systems; (**b**) fluvial-aeolian system; (**c**) sabkha aeolian sytems (Image courtesy C.Y. Hern 2000)

The hierarchical packaging of dune systems by bounding surfaces has been well described (e.g. Hunter 1977; Kocurek 1981; Fryberger 1990b) and the potential impact of their arrangement on reservoir sweep efficiency investigated (e.g. by Ciftci et al. 2004). In the Ciftci et al. study, aeolian bounding surfaces were seen to act as barriers to flow, based on observations of the Tensleep Sandstone in Wyoming, whereas in the Scottish outcrop example shown in Fig. 6.5 the bounding surfaces are clearly open to flow. Either scenario is possible.

Assuming the permeability of the bounding surfaces can be determined, the central questions for forecasting reservoir flow patterns (sweep efficiency) are:

- which reservoir element is the connecting medium, and
- what is the scale of the element distribution relative to the well spacing (for a given production mechanism, e.g. water injection)?

If high permeability slip-face sands are embedded in poorer quality sands on a scale significantly below that of the well spacing, the permeability of the overall system is dominated by the poorer quality unit (Fig. 6.8). In this case it can be argued that explicit modelling of the 'detail' is not necessary because irregularities in the sweep pattern disperse over the inter-well volume and the permeability of the reservoir system will start to approximate a predictable average.

However, if the slip-face sands connect, or congregate preferentially in specific units, the heterogeneity needs to be explicitly captured.

6.1.4 Aeolian System Anisotropy

For aeolian systems the key is therefore to identify the dune types and internal stacking patterns. A strong overprint on aeolian architecture is commonly the effect of changing base levels (the 'stokes surfaces' of Stokes 1968) or climatic

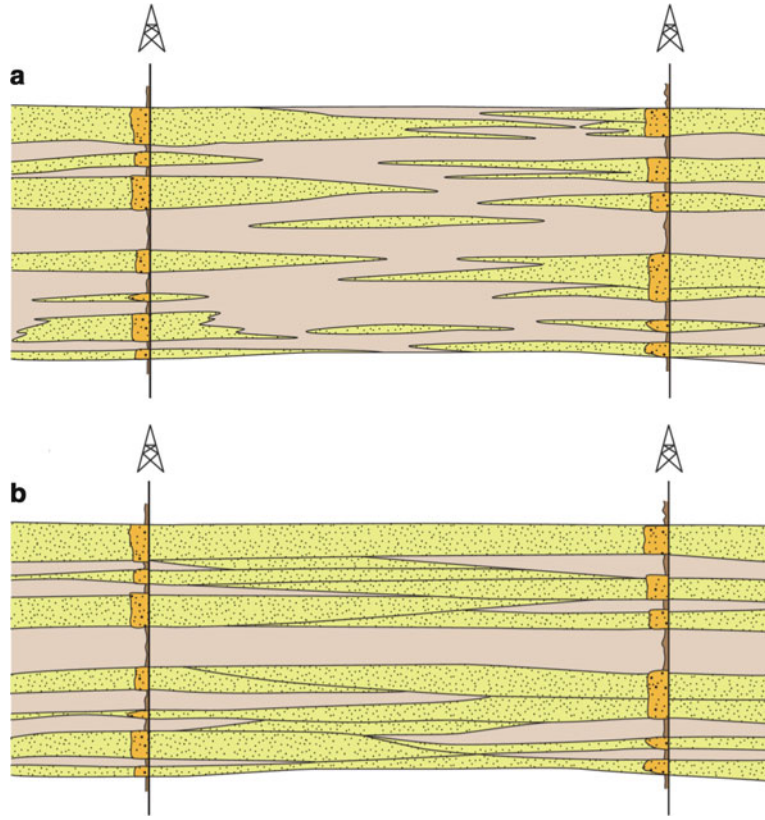

Fig. 6.8 Finding the connecting medium: comparing the length scale of the heterogeneity with the length scale of the development question (in this case, the well spacing). In (**a**) the connecting medium is the poor quality element, whereas in (**b**) the good quality elements are connecting

fluctuations, as exemplified by the work of Meadows on Triassic reservoirs of the Irish Sea (e.g. Meadows and Beach 1993). As these trends are operating on a regional (basin) scale, high degrees of correlation within-field can occur. Productivity is driven by inter-well connectivity along correlatable dry-dune belts, such as that shown in Fig. 6.7 (lower image).

On a regional scale, even without base level changes, effective permeability anisotropy occurs if the dune systems are themselves strongly anisotropic (Krystinik 1990), with effective permeabilities parallel and perpendicular to dune ridges varying by up to an order of magnitude. Well spacing and preferred sweep directions are influenced by such anisotropy, which places value on the interpretation of dune type, and this can be imparted on reservoir models using variograms (for pixel-based workflows) or the superimposition of trends (discussed in Chap. 2).

6.1.5 Laminae-Scale Effects

A final important issue for aeolian systems, characterised by the widespread presence of fine-scale laminated lithologies, is whether these laminated elements in the reservoir system promote capillary trapping effects. That is, are the multiphase flow effects of strongly contrasting laminations important and adequately represented in the reservoir model?

This has been studied by Huang et al. (1995) who showed the impact of capillary forces on both the initial hydrocarbon distribution and the waterflood oil recovery. The low-permeability laminae cause a trapping effect due to locally high water saturations during water-oil displacement (see Chap. 4). The impact of small-scale heterogeneity on multiphase flow also depends on wettability (Huang et al. 1996), and wettability appears to vary – in this case more oil-wet in the poorer-permeability laminae and more

water-wet in the higher permeability laminae. Capillary trapping will generally be a more important issue to consider in more water-wet systems.

If determined to be important, the rock unit associated with capillary trapping (e.g. in grainfall or wind ripple strata) needs to be defined and included as a discrete modelling element. The impact of that element can then either be modelled explicitly as a 3D object or captured as part of an REV in small-scale models used to determine effective properties (notably effective relative permeabilities) for a larger scale model.

6.2 Fluvial Reservoirs

6.2.1 Fluvial Systems

Fluvial reservoirs were one of the first reservoir types to receive the attention of object-based (Boolean) geological modelling efforts (e.g. Haldorsen and MacDonald 1987; King 1990; Holden et al. 1998; Larue and Hovadik 2006). Finding the location of sand-rich channel objects within a more or less muddy background is a key issue, which lends itself to some form of probabilistic modelling, and establishing the degree of connectivity between channels is the ultimate factor which determines hydrocarbon recovery. However, the proportion of channel sands and the internal character of the channels vary enormously.

Fluvial reservoirs fall into two broad groups: braided and meandering. Braided channels are formed in wide braid-plain systems (Fig. 6.9) with high sediment flux, whereas meandering channels form in more mature channel systems with overall lower sediment discharge. Braided systems tend to have a higher density of channels, which have lower sinuosity, whereas meandering systems tend to have a lower density of channels, with higher individual channel sinuosity.

Individual channels are typically grouped to form multi-channel complexes, and when we look at any individual channel we find it usually contains hierarchically-organised components – channel fill, barforms (Fig. 6.9), point bars, lateral accretion surfaces, over-bank deposits, etc.

Fluvial sandbody architecture is covered in detail elsewhere, notably by Miall (1985, 1988), and many resources have been devoted to understanding fluvial sandbody architecture in outcrop (e.g. Dreyer et al. 1993) as illustrated in Fig. 6.10.

6.2.2 Geometry

The key questions to ask when modelling fluvial reservoirs are typically geometric:

1. What is the fluvial system – braided or meandering – or something in between?
2. What is the channel density – channels proportion well over 50 % or much less?
3. What is the channel sinuosity?
4. What are the typical channel dimensions?
5. Should we be focussing on individual channels or multi-channel complexes?
6. What is the internal channel architecture? Is it essentially sand rich – and therefore effectively homogeneous, or is it composed of many variable elements including muddy, silty and sandy sub-elements?

Figure 6.11 shows examples of high-resolution models of meandering channel systems, illustrating typical model elements. In one example (Fig. 6.11, left), the focus is on channel stacking patterns and internal channel fill. The overbank crevasse-splay sands (green) have been represented as simple ellipsoids, whereas the sinuous channels have been modelled in more detail with layers of sand (yellow) and silt (purple) in the channel fill, and lateral accretion surfaces (red), all within a muddy background (blue). Alternatively (Fig. 6.11, right), less effort may given to the internal channel architecture and more attention paid to capturing the channel types, intersections and connectivity.

Whatever the choice of approach, the key issue is not to attempt to model all lithofacies but to

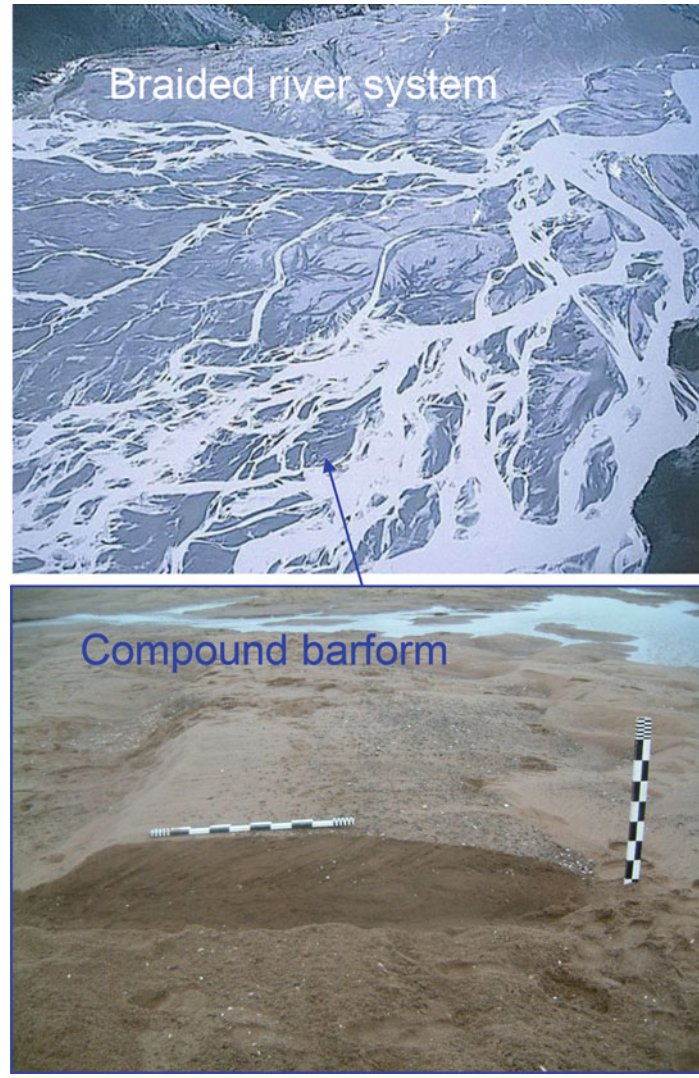

Fig. 6.9 A modern braided fluvial system, with inset showing a compound barform (Photo A. Martinius/Statoil © Statoil ASA, reproduced with permission)

define the appropriate *modelling elements*. Typical modelling elements for a fluvial system are:

- one or two channel elements, e.g. coarse-grained channel lag deposits and the main (typically finer) active channel fill,
- discrete barforms within the channel complexes,
- overbank deposits giving thin lateral communication paths within the non-reservoir background, and
- mudstone-dominated background facies (the floodplain).

6.2.3 Connectivity and Percolation Theory

Understanding sandstone connectivity in fluvial reservoirs is nearly always a dominant issue, and is best understood in terms of *percolation theory*, which describes the statistics of connectivity. In the context of sandstone connectivity, the essential problem is whether we can say a sandstone observed in one well will connect with a sandstone observed in another well (Fig. 6.12).

Fig. 6.10 The Escanilla Formation (Pyrenees, Spain) – a fluvial channel analogue illustrating large-scale stacked channel architecture (Photo, Statoil image archive, © Statoil ASA, reproduced with permission)

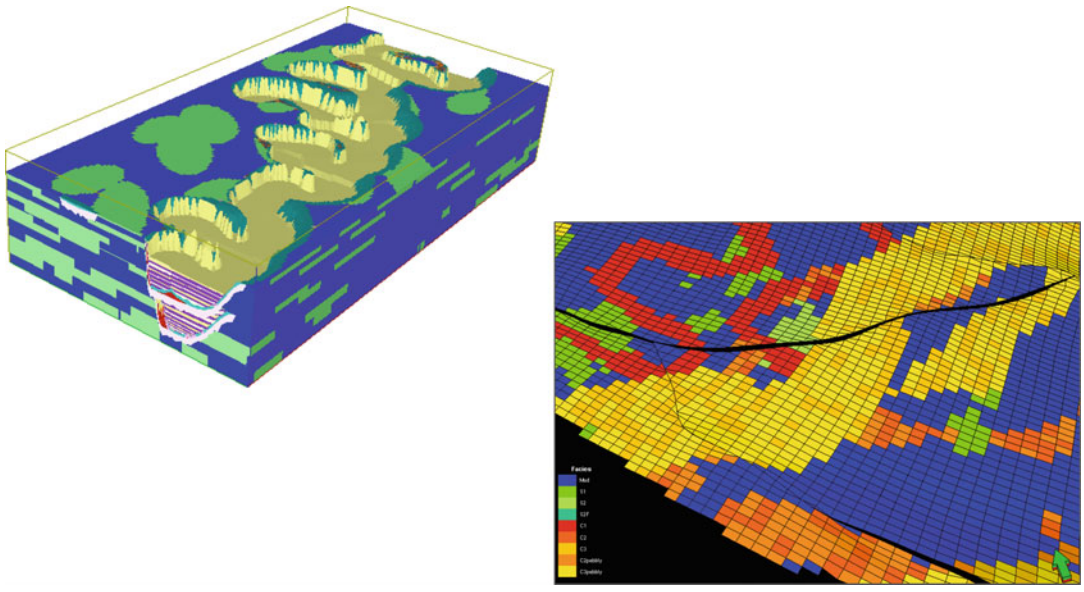

Fig. 6.11 Example models of fluvial systems. *Left*: stacked meandering channel systems with heterogeneous fill (model area approximately 1km × 2 km); *right*: model of mutually erosive channels (*yellow*, *red*) and crevasse splays (*green*) – channels approximately 200–1,000 m wide (*Left image*, R. Wen/Geomodelling Corp., reproduced with permission)

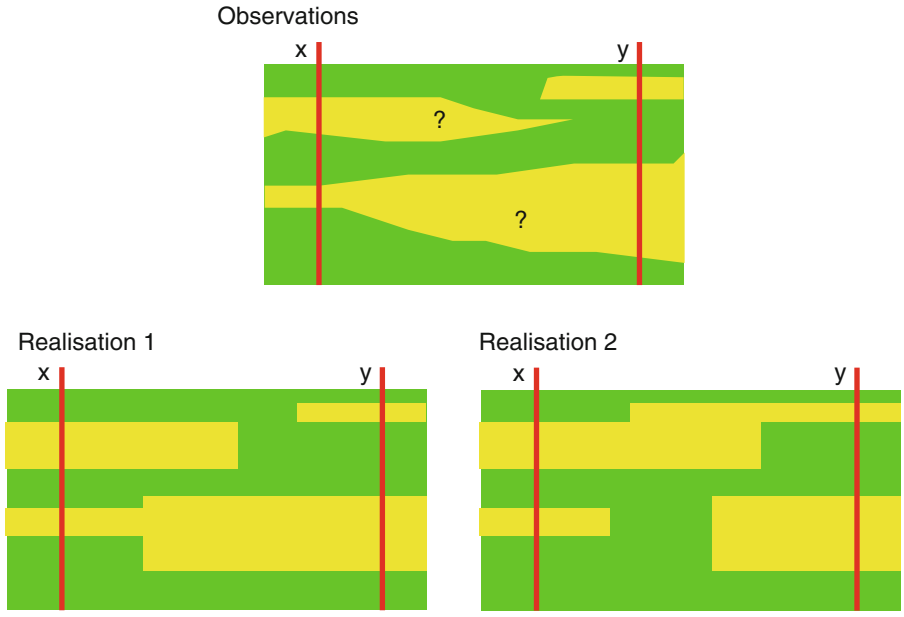

Fig. 6.12 Simple illustration of the sand connectivity problem

Percolation theory, widely used in many branches of applied physics, describes connectivity in a statistical network using probability theory. To summarise the concept, it has been found that by adding conducting elements randomly in a non-conductive network or lattice, connectivity occurs (statistically) when a predictable number of nodes or sites are filled. This point is the percolation threshold, p_c. The value for p_c depends on the dimensions and geometry of the system being considered. The theory is applied to a wide range of physical phenomena (de Gennes 1976) and has been widely applied in subsurface flow studies (e.g. Stauffer and Ahorony 1994). King (1990) showed how the theory can be applied to overlapping sand bodies in reservoir characterisation studies and Table 6.1 shows some example percolation thresholds.

When the theory is applied to permeability (e.g. Deutsch 1989; King 1990; Renard and de Marsily 1997) we find that the effective permeability, k_{eff}, in such a system follows a power law defined by p_c:

$$\begin{aligned} &\text{For } p < p_c \quad k_{eff} = 0 \\ &\text{For } p > p_c \quad k_{eff} = A(p - p_c)^e \end{aligned}$$

where A and e are characteristic constants.

Table 6.1 Some example percolation thresholds

System	Percolation threshold	References
Square Lattice (bond percolation)	0.5000	Stauffer and Ahorony (1994)
Simple cubic lattice (site percolation)	0.3116	Stauffer and Ahorony (1994)
Simple cubic lattice (bond percolation)	0.2488	Stauffer and Ahorony (1994)
Overlapping sandstone objects (rectangles in 2D)	~0.667	King (1990)
Overlapping sandstone objects (boxes in 3D)	~0.25	King (1990)
Multiple stochastic models of intersecting sinuous channels	~0.2 to ~0.6	Larue and Hovadik (2006)

The simple case of 2D overlapping sand bodies is illustrated in Fig. 6.13 (based on results from King 1990). For more realistic systems, the problem is how the constants are to be estimated. However, all object-based geological reservoir models will tend to exhibit characteristics related to percolation phenomena, and it is useful to establish the expected

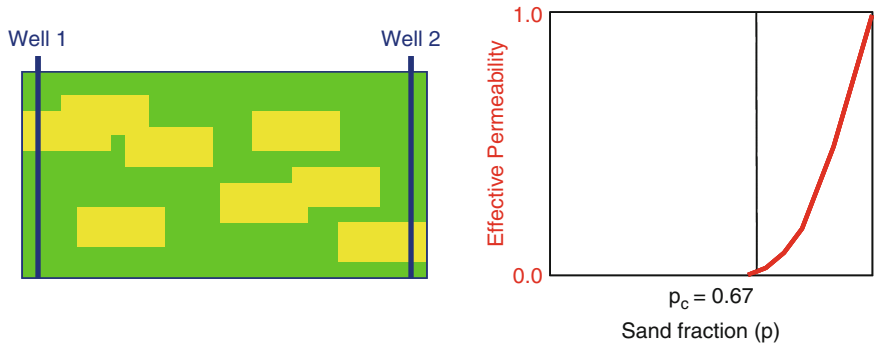

Fig. 6.13 Illustration of the sand connectivity and effective permeability using percolation theory

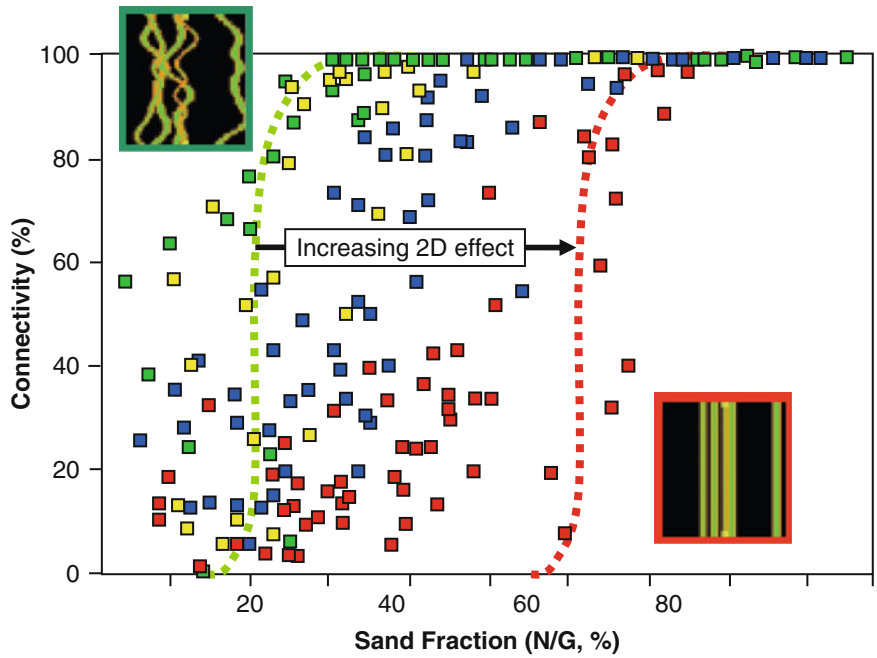

Fig. 6.14 Connectivity as a function of channel sandstone fraction (N/G), for a wide range of stochastic 3D channel models (Redrawn from Larue and Hovadik 2006). Sinuous channels (*green*) show characteristic 3D percolation behaviour, while straighter channels (*red*) show more 2D percolation behaviour. *Yellow* and *blue* points have intermediate sinuosity (Redrawn from Larue and Hovadik 2006, Petroleum Geoscience, v. 12 © Geological Society of London [2006])

connectivity behaviour of the system at hand. A simple reference point is that a reservoir with sand volume fraction of around 0.25 would be expected to be close to the percolation threshold (in 3D) and therefore have connectivity strongly dependent on the sand volume fraction and geometrical assumptions.

Larue and Hovadik (2006) completed a very comprehensive analysis of connectivity in models of channelized fluvial reservoirs (Fig. 6.14). They showed that actual connectivity (measured in terms of percolation exponents) varies enormously, depending on the details of the channel system, especially the sinuosity. In general, for 3D models, the rapid fall in connectivity occurs at around 20 % sand fraction – a little lower than the theoretical value of 25 % due to sinuosity and overlap of sandstone objects.

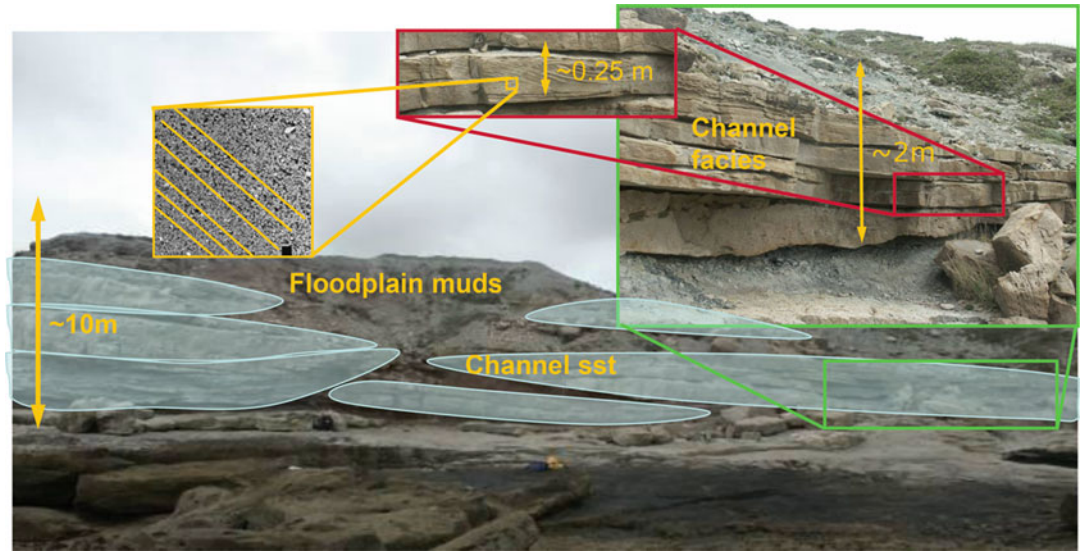

Fig. 6.15 Hierarchy of sedimentary structures in fluvial channel system (Lourinha Formation, Portugal) (Photo K. Nordahl/Statoil © Statoil ASA, reproduced with permission)

However, as the sinuosity and dispersion in channel orientation reduces, 3D channel systems begin to behave like 2D systems, with the rapid change in connectivity occurring at around 60 % sand fraction – close to the theoretical value of 66.7 %.

This wide range in reservoir connectivity for fluvial channel models highlights the need for careful model design based on good characterisation of the fluvial depositional system at hand. There is no point in making an attractive-looking fluvial reservoir model if it 'misses the target' with regard to the likely sandstone connectivity.

6.2.4 Hierarchy

Figure 6.15 illustrates the multi-scale nature of fluvial channels – the 'channel' is composed of several sandstones bodies, and each sandstone has variable lithofacies types (typically trough cross-bedded and ripple-laminated sandstones). Although challenging, these multiple scales lend themselves well to a multi-scale modelling approach – the detail within each channel cannot practically be modelled field-wide, but the effective permeability of a generic channel – the 'channel REV' – can be quantified through small-scale modelling (Chap. 4) and fed into a larger-scale model, field-scale if necessary. Keogh et al. (2007) give a good review of the use of probabilistic geological modelling methods for building geologically-realistic multi-scale models of fluvial reservoirs.

6.3 Tidal Deltaic Sandstone Reservoirs

6.3.1 Tidal Characteristics

Tidal deltaic reservoir systems have earned a special focus in reservoir studies, because although they represent only one class of deltaic systems they present special challenges. Delta systems can be fluvial-, wave- or tidal-dominated. In terms of reservoir modelling fluvial-dominated or wave-dominated delta systems could generally be handled using similar modelling approaches to those used for fluvial and shallow marine settings (discussed elsewhere in this chapter). However, the influence of tidal processes tends to result in highly heterolithic

Fig. 6.16 Example tidal heterolithic facies from core – in this case an inter-tidal wavy-bedded unit showing flow ripples and some bioturbation (Photo A. Martinius/Statoil © Statoil ASA, reproduced with permission)

reservoirs and these are now appreciated as being a widespread and important class of petroleum reservoir (e.g. offshore Norway, Alaska, Canada, Venezuela and Russia).

They form in estuarine settings (Dalrymple et al. 1992) where tidal influences tend to dominate the depositional system (Dalrymple and Rhodes 1995). They have highly complex architectures and stacking patterns, with bars, channels and inter-tidal muddy deposits intermixed and difficult to correlate laterally. The oscillatory nature of tide-dominated currents results in mixed sandstone/mudstone lithofacies, conveniently referred to as 'heterolithics'. Heterolithics are defined as sedimentary packages with a strongly bimodal grain-size distribution, typified by moderate to high frequency alternation of sandstone layers with siltstone/clay layers in which layer thicknesses are commonly at the centimetre to decimetre scale (Martinius et al. 2001, 2005).

Heterolithic tidal sandstones represent particularly challenging reservoir systems because they display:

- generally marginal reservoir quality,
- highly variable net-to-gross ratios,
- highly anisotropic reservoir properties,
- fine-scale heterogeneities which are not easily handled with conventional reservoir modelling tools.

Recovery factors in heterolithics are typically low, in the range 15–40 %.

6.3.2 Handling Heterolithics

Typically, the first inspection of heterolithic sandstones facies (e.g. Fig. 6.16) leads to the response "so where is the reservoir?" Often, the sandstone is so intermixed with the mudstone/siltstone facies that identification of good and

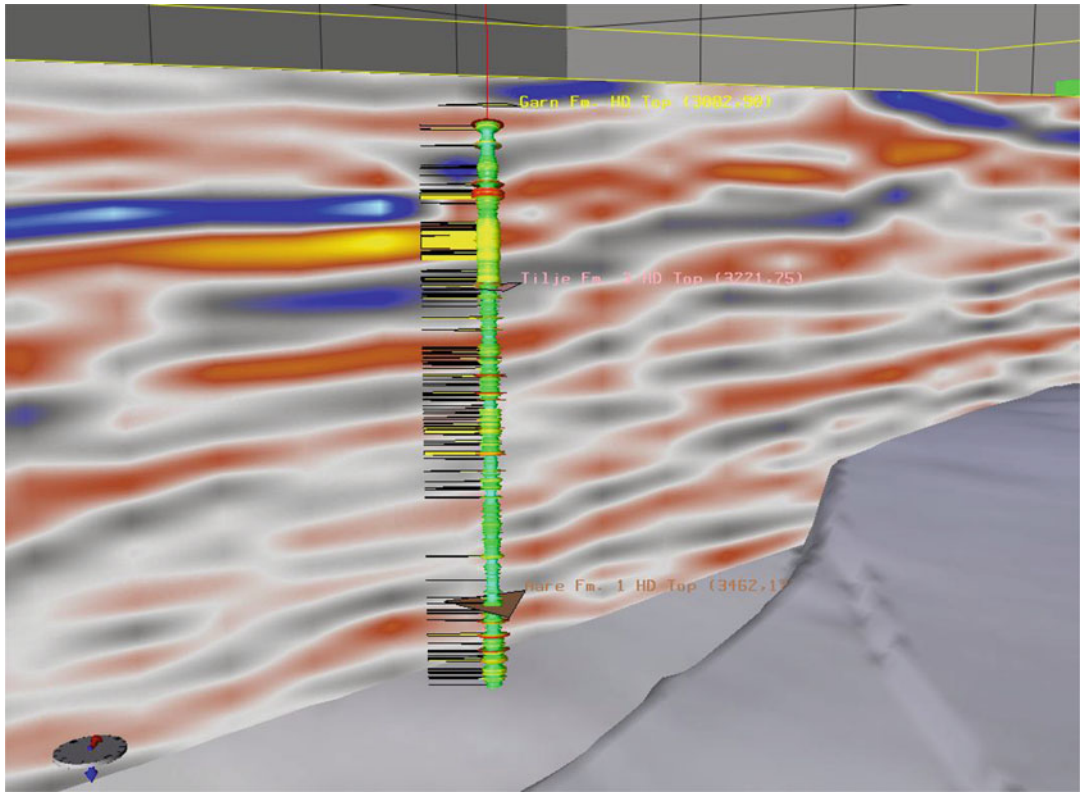

Fig. 6.17 Tidal deltaic sand log shown alongside the corresponding seismic section, where only the thickest sands are evident on seismic

bad reservoir facies becomes quite a challenge. Furthermore, the integration of thin-bedded well logs with seismic data in such units is simply difficult (Fig. 6.17).

In reservoir modelling, it is conventional to model the reservoir (the foreground facies) and to neglect the non-reservoir (the background facies), but in heterolithic, tide-dominated reservoir systems, there is often a gradation between reservoir and non-reservoir. In tidal deltaic systems, it is therefore essential to represent both background and foreground facies explicitly (e.g. Brandsæter et al. 2001a, b, 2005).

It was in this context that many of the concepts for total property modelling (*cf*. Fig. 3.33) and multi-scale modelling (*cf*. Fig. 4.1) were developed, and when working these fields it is quickly evident that multi-scale modelling is not optional for tidal-delta systems – it is essential.

Some form of effective flow property has to be estimated for the heterolithics, because neither core data, well logs or seismic give direct indicators of the presence of sandstone or high quality reservoir zones. There are many possible approaches to multi-scale modelling in such systems, but as a guide, Fig. 6.18 illustrates the workflow for upscaling heterolithic tidal deltaic reservoir systems, developed by Nordahl et al. (2005) and Ringrose et al. (2005). Core data is interpreted, ideally with the aid of near-wellbore models to allow rescaling of core and wireline logs to the lithofacies REV. Rock property models (at the lithofacies REV) are then used to estimate flow functions. These could be permeability as a function of mud/sand ratio [e.g. $k_v = f(V_m)$] as shown in Fig. 6.18, or any other useful function such as acoustic properties as a function of porosity or water saturation as a function of k_h. Upscaled flow functions are then applied to

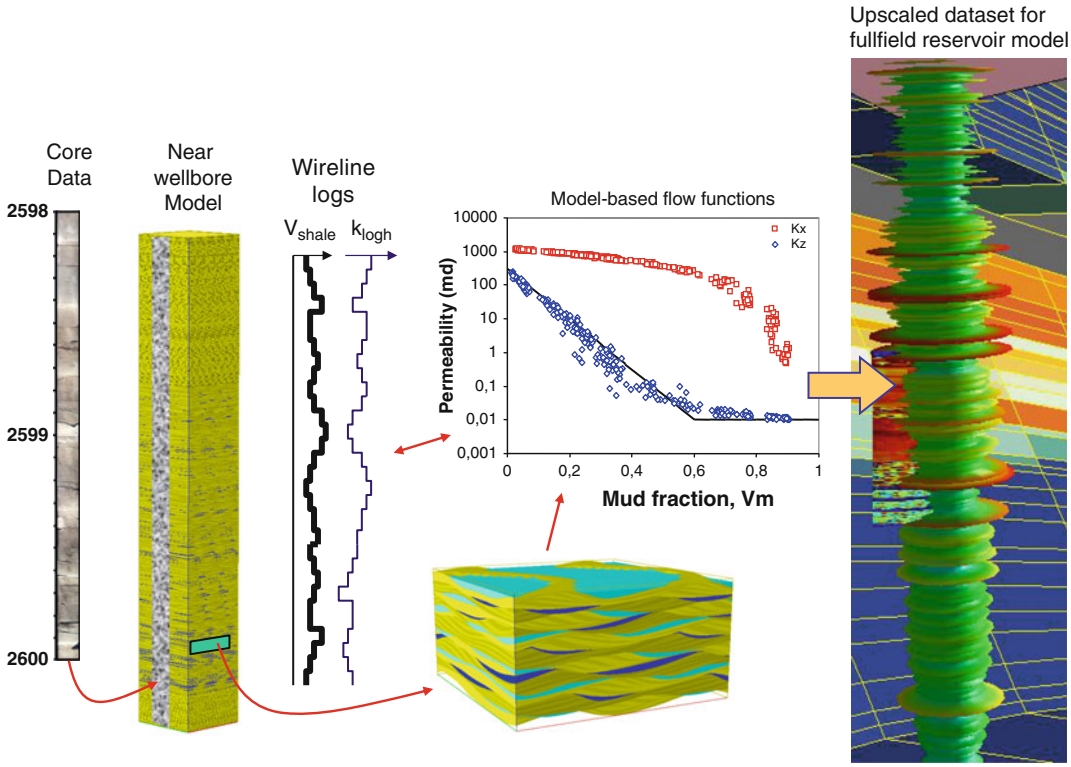

Fig. 6.18 Workflow for upscaling heterolithic tidal deltaic reservoir systems

the reservoir scale directly, or as part of further upscaling steps at the geological architecture scale.

The extra effort involved in multi-scale modelling of tidal deltaic systems clearly pays off in terms of the value gained by achieving realistic oil recovery factors from these relatively low quality reservoirs (Elfenbein et al. 2005). Good modelling can lead to significant commercial benefit.

6.4 Shallow Marine Sandstone Reservoirs

6.4.1 Tanks of Sand?

Shallow marine sandstones are among the most prolific class of reservoirs in terms of volumes of oil produced and are characterised by especially good recovery factors – up to 70 % or even 80 % (Tyler and Finlay 1991). They account for a large portion of the Jurassic North Sea reservoirs and the majority of onshore US oilfields. They might well be regarded as an 'easy kind' of reservoir in terms of oilfield development and are indeed one of the few reservoir types to occasionally behave like 'tanks of sand' – the reservoir engineer's dream. However, shallow marine (paralic) reservoir systems are in fact very varied and can contain important heterogeneities at the sub-log scale.

Under the shallow marine group we include fluvial- and wave-dominated deltaic systems which characteristically build out into true shallow marine shoreface and offshore transition zones. The principal depositional settings involved are:

- delta plain and delta front,
- upper shoreface (usually storm and wave dominated),
- middle and lower shoreface (mainly below the fair-weather storm wave base),
- offshore and offshore transition zone (mud-dominated or heterolithic).

For a fuller discussion of the sedimentology and stratigraphy of these systems refer to the literature, including Van Wagoner et al. (1990), Van Wagoner (1995), Reading (1996), and Howell et al. (2008).

Alongside a fairly wide range of depositional processes, including waves and storms, fluvial delta dynamics, and re-adjustments to base level change, shallow marine systems are characterised by active benthic fauna, 'worms and critters', which churn up and digest significant quantities of the sandstone deposits. The trace fossils from these creatures (the ichnofacies) provide an important stratigraphic correlation tool, and give vital clues about the depositional setting (e.g. Bromley 1996; McIlroy 2004). They can also modify the rock properties.

6.4.2 Stacking and Laminations

Many reservoir characterisation and modelling studies of these systems have been published, (e.g. Weber 1986; Weber and van Geuns 1990; Corbett et al. 1992; Kjønsvik et al. 1994; Jacobsen et al. 2000, and Howell et al. 2008). The last of these was part of a very comprehensive analysis of the geological factors which most affect oil production in faulted shallow marine reservoir systems (Manzocchi et al. 2008a, b). They concluded the most important factors were:

1. The large-scale sedimentary stacking architecture (determined by the aggradation angle and progradation direction), and
2. The small-scale effects of lamination on two-phase flow (determined by the shape of the capillary pressure function).

That is, both the large-scale architecture and the small-scale laminations are important in these systems (as also concluded by Kjønsvik et al. 1994).

In wave-dominated shallow-marine settings, fine scale laminations are common in the form of swaley or hummocky cross-stratified lithofacies (Fig. 6.19). These represent bedforms produced as the result of either wave-related oscillatory currents at the seabed or unidirectional currents (Allen and Underhill 1989) and are visible in core as bedsets with low-angle intersections (typically <5°). The laminations are sub-log scale and may be poorly sampled at the core-plug scale too, but make a significant contribution to flow heterogeneity. Such heterogeneity lends itself well to effective property modelling using small-scale models (such as that shown in Fig. 6.19).

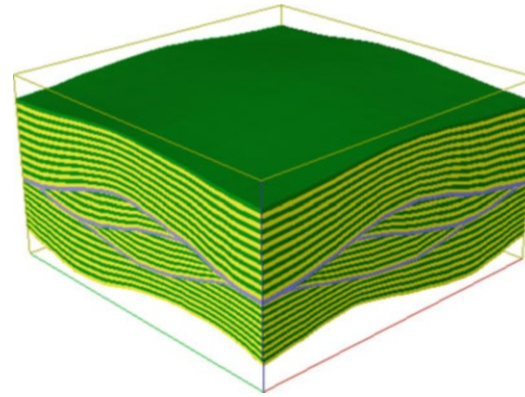

Fig. 6.19 Example model of hummocky cross stratification (HCS) from a shallow marine shoreface system (model is 2.5 × 2.5 × 0.5 m)

6.4.3 Large-Scale Impact of Small-Scale Heterogeneities

To illustrate the dynamic interplay of geological factors with flow processes in shallow marine reservoirs, we use the case study presented by Ciammetti et al. (1995). They used a detailed outcrop model of a shallow marine parasequence (1,370 m long and 45 m high) to study the effects of geological architecture on a simulated waterflood (Fig. 6.20).

Of the many cases run, the three cases shown in Fig. 6.21 illustrate the main effects. Water override generally occurs due to the coarsening-up (permeability increasing upwards) nature of the prograding shallow-marine parasequence. This is generally positive, as it is in opposition to gravity which drives the water downwards, thus giving a balance between gravity slumping and viscous override of the water front.

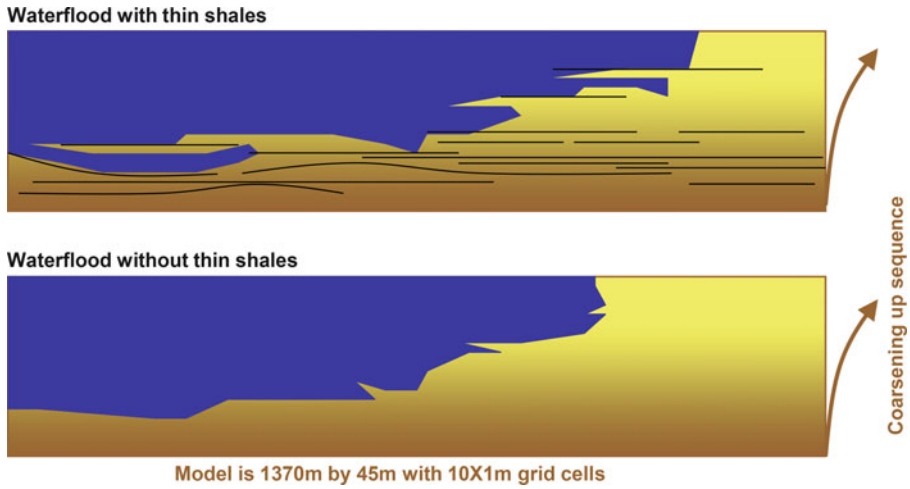

Fig. 6.20 Detailed flow modelling of a shallow marine parasequence – Grassy member, Blackhawk Formation, Book Cliffs, Utah. Images show waterflood flow front (*blue*) prior to breakthrough at a producing well on the right (Redrawn from Ciammetti et al. 1995, ©1994, Society of Petroleum Engineers Inc., reproduced with permission of SPE. Further reproduction prohibited without permission)

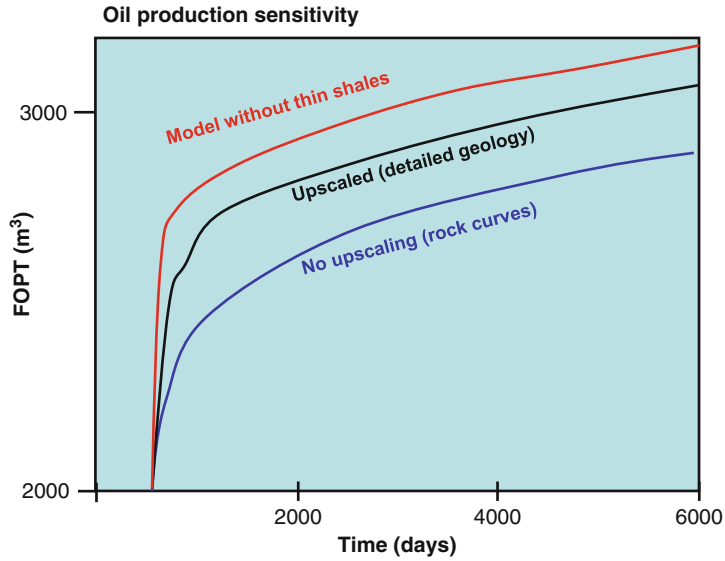

Fig. 6.21 Oil production profiles for three cases from the shallow marine outcrop simulations (Redrawn from Ciammetti et al. 1995); *FOPT* field oil production total (Redrawn from Ciammetti et al. 1995, ©1994, Society of Petroleum Engineers Inc., reproduced with permission of SPE. Further reproduction prohibited without permission)

Geologically-based upscaling captures this effect better than simple averaging and the application of rock curves. However, failure to include the effects of thin shales in the model, easy to overlook in log analysis, gives a reduced water override, and leads to an over-optimistic estimate of oil recovery.

All these models included the effects of capillary-dominated two-phase flow at the lamina scale (via upscaling). Omission of small-scale lamina architecture leads to difference in oil recovery of at least 5 % (less recovery if small-scale effects are neglected), as shown by the oil production curves (Fig. 6.21). It is quite intriguing that for this shallow-marine case study, both the small-scale lamination and the coarsening-up permeability profile give a positive effect on recovery. In part, this explains why

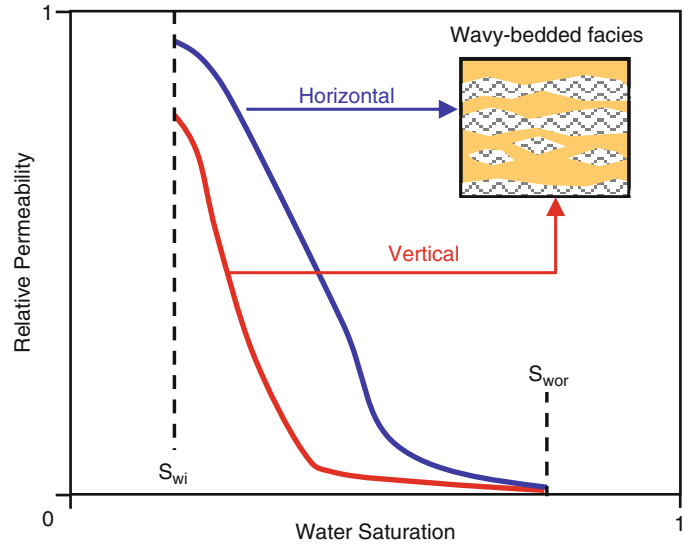

Fig. 6.22 Anisotropic relative oil permeability for an example shallow marine facies (wavy-bedded facies, Rannoch Formation, Ringrose and Corbett 1994) (Redrawn from Ringrose and Corbett 1994, The Geological Society, London, Special Publications, No. 78 © Geological Society of London [1994])

shallow marine reservoirs have such good overall recovery factors. Thin shales, however, have a negative impact.

The small-scale (microscopic) effects of capillary forces in causing strong directional anisotropy on two-phase immiscible flow processes (Fig. 6.22) are surprising to many, although the effect has been clearly documented using modelling (Corbett et al. 1992; Ringrose et al. 1993), laboratory analysis (Huang et al. 1995) and full-field history matching (Rustad et al. 2008).

Reluctance to acknowledge the importance of small-scale heterogeneities may also be due to the fact that the effect operates at a scale much smaller than most models can resolve, and so must be incorporated implicitly – using upscaled relative permeability functions. Here, the fluid system itself plays a determining role – the geological factors discussed above are for water displacing oil, an immiscible flow process. Gas displacing oil – generally a miscible flow process – tends to be most influenced by the large-scale permeability architecture. Strong gas over-ride should be expected, driven by both gravity and viscous forces working in concert, leading to a gas thief zone at the top of any progradational shallow marine unit, in contrast to the waterflood shown in Fig. 6.20.

The same parasequence model was used by Carruthers (1998) to simulate oil migration into a detailed model of a rock formation. Oil was introduced at the base and allowed to invade the rock model, using a capillary-dominated invasion-percolation technique (Carruthers and Ringrose 1998). The result (Fig. 6.23) illustrates how a capillary-dominated drainage flow process picks out critical flow pathways, filling individual sand layers as local accumulations. If oil migration is allowed to continue out of the model then little more than a few percent of the rock volume is contacted by oil. However, imposition of a structural closure on the model would result in the unit back-filling to create an oil reservoir.

In summary, shallow marine reservoir systems generally provide us with a 'dream ticket' for oil recovery. This is due partly to geology – shallow marine systems are generally laterally-continuous, sand-rich and well-sorted – but also due to the positive interaction between flow processes and geology. Two-phase flow effects at the lamina-scale and the coarsening up profile both have a positive effect on lateral water injection strategies; the geology assists the reservoir engineer. However, the small scale factors are important and need to be included in any modelling exercise.

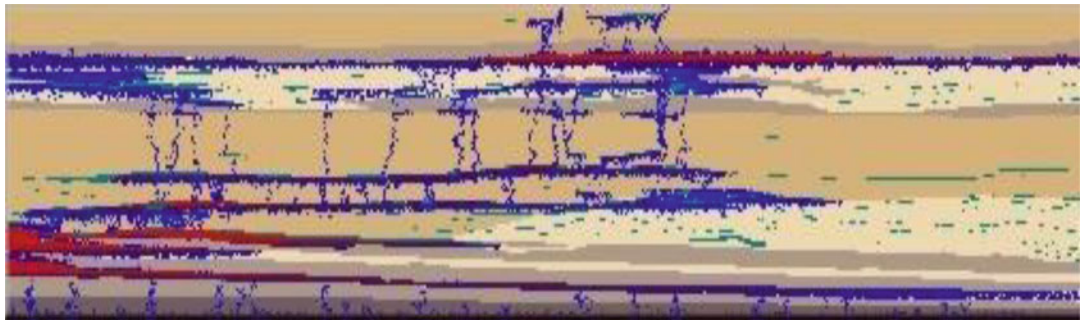

Fig. 6.23 Simulation of oil migration into shallow marine rock unit (Carruthers 1998) (Redrawn from Carruthers 1998 (Courtesy of D. Carruthers))

Other flow processes, such as gas injection, would not benefit in the same way from the geology so care is needed to ensure a rock model design that fits the flow process at hand. For a gas injection scheme, the most important geological feature is likely to be the location and continuity of the parasequence tops.

6.5 Deep Marine Sandstone Reservoirs

Deep marine systems are dominated by processes associated with density flows: gravity-driven currents moving sediments in suspension or by traction and depositing them along continental margins. Deep-water systems include but are not synonymous with 'turbidites' (Kneller 1995).

Emphasis in deep marine reservoirs has been placed firmly on depositional geometries and reservoir frameworks which are commonly determined from seismic, in some cases of spectacular quality. In reservoir modelling, the strength has been the ability to integrate seismic attributes into conditioned reservoir models; the weakness has been in the underestimation of small-scale heterogeneities and in not seeing what lies below seismic resolution.

The tendency to miss significant reservoir features has been encouraged by the observation that seismic data and reservoir simulation work at similar resolutions. It is therefore tempting to avoid sub-seismic architecture and work directly from 'seismic-to-simulation'. This can work, but requires the seismic to be fortuitously resolved at the REV scale pertinent to the model purpose. This can be the case for gas reservoirs but, recalling Flora's guiding rule (Chap. 2), this is unlikely to be the general case for oil reservoirs.

Sub-seismic architectural understanding is usually required, and from reference to a compendium of architectures (e.g. Nilson et al. 2008) it is immediately apparent that there are a considerable range of possibilities. The question to ask is: "What's inside the seismic loop?", and for model-related issues a consideration of *confinement* is a good place to start.

6.5.1 Confinement

Confinement describes the extent to which a submarine gravity flow 'feels' physically constrained by surrounding topography. Is the flow being funnelled through a narrow canyon ('confined') or is it depleting on to the floor of a large open basin ('unconfined')? Confinement is important as a concept because it is the primary underlying factor guiding the permeability architecture we are attempting to capture in reservoir modelling and simulation.

In confined systems, new density flows tend to erode into deposits of earlier flows and hence sands from different flows tend to amalgamate (Fig. 6.24). The erosional elements of the new flow are typically sand-rich and the fill within the erosional scour will also tend to be sand-rich, whether deposited by the initial confined flow

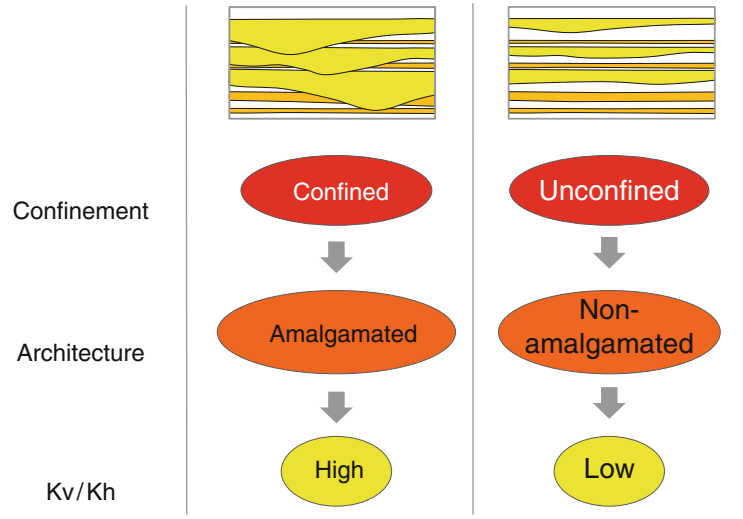

Fig. 6.24 Summary of the effect of confinement on deep-water reservoir architecture

or subsequent flows through the same conduit. The amalgamation of sand-rich units results in permeability architectures with favourable k_v/k_h ratios.

In unconfined systems, flows are more depletive, less erosive and prone to the generation of a more layer-cake architecture (Fig. 6.24). Sand amalgamation is limited and the finer-grained, lower-permeability units separating the sands tend to remain continuous. The resulting k_v/k_h ratio is low.

The degree of confinement and the resulting amalgamation ratio therefore link directly to permeability architecture (Stephen et al. 2001) and an understanding of the reservoir in terms of confinement is an essential aspect of the conceptual sketch which we have argued underpins any good modelling exercise (Chap. 2).

Figure 6.25 illustrates the degree of confinement in terms of two controlling factors: the size of the gravity flow depositing the sediment and the size of the container it flows in to. Similar geometries may result from large flows entering a large basin as those from small flows entering a smaller space (e.g. Stanbrook and Clark 2004). Confinement is thus a *relative* issue, and a series of flows making up one gross reservoir interval may be a combination of confined and unconfined components. Variations in confinement, via changes in amalgamation ratio, lead to variations in permeability architecture, k_v/k_h ratio and recovery efficiency.

6.5.2 Seismic Limits

Once a reservoir prospect has been identified from seismic attributes and proven by drilling, the reservoir often becomes clearly 'visible on seismic' leading to three common tendencies in reservoir modelling:

1. To limit the field description to the observed seismic attributes,
2. To treat the reservoir as largely connected within-attribute, and
3. If high N/G sands are encountered initially, to assume the field is relatively tank-like within the seismically-constrained envelope.

These simplifying tendencies may occasionally work (the rare 'sand tank' reservoir) but subseismic heterogeneities usually emerge during the producing life of a field.

A distinctive feature of deep water systems is the predominance of stratigraphic traps. Unlike structurally closed fields, where there is a geometric limit to how much volume can be contained in a defined closure, the addition of previously undetected connected HCIIP beyond

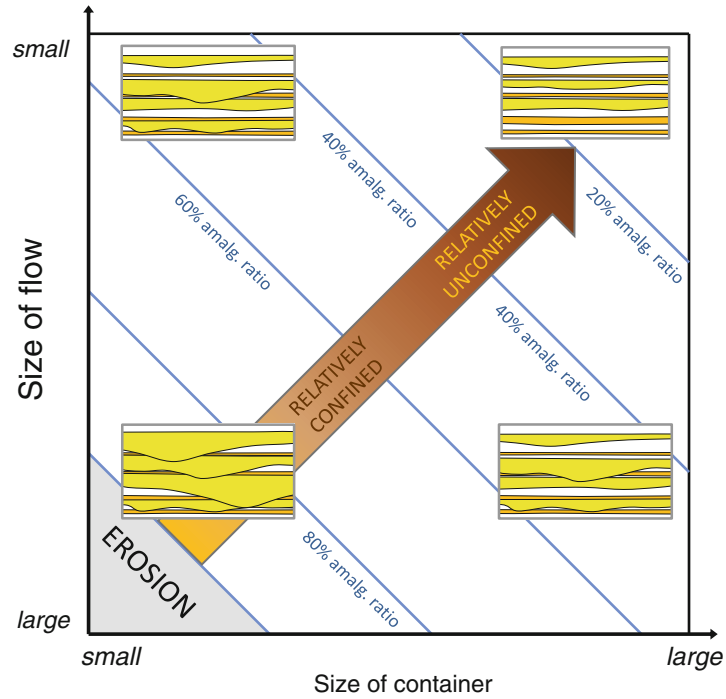

Fig. 6.25 The relationship between permeability architecture (anisotropy expressed in terms of an amalgamation ratio) and key underlying controls on confinement (Based on discussions with D. Stanbrook and E. Stephens)

the seismically-observed reservoir can be considerable. This is particularly the case in unconfined systems. The challenge is therefore to see beyond the seismic, particularly if the reservoir has a stratigraphic trap with no direct means of defining the field extent.

For reservoir modelling, the possibility of unseen HCIIP requires a concept, and ideas on confinement (and hence likely connectivity) can be tested against information from material balance. There is therefore greater emphasis than usual on starting the modelling exercise with guidance from dynamic data, as this can inform the first conceptual sketches of the reservoir.

The example shown in Fig. 6.26 is from a gas field in the UK Central North Sea modelled after 5 years of production (Bentley and Hartung 2001). The structure is a small field in which gravity flows were observed to onlap a palaeotopographic high above a salt dome. Models limited to observations of sand intervals in the wells could be history matched but simple matches could only be achieved if additional volumes were present in beds not initially identified from seismic. In the analysis of uncertainty, it was therefore valid to consider scenarios including additional, unobserved reservoir sands, an interpretation which would be consistent with additional confined flows depositing around the palaeo high. 4D seismic data from this field subsequently supported this hypothesis.

6.5.3 Thin Beds

Incorrect representation of thin beds is prevalent in deep water stratigraphic traps where significant undrilled sub-seismic HCIIP may be present. Even when penetrated by wells, the thin beds may be unresolved on logs and reservoir pay intervals will typically be underestimated.

The impact of the log sampling problem in a reservoir modelling workflow is illustrated in Fig. 6.27. Modellers will usually check blocked property (porosity) logs against raw log data as a QC step, but this is only worthwhile if the raw data points are valid in the first place. If not, the subsequent cross-plotting of incorrect blocked log data with permeability data is invalid.

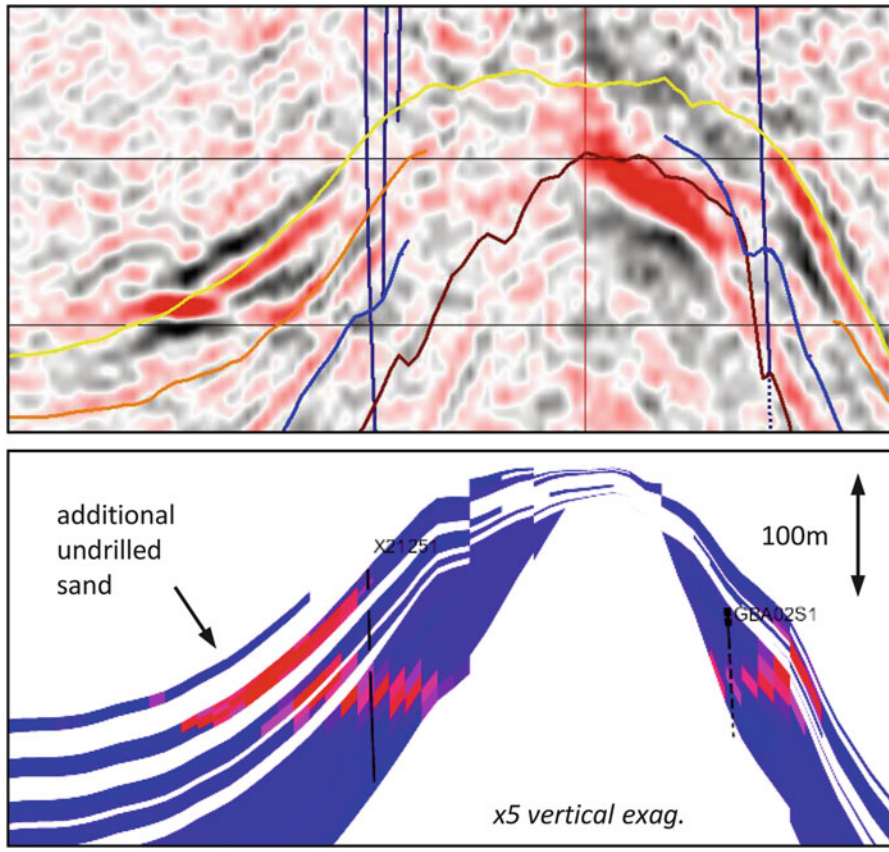

Fig. 6.26 *Top*: amplitude change after 5 years of production in gravity flows onlapping a salt dome; *bottom*: forward-modelled acoustic impedance change in the sand-rich layers, including an additional upper layer not seen in the wells (Bentley and Hartung 2001) (Redrawn from Bentley and Hartung 2001, ©EAGE reproduced with kind permission of EAGE Publications B.V., The Netherlands)

An important error occurs if the core plug data is not sampling an REV, which tends to be the case in very finely laminated intervals. The resulting permeability values inserted into model cells are somewhat meaningless numbers, which are then upscaled for simulation. The resulting simulation forecasts are unlikely to be useful.

A less error-prone workflow is illustrated in Fig. 6.28, in which the key step is to decouple the handling of porosity and permeability. The porosity log may not reflect the porosity of the thin net reservoir beds correctly, but it may be a reasonable average of porosity in the net/non-net package. The logging tool is effectively measuring an upscaled porosity, which can be applied to a cell with N/G = 1 at least as a first approximation of the pore volume. The validity of this can be checked with reference to core data.

Permeability cannot be directly derived by transforming the log-average of core values, however, and this is where the modelling of porosity and permeability is decoupled. Effective permeability can instead be calculated using small-scale modelling based on data which samples the REVs of the small scale reservoir elements, as described in Chap. 4, and illustrated in this chapter for tidal heterolithics and fine aeolian laminae. The input data may be core plug permeabilities, mini-permeameter data or estimates from thin sections – whichever scale samples the appropriate REV. The final outcome should be checked against well test data.

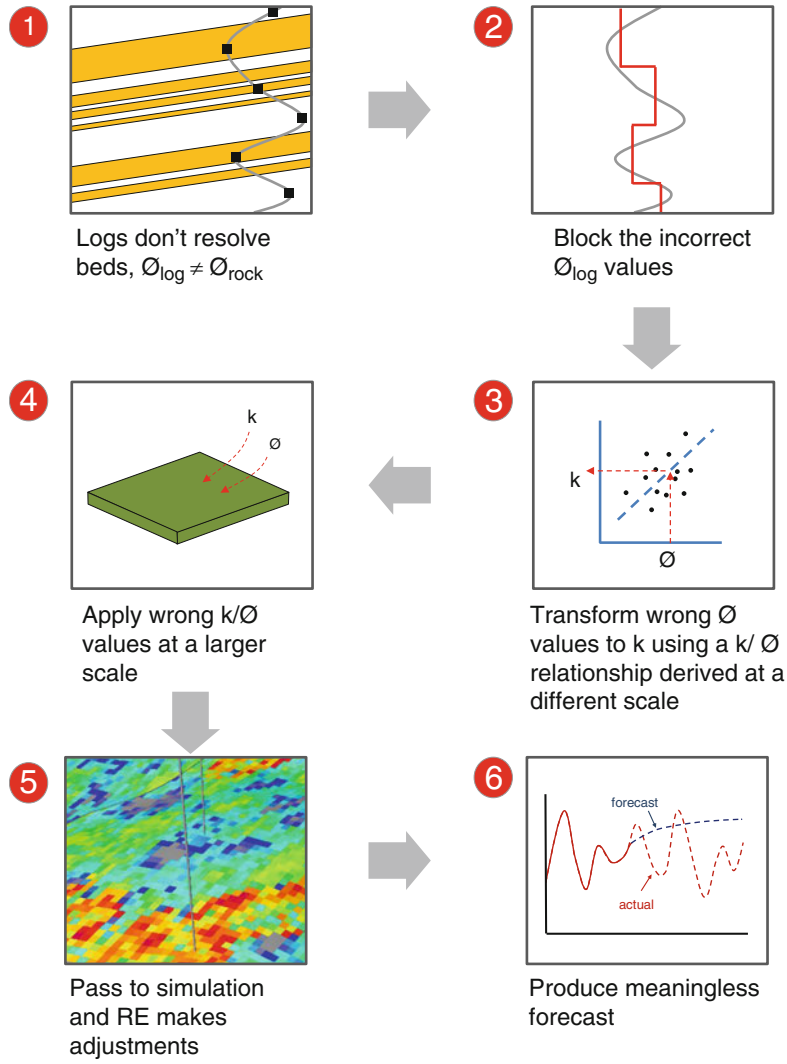

Fig. 6.27 Modelling of thin beds: when it goes wrong

6.5.4 Small-Scale Heterogeneity in High Net-to-Gross 'Tanks'

For confined systems in which the reservoir is detectable from seismic attributes, it is tempting to work directly from seismic and treat the field as a 'tank of sand', albeit an irregularly-shaped one. What tends to be overlooked is the contribution of low-net thin beds within the generally high N/G system; the inverse condition of the 'thin bed' scenarios described above.

An example of this is shown below from the well-studied high N/G ratio reservoir analogues of the Annot region in SE France (Pickering and Hilton 1998). Massive sand intervals are partitioned by thin but extensive heterolithic intervals with low permeability which would be poorly resolved on logs (Fig. 6.29). The issue is whether or not such heterolithic intervals would have significant vertical permeability and how laterally extensive the intervals would be, i.e. do they constitute barriers or baffles?

Without very good log resolution a similar logic is needed to that applied to thin beds – effective permeability needs to be estimated from small-scale modelling. This is a simpler exercise, however, as the key issue is vertical permeability; the horizontal permeability in the gross sand interval will always be dominated by the high N/G sands above and below the heterolithics.

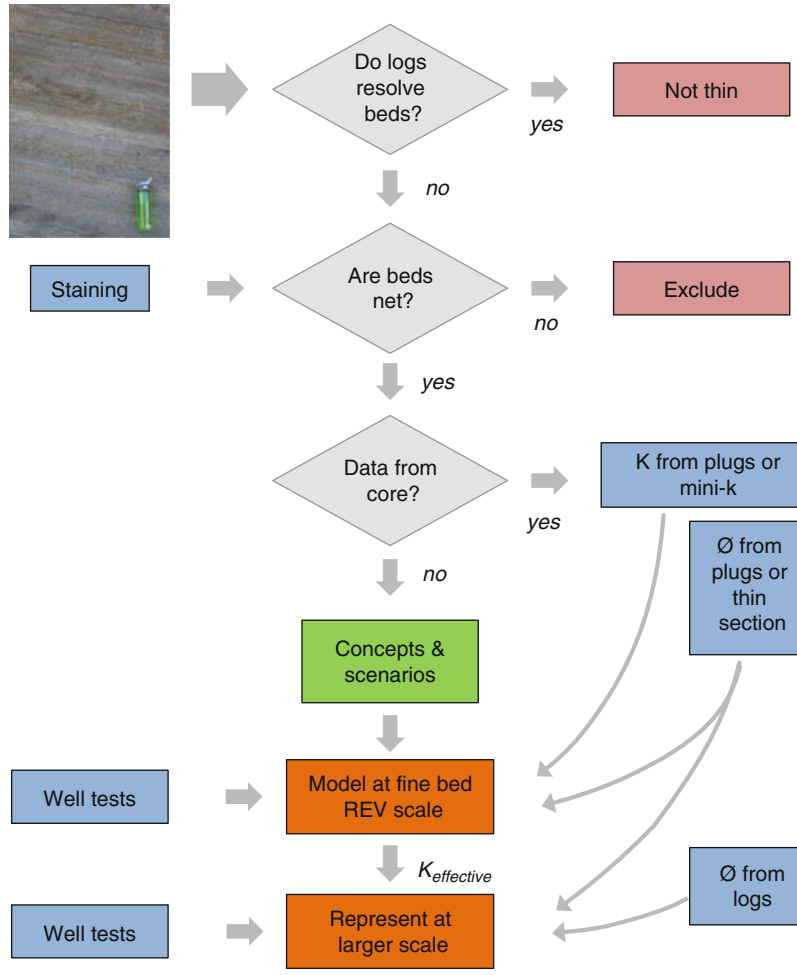

Fig. 6.28 Reservoir modelling in thin beds: a better approach, partly decoupling the modelling of porosity and permeability modelling

The heterolithic facies can be extensive, even in high N/G systems, and in this example can be traced along the cliff line for 4 km (Fig. 6.30). The impact of this architecture is illustrated in 2D sections through a 3D model (Fig. 6.31), in which the heterolithic intervals seen in Fig. 6.29 are included as discrete elements with contrasting effective vertical permeabilities.

The effective vertical permeability in the heterolithic units determines the sweep pattern. In this case the heterogeneity improves recovery; water breakthrough times increase from 3 months to 3 years and recovery increases from 21 to 37 % (after 16 years production) as the baffling effect of the low-permeability interval holds back water coning. The addition of higher permeability channels within the sheet-like sands (the 'Jardin de Roi' section in Fig. 6.31) has the reverse effect by provoking earlier water breakthrough. Both the heterolithic facies and the channel facies are likely to be sub-seismic, and these effects will be missed by "seismic-only" workflows.

6.5.5 Summary

Despite huge advances in deep marine reservoir developments, the experiences of the last decade confirm that no matter how good the seismic data is, there is typically essential sub-seismic heterogeneity in deep marine systems, especially in fields to be developed under waterflood. Once under production, 4D seismic is an invaluable tool to help explain field behaviour, but by this

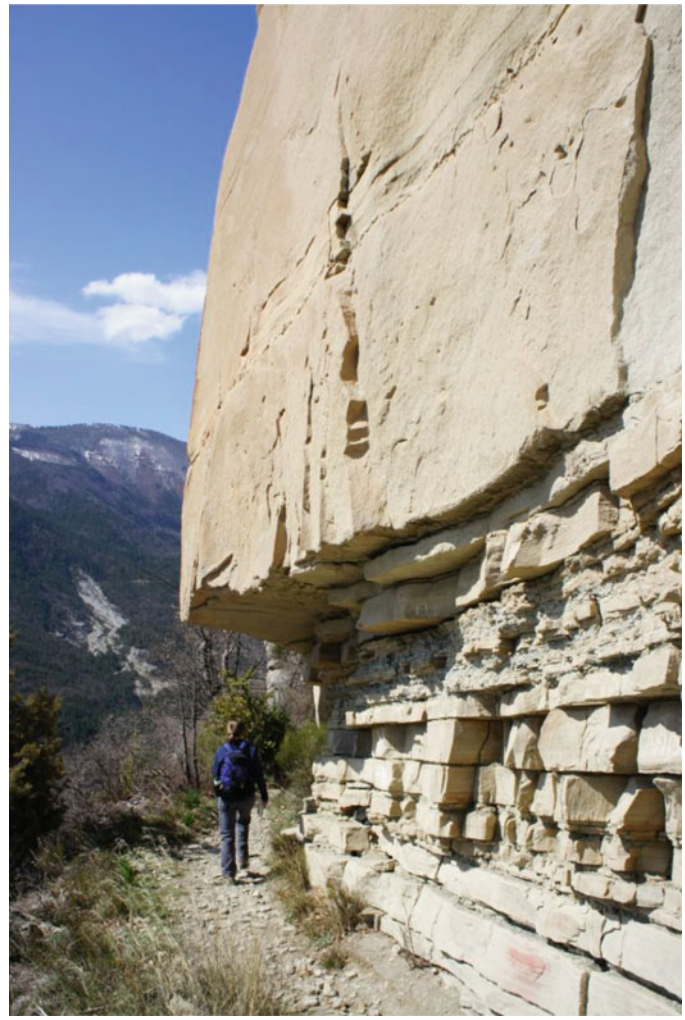

Fig. 6.29 Heterolithics in the otherwise high N/G of the Gres d'Annot, outcrops above Annot town

time the biggest investment decisions have been made. Even with 4D data, key heterogeneities may remain sub-seismic.

Reservoir modelling in deep marine systems therefore requires an understanding of the fine-scale architectural concepts, steered by an overarching understanding of confinement.

6.6 Carbonate Reservoirs

To the frustration of some sedimentologists, carbonate reservoir modelling suffers from two common labels:

- Carbonate systems are as varied as siliciclastic systems, but whilst much attention is paid to different types of clastic reservoir, carbonates are often lumped as one (as in this chapter), and
- Carbonates are seen as 'just difficult.'

The bias towards clastic systems in reservoir modelling is certainly strong, but the principles of model design described in Chaps. 1, 2, 3, 4, and 5 apply equally well to all reservoir types. Are carbonates more difficult to model? Not necessarily, but they do tend to be different, as reviewed by Burchette (2012).

For carbonate reservoir modelling, five areas are highlighted for consideration:

1. Depositional architecture,
2. Pore fabric,
3. Diagenesis,
4. Fractures,
5. Hierarchies of scale (the carbonate REV).

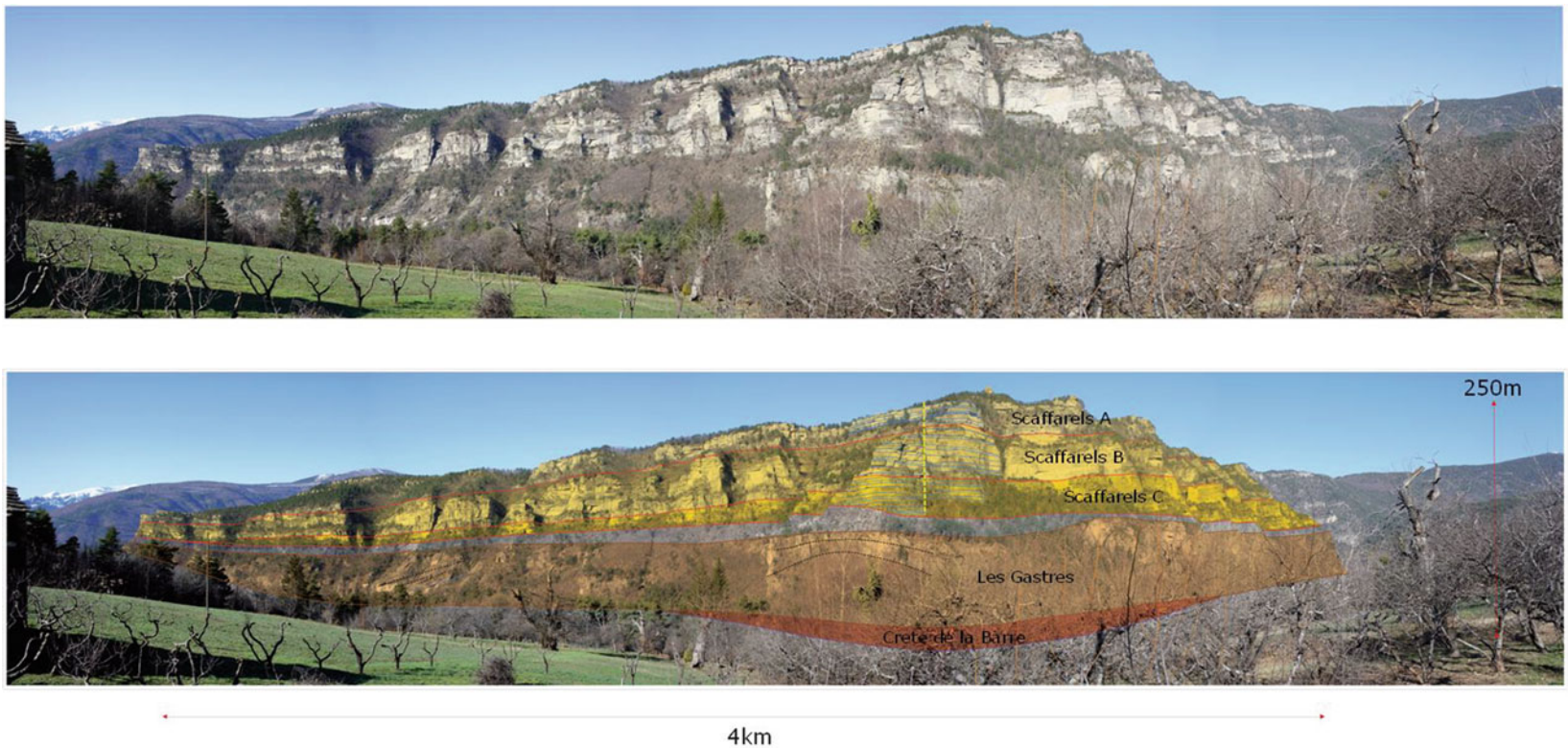

Fig. 6.30 Architecture of the Gres d'Annot of the Coulomp Valley; the heterolithics in Fig. 6.29 are at the base of the unit labelled 'Scaffarels A'

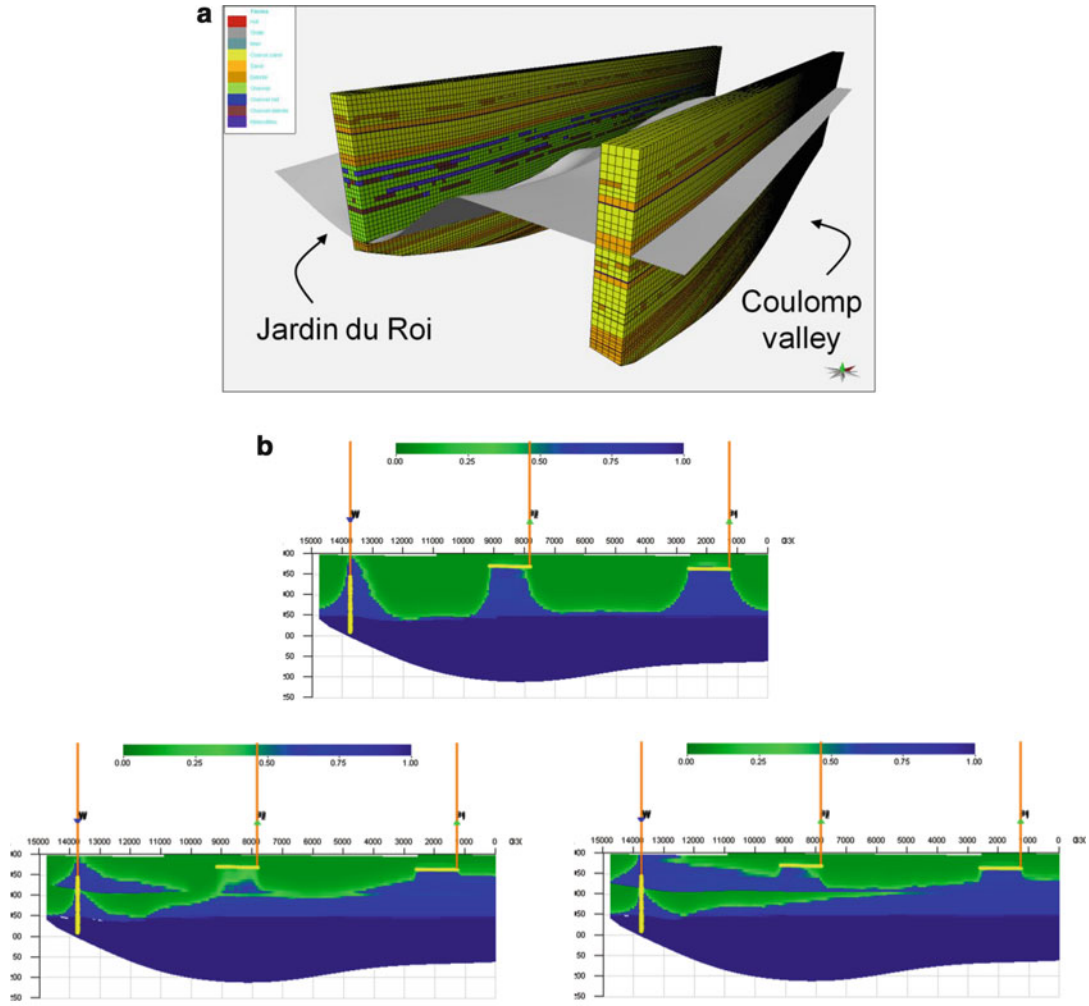

Fig. 6.31 Modelling the Gres d'Annot. (**a**) Static well model sections with heterolithics in *orange*. (**b**) Impact of heterolithics in a high N/G reservoir (Coulomp Valley section) on sweep efficiency during a water flood of a viscous oil; *green* = oil, *blue* = water, injection from *left*. Production is from horizontal wells in the upper reservoir. *Upper image*: no heterolithics; *lower left*: heterolithics with effective $k_v = 1$ mD; *lower right*: heterolithics with effective $k_v = 0.1$ mD (Image courtesy of M. Bentley & E. Stephens)

6.6.1 Depositional Architecture

Where reservoir heterogeneity is controlled by original depositional patterns and processes, carbonate modelling is open to the same options for rock modelling as those which apply for siliciclastic reservoir models. An important difference is the more limited reservoir modelling database for carbonates, and the tendency is therefore to rely more on modern environmental analogues (Burchette 2012). However, the link to modern analogues is weaker than for clastic systems simply because of the organic aspect of carbonate sedimentology – modern day organisms do not necessarily build carbonate reservoirs the same way as their ancestors, and current climatic changes do not automatically match those of the past. There is therefore a greater need to derive geometric data from stratigraphically and environmentally appropriate settings than is the case for many clastic reservoirs.

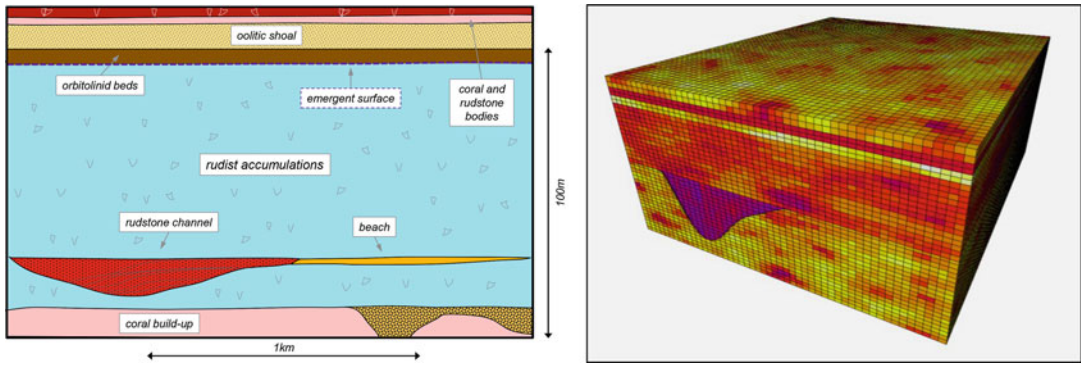

Fig. 6.32 Facies interpretation of a platform margin from outcrops near Rustrel, France (Leonide et al. 2012) (*left*) and a cellular representation of the same (*right*) (Left image redrawn from Leonide et al. 2012, © SEPM Society for Sedimentary Geology [2012], reproduced with permission)

In the example shown in Fig. 6.32, outcrop analogues for the Shuaiba reservoir are drawn from examples in Provence (Leonide et al. 2012) and detailed mapping of limestone facies provides insight into the distribution of reservoir types in age-equivalent Middle Eastern reservoirs. Even here, though, the palaeo-environments between reservoir and analogue locations differ – the two areas lay on opposite sides of the ancient Tethys Ocean and are characterised by different faunal assemblages.

Other carbonate environments display impressive lateral continuity and might appear to make little call on the rock modelling toolbox. This is reported from field studies by Palermo et al. (2012) working on the Muschelkalk, where laterally consistent reservoir properties have been measured in platform carbonates and traced over several 100's of metres, contrasting markedly with very abrupt vertical variations. Similar patterns are common in platform carbonates of the Middle East (Fig. 6.33).

This extreme anisotropy is also familiar in carbonate-evaporite sequences where heterogeneities are controlled laterally by gentle basin-wide chemical gradients but vertically by fluctuations in basin inputs and outputs, such as periodic connection and disconnection with open seawater and periodic basin desiccation (Fig. 6.34).

Similar high frequency, laterally-correlatable cyclicity is also common to chalk fields, and the regularity can be picked out from vertical variograms of porosity and permeability measured on core (Almeida and Frykman 1994) (Fig. 6.35).

Depositional environments can therefore dictate the need for simple, very thinly layered models, or heterogeneous object-based models, although the latter potentially lack good analogue data. In this respect, carbonate modelling workflows may be comparable to workflows for clastic reservoirs.

6.6.2 Pore Fabric

Where carbonates and clastics differ most markedly is in their pore fabric. Clastic systems can generally be broken down into elements with reasonable porosity-permeability relationships, reflecting a consistency of carbonate pore type for a given model element. This is often not the case in carbonates, where there may be little or no relationship between porosity and permeability.

The underlying reason is pore size distribution, which can vary over very short distances in carbonates owing to the irregularity of pore shapes. Not all carbonates behave this way: as pore shapes become more uniform, such as in some chalks or well sorted grainstones, regular k/ϕ relationships emerge. However, classifying core plug data using the Dunham (1962) descriptive scheme, useful for

Fig. 6.33 Highly layered platform carbonates from the Natih-E at Jabal Madmar, Oman

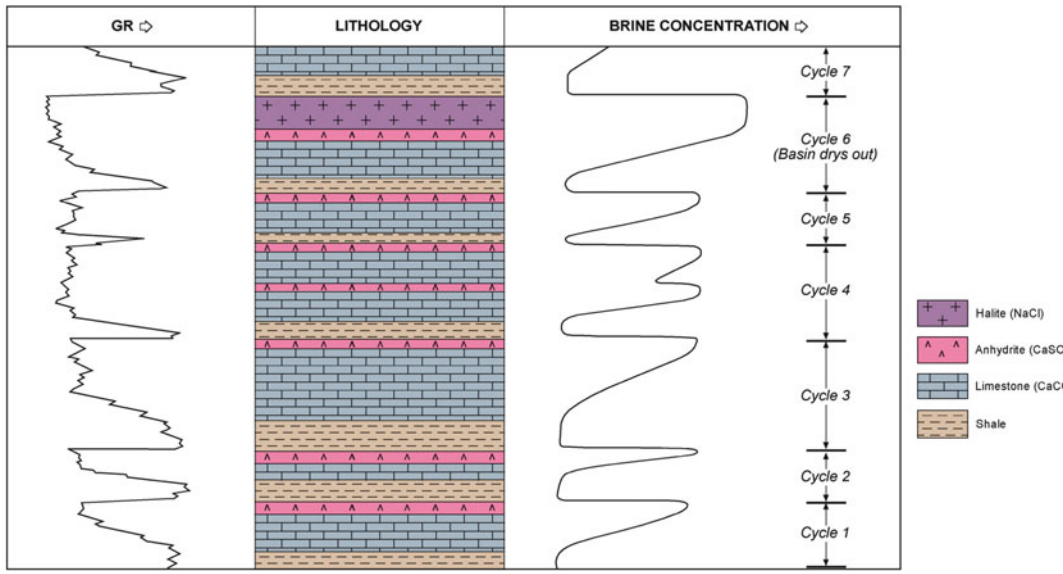

Fig. 6.34 Vertical distribution of elements in a carbonate-evaporite interval; individual 5 m thick cycles are correlatable for 10's of km laterally

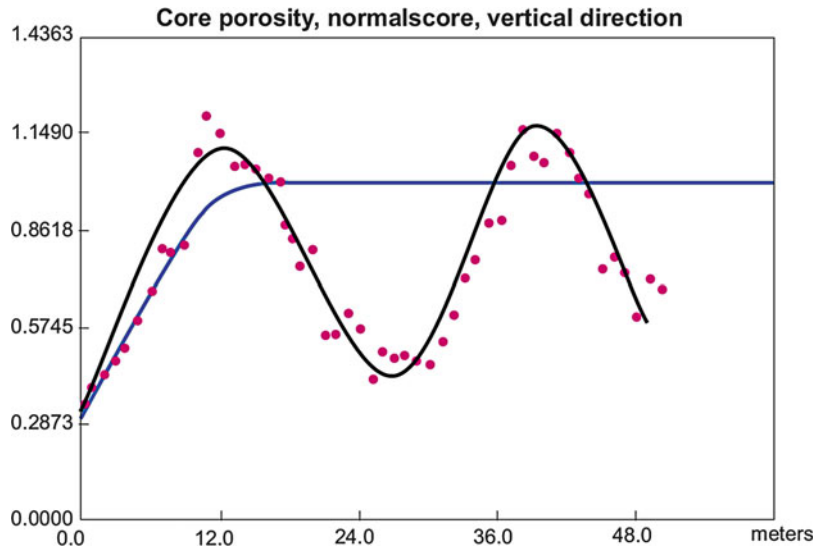

Fig. 6.35 A variogram for vertical porosity measured in chalk core (Almeida and Frykman 1994). The pattern is a 'hole' variogram, showing alternating high and low variance between porosity values, suggesting regular 12 m layering (Redrawn from Almeida and Frykman 1994, AAPG©1994, reprinted by permission of the AAPG whose permission is required for further use)

objective description of the lithology, often fails to break a reservoir system down into elements with clear k/ϕ relationships.

A pragmatic method of carbonate characterisation at the pore scale is presented in Lucia (1983) and the summaries given by Lucia (2007) remain a very good starting point for characterising carbonate reservoirs as a basis for reservoir modelling. Lucia classifies pore systems into two broad groups:

1. Inter-particle, in which porosity sits between grains or crystals, and
2. Vuggy (which is everything else).

Vuggy systems divide again into separate-vug and touching-vug fabrics. Any carbonate classification system can be mapped onto this simple scheme, and indeed Lucia (2007) subdivides the scheme to accommodate common carbonate descriptive terms (moldic pores, fenestral pores, breccias, etc.). The advantage of Lucia's scheme is that it captures heterogeneity in terms of pore fabric which lends itself to petrophysical characterisation, and it is therefore more predictive than the Dunham scheme.

With reservoir modelling in mind, a generalisation of Lucia's scheme is shown in Fig. 6.36. This is set against the Dunham classification but with joint systems separated out, rather than being treated as a special case of touching-vug fabrics, as in the Lucia classification scheme. The latter distinction is somewhat semantic but is made here because of the dramatically different permeability of connected fractures and the different scale on which connected fracture systems work (see next section). We would argue that this imparts a distinctly different fabric on the reservoir than more localised touching-vug fabrics, even those including micro-fractures. Lucia's work is primarily focussed on carbonate sedimentology and petrophysics, with fractures given a reduced role; the modified scheme proposed in Fig. 6.37 allows for the fracture classifications of Nelson (2001) to be incorporated.

The typical porosity-permeability characteristics of the Lucia rock fabrics are shown in Fig. 6.37, with a fracture group added alongside.

These classification schemes attempt to isolate the underlying controls on rock properties, particularly permeability. It should however be emphasized that if the origin of reservoir permeability for any given case is not known and cannot be characterised conceptually, there is little point in embarking on a model, certainly if the end-result is to be simulation. Simple log-based porosity modelling and application of a linear transform from porosity to permeability is likely to produce a weak model (discussed further below).

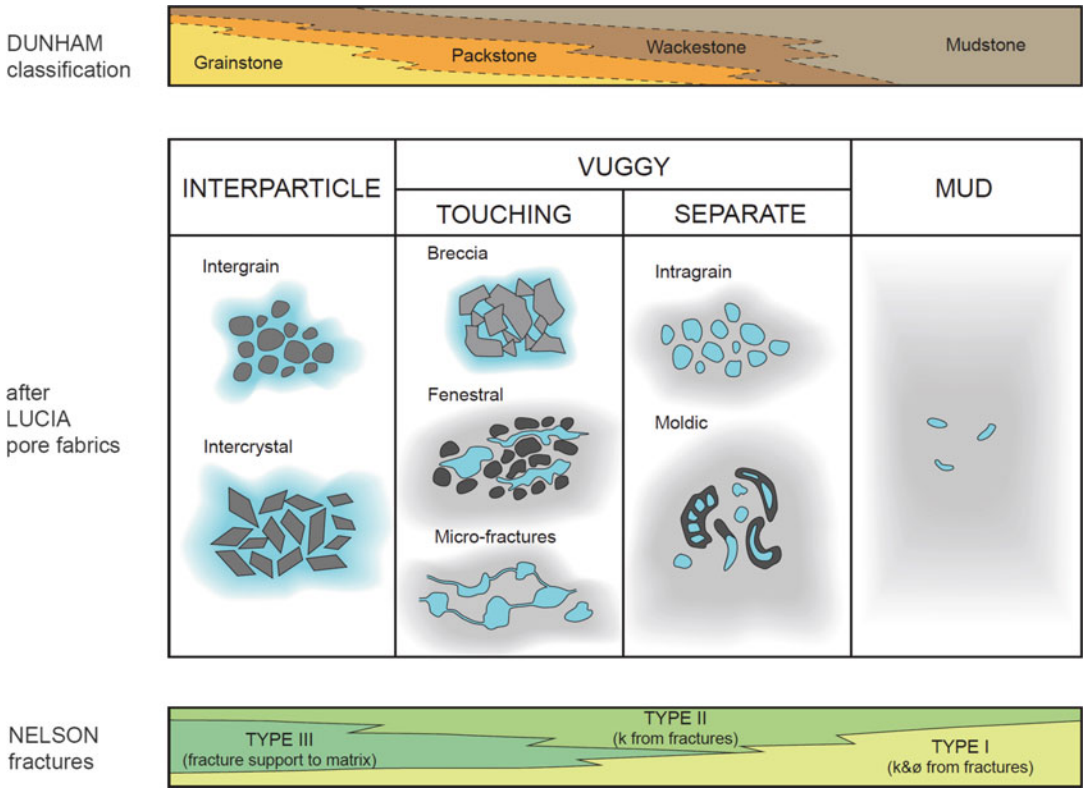

Fig. 6.36 Carbonate pore fabrics; modified after Lucia (2007) for selecting reservoir modelling elements but including fracture sets, mudstone, the Dunham classification and the typical overlap with Nelson's fracture classification

6.6.3 Diagenesis

A second key difference between clastic and carbonate reservoir characterisation is the complexity of the diagenetic history. The diagenetic history will provide much of the back story to the concept for small-scale permeability architecture – deemed necessary from the discussion above. For reservoir modelling, the diagenesis storyline needs to be converted into a model parameter which can be overlain, or may completely replace, the depositional architecture. In clastics, it is unusual for the original depositional fabric to be completely obscured during diagenesis. In carbonates, this is much more common, to the point that traditional rock modelling as described in Chap. 2 may no longer be necessary, and the process of modelling can begin with effective property modelling.

In this case, the desired reservoir model may in fact be a description of the diagenetic history, parameterised into a set of overlying trends or functions. The example in Fig. 6.38 illustrates this for a thick carbonate-evaporite interval in which diagenesis dominates the depositional fabric and matrix permeability is controlled by dolomitisation. The conceptual model is for the expulsion of dolomitising fluids due to compaction in the basin centre, leading to best reservoir properties along the basin margins. The permeability distribution can therefore be modelled regionally by applying trends sensitive to depth and structural location. The porosity model is generated from upscaled (core calibrated) porosity logs, but there is no porosity-permeability relationship *per se*.

6.6.4 Fractures and Karst

The third key difference between carbonates and clastics lies in the mechanical properties of limestones and dolomites. These predispose carbonates to natural fracturing, notably jointing, to a much

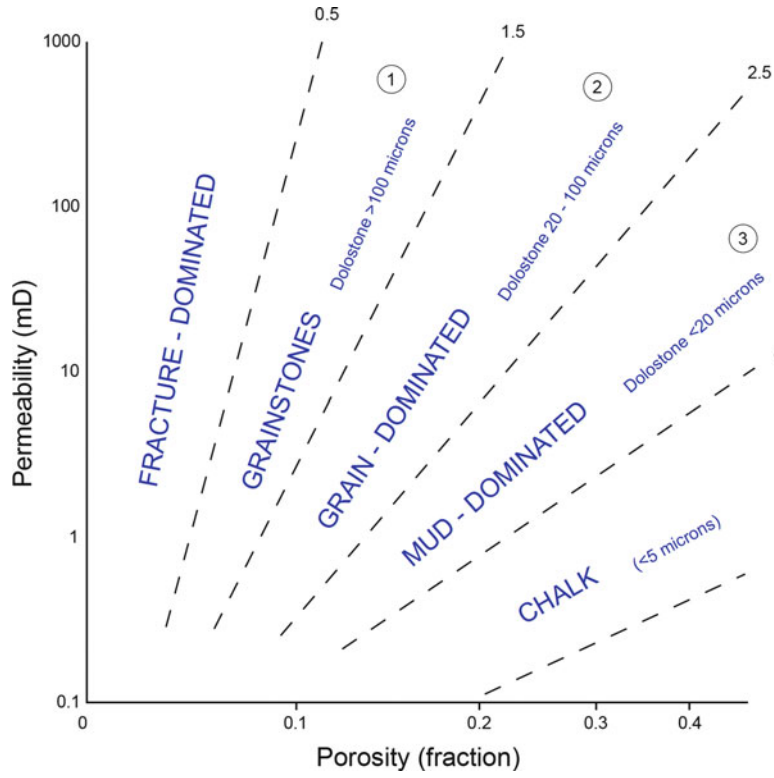

Fig. 6.37 Pore fabric k/ø transforms (Modified after Lucia (2007))

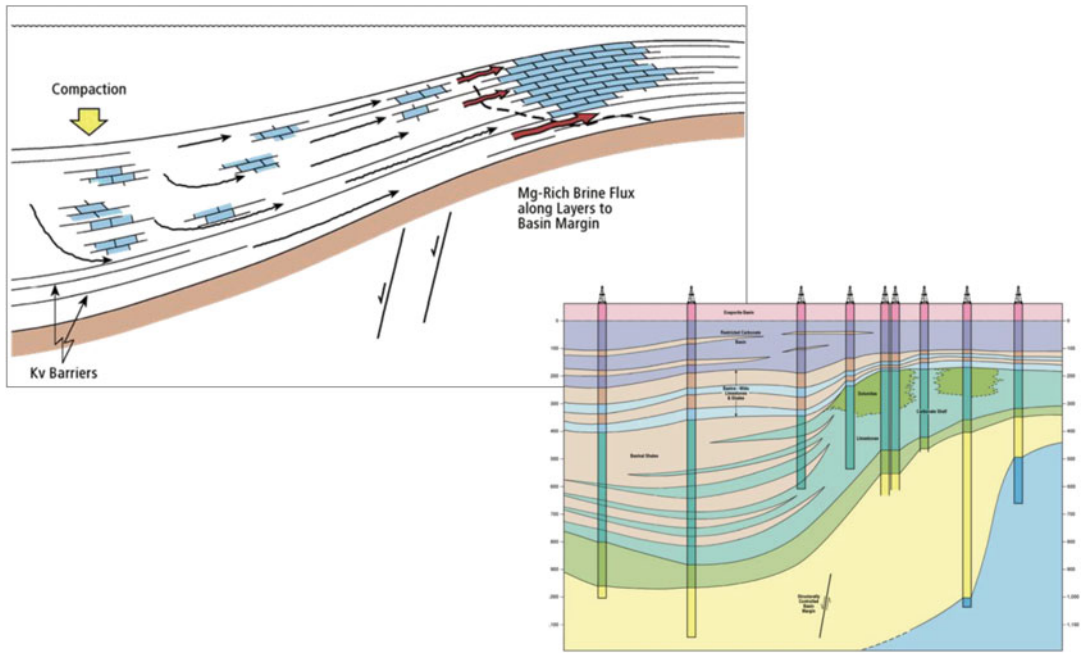

Fig. 6.38 Localisation of high permeability dolomite along structurally-controlled basin margins

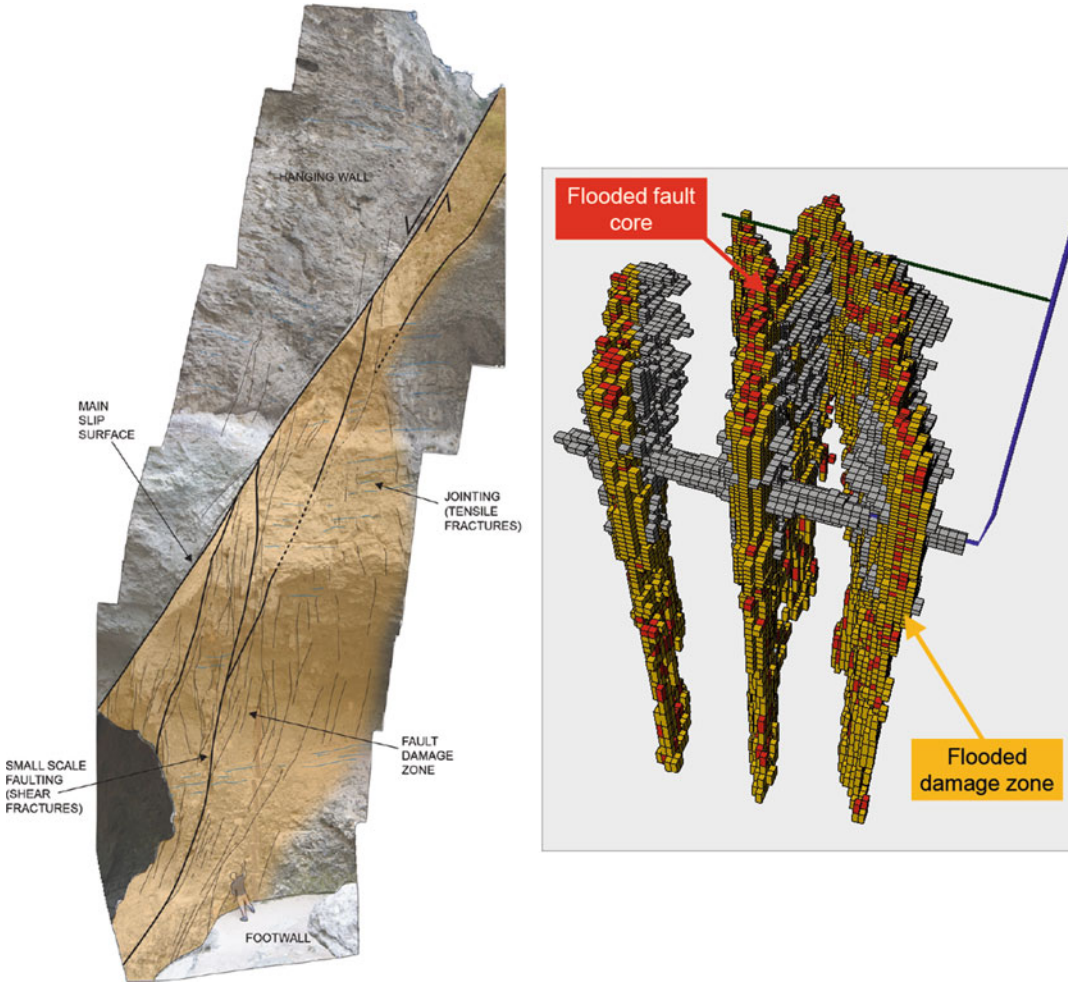

Fig. 6.39 Karstified natural fracture system from the Fontaine du Vaucluse, Provence, France: *left:* outcrop at the abyss; *right*: simulation of a waterflood across the fracture/matrix network, *horizontal* injector in *blue*, producer in *green*; open fractures in the flooded fault damage zone dominate flow, which diverts along only the highest permeability matrix (colours represent injection water saturation, *red* = high)

greater extent than their more argillaceous, clastic counterparts. Near-surface dissolution processes in carbonate rocks, which result in karst topography and related weathering structures, are another key factor for modelling carbonate reservoirs.

Fractured reservoirs are discussed separately below, and it suffices to say here that in the absence of information to the contrary it is wise to assume some degree of natural fracturing in *any* carbonate reservoir. As carbonates typically have little argillaceous content, these fractures are more likely to remain open than they are in clastic reservoirs.

Figure 6.39 shows a spectacular modern example of a karstified fracture system, in which the 'matrix' fabric plays a secondary role. The simulation model of the system captures the dominance of the fracture network for a waterflood scenario, with high permeability matrix rock fabrics providing secondary shortcuts for the flood front.

6.6.5 Hierarchies of Scale – The Carbonate REV

A starting point for the characterisation of a carbonate reservoir for reservoir modelling is therefore to view the depositional architecture, the diagenesis

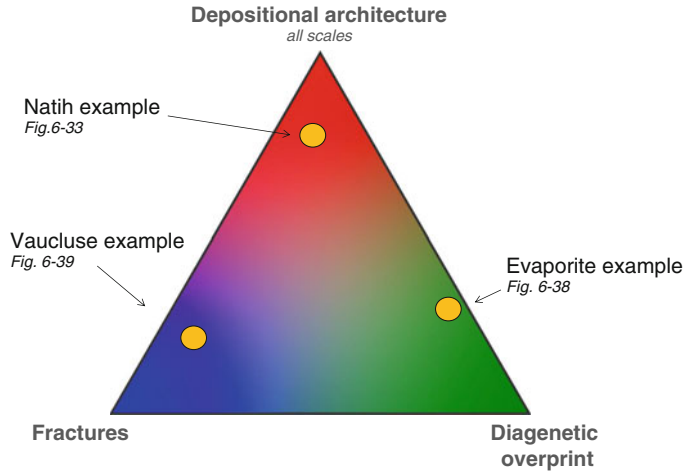

Fig. 6.40 Ternary diagram of influences on carbonate reservoir modelling with examples from this section

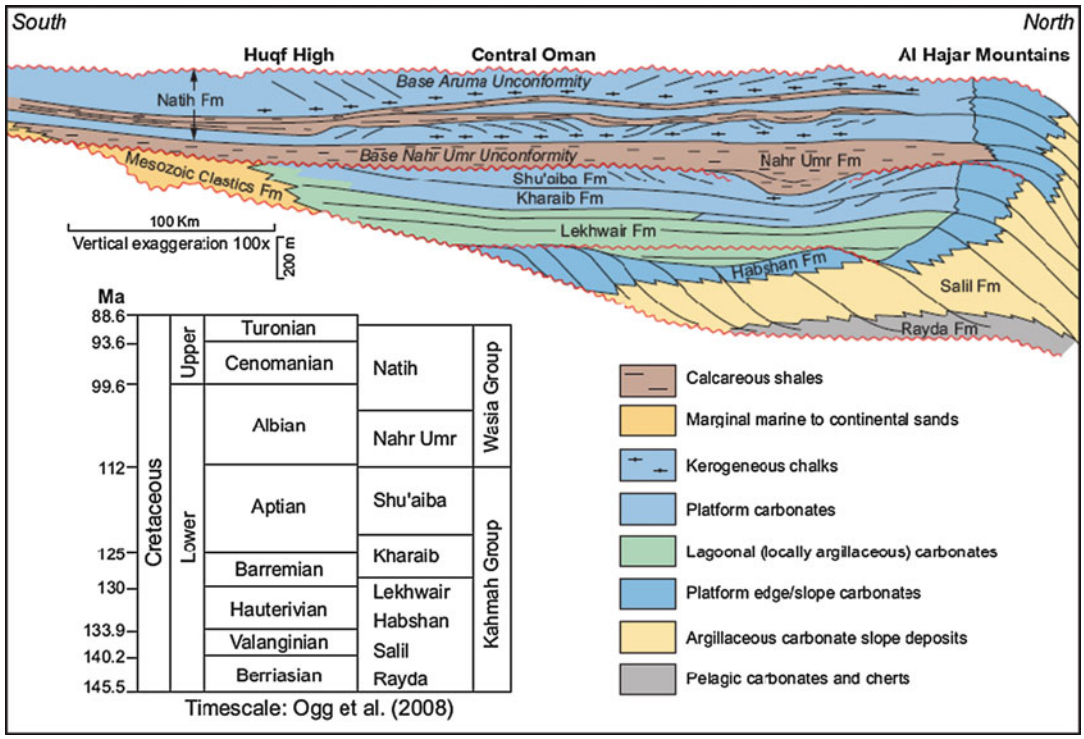

Fig. 6.41 Sequence-based framework for the Kahmah and Wasia Group reservoirs in North Oman (After Droste and Van Steenwinkel 2004) (Redrawn from Almeida and Frykman 1994, AAPG©1994, reprinted by permission of the AAPG whose permission is required for further use)

and fracture patterns all as potential inputs, and determine the relative importance of each on permeability, at the scale of interest (Fig. 6.40).

Having determined dominant influences on reservoir quality, these then need to be placed in a large-scale framework, which for carbonate environments is usually a sequence-based hierarchy, such as the example from Oman (Droste and Van Steenwinkel 2004; Fig. 6.41).

A key topic for attention in carbonate reservoir modelling is how to take interpretations of small-scale pore fabric (Fig. 6.36) and map these

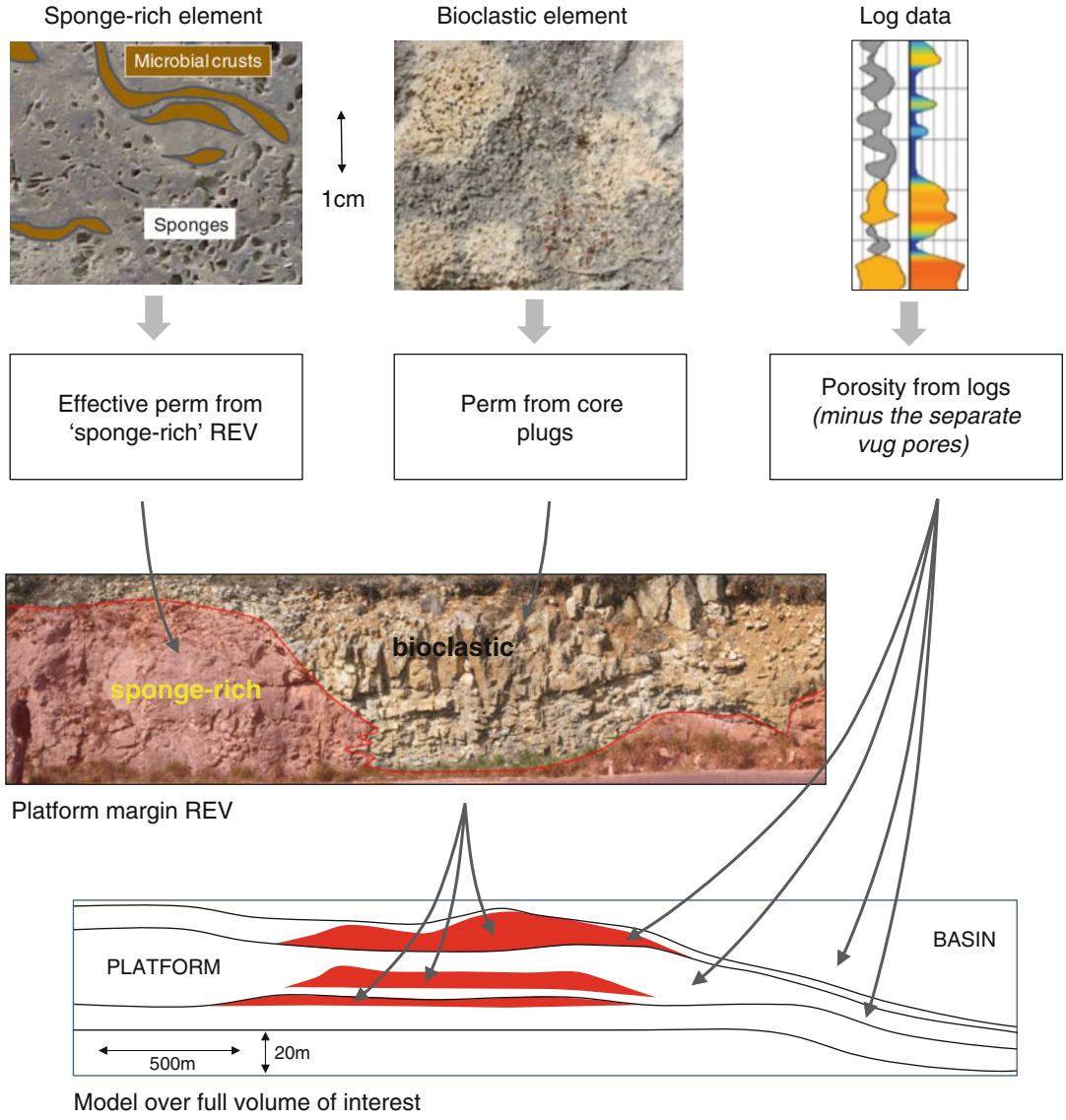

Fig. 6.42 Workflow for modelling pore-scale detail in a larger scale carbonate model for a platform margin. *Top*: pore scale elements, the REV for one of which is captured at the core plug scale, the other requiring effective property modelling to quantify; *middle*: outcrop analogue guiding the concept for architectural arrangement of elements within a layer, the second REV scale; *lower*: sequence-based framework showing the location of the sponge-dominated REVs, scale informed from the work of Leonide et al. (2012). Porosity is modelled directly from logs

onto a large-scale chronostratigraphic framework such as that in Fig. 6.41. In a clastic reservoir the route would be via depositional architecture (facies, facies associations), but this only applies to carbonates at one tip of the ternary set of influences (Fig. 6.40). Even then the task remains of finding the REVs for the intermediate scales between pore and region. Carbonate modelling requires the integration of all three nodes of the ternary in Fig. 6.40, encapsulating the model purpose (Chap. 1) and the scale at which the model purpose applies, which usually relates to the current and planned well spacing.

These issues have been further explored in recent studies (e.g. Kazemi et al. 2012) which relate to the hierarchies of REVs (described in Chap. 4). An example of how this can be done is shown in Fig. 6.42, working up from the pore

scale. The problem at hand is the value of infill drilling in a platform-margin reservoir; the scale of the question is therefore the well spacing, in this case 500–1,000 m. The reservoir is characterised by local sponge build-ups in a bioclastic background, as observed at outcrop analogue (centre of Fig. 6.42). In this case permeability does relate to the original depositional architecture, which places this case at the top apex of the ternary plot (Fig. 6.40). The difficulty is that the pore fabric in the sponges is not sampled in a representative way by core plugs, so the core-based data source for permeability estimation is insufficient.

As in the case of thin beds in siliciclastic reservoirs, a solution lies in the decoupling of porosity and permeability modelling, but this time at the pore fabric scale (Fig. 6.42). The sponge-dominated model element is a combination of separate-vug and touching-vug pore fabric in a very low permeability mudstone background mixed with algal crusts which have no effective porosity. Small-scale modelling can deliver estimates of the effective permeability of the sponge-rich element which can be combined with the bioclastic element at the next scale up (layer scale). The inter-particle permeability for the bioclastic facies is, however, sampled reasonably well at the core plug scale, so this part of the layer-scale model can be populated directly from core data.

The effective permeability of the layer-scale model can be determined by a small-scale model on the scale of metres (the outcrop-analogue scale and the 'platform margin' REV), and this can be fed into the sequence-based framework of the larger scale model, scaled appropriately to answer the infill well spacing question. Note that a full-field model is not required to address the question at hand.

Porosity meanwhile can simply be derived from logs upscaled into the largest scale model, unless there is a reason to believe the averaging of the tool is significantly non-additive (see Chap. 3). A common cause for this in carbonates is non-contributing vuggy pore space (i.e. porosity that does not contribute to flow), and this needs to be compensated for in the petrophysical model (see Lucia 2007, for an approach to this issue).

The handling of porosity and permeability is therefore largely decoupled in this workflow. This is a necessary step here, not because there is no k/ϕ relationship (ultimately, permeability is related in some way to porosity) but because the relationship is not captured at the scales at which the porosity and permeability data are gathered. Arguably, average porosity could also be derived from the multi-scale models. The disadvantage of this approach is that the average porosity variation captured by the field-wide log dataset would be missed, and this would degrade the other main model purpose, which is to estimate pore volume across the volume of interest.

Small-scale complexity does not therefore rule out reservoir modelling, it simply means an alternative workflow is required, in which the modelling of porosity and permeability may be decoupled. Porosity may justifiably be modelled from log values. Permeability may need to be forward-modelled from small-scale data, accompanied by an architectural concept for permeability distribution – the conceptual sketch.

6.6.6 Conclusion: Forward-Modelling or Inversion?

Are carbonate reservoirs more difficult to model than clastic reservoirs? We would suggest not necessarily, but the model designs *will* be different. Agar and Hampson (2014) give a good summary of future directions in carbonate modelling. The same design elements apply to all reservoirs: concept – element selection – architectural arrangement – algorithm choice – model scaling – uncertainty-handling, but different choices will be made.

The total property modelling concept (Chap. 3) is especially applicable to carbonate reservoirs, as is the multi-scale effective property modelling approach (in place of simple poro-perm cross-plots), as described in Chap. 4. The need to overlay an open natural fracture network on the matrix properties is also more common.

When carbonate reservoir modelling becomes especially complex (e.g. multi-scale, with matrix and fractures), the expectation of an accurate forward model of the reservoir should be reduced, and more emphasis placed on inversion from production data. This philosophy is explored further in the section on fractured reservoirs, below.

6.7 Structurally-Controlled Reservoirs

All reservoirs are to some extent influenced by fractures, and there is something slightly artificial in separating out a group of reservoirs that are 'structurally controlled'. It is truer to say that for some reservoirs the effects of fracturing are minor and can be neglected, whereas for other reservoirs the structural effects are so important that it is the sedimentary aspects which turn out to play a minor role. It is also often true that the effects of fractures are initially assumed to be of minor importance, but once more detailed reservoir data becomes available, especially dynamic production data, the fractures start to reveal themselves.

Modelling fractures requires an underlying concept, as for all reservoir models. The first step in forming a concept is the description of the significant fracture types, the key distinction being between joints (tensile fractures) and faults (shear fractures). Although most fractured reservoirs will contain a mixture of both, the distinction is important because joint-dominated systems tend to form high density fracture systems – these are generally what is being referred to when the term 'naturally fractured reservoir' is used – whereas fault-dominated systems tend to form low density systems. Joint-dominated systems tend to be open, whereas is it common to encounter both open and closed fractures in fault dominated systems.

In this section, high- and low-density fracture systems will be treated separately because the modelling workflows required to describe them are very different.

6.7.1 Low Density Fractured Reservoirs (Fault-Dominated)

6.7.1.1 Terminology

A fault is a zone, either side of which relative displacement of the host rock has occurred during failure, as a result of *shear* when the deviatoric stress exceeds the rock strength. Note that rocks are always in net compression at shear failure, irrespective of whether the regional tectonic picture is described as 'extensional', 'compressional' or 'strike-slip'. The latter terms simply describe the relative position of the principal stresses at failure.

Faults form as part of a fault network (e.g. Fig. 6.43), and a key characteristic of fault networks is their scale invariance – the same fault patterns can be observed on a range of scales. They are fractal.

Faults are formed in three principle settings, the contrasts between which are important for an understanding of their impact on reservoir performance:

1. *Normal faults*, mainly occur in extensional tectonic settings and tend to be steeply-dipping (with fault-plane dips typically in the range of 60°–90°) and with mainly dip-slip motion vectors.
2. *Thrust faults*, which occur in compressional tectonic settings and tend to be shallow-dipping (with fault-plane dips mainly in the range of 0°–30°) and with mainly dip-slip motion vectors.
3. *Strike-slip faults*, which are near-vertical and created by lateral-slip motions in compressional tectonic settings (e.g. mountain belts) and at transform plate margins.

All intermediate cases between these three end-member cases are possible, hence the terms 'oblique-slip', 'transtensional' and 'transpressional' to cover hybrid cases. Faults also tend to reactivate, for example normal faults in extensional basins may subsequently experience reverse fault motion during later phases of basin compression – the process of 'structural inversion'.

A founding principle in structural geology is the Anderson (1905) theory of faulting, which relates the stress system to the style of faulting. The stress field is summarised by three principle stresses:

$$\sigma_1 > \sigma_2 > \sigma_3$$

Anderson showed that (Fig. 6.44):

- Normal (extensional) faulting occurs when σ_1 is vertical and σ_2 and σ_3 are horizontal;

Fig. 6.43 Extensional fault network in Somerset – comparable geometries can also be observed on a seismic scale

- Thrust faulting occurs when σ_3 is vertical and σ_1 and σ_2 are horizontal;
- Strike-slip faulting occurs when σ_2 is vertical and σ_1 and σ_3 are horizontal.

This simple theory is founded in rock mechanical principles, where brittle failure occurs along surfaces of maximum shear. Failure occurs on one preferred slip plane, often accompanied by smaller movements on conjugate planes oriented approximately 60° from the main plane of shear failure.

For a fuller understanding of the processes involved we refer you to texts such as Twiss and Moores (1992) and Mandl (2000).

In practice, faults in reservoirs are not single 2D planes, but form zones in which many fractures coalesce. The result is a highly deformed fault core surrounded by a wider, less deformed damage zone. *Faults are therefore volumetric*. This is important to appreciate because on seismic, faults are usually interpreted as 2D planes, and are typically represented as 2D surfaces in reservoir and simulation models with little more analysis. The acknowledgment that fault zones represent volumes has a bearing on the world of modelling and simulation because faults then become 3D model elements, and all model elements must have petrophysical properties.

The best way to understand faults is to visit some. Essential fault terminology began in the mining industry, such that a mining geologist standing within a fault found the footwall at his feet and the hangingwall overhead (Fig. 6.45). With normal faults the hangingwall has moved *downwards* with respect to the footwall (in reverse or thrust faults the hangingwall has moved upwards). This basic terminology has developed into a wide set of vocabulary (e.g. Sibson 1977; Wise et al. 1984). In reservoir modelling it is convenient to treat fault zones in terms of two key components: the thin, very highly deformed fault core around the main slip surface (centimetres or 10's of centimetres across) and a wider fault damage zone, which is can be several metres or 10's of metres across.

6.7.1.2 Handling the Effects of Faulting

In reservoir modelling we are mainly concerned with the effects which faults have on fluid flow.

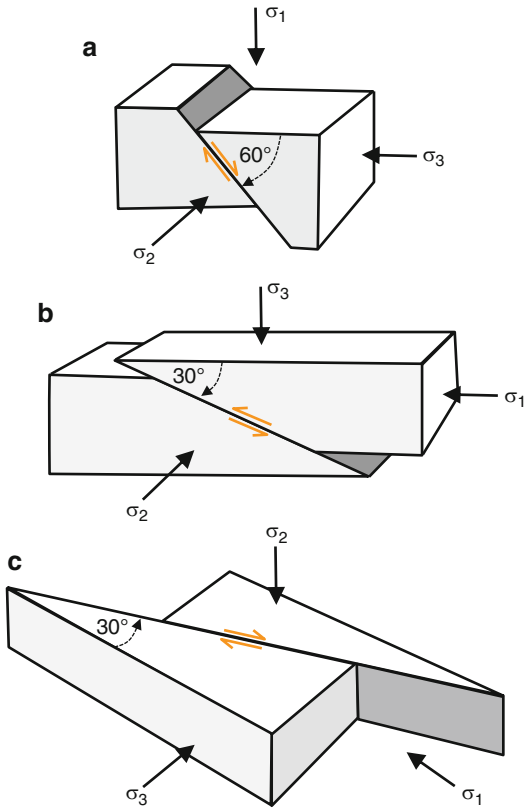

Fig. 6.44 Anderson theory of faulting relating faults to the principal stress directions: (**a**) normal faults, (**b**) thrust faults, and (**c**) strike-slip faults

We therefore need to translate structural geological features into their flow properties, and this is not an easy task. Faults often give rise to 'tales of the unexpected' in reservoir modelling studies because:

- They are relatively narrow features, hard to sample in well and core data and usually present on a sub-seismic scale;
- They generally have very low permeability and high capillary entry pressure;
- They are very heterogeneous, both in the plane of the fault zone and perpendicular to that plane;
- They introduce new layer connections due to fault offsets.

To have any chance of anticipating the potential effects of faults on flow behaviour in a reservoir, we need some appreciation of the mechanics of faults and the nature of their sealing properties. In reservoir modelling studies there are two main activities:

1. Representing fault geometry as accurately as possible based on the best available seismic data.
2. Representing the fault flow properties, using various methods for fault seal analysis.

6.7.1.3 Geometry

Estimating fault throw is a key uncertainty, as seismic image quality tends to deteriorate close to faults. Fault connections in the 3D network are a particular issue as fault intersections are rarely resolved accurately from seismic. It is therefore typically necessary to edit raw fault interpretations from seismic to produce a network which is structurally plausible (Fig. 6.46).

Judging whether the fault network interpreted from seismic is indeed plausible and reasonable is assisted by the knowledge that fault systems – unlike joint systems – are fractal in nature (Scholz and Aviles 1986; Walsh et al. 1991) so fault networks show size and property distributions which usually follow a power law. Walsh and Watterson (1988) showed that for many real fault datasets the length of a fault, L, is correlated with the maximum displacement on the fault, D, such that $D = L^2/P$ (where P is a rock property factor). A 10 km-long fault would typically have a maximum displacement of around 100 m. Similar relationships between fault thickness and displacement have also been established by Hull (1988) and Evans (1990).

6.7.1.4 Sealing Properties

Figure 6.47 shows an example fault where a few metres of displacement have created a fault with a thickness of a few centimetres. Also clearly seen in this example is the drag of a shale layer along the fault surface creating a baffle or seal between juxtaposed sandstone layers – the formation of a 'fault gouge' (Yielding et al. 1997; Fisher and Knipe 1998).

Empirical data from fault systems has led to a set of quantitative methods for predicting the sealing properties of faults. The most widely used method is the shale gouge ratio, SGR, proposed by Yielding et al. (1997) who showed that the cumulative shale bed thickness in a faulted siliciclastic reservoir sequence could be used to

Fig. 6.45 Normal fault exposed in Permian dune sands at Clashach near Elgin, Scotland, with essential fault terms indicated

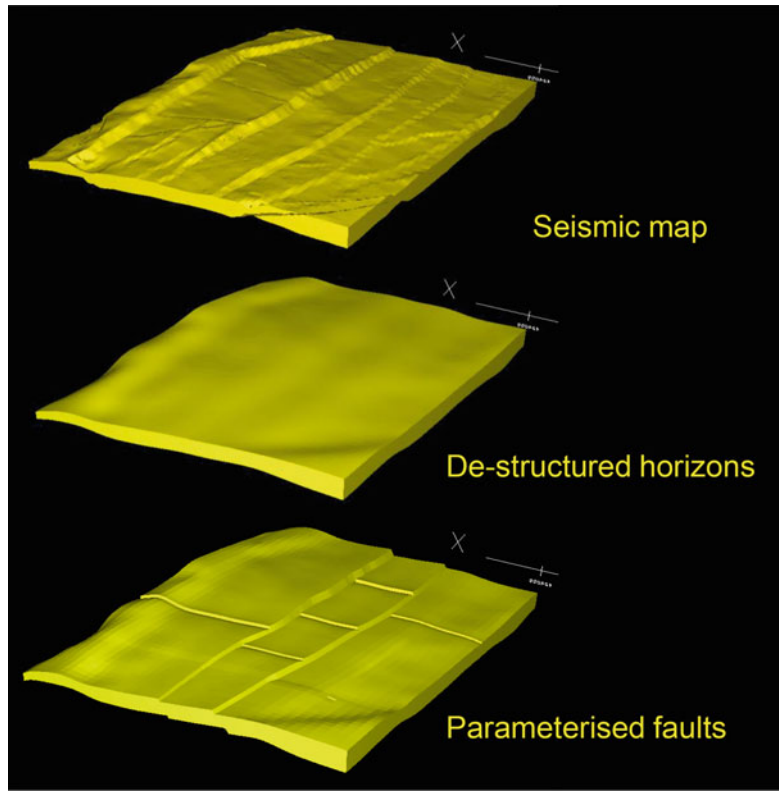

Fig. 6.46 Example workflow for modelling faults from seismic data (central fault block is ~1 km wide) (Statoil image archive, © Statoil ASA, reproduced with permission)

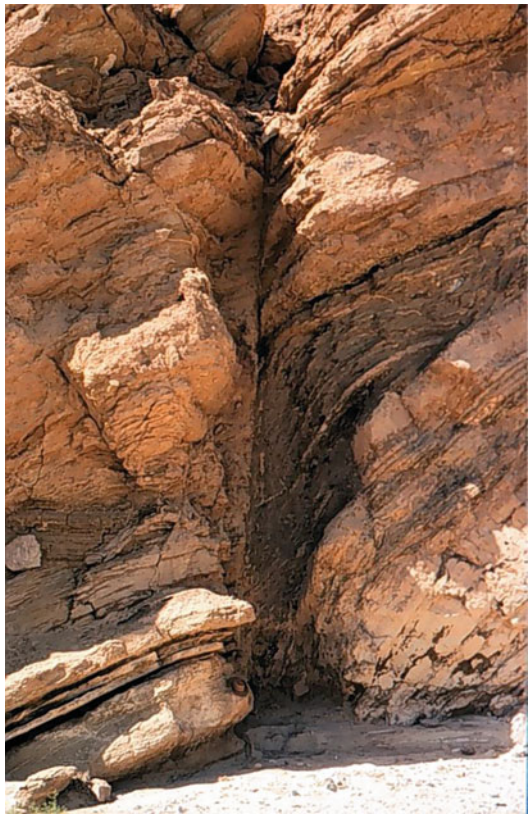

Fig. 6.47 Small normal fault in an inter-bedded sand-shale sequence (width of image 2 m)

predict fault seal based on observed across-fault pressure differences. They defined the SGR for a specific reservoir interval as:

$$SGR = \frac{\Sigma(Shale\,bed\,thickness)}{Fault\,throw} \times 100\,\%$$

Other factors used in fault seal analysis include the clay smear potential (CSP) and the shale smear factor (SSF), but the SGR method is most widely applied. Modifications to the SGR method include corrections for actual clay mineral content of shaly beds (Sperrevik et al. 2002).

The effects of fault seal variation across fault zones intersecting a multi-layer reservoir interval can then be mapped using fault juxtaposition diagrams, to which a measure of seal potential can be added (Bentley and Barry 1991; Knipe 1997).

Despite the utility of proposed predictive tools for fault seal analysis such as SGR, it should be appreciated that faults are highly complex geological features containing multiple elements acting both as flow conduits and barriers (e.g. Caine et al. 1996; Manzocchi et al. 1998, 2010). Fault flow properties also depend on the *in situ* stress field, a factor we will consider further in the high-density fractured reservoir section below.

Fig. 6.48 Simple analytical petroleum trap filled to the spill point and leaking through a fault with a lower P_{CT} than the caprock (from Ringrose et al. 2000)

6.7.1.5 Flow Properties

Although sometimes acting as flow barriers, faults can also be open to cross-flow and can discriminate between fluids – that is, they have multiphase flow properties related to capillary and surface tension effects. These effects can be subtle and quite substantial. In some cases a fault can retain an oil column of several 10's of metres while still being permeable to water.

For the simplest case of a water-wet low-permeability fault rock, we can define the capillary threshold pressure, P_{CT}, required to allow the non-wetting phase to flow (Manzocchi and Childs 2013), e.g. for a static oil-water system:

$$P_{CT} = (\rho_w - \rho_o) g\, h_o$$

where h_o is the oil column height.

If the fluid pressure of the oil column exceeds the P_{CT} of the fault then oil will flow across the fault, if not then the fault will be permeable only to water. Figure 6.48 shows an example of a simulated leaky fault seal, using these capillary-controlled flow conditions.

In the case of non-static conditions, where natural hydrodynamic gradients exist or lateral pressures are applied (by injection or production) additional terms for lateral pressure gradients in the water or oil phase need to be taken into account (see Manzocchi and Childs 2013).

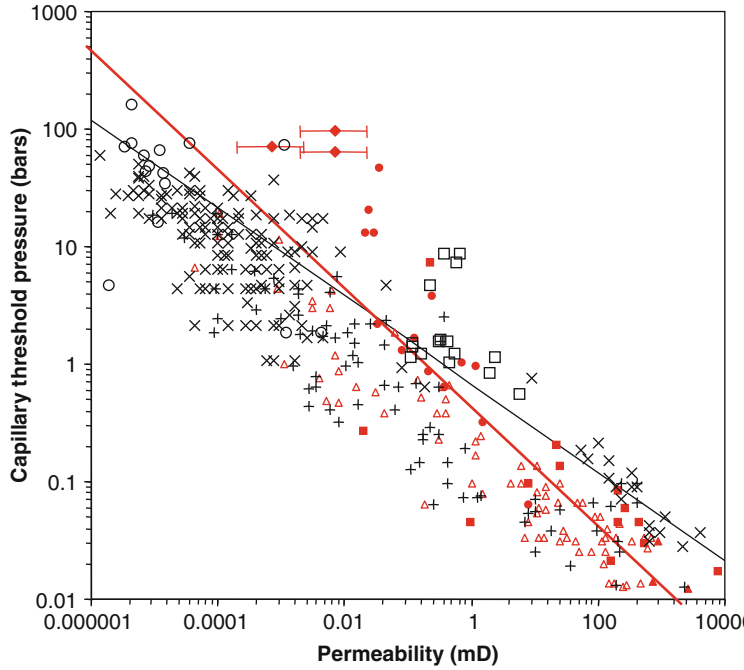

Fig. 6.49 Capillary threshold pressure versus permeability from a compiled dataset of fault-rock samples (*solid symbols*) and unfaulted rock samples (*crosses* and *open symbols*) from Manzocchi et al. (2002) and T. Manzocchi (pers. comm.). The two lines are published model relationships for unfaulted rocks (*black line*, Ringrose et al. 1993) and faulted rocks (*red line*, Harper and Lundin 1997). For sources of datasets see Manzocchi et al. (2002). Data have been normalized for a moderately water-wet oil-water system (Redrawn from Manzocchi et al. 2002, Petroleum Geoscience, v. 8 © Geological Society of London [2002])

Wherever faults are important in reservoir modelling studies, considerable efforts are needed to measure fault rock properties (e.g. Sperrevik et al. 2002). Figure 6.49 shows a compiled set of measured values for P_{CT} as a function of permeability. Despite some spread in the data, general empirical transforms between permeability and capillary threshold pressure can be established. The trends for faulted and un-faulted rock samples are broadly similar, although low-permeability clay-rich fault rocks tend to have significantly higher P_{CT}.

In order to represent the effects of faults in reservoir flow simulation models, there are several options:

1. Represent the fault as a transmissibility multiplier on the simulation cell boundary which coincides with the fault plane (no multi-phase effects included);
2. Represent the fault as a two-phase flow transmissibility multiplier on the simulation cell boundary which coincides with the fault plane;
3. Represent the fault explicitly as a volume, using grid cells within the fault zone and adjacent to the fault zone or damage zone (with multi-phase effects included).

The third option allows detailed analysis of the effects of faults on flow, but is rarely used because it may be computationally demanding. The use of simple transmissibility multipliers allows for more efficient reservoir simulations, but neglects potentially important multi-phase flow effects. Manzocchi et al. (2002) proposed a versatile approach for inclusion of two-phase transmissibility multipliers to represent faults in reservoir simulation studies, allowing more structural geological detail to be included in reservoir models (e.g. Brandsæter et al. 2001b; Manzocchi et al. 2008a, b).

6.7.1.6 Open Damage Zones

The discussion above concerns situations in which low density fracture systems tend to seal or at least reduce permeability *across* the fault

zone. There is now an increasing awareness that even if a fault core is sealing, the fractures in the fault damage zone may be open to flow *up or along* the fault zone.

The Douglas Field in the East Irish Sea provides an example of this, for which a simple modelling workflow was designed (Bentley and Elliott 2008). The interpretation of open damage zones was prompted by the anomalous water-cut behaviour of some wells and the inability to match history using conventional simulation modelling of the reservoir matrix. The anomalous behaviour took three forms:

1. Water breakthrough not matched in wells drilled close to or through major faults.
2. Gas breakthrough not matched in wells post gas injection into a flank well in the field.
3. Flowing bottom-hole pressures not matched in most wells.

In order to address these observations, three activities were initiated (a) re-visit the core store; (b) understand fault-related processes using outcrop analogues, and (c) re-design the reservoir modelling approach using the new insights.

The revised geological concept which emerged from these studies was one of zones of damage around seismic-scale faults containing both permeability-reducing and permeability-enhancing elements. The sealing elements were the small shear fractures, observed as deformation bands in quartz-rich layers or as small discrete faults in more mud-rich intervals, and the master fault slip surfaces themselves. Evidence of fracturing in the core material is sparse, as the core was taken in vertical appraisal wells. Fracturing was nevertheless observed in core in the form of deformation bands and small faulted intervals. One fault plane in particular was well preserved in core, was not cemented and, crucially, was observed to be hydrocarbon stained (Fig. 6.50). Some fractures were clearly permeable.

The structural concept which emerged from the review is summarised in Fig. 6.51. Although major faults tend to seal to lateral cross-flow, either through juxtaposition, the formation of a sealing fault gouge or the generation of deformation bands, the damage zones around the faults include open fractures, either joints or small faults. The joints will tend to be stratigraphically sensitive and bed-limited to the quartz-rich intervals, but the slip surfaces will be throughgoing. The major faults therefore exhibit a tendency to seal laterally but also a tendency for vertical flow along open damage zones.

Fig. 6.50 Open fractures associated with deformation bands in Ormskirk Sandstone core from the Douglas Field

In order to model the effects of this concept, involving both conductive fractures and sealing faults, a novel approach to modelling the fault damage zones was implemented, using artificial wells ('pipes') to create flow conduits along suspected fracture zones.

The pipes were assigned with open flow completions in each simulation grid block along the fracture corridor to allow cross-flow within the formation. Altering the radii of the pipes provided a method of history matching the rapid onset of water production (Fig. 6.52). The approach readily allowed a successful history match, successfully replicating the observed water break through patterns, the gas-oil ratio changes and the recorded flowing bottom-hole pressures.

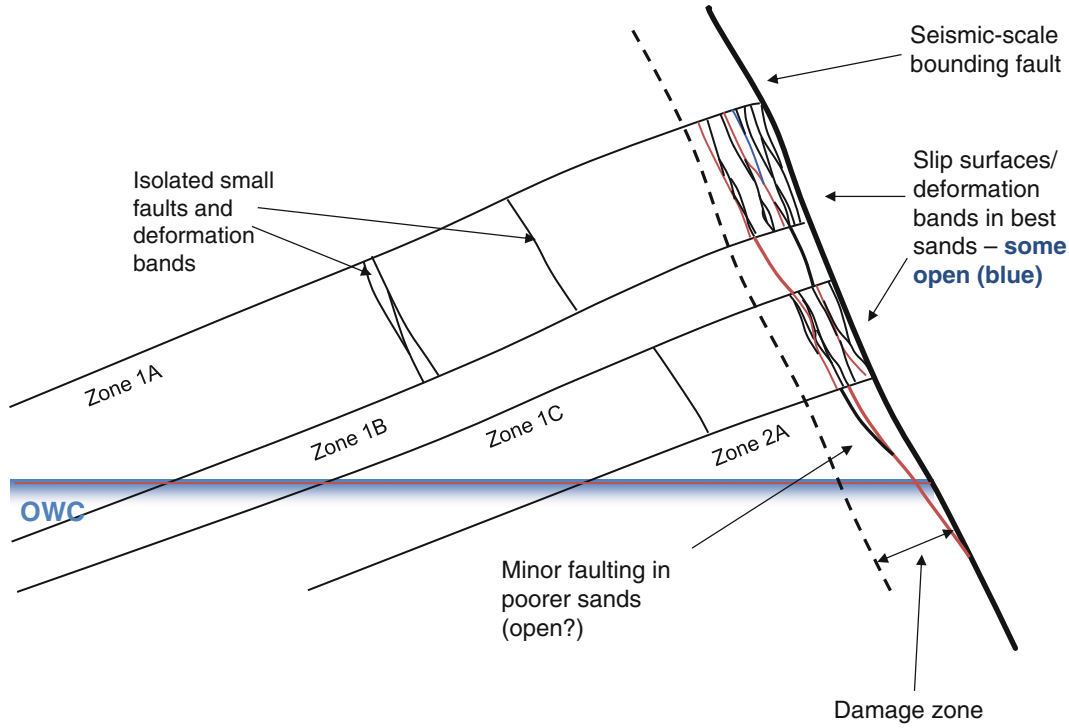

Fig. 6.51 Structural concept for the major fault terraces in the Douglas field (Redrawn from Bentley and Elliott 2008, ©2008, Society of Petroleum Engineers Inc., reproduced with permission of SPE. Further reproduction prohibited without permission)

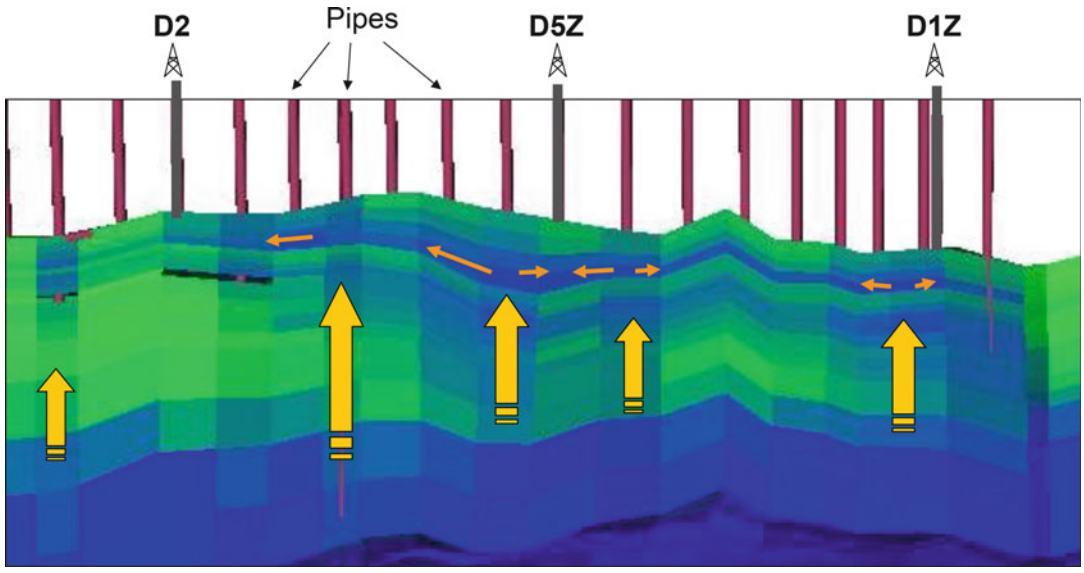

Fig. 6.52 Use of 'pipes' (dummy wells) to represent open fault damage zones in the Douglas Field (Bentley and Elliott 2008); view is towards the footwall of a seismic-scale fault; *blue* = water; *green* = oil, pipes (*red*) are positioned in simulation grid cells adjacent to the fault. Water is drawn up the damage zone and along the highest permeability matrix towards the producers (*black*) in response to depletion (Redrawn from Bentley and Elliott 2008, ©2008, Society of Petroleum Engineers Inc., reproduced with permission of SPE. Further reproduction prohibited without permission)

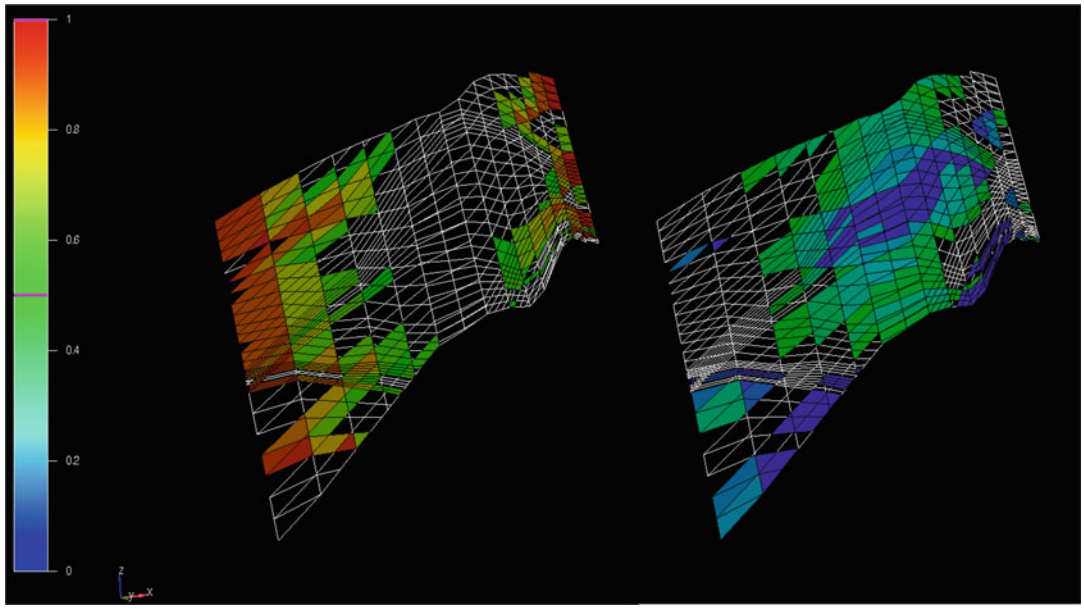

Fig. 6.53 Example fault-plane mesh (circa 5 km long and 100 m high) showing hanging-wall to footwall grid connections with estimated fault transmissibility multipliers: *hot colours* representing higher transmissibility at fault margins (*left*) and *cold colours* representing lower transmissibility closer to the centre of the fault (*right*) (Statoil image archive, © Statoil ASA, reproduced with permission)

This example illustrates, once again, the importance of the conceptual geological model as a foundation for reservoir modelling. In this case, failure of the initial conceptual model to include the effects of low-density fracture systems was the source of the failure to match the dynamic field data. The change in the geological interpretation was prompted by an accumulation of production data which was inconsistent with other interpretations. Once sense-checked against core data, outcrop data and structural geological theory, a new model emerged, which was not only geologically plausible but also led to significantly improved interpretation of rather complex subsurface flow behaviour. This case also highlights the importance of understanding faults as heterogeneous 3D zones, rather than 2D planes of offset.

6.7.1.7 Fault-Related Uncertainties

The Douglas Field Example highlights the limitation of becoming locked into a best-guess or base-scale conceptual geological model.

Although it is critical to maintain alternative reservoir concepts through the life cycle of a reservoir development, there is often a reluctance to expend the additional effort required to build alternative structural models. This is unwise, especially as fault uncertainties are always significant – they are never perfectly imaged on seismic data and their fractal nature means sub-seismic fault populations will always exist. The question is how important are the effects of faults compared with other factors? These uncertainties are best handled by establishing fault-model workflows (e.g. Fig. 6.53) and testing alternative models within the uncertainty span. If deemed significant, fault-related uncertainties should be evaluated either using a relatively simple sensitivity analysis (e.g. Brandsæter et al. 2001b), a practical modelling work-around such as the Douglas Field case (Bentley and Elliott 2008), or using an integrated experimental design scheme for assessing the impact of different factors on reservoir performance metrics (e.g. Lescoffit and Townsend 2005; Manzocchi et al. 2008a).

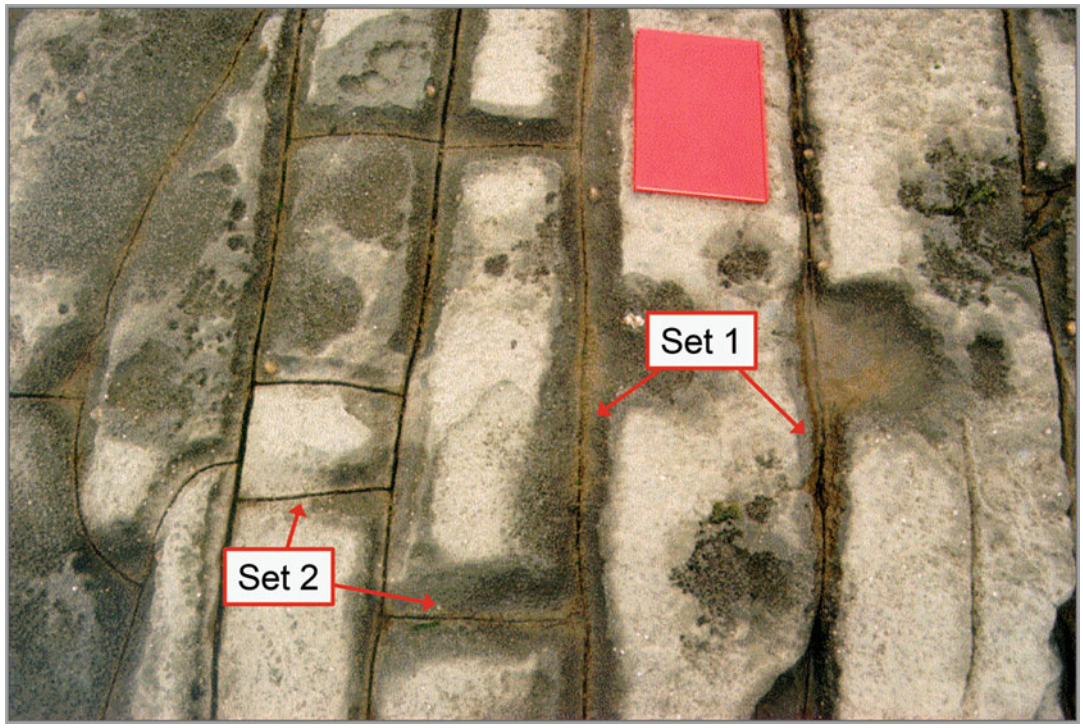

Fig. 6.54 Two joint sets abutting in a sandstone layer (view *down* on to the layer *top*)

A typical uncertainty list for handling fault-related factors would be:

1. *How many faults*? Scenarios might include (a) all seismically-mapped faults, (b) uncertain faults evident from seismic coherence analysis, edge-detection or curvature analysis, (c) sub-seismic faults generated from structural deformation models.
2. *Fault displacement uncertainty*. Using maximum fault displacements observed from seismic data with a range of ±5 to ±10 m to reflect interpretation uncertainties.
3. *Fault seal uncertainty*. Testing fully-sealed versus open fault scenarios, using a shale gouge ratio (SGR) method linked to displacement uncertainties, or using a range of measured fault-seal values.
4. *Development scenario uncertainty*. Well placement strategy is usually closely linked to the overall structural model (bounding faults and internal fault compartments). Why allow the whole field development strategy to depend entirely on an uncertain base-case structural model? Better to test the well placement strategy against a range of models to ensure some degree of robustness.

6.7.2 High Density Fractured Reservoirs (Joint-Dominated)

6.7.2.1 Terminology

Joints are extensional fractures, formed when rocks enter tensile space (the left-hand side of the Mohr diagram) under a deviatoric stress in excess of the tensile rock strength. They tend to form regularly-spaced fractures (Fig. 6.54) often in more than one set, with sets mutually abutting. Lateral displacement on joints is minimal, although not necessarily zero as once a tensile fracture has formed there may be millions of years of isostatic activity to follow during which some movement on any open fracture is inevitable.

The properties of joint sets are influenced strongly by the mechanical properties of the

Fig. 6.55 Classic natural fracture (joint) systems in Shuaiba-analogue limestones near Cassis, Southern France

host rock – brittle rocks form joints more readily – so joints are often bed-limited. Mechanical stratigraphy is therefore important in understanding joint patterns. Unlike fault networks the statistics of joint sets (in terms of frequency vs. size) are typically lognormal. The classic 'naturally-fractured reservoir' is typically a joint-network reservoir, in which production is dominated by flow from widespread, high-density fracture networks such as those seen at outcrop in Fig. 6.55.

In addition to the dispersed joint systems shown in Fig. 6.55, more localised joint networks occur in response to the development of other structures. Two common relationships are illustrated in Figs. 6.56 and 6.57. The first is fold-related, in which the hinge of a folded but competent mechanical layer is 'nudged' into tensile failure. Note how the underlying, more ductile layer lacks the joints – it doesn't fail in the same way.

The second is fault-related. This can produce highly localised features – as in the open damage zone case of the Douglas Field described in the previous section. If the fault density is high, however, or the reservoir rock brittle (as in carbonate reservoirs), fault-related fracturing can generate widespread open fracture systems.

The expected flow behaviour of the three joint systems shown in Figs. 6.55, 6.56, and 6.57 is also very different – so once again the key is to develop plausible fracture distribution concepts before starting the modelling – simple sketches are needed. These can be used as the basis for choosing optimal model designs, of which there are several to select.

Fig. 6.56 Fold-related jointing, Carboniferous exposures, Northumberland, UK

Fig. 6.57 Fault-related jointing in a fault damage zone, Brushy Canyon, USA

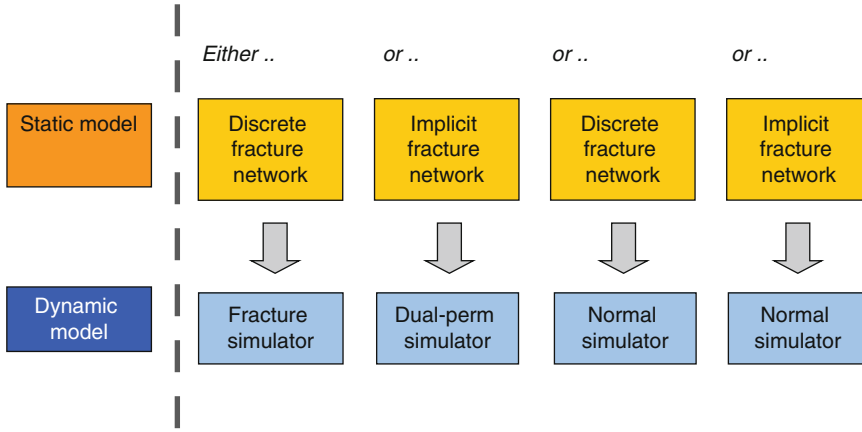

Fig. 6.58 Alternative modelling workflows for high density fracture systems

6.7.2.2 Handling High-Density Fracture Systems

There are numerous ways of modelling high-density fracture systems, ranging from the very simple to the complex. From the reservoir engineering viewpoint, the focus is on whether the fracture and matrix should both be permeable and porous (i.e. should neighbouring grid cells connect through the matrix, the fractures, or both). Hence, the distinction between dual-permeability/dual-porosity models, dual-permeability/single-porosity, or single-permeability/single-porosity models.

In terms of choosing a model design, another distinction of the static and dynamic workflows is whether the fractures are to be modelled as explicit or implicit model properties. All combinations are possible (Fig. 6.58) and all are workable.

The big issue for reservoir modellers is that explicit methods are generally more time-consuming, both in terms of people-time and computer-time.

6.7.2.3 Discrete Fracture Network (DFN) Models

Explicit fracture modelling methods are generally described as discrete fracture network models (DFNs) and involve building digital representations of the fracture planes (Fig. 6.59).

These packages were designed for high density networks and were built for classic joint-dominated naturally fractured reservoirs. Having built them, specialist simulators are then required to model flow through the discrete fracture planes (Fig. 6.60).

On the computing side, fracture modelling algorithms are a lot less mature than standard modelling tools. They also tend to exhibit incompleteness, in that there is only so much detail the current algorithms can capture explicitly e.g. are fractures assumed to have constant properties? Technical guidance for correctly upscaling multiphase fracture properties is limited, but also more practical matters such as hardware memory limitations may limit what can currently be achieved.

Whilst appearing to offer an ultimate solution to the fracture modelling need, the DFN solution is therefore not always manageable or practical, and high levels of approximation must often be accepted to implement this approach. Attempts at full-field DFN models – literally modelling every crack in the reservoir – are generally unrealistic and at a certain level of approximation, it can be queried whether the discrete model description is adding much value beyond visualisation.

The most successful implementations of DFN models are those built at the well-model scale, and used to match well test data (e.g. Fig. 6.59). The outputs from this type of explicit fracture

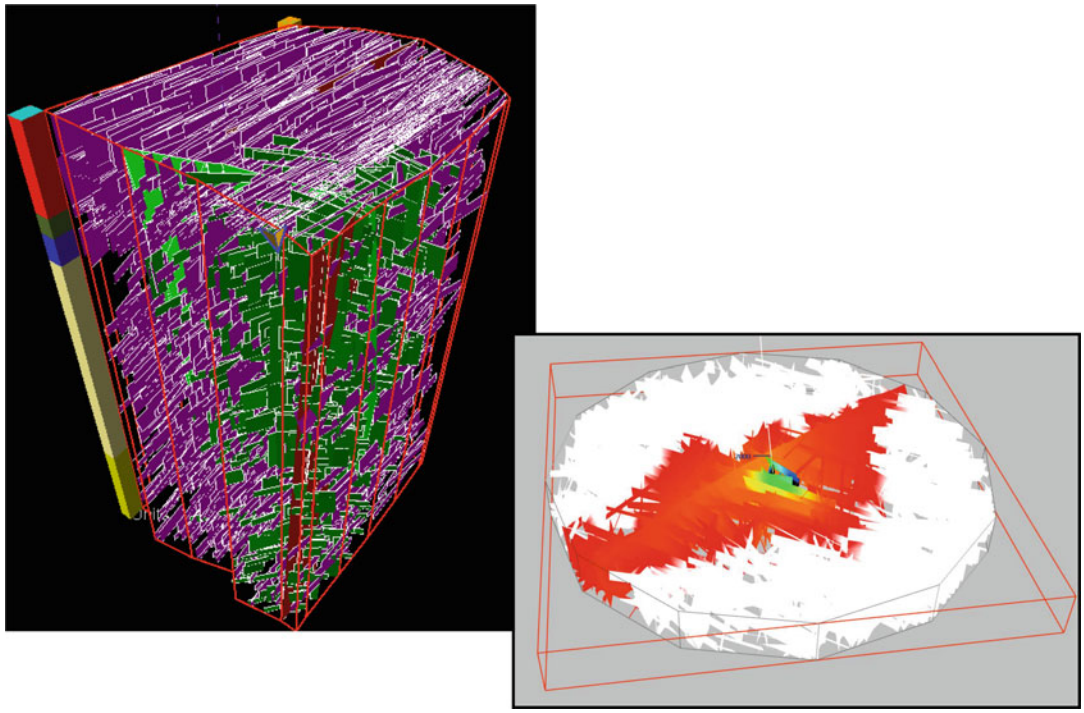

Fig. 6.59 Discrete Fracture Network (DFN) models: *Main image:* a static fracture model for a near-wellbore volume; *inset:* simulated well test in a dynamic DFN (Images courtesy of J. Hadwin and T. Wynn, Tracs International)

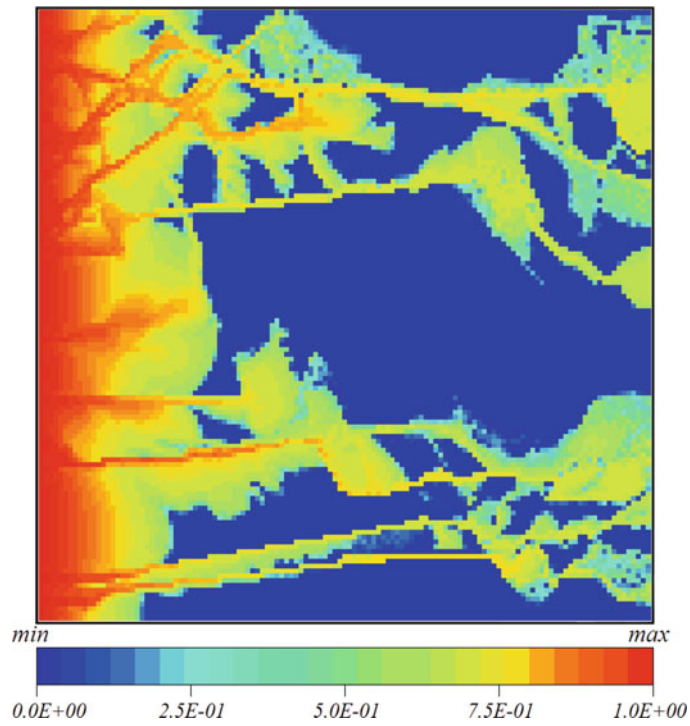

Fig. 6.60 Example simulation of water (*red*) displacing oil (*blue*) in a permeable rock model with open fractures (Redrawn from Bech et al. 2001) (Image courtesy of N. Odling (U. Leeds), modified from Bech et al. 2001)

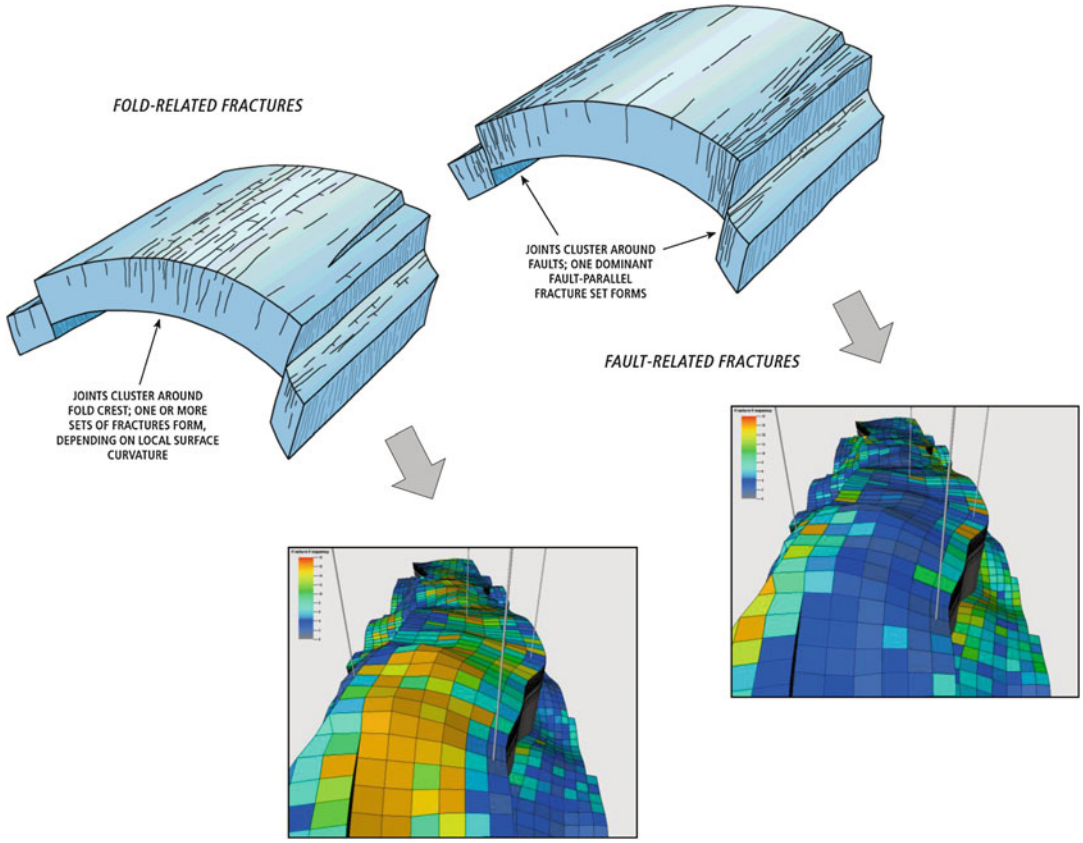

Fig. 6.61 Alternative concepts for fracture distribution (fold- or fault-related), and property models for fracture density which honour those concepts implicitly (*hot colours* = higher fracture density)

modelling (in terms of effective permeabilities) then become the inputs to more implicit modelling methods at the full-field scale, as discussed below.

6.7.2.4 Implicit Fracture Property Models

Implicit methods abandon the aspiration to represent fractures as planes, and instead treat the dense fracture systems as a volumetric property of a standard cellular model.

Simulators can accomplish this when working in 'dual permeability' mode. Two modelling grids are set up: one to handle the matrix properties and one to handle the fractures. The two grids exist in the same geographic space and a functional relationship (often termed the 'shape factor') is used to control how the two grid-cell meshes should 'talk to each other' and exchange fluids. A common assumption is that capillary flow processes dominate the fluid exchange between the matrix block and the fracture network, while viscous (Darcy) flow processes dominate in the fracture network. Note also that flow in fractures is governed by Poiseuille's law (Chap. 3.2).

Given that dual-permeability mode simulation needs implicit fracture properties, modelling workflows can be devised to provide these inputs from standard geocellular modelling software packages. One such example is shown in Fig. 6.61, following a workflow described in Fig. 6.62 – which involves the production of reservoir property models for fracture permeability, fracture density, fracture porosity and fracture geometry (affecting the shape factor).

The advantage of implicit fracture modelling methods is that they can be applied in conventional modelling packages, and therefore easily

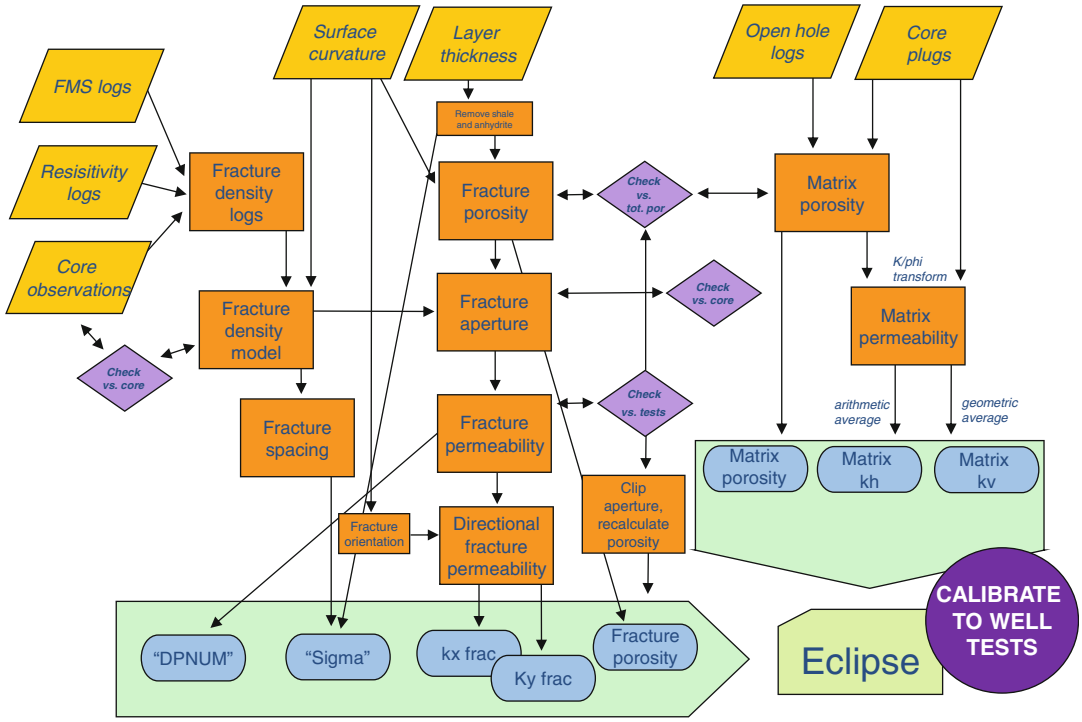

Fig. 6.62 Workflow for implicit static description of fractures, feeding into standard dual-permeability simulations

combined with standard workflows for modelling the matrix (the right hand side of Fig. 6.62).

The same logic can be applied to the dynamic model, in which the effective flow properties of a 'fracture REV' can be established using small-scale models, and applied directly in a standard single porosity, single permeability simulator. Numerous assumptions must be made along the way, and it is important to check whether the underlying fracture concept has been compromised in the process. This is particularly the case for ensuring an appropriate level of network connectivity on the cell-to-cell scale: if the concept is for field-wide fracture continuity in a particular direction, is that appropriately represented in the dynamic model?

6.7.2.5 Handling the Effects of Stress

A prescient challenge for fracture modelling, for both the explicit and implicit approaches, is capturing the effects of stress. The present-day stress system will act on the inherited sets of fractures to determine their fluid flow properties. Fractures which are favourably aligned to the present-day stress field will tend to be more open and conductive than fractures which are in compression. In reservoir modelling, conditioning static fracture models to dynamic data (well tests and production data) often acts as a proxy to stress-modelling, since the dynamic data indicates which fractures are actually flowing. However, this may not be very predictive, and so it may be preferable to try and forward-model or 'forecast' which fractures are most likely to be conductive.

Predicting the effects of the stress field on fracture flow properties is a significant challenge, so that a more realistic modelling objective is to allow fracture flow properties to be 'stress sensitive' – that is to try to capture the relationship between fracture conductivity and orientation. Bond et al. (2013) successfully demonstrated this approach by modelling fracture anisotropy as controlled by the stress field, for a CO_2 storage modelling study. They used dilation tendency T_d, as the controlling factor:

$$T_d = (\sigma_1 - \sigma_n)(\sigma_3 - \sigma_n)$$

where σ_n is the normal stress on the fracture plane.

This allows the stress field to operate as a control on the fracture flow properties, generating a tensor permeability matrix for the fracture permeability (*cf.* Sect. 3.2). The fracture network properties still need to be calibrated to static and dynamic data (e.g. image logs, seismic data and well tests), but now the effects of stress are also included. The stress field in itself may be hard to determine accurately, and alternative stress field scenarios may need to be evaluated, ideally within a framework of multiple deterministic scenarios.

6.7.2.6 Forward-Modelling or Inversion?

In discussing carbonate reservoirs (Sect. 6.6), the point was made that once a significant number of assumptions have been made in a complex modelling workflow it can be questioned whether attempts to forward-model reality from limited data are still valid. This is particularly the case for fractured reservoirs, where necessary static field data is limited and the sensitivity to the missing data is high. For example, fracture permeability is particularly sensitive to fracture aperture, yet *in situ* aperture data is extremely difficult to determine. Average aperture can be back-calculated if fracture density and gross fracture porosity are known, but fracture porosity is also difficult to measure and even estimates of fracture density are usually built on very limited data sets. Many assumptions must be made, in addition to those routinely made for modelling the matrix properties. By definition, fractured reservoir models involve a greater degree of approximation than models for un-fractured reservoirs.

Because of this, there is a greater reliance on using production data, and in this sense fracture models are typically 'inverted' from production data rather than forward-modelled from logs and core. Indeed, one of the most useful roles of DFN software is to reconcile well test data with potential fracture network properties – the missing fracture data is effectively inverted from the well test data.

This is captured in the workflow shown in Fig. 6.62 in which the forward modelling steps culminate in the need to 'calibrate to well tests', after which several of the fracture parameters may need to be significantly adjusted. It is not uncommon for orders of magnitude permeability adjustments to be made in order to reconcile models with production data; in matrix-only reservoirs the permeability adjustments are more normally no more than a factor 2 or 3, or none at all.

This leads to some general implications for the use of fracture models:

1. In inversion-style workflows the production data is often treated as representative for the field; if based on a single well test, this is unlikely to be the case.
2. The inversion process is itself non-unique.
3. Because of the above, base-case fracture models are of even less value than base-case matrix models – multi-model uncertainty-handling based on alternative fracture concepts and scenarios is essential.

6.8 Fit-for-Purpose Recapitulation

The preceding sections have discussed different reservoir types in terms of their geology, identifying the key issues for reservoir modelling with an underlying assumption that we are generally talking about oil fields. However, as pointed out in Chap. 2 (Ref. Fig. 2.14) and then developed further in Chap. 4 (Ref. Fig. 4.29) the type of fluid is as important as the type of rock system. The effects of fluid physics have to be considered alongside the effects of rock architecture.

To reiterate the underlying principle, for any given reservoir architecture (e.g. fluvial, shallow marine, carbonate, or structurally complex fields) the impact of the reservoir heterogeneities on flow depends on the fluid system. Using the handy rule of thumb (Flora's rule, Chap. 2):

- A gas reservoir is only sensitive to 3 orders of magnitude of permeability variation;
- An oil reservoir is sensitive to 2 orders of magnitude of permeability variation;
- Heavy oil reservoirs or lighter crudes under secondary recovery (waterflood) are sensitive to 1 order of magnitude of permeability variation.

This is only intended as a rule of thumb, but reminds us to consider the fluid system before launching into a detailed reservoir modelling study. Gas reservoirs under depletion will require much less modelling and characterisation effort than oil reservoirs under waterflood, and heavy oil reservoirs may require very intense efforts to identify the critical effects of rock architecture on the fluid displacement mechanism.

One important caveat to this principle is that it assumes you know what the permeability variation of your reservoir is *a priori*. We know from our discussion of the treatment of generally incomplete subsurface datasets (Chap. 3) that a few core plugs from an appraisal well may give a false impression of the permeability variation in the reservoir. Several gas reservoir developments started with the assumption that internal permeability variations in the reservoir were insignificant, and that a 'reservoir tank' model was therefore adequate, only to find later that certain previously unidentified high-k thief zones or barriers did in fact have a major impact on the gas depletion rates.

Every heterogeneous reservoir is heterogeneous in its own way. Although this is true, generic issues can be extracted for different reservoir types, as the preceding pages have aimed to illustrate. These common features should allow the reservoir modeller to achieve a fit-for-purpose approach to the case at hand. In all cases three things are essential:

(a) Developing good conceptual reservoir models;
(b) Understanding how the fluid system interacts with the reservoir heterogeneity;
(c) Maintaining alternative concepts in order to handle uncertainties.

References

Agar SM, Hampson GJ (2014) Fundamental controls on flow in carbonates: an introduction. Petrol Geosci 20 (1):3–5. doi:10.1144/petgeo2013-090

Allen PA, Underhill JR (1989) Swaley cross stratification produced by unidirectional flows, Beneliff Grit (Jurassic), Dorset, U.K. J Geol Soc Lond 146:241–252

Almeida AS, Frykman P (1994) Geostatistical modeling of chalk reservoir properties in the Dan field, Danish North Sea. In: Computer application, vol 3. The American Association of Petroleum Geologists, Tulsa, pp 273–286

Anderson EM (1905) The dynamics of faulting. Trans Edinb Geol Soc 8(3):387–402

Bech N, Bourgine B, Castaing C, Chilés J-P, Christensen NP, Frykman P, Genter A, Gillespie PA, Høier C, Klinkby L, Lanini S, Lindgaard HF, Manzocchi T, Middleton MF, Naismith J, Odling N, Rosendal A, Siegel P, Thrane L, Trice R, Walsh JJ, Wendling J, Zinck-Jørgensen K (2001) Fracture interpretation and flow modelling in fractured reservoirs. European Commission Publication, Brussells. ISBN 92-894-2005-7

Bentley MR, Barry JJ (1991) Representation of fault sealing in a reservoir simulation: Cormorant block IV UK North Sea. SPE paper 22667 presented at the SPE annual technical conference and exhibition, Dallas, Texas, 6–9 October

Bentley M, Elliott A (2008) Modelling flow along fault damage zones in a sandstone reservoir; an unconventional modelling technique using conventional modelling tools in the Douglas Field, Irish Sea, UK. SPE paper 113958 presented at Europec/EAGE conference and exhibition, Rome, Italy, 9–12 June 2008

Bentley M, Hartung M (2001) A 4D surprise at Gannet B; a way forward through seismically-constrained scenario-based reservoir modelling. Extended abstract, EAGE annual conference, Amsterdam

Bond C, Wightman R, Ringrose P (2013) The influence of fracture anisotropy on CO_2 flow. Geophys Res Lett 40:1284–1289. doi:10.1002/grl.50313

Brandsæter I, Wist HT, Næss A et al (2001a) Ranking of stochastic realizations of complex tidal reservoirs using streamline simulation criteria. Petrol Geosci Spec Issue 7:S53–S63

Brandsæter I, Ringrose PS, Townsend CT, Omdal, S (2001b) Integrated modeling of geological heterogeneity and fluid displacement: Smørbukk gas-condensate field, Offshore Mid-Norway. SPE paper 66391, Society of Petroleum Engineers, Richardson, pp 11–14. doi:10.2118/66391-MS

Brandsæter I, McIlroy D, Lia O, Ringrose PS (2005) Reservoir modelling of the Lajas outcrop (Argentina) to constrain tidal reservoirs of the Haltenbanken (Norway). Petrol Geosci 11:37–46

Bromley RG (1996) Trace fossils: biology, taphonomy and applications. Chapman & Hall, London

Burchette TP (2012) Carbonate rocks and petroleum reservoirs: a geological perspective from the industry. Geol Soc Lond Spec Publ 370(1):17–37

Caine JS, Evans JP, Forster CB (1996) Fault zone architecture and permeability structure. Geology 24(11):1025–1028

Carruthers DJF (1998) Transport modelling of secondary oil migration using gradient-driven invasion percolation techniques. PhD thesis, Heriot-Watt University, UK

Carruthers DJF, Ringrose PS (1998) Secondary oil migration: oil-rock contact volumes, flow behaviour and

rates. In: Parnell J (ed) Dating and duration of fluid flow and fluid rock interaction, Geological Society special publication, 144. The Geological Society, London, pp 205–220

Ciammetti G, Ringrose PS, Good TR, Lewis JML, Sorbie KS (1995) Waterflood recovery and fluid flow upscaling in a shallow marine and fluvial sandstone sequence. SPE 30783, presented at the SPE annual technical conference and exhibition, Dallas, USA, 22–25 October 1995

Ciftci BN, Aviantara AA, Hurley NF, Kerr DR (2004) Outcrop-based three-dimensional modeling of the Tensleep Sandstone at Alkali Creek, Bighorn Basin, Wyoming. In: Integration of outcrop and modern analogs in reservoir modeling. American Association of Petroleum Geologists, Tulsa, pp 235–259 (archives.datapages.com)

Corbett PWM, Ringrose PS, Jensen JL, Sorbie KS (1992) Laminated clastic reservoirs: the interplay of capillary pressure and sedimentary architecture. SPE paper 24699, presented at the SPE annual technical conference, Washington, DC

Dalrymple RW, Rhodes RN (1995) Estuarine dunes and bars. In: Perillo GME (ed) Geomorphology and sedimentology of estuaries, Developments in sedimentology, 53. Elsevier, Amsterdam, pp 359–422

Dalrymple RW, Zaitlin BA, Boyd R (1992) Estuarine facies models: conceptual basis and stratigraphic implications. J Sediment Petrol 62:1130–1146, Geoscience 11:37–46

de Gennes PG (1976) La Percolation: un concept unificateur. La recherche 7:919

Deutsch C (1989) Calculating effective absolute permeability in sandstone/shale sequences. SPE Form Eval 4:343–348

Dreyer T, Fält L-M, Høy T, Knarud R, Steel R, Cuevas J-L (1993) Sedimentary architecture of field analogues for reservoir information (SAFARI): a case study of the fluvial Escanilla formation, Spanish Pyrenees. In: Flint S, Bryant ID (eds) Quantitative description and modeling of clastic hydrocarbon reservoirs and outcrop analogues, Special publication of the international association of sedimentologists, vol 15, Blackwell Publishing Ltd

Droste H, Van Steenwinkel M (2004) Stratal geometries and patterns of platform carbonates: the Cretaceous of Oman. In: Eberli GP, Masaferro JL, Rick Sarg JF (eds) Seismic imaging of carbonate reservoirs and systems, AAPG memoir 81. American Association of Petroleum Geologists, Tulsa, pp 185–206

Dunham RJ (1962) Classification of carbonate rocks according to depositional texture. In: Classification of carbonate rocks: a symposium, vol 1. American Association of Petroleum Geologists, Tulsa, p 108

Elfenbein C, Ringrose P, Christie M (2005) Small-scale reservoir modeling tool optimizes recovery offshore Norway. World Oil 226(10):45–50

Evans JP (1990) Thickness-displacement relationships for fault zones. J Struct Geol 12(8):1061–1065

Fisher QJ, Knipe R (1998) Fault sealing processes in siliciclastic sediments. Geol Soc Lond Spec Publ 147(1):117–134

Fryberger SG (1990a) Eolian stratification. In: Fryberger SG, Krystinik LF, Schenk CJ (eds) Modern and ancient eolian deposits: petroleum exploration and production. SEPM Rocky Mountain Section, Denver, pp 4-1–4-12

Fryberger SG (1990b) Bounding surfaces in eolian deposits. In: Fryberger SG, Krystinik LF, Schenk CJ (eds) Modern and ancient eolian deposits: petroleum exploration and production. SEPM Rocky Mountain Section, Denver, pp 7-1–7-15

Haldorsen HH, MacDonald A (1987) Stochastic Modeling of Underground Reservoir Facies (SMURF). SPE paper 16751, presented at the 62nd annual technical conference and exhibition of the society of petroleum engineers, Dallas, TX, 27–30 September 1987

Harper TR, Lundin ER (1997) Fault seal analysis: reducing our dependence on empiricism. In: Møller-Pedersen P, Koestler AG (eds) Hydrocarbon seals: importance for exploration and production, Norwegian Petroleum Society special publications, 7. Elsevier, Amsterdam, pp 149–164

Hern CY (2000) Quantification of Aeolian architecture and the potential impact on reservoir performance. Institute of Petroleum Engineering, Heriot-Watt University. PhD, Unpublished thesis

Heward AP (1991) Inside Auk: the anatomy of an eolian oil reservoir. In: Miall AD, Tyler N (eds) The three-dimensional facies architecture of terrigenous clastic sediments and its implications for hydrocarbon discovery and recovery. SPEM, Tulsa, pp 44–56

Holden L, Hauge R, Skare Ø, Skorstad A (1998) Modeling of fluvial reservoirs with object models. Math Geol 30(5)

Howell JA, Skorstad A, MacDonald A, Fordham A, Flint S, Fjellvoll B, Manzocchi T (2008) Sedimentological parameterization of shallow-marine reservoirs. Petrol Geosci 14(1):17–34

Huang Y, Ringrose PS, Sorbie KS (1995) Capillary trapping mechanisms in water-wet laminated rock. SPE Reserv Eng 10:287–292

Huang Y, Ringrose PS, Sorbie KS, Larter SR (1996) The effects of heterogeneity and wettability on oil recovery from laminated sedimentary Structures. SPE J 1(4):451–461

Hull J (1988) Thickness-displacement relationships for deformation zones. J Struct Geol 10(4):431–435

Hunter RE (1977) Basic types of stratification in small eolian dunes. Sedimentology 24:361–387

Jacobsen T, Agustsson H, Alvestad J, Digranes P, Kaas I, Opdal S-T (2000) Modelling and identification of remaining reserves in the Gullfaks field. Paper SPE 65412 presented at the SPE European petroleum conference, Paris, France, 24–25 October

Kazemi A, Shaikhina D, Pickup G, Corbett P (2012) Comparison of upscaling methods in a heterogeneous carbonate model. SPE 154499 presented at SPE Europec/EAGE annual conference, Copenhagen, Denmark, 4–7 June 2012

Keogh KJ, Martinius AW, Osland R (2007) The development of fluvial stochastic modelling in the Norwegian oil industry: a historical review, subsurface implementation and future directions. Sediment Geol 202(1):249–268

King PR (1990) The connectivity and conductivity of overlapping sand bodies. In: Buller AT et al (eds) North sea oil and gas reservoirs II. Graham and Trotman, London, pp 353–358

Kjønsvik D, Doyle J, Jacobsen T, Jones A (1994) The effect of sedimentary heterogeneities on production from a shallow marine reservoir – what really matters? SPE paper 28445 presented at the European petroleum conference, London, 25–27 October 1994

Kneller BC (1995) Beyond the turbidite paradigm: physical models for deposition of turbidites and their implications for reservoir prediction. In: Hartley AJ, Prosser DJ (eds) Characterisation of deep marine clastic systems, Special publication 94. Geological Society, London, pp 31–49

Knipe RJ (1997) Juxtaposition and seal diagrams to help analyze fault seals in hydrocarbon reservoirs. AAPG Bull 81(2):187–195

Kocurek GA (1981) Significance of interdune deposits and bounding surfaces in eolian dune sands. Sedimentology 28:753–780

Krystinik LF (1990) Early diagenesis in continental eolian deposits. In: Fryberger SG, Krystinik LF, Schenk CJ (eds) Modern and ancient eolian deposits: petroleum exploration and production. SEPM Rocky Mountain Section, Denver, pp 79–89

Larue DK, Hovadik J (2006) Connectivity of channelized reservoirs: a modelling approach. Petrol Geosci 12(4):291–308

Leonide P, Borgomano J, Masse JP, Doublet S (2012) Relation between stratigraphic architecture and multi-scale heterogeneities in carbonate platforms: The barremian-lower aptian of the monts de vaucluse, S.E. France. Sediment Geol 265:87–109

Lescoffit G, Townsend C (2005) Quantifying the impact of fault modeling parameters on production forecasting for clastic reservoirs. In: Evaluating fault and cap rock seals, AAPG special volume Hedberg series, no. 2. American Association of Petroleum Geologists, Tulsa, pp 137–149

Lucia FJ (1983) Petrophysical parameters estimated from visual descriptions of carbonate rocks: a field classification of carbonate pore space. J Petrol Tech 35(03):629–637

Lucia FJ (2007) Carbonate reservoir characterization: an integrated approach. Springer, Berlin

Mandl G (2000) Faulting in brittle rocks: an introduction to the mechanics of tectonic faults. Springer, New York

Manzocchi T, Childs C (2013) Quantification of hydrodynamic effects on capillary seal capacity. Petrol Geosci 19(2):105–121

Manzocchi T, Ringrose PS, Underhill JR (1998) Flow through fault systems in high-porosity sandstones. Geol Soc Lond Spec Publ 127(1):65–82

Manzocchi T, Heath AE, Walsh JJ, Childs C (2002) The representation of two phase fault-rock properties in flow simulation models. Petrol Geosci 8(2):119–132

Manzocchi T, Carter JN, Skorstad A et al (2008a) Sensitivity of the impact of geological uncertainty on production from faulted and unfaulted shallow-marine oil reservoirs: objectives and methods. Petrol Geosci 14:3–15

Manzocchi T, Heath AE, Palananthakumar B, Childs C, Walsh JJ (2008b) Faults in conventional flow simulation models: a consideration of representational assumptions and geological uncertainties. Petrol Geosci 14(1):91–110

Manzocchi T, Childs C, Walsh JJ (2010) Faults and fault properties in hydrocarbon flow models. Geofluids 10(1–2):94–113

Martinius AW, Kaas I, Næss A, Helgesen G, Kjærefjord JM, Leith DA (2001) Sedimentology of the heterolithic and tide-dominated Tilje Formation (Early Jurassic, Halten Terrace, offshore mid-Norway). In: Martinsen OJ, Dreyer T (eds) Sedimentary environments offshore Norway – paleozoic to recent, Norwegian Petroleum Society, special publications, 10. Elsevier, Amsterdam, pp 103–144

Martinius AW, Ringrose PS, Brostrøm C, Elfenbein C, Næss A, Ringås JE (2005) Reservoir challenges of heterolithic tidal hydrocarbon fields (Halten Terrace, Mid Norway). Petrol Geosci 11:3–16

McIlroy D (2004) Some ichnological concepts, methodologies, applications and frontiers. Geol Soc Lond Spec Publ 228:3–27

Meadows NS, Beach A (1993) Controls on reservoir quality in the Triassic Sherwood sandstone of the Irish Sea. In: Petroleum geology conference series, vol 4. Geological Society, London, pp 823–833

Miall AD (1985) Architectural-element analysis: a new method of facies analysis applied to fluivial deposits. Earth Sci Rev 22:261–308

Miall AD (1988) Reservoir heterogeneities in fluvial sandstones: lessons learned from outcrop studies. Am Assoc Petrol Geol Bull 72:882–897

Nelson RA (2001) Geologic analysis of naturally fractured reservoirs, 2nd edn. Butterworth-Heinemann, Houston

Nilsen T, Shew R, Steffens G, Studlick J Eds. (2008) Atlas of deep-water outcrops. AAPG Stud Geol 56:181–184

Nordahl K, Ringrose PS (2008) Identifying the representative elementary volume for permeability in heterolithic deposits using numerical rock models. Math Geosci 40(7):753–771

Nordahl K, Ringrose PS, Wen R (2005) Petrophysical characterisation of a heterolithic tidal reservoir interval using a process-based modelling tool. Petrol Geosci 11:17–28

Palermo D, Aigner T, Seyfang B, Nardon S (2012) Reservoir properties and petrophysical modelling of carbonate sand bodies: outcrop analogue study in an

epicontinental basin (Triassic, Germany). Geol Soc Lond Spec Publ 370(1):111–138
Pickering KT, Hilton VC (1998) Turbidite systems of SE France. Vallis Press, London
Pickup GE, Hern CY (2002) The development of appropriate upscaling procedures. Transp Porous Media 46:119–138
Reading HG (ed) (1996) Sedimentary environments: processes, facies and stratigraphy, 3rd edn. Blackwell Science, London
Renard P, de Marsily G (1997) Calculating equivalent permeability: a review. Adv Water Resour 20:253–278
Ringrose PS, Corbett PWM (1994) Controls on two-phase fluid flow in hetrogeneous sandstones. In: Parnell J (ed) Geofluids: origin, migration and evolution of fluids in sedimentary basins, Geological Society special publication No. 78. Geological Society, London, pp 141–150
Ringrose PS, Nordahl K, Wen R (2005) Vertical permeability estimation in heterolithic tidal deltaic sandstones. Petrol Geosci 11:29–36
Ringrose PS, Sorbie KS, Corbett PWM, Jensen JL (1993) Immiscible flow behaviour in laminated and cross-bedded sandstones. J Petrol Sci Eng 9:103–124
Ringrose PS, Yardley G, Vik E, Shea WT, Carruthers DJ (2000) Evaluation and benchmarking of petroleum trap fill and spill models. J Geochem Explor 69:689–693
Rustad AB, Theting TG, Held RJ (2008) Pore-scale estimation, upscaling and uncertainty modelling for multiphase properties. SPE paper 113005, presented at the 2008 SPE/DOE improved oil recovery symposium, Tulsa, OK, UK, 19–23 April 2008
Scholz CH, Aviles CA (1986) The fractal geometry of faults and faulting. In: Das S et al (eds) Earthquake source mechanics, vol 37. American Geophysical Union, Washington, DC, pp 1–341
Sibson RH (1977) Fault rocks and fault mechanisms. J Geol Soc 133(3):191–213
Sperrevik S, Gillespie PA, Fisher QJ, Halvorsen T, Knipe RJ (2002) Empirical estimation of fault rock properties. In: Koestler AG, Hunsdale R (eds) Hydrocarbon seal quantification, Norwegian Petroleum Society special publications, 11. Elsevier, Amsterdam, pp 109–125
Stanbrook DA, Clark JD (2004) The Marnes Brunes Inférieures in the Grand Coyer remnant: characteristics, structure and relationship to the Grès d'Annot. In: Joseph P, Lomas SA (eds) Deep-water sedimentation in the Alpine Basin of SE France: new perspectives on the Grès d'Annot and related systems, Special Publications, 221. Geological Society, London, pp 285–300
Stauffer D, Ahorony A (1994) Introduction to percolation theory, Rev. 2nd edn. Routledge/Taylor & Francis Group, London
Stephen KD, Clark JD, Gardiner AR (2001) Outcrop based stochastic modelling of turbidite amalgamation and its effects on hydrocarbon recovery. Petrol Geosci 7:163–172
Stokes WL (1968) Multiple parallel-truncation bedding planes – a feature of wind-deposited sandstone formations. J Sediment Petrol 38:510–515
Twiss RJ, Moores EM (1992) Structural geology. Freeman and Co., New York, 532 pp
Tyler N, Finlay RJ (1991) Architectural controls on the recovery of hydrocarbons from sandstone reservoirs. In: Miall AD, Tyler N (eds) The three dimensional facies architectures of terrigeneous clastic sediments and its implications for hydrocarbon discovery and recovery. SEPM concepts in sedimentology and palaeontology, vol 3, SEPM, Tulsa, pp 1–5
Van Wagoner JC (1995) Sequence stratigraphy and marine to nonmarine facies architecture of foreland basin strata. In: Van Wagoner JC, Bertram GT (eds) Sequence stratigraphy of foreland basin deposits, AAPG memoir, 64. American Association of Petroleum Geologists, Tulsa, pp 137–224
Van Wagoner JC, Mitchum RM, Campion KM, Rahmanian VD (1990) Siliciclastic sequence stratigraphy in well logs, cores, and outcrops, AAPG methods in exploration series, No. 7. American Association of Petroleum Geologists, Tulsa
Walsh JJ, Watterson J (1988) Analysis of the relationship between displacements and dimensions of faults. J Struct Geol 10(3):239–247
Walsh J, Watterson J, Yielding G (1991) The importance of small-scale faulting in regional extension. Nature 351:391–393
Weber KJ (1986) How heterogeneity affects oil recovery. In: Lake LW, Carroll HB (eds) Reservoir characterisation. Academic, Orlando, pp 487–544
Weber KJ (1987) Computation of initial well productivities in aeolian sandstone on the basis of a geological model, Leman gas field, U.K. In: Tillman RE, Weber KJ (eds) Reservoir sedimentology, SEPM special publication, 46. Society of Economic Paleontologists and Mineralogist, Tusla, pp 333–354
Weber KJ, van Geuns LC (1990) Framework for constructing clastic reservoir simulation models. J Petrol Tech 42:1248–1297
Wise DU, Dunn DE, Engelder JT et al (1984) Fault-related rocks: suggestions for terminology. Geology 12(7):391–394
Yielding G, Freeman B, Needham DT (1997) Quantitative fault seal prediction. AAPG Bull 81(6):897–917

Epilogue

7

Abstract

If making forecasts from fit-for-purpose reservoir models is difficult, predicting future trends in reservoir modelling technology is no more than speculation. Nevertheless, we conclude with some reflections on key issues for further development of sub-surface reservoir model design.

Geological systems are highly complex and efforts to understand the effects of ancient rock strata on fluid flow processes several km beneath the surface are ambitious, to say the least. However, some of the underlying principles in geology help point us in the right direction. In the study of geological systems, we know that:

> *The present is the key to the past*
> *– Sir Archibald Geikie* (1905)

However, in most forms of forecasting we also realise that:

> *The past is the key to the future*
> *– Doe* (1983)

Reservoir modelling requires both

P. Ringrose and M. Bentley, *Reservoir Model Design*, DOI 10.1007/978-94-007-5497-3_7,

Multiscale geological bodies and associated erosion, Lower Antelope Canyon, Arizona (Photo by Jonas Bruneau, © EAGE reproduced with permission of the European Association of Geoscientists & Engineers)

7.1 The Story So Far

This book set out to offer practical advice and guidelines on the design and construction of subsurface reservoir models. This was an ambitious goal and it is clear we have only touched the surface of many of the issues involved.

The overall objective has been to develop the skills and procedures for the design of fit-for-purpose models that allow the reservoir modeller to make useful estimates of reservoir resources and forecasts of fluid behaviour within reasonable bounds of uncertainty.

The main design elements we proposed were:

1. Model Purpose
2. The Rock Model
3. The Property Model
4. Upscaling Flow Properties
5. Handling Uncertainty

In order to fulfil these design elements, we need access to a selection of data manipulation and mathematical modelling tools, including tools for seismic analysis, petrophysical analysis, geological modelling, statistical estimation, fluid flow simulation and analysis of outcomes. This is a rather long list of tools and functions – which in today's world is typically handled by several different computer software packages often linked by spreadsheets. The quest for a fully integrated subsurface data package will no doubt continue – and we welcome those efforts – but they will tend to be frustrated by the complexity of the challenge.

The primacy of the geological concept in deciding what information to capture in a reservoir model does, however, give us a framework for addressing the subsurface data integration challenge. The first step in reservoir modelling is always to think rather than to click.

We have tried to hold two important themes in balance:

(a) *The conceptual geological model:* Your first concept (e.g. "it's a fluvial delta") could be wrong – but that is a lot better than having no concept formulated at all. Better still, have several geological concepts that can be tested and refined during the modelling process. e.g. "we think it's a fluvial delta, but some indications of tidal influence are evident, and so we need to test tidal versus fluvial delta models."

(b) *The importance of the fluid system:* Fluid flows have their own natural averaging processes. Not all geological detail matters, and the geological heterogeneities that do matter depend on the fluid flow system.

Low viscosity fluids (e.g. gases) are more indifferent to the rock variability than high viscosity fluids (e.g. heavy oil) and all multiphase fluid systems are controlled by the balance of capillary, viscous and gravity forces on the fluid displacement processes.

Because these rock-fluid interactions are multi-scale – from the microscopic pore-scale (μm) to the macroscopic rock architecture scale (km) – we need a framework for handling data as a function of scale. The concept of the Representative Elementary Volume (REV) has been identified as absolutely fundamental to understanding and using reservoir property data. If your measurements are not representative and your flow properties are estimated at the wrong length scale the modelling effort is futile and the outcomes almost random. The multi-scale REV concept gives us a framework for determining which measurements (and averages of measurements) are useful and which model scales and grid sizes allow us to make reasonable forecasts given that data. This is not a trivial task, but it does give us a basis for deciding how confident we are in our analysis of flow properties.

Subsurface data analysis leads us quickly into the domain of 'lies and statistics.' Geostatistical tools are immensely useful, but also very prone to misuse. A central challenge in reservoir modelling is that we never have enough data – and that the data we do have is usually not statistically sufficient. When making estimates based on incomplete data we cannot rely on statistics alone – we must employ intuition and hypothesis. To put this simply in the context of reservoir data, if you wish to know the porosity and permeability of a given reservoir unit that answer is seldom found in a simple average. The average can be wrong for several reasons:

- some data points could be missing (incomplete sampling),
- the model elements could be wrongly identified (the porosity data from two distinct lithofacies do not give you the average of lithofacies 1 or lithofacies 2),
- you may be using the wrong averaging method – effective permeability is especially sensitive to the choice of averaging (the usefulness of the arithmetic, harmonic and geometric averages are controlled by the rock architecture),
- you may be estimating the average at an inappropriate scale – estimates close to the scale of the REV are always more reliable.
- the average may be the wrong question – many reservoir issues are about the inherent variability not the average.

Because of these issues, we need to know which average to use and when. Averaging is essentially a form of upscaling – we want to know which large-scale value represents the effects of small-scale variations evident within the reservoir. It is useful to recall the definition of the upscaled block permeability, k_b (Chap. 3.2):

> *k_b is the permeability of an homogeneous block, which under the same pressure boundary conditions will give the same average flows as the heterogeneous region the block is representing.*

If the upscaled permeability is closely approximated by the arithmetic average of the measured (core plug) permeability values, then that average is useful. If not, then other techniques need to be applied, such a numerical estimation methods or the power average.

Assuming, then, that we have the first four elements of reservoir design in place – a defined model purpose, a rock model based on explicit geological concepts, a property model estimated at an REV, and then upscaled appropriately – we have one element remaining. We are still not sure about the result, because we have the issue of uncertainty. No amount of careful reservoir model design will deliver the 'right' answer. We must carry uncertainty with us along the way. The model purpose might be redefined, the geological concept could be false, the property model may be controlled by an undetected flow unit, and upscaling may yield multiple outcomes.

In order to handle reservoir uncertainty we have advocated the use of multiple deterministic scenarios. It may at first appear dissatisfying to argue that there may be several possible outcomes after a concerted period of reservoir data analysis, modelling and simulation. The asset manager or financial investor usually wants only one answer, and becomes highly irritated

by the 'two-handed' geologist ("on the other hand. . ."). Some education about reservoir forecasting is needed at all levels. It is never useful to say that the sky tomorrow will be a shade of blue-grey (it seldom is). It is however, accurate to say that the skies tomorrow may be blue, white or grey – depending on the weather patterns and the time of day – and it is useful to present more explicit scenarios with probabilities, such as that there is a 60 % of blue sky tomorrow and a 10 % chance of cloud (if based on a sound analysis of weather patterns).

In the same way, multiple deterministic scenarios describing several possible reservoir model outcomes do provide useful forecasts. For example, who wouldn't invest in a reservoir development plan where nine out of ten fully integrated and upscaled model scenarios gave a positive net present value (NPV), but where one negative scenario helped identify potential downsides that would need to be mitigated in the proposed field-development plan.

The road to happiness is therefore good reservoir model design, conceptually-based and appropriately scaled. The outcome, or forecast, should encompass several deterministic scenarios, using probabilistic methods constrained by the model design.

7.2 What's Next?

7.2.1 Geology – Past and Future

Reservoir systems are highly complex, and so the ambition of reservoir modellers to understand the effects of ancient subsurface rock strata on fluid flow processes several km beneath the surface is a bold venture. However, we may recall the underlying principles of geology to guide us in that process. One of the founders of geology, Sir Archibald Geikie (1905), established the principle:

The present is the key to the past

This concept is now so embedded in sedimentology that we can easily forget it. We use our understanding of modern depositional processes to interpret ancient systems. Modern aeolian processes in the Sahara desert can tell us a lot about how to correctly describe, for example, a North Sea reservoir built from Permian aeolian sands. The many efforts to understand outcrop analogues for subsurface reservoir systems (such as Fielding and Crane 1987; Miall 1988; Brandsæter et al. 2005; Howell et al. 2008) are all devoted to this goal and will continue to bring important new insights into the reservoir description of specific types of reservoir.

Modern dune systems in the Sahara, central Algeria (Photo B. Paasch/Statoil © Statoil ASA, reproduced with permission)

A wide range of advanced imaging techniques are now being used in outcrop studies (Pringle et al. 2006) in order to obtain more quantitative and multi-scale information on outcrop analogues of reservoir systems. These include digital aerial photogrammetry, digital terrain models, satellite imaging, differential GPS location data, ground-based laser scanning (LIDAR) and ground penetrating radar. While these new high-resolution outcrop datasets provide more valuable information at faster rates of acquisition, they still require sound geological interpretation to make sense of the data and to apply them to reservoir studies.

Despite the growing body of knowledge, reservoirs and the ancient sedimentary record will always present us with surprises – features which we cannot explain or fully understand. For this reason, and because of the inherent challenge of the estimation of inter-well reservoir properties, reservoir forecasting will always carry large uncertainties.

In the process of making predictions about the subsurface (forecasting in the Earth sciences) we also employ a variation of the dictum, the *present is the key to the past,* because we use our knowledge of the geological record to make these forecasts, such that:

The past is the key to the future

This principle has grown in its use in the last decades, and formally elaborated as a branch of geological research by Doe (1983). Geological forecasting has received most attention in the study of climate change (e.g. Sellwood and Valdes 2006), but also in the fields of earthquake hazard forecasting and in subsurface fluid flow modelling.

In reservoir modelling studies we use the *past is the key to the future* principle in several ways:

1. We use our knowledge of the rock system to make credible 3D models of petrophysical properties giving us some confidence in our flow predictions. This principle is axiomatic to the proposed basis for reservoir model design – that there must be some level of belief in the geological concepts embodied in the model for there to be any value in the forecasts made using that model.
2. We use our experience from other similar reservoirs to gain confidence about new reservoirs. This includes the 'petroleum play' concept and the use of subsurface reservoir analogues. We have much more confidence in reservoir forecasting in a mature petroleum basin (such as the North Sea Brent play) than we do in a frontier province (such as deep water South Atlantic).
3. We use our growing body of knowledge on rock-fluid interactions to make better forecasts of fluid flow. One important example of this is the role of wetting behaviour in multiphase flow. There was a time (1950s to 1980s) when most petroleum engineers assumed water-wet behaviour for oil mobility functions, i.e. the oil had negligible chemical interaction with the rock. The growing appreciation that most rock systems are mixed wet (that is that they contain both water-wet and oil-wet pores controlled by the surface chemistry of silicate, carbonate and clay minerals) led to improved two- and three-phase relative permeability functions and to the use of different chemicals and altered water salinity to improve oil mobility.

The tools available for understanding rock-fluid interactions are constantly improving. New technology is being applied at the macroscopic scale, such as the use of advanced inversion of seismic data and electromagnetic data (Constable and Srnka 2007) and at the nanoscopic to microscopic scale, such as the use of scanning electron microscopes (SEM) to study pore-surface mineralogy.

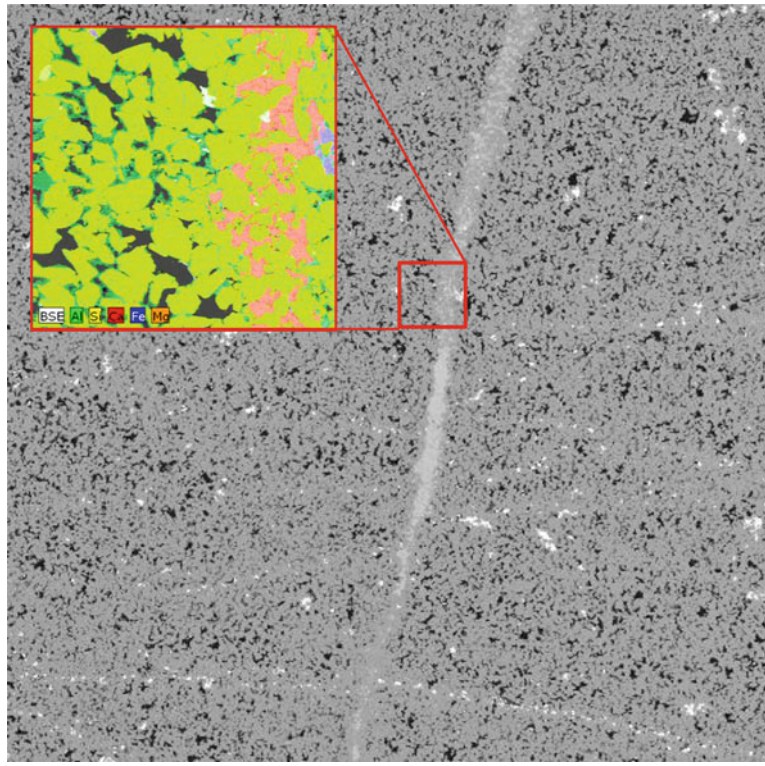

SEM petrography and spectroscopic analysis used to identify pore mineralogy and their controls on porosity and permeability. A fracture filled with carbonate cements (*pink*) and a sandstone pore space with grain coatings of chlorite (*green*) can be identified using the Energy-Dispersive X-ray Spectroscopy (EDS) image, shown on the *inset* which is 500 μm across (Photo T. Boassen/Statoil © Statoil ASA, reproduced with permission)

Thus it is clear that the future of reservoir modelling will ultimately be governed by our ability to use improved knowledge of geological systems to make more informative and accurate predictions of fluid distributions and flow processes. And we will use geology both in the classical reverse mode – understanding the past – and in the forward mode – forecasting.

7.3 Reservoir Modelling Futures

Computer modelling software tools applied to reservoir modelling are constantly evolving, and at an increasing pace. It would be foolish to attempt to predict innovations that might occur in this field – we welcome novel tools and methods when they become available. Rather we wish to highlight some of the current gaps which, from the user's point of view, might be filled by new software packages and upgrades.

Today's toolset for reservoir modelling is lacking in many aspects – the fields of integration, data rescaling and uncertainty handling being foremost in the wish list:

- *Integration:* Different parts of the reservoir modelling workflow are often addressed by different software tools. Whilst this can be frustrating, it is also inevitable as specialist functions often require special tools. Arguably, the most time-consuming part of the generic workflow is construction of the structural framework and iteration between the framework model and the property model updates. Improved integration across this link will be welcome to many users, including flexible gridding using structured and unstructured meshes.

- *Data re-scaling:* Upscaling workflows in reservoir modelling needs to move from a specialist reservoir simulation function to being a routine part of the reservoir model workflow. Nearly all data has to be re-scaled from one model/data domain to another. Several averaging options and numerical scaling recipes need to be offered to the user to allow the right data to the applied at the appropriate scale. The multi-scale REV concept gives us a framework for linking these rescaling functions to the natural length scales of the rock system.
- *Uncertainty handling:* Living with uncertainty means that we need the tools for handling uncertainty readily to hand. The ability to generate multiple equi-probable stochastic realisations of a model is only a small part of the solution. The main requirement is an ability to create and handle multiple deterministic concepts in the reservoir modelling workflow. 'Smart determinism' is, we propose, an ideal balance that combines geologically-based scenarios (determined) with stochastic methods for handling natural variability.

These three issues merely represent some key issues for future developments in reservoir modelling, and we look forward to the products of future research and innovation in this field. However, developments in software and modelling tools are only half of the answer to challenges of reservoir modelling. The other half, arguably the biggest half, lies with the user and the nature of the human mind-set.

We have shown many examples where reservoir data may be misleading or where model outcomes can be completely false. The problem lies ultimately not with the data or the model, but with the user's ability to intelligently interpret data and results. This is more about human psychology than geoscience, or more specifically about the human inability to make informed decisions. Human beings are, in fact, notoriously poor at making good intuitive judgements where chance or probability is involved. This tendency for people to be deluded by their own biases has been neatly explained a ground-breaking paper on 'Judgement under Uncertainty' by Tversky and Kahneman (1974). Daniel Kahneman went on to win the Nobel Prize for Economics in 2002 for "his insights from psychological research into economic science, especially concerning human judgment and decision-making under uncertainty" and has since then written a popular and very accessible book on the nature of human judgement (Kahneman 2011).

Tversky and Kahneman (1974) identified several heuristics that are used when making judgements under uncertainty. Many of their examples and arguments were set in the framework of economics – but apply equally well to reservoir modelling (Bentley and Smith 2008). Many heuristics have been identified since this early work, but three of the original biases are particularly pertinent to our efforts:

- Representativeness (mistaking plausibility for probability),
- Availability of information (bias towards interpretations that come easily to mind, hence ignorance of an important and relevant scenario),
- Adjustment from an anchor (the human tendency to become anchored by local or limited experience, and to find difficulty in estimating ranges far from the anchor point).

Improved decision making involves better understanding of these heuristics and biases. It is exactly this mind-set that needs to be applied more often in reservoir modelling, which points us to three key questions that must always be posed:

1. Is the sample representative?
2. Have you ignored important alternatives?
3. Is your forecast anchored to a premature best guess?

With that mind-set, and together with the many skills involved in geologically-based reservoir modelling, we are well prepared to make good reservoir models.

References

Bentley M, Smith S (2008) Scenario-based reservoir modelling: the need for more determinism and less anchoring. Geol Soc Lond Spec Publ 309:145–159

Brandsæter I, McIlroy D, Lia O, Ringrose PS (2005) Reservoir modelling of the Lajas outcrop (Argentina) to constrain tidal reservoirs of the Haltenbanken (Norway). Petrol Geosci 11:37–46

Constable S, Srnka LJ (2007) An introduction to marine controlled-source electromagnetic methods for hydrocarbon exploration. Geophysics 72(2): WA3–WA12

Doe BR (1983) The past is the key to the future. Geochemica et Cosmochemica Acta 47:1341–1354

Fielding CR, Crane RC (1987) An application of statistical modelling to the prediction of hydrocarbon recovery factors in fluvial reservoir sequences, SEPM Special Publication, Tulsa, No. 39

Geikie A (1905) The founders of geology. Macmillan and Co., Limited, London, p 299. Reprinted by Dover Publications, New York, in 1962

Howell JA, Skorstad A, MacDonald A, Fordham A, Flint S, Fjellvoll B, Manzocchi T (2008) Sedimentological parameterization of shallow-marine reservoirs. Petrol Geosci 14(1):17–34

Kahneman D (2011) Thinking fast and slow. Farrar, Straus and Giroux, New York, 499 p

Miall AD (1988) Reservoir heterogeneities in fluvial sandstones: lessons learned from outcrop studies. Am Assoc Petrol Geol Bull 72:882–897

Pringle JK, Howell JA, Hodgetts D, Westerman AR, Hodgson DM (2006) Virtual outcrop models of petroleum reservoir analogues: a review of the current state-of-the-art. First Break 24:33–42

Sellwood BW, Valdes PJ (2006) Mesozoic climates: general circulation models and the rock record. Sediment Geol 190:269–287

Tversky A, Kahneman D (1974) Judgment under uncertainty: heuristics and biases. Science 185:1124–1131

Nomenclature

Symbol	Definition
A	Area
$AI_{p,s}$	Acoustic Impedance (p and s wave)
C_a	Capillary number
C_v	Coefficient of Variation
E(p)	Expected value for the variable, p
f	Variance adjustment factor or frequency
f(x), g(x)	Functions of the variable x
F_D	Fracture density
g	Acceleration due gravity at the Earth's surface. (~9.81 ms^{-2})
H, h	Height or spatial separation (lag)
HCIIP	Hydrocarbon volume initially in place
$J(S_w)$	Water saturation function
K	Constant of hydraulic conductivity or coefficient of permeability
k	Permeability, or strictly the intrinsic permeability
$\underline{\mathbf{k}}$	Permeability tensor
k_b	Block permeability
k_{eff}	Effective permeability
k_h, k_v	Horizontal and vertical permeability
k_{ro}, k_{rg}, k_{rw}	Relative permeability to oil, gas and water
k_x, k_y, k_z	Directional permeabilities in a Cartesian grid coordinate system
L	Length
ln(x)	Natural logarithm of x
N_o	Sample number sufficiency statistic
N/G	Net to Gross ratio
p, p_c	Statistical variable, critical value of p
P_c	Capillary pressure
PDF	Probability density function
∇P	Pressure gradient
Q, q	Volume flux of fluid

QC	Quality Control
REV	Representative Elementary Volume
STOIIP	Stock tank oil initially in place
S_{ro}	Remaining oil saturation
S_{wi}	Initial water saturation
S_{wc}	Connate water saturation
S_w, S_o, S_g	Water, oil and gas saturation
u	Intrinsic flow velocity
V_m, V_s	Volume fraction of mud and sand
V_{shale}	Volume fraction of shale
v_p	Seismic compressional wave velocity
v_s	Seismic shear wave velocity
X	General variable parameter
δX, δY, δZ	Grid cell increment in X, Y, and Z
ΔX, ΔY, ΔZ	System dimension in X, Y, and Z
Z(x)	Spatial variable
$\gamma(h)$	Semi-variance at distance h (the Variogram function)
θ	Angle (radians or degrees)
κ	Number of standard deviations
λ	Correlation length or power exponent
μ	Mean value (statistics) or viscosity (physics)
π	Mathematical constant (ratio of circle circumference to diameter)
ρ	Correlation coefficient
ρ_g	Grain density
ρ_b	Bulk formation density
σ	Standard deviation (statistics) or interfacial tension (physics)
$\sigma_{1,2,3}$	Principle components of the stress field
ϕ	Porosity
ω	Weighting factor

P. Ringrose and M. Bentley, *Reservoir Model Design*, DOI 10.1007/978-94-007-5497-3,

Solutions

Exercise 2.1. Estimation of variograms for an outcrop image

Variograms for the pixelated grey-scale version of the outcrop image are shown below. If your sketch was close to these your intuition was pretty good.

(a) Horizontal variogram with range of c. 40 pixels

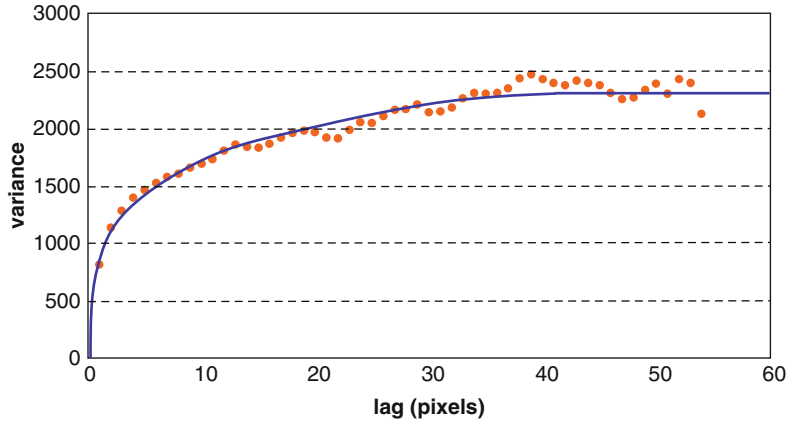

(b) Vertical variogram with range of c. 5 pixels

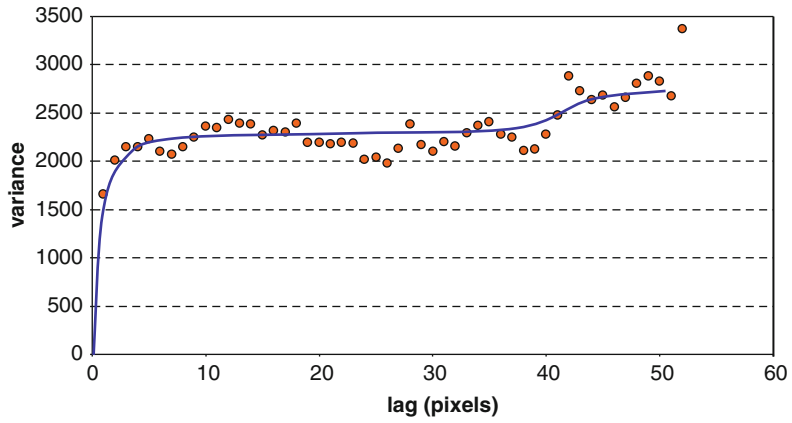

P. Ringrose and M. Bentley, *Reservoir Model Design*, DOI 10.1007/978-94-007-5497-3,

Exercise 3.1. Which modelling methods to use?

There is no automatic right answer – the table is ordered in approximate correspondence between simpler approaches and complexity of purpose. 3D approaches are nearly always essential for well placement and design of IOR/EOR strategies, while 2D maps or simple averages may be quite adequate for initial fluids-in-place or reserves estimates.

Exercise 3.2. Additive properties

The key factor is that if the property involves a vector (e.g. related to field fluxes or gradients) then it is generally non-additive, while scalar properties are additive. The following properties are essentially additive: net-to-gross ratio, fluid saturation, porosity and bulk density. Permeability, formation resistivity, seismic velocity, and acoustic impedance are non-additive. However, fluid saturation could be considered non additive by virtue of its dependence on permeability.

Exercise 3.3. Dimensions of permeability

The SI unit for intrinsic permeability, k, is m^2 and the dimensionless form of Darcy's law is $[LT^{-1}] = ([L^2]/[ML^{-1}\ T^{-1}])\ .\ [ML^{-2}\ T^{-2}]$. Note: One Darcy $= 0.987 \times 10^{-12}\ m^2$.

Exercise 3.4. Comparing model distributions to data

The warning indicator here is that although the arithmetic averages are similar, the geometric average of the well data is half the value for the model while the harmonic average of the model is much lower than the value for the well data. Two things are happening here illustrated in the graph below: (a) there is a facies group, or population, in the well data that has not been captured in the model and (b) the model has included some barriers that are not present in the data (due to insufficient sampling of thin shales). The model may in fact be quite a good one – if it is assumed that it captures the key features of the geology. Gaussian distributions are shown representing the hypothetical "true" rock property distributions.

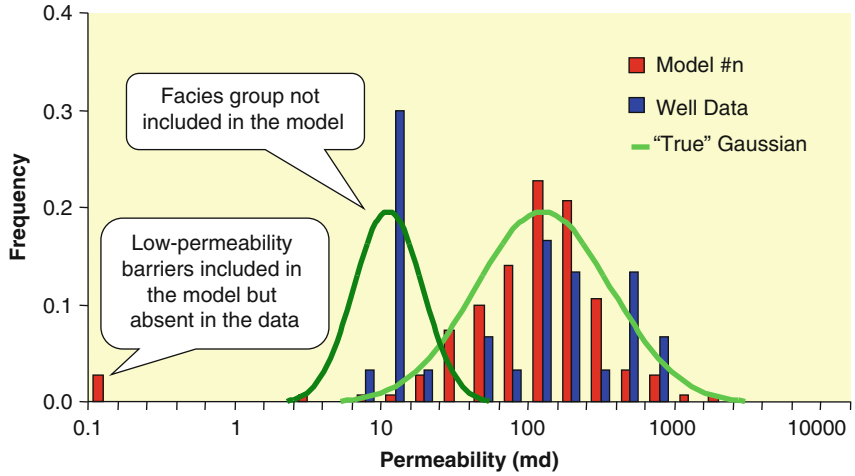

Exercise 3.5. Bayes and the cookie jar

The probability that Fred picked the cookie from the first cookie jar is 0.6 because:

$$P(A|B) = \frac{P(B|A)\,x\,P(A)}{P(B)} = \frac{0.75\,x\,0.5}{0.625} = 0.6$$

where

P(A) is the probability of picking jar 1;

P(B), is the probability of getting a plain cookie;

P(B|A), or the probability of getting a plain cookie assuming Fred picked from jar l.

Exercise 4.1. Permeability upscaling for a simple layered model

(a) The upscaled horizontal and vertical single-phase permeabilities are estimated using arithmetic and harmonic averages to give $k_h = 550$ md and $k_v = 181.8$ md.

(b) Analytical values for the upscaled directional relative permeabilities for two values of Pc (assuming capillary equilibrium) are given below, where k_{rox} is the oil relative permeability in the horizontal direction, etc. (The method is illustrated in Fig. 4.9 and the complete upscaled curves are shown in Fig. 4.11.)

Pc	Sw	krox	kroz	krwx	krwz
0.5	0.137	0.892	0.873	1.022E-05	3.058E-05
3	0.132	0.899	0.898	4.74E-08	1.419E-07

Exercise 4.2. Find the REV's for your reservoir.

There is no correct answer – every reservoir is unique, although many lithofacies show characteristic behaviours. An example multi-scale REV sketch might look something like the example below. In practice we want to identify scales where the variance is relatively low and where an REV may be defined. Measurements will be most representative where an REV can be established. Reservoir models are best designed if their length scales (cell sizes and model domains) match the REV's. This may not always be possible.

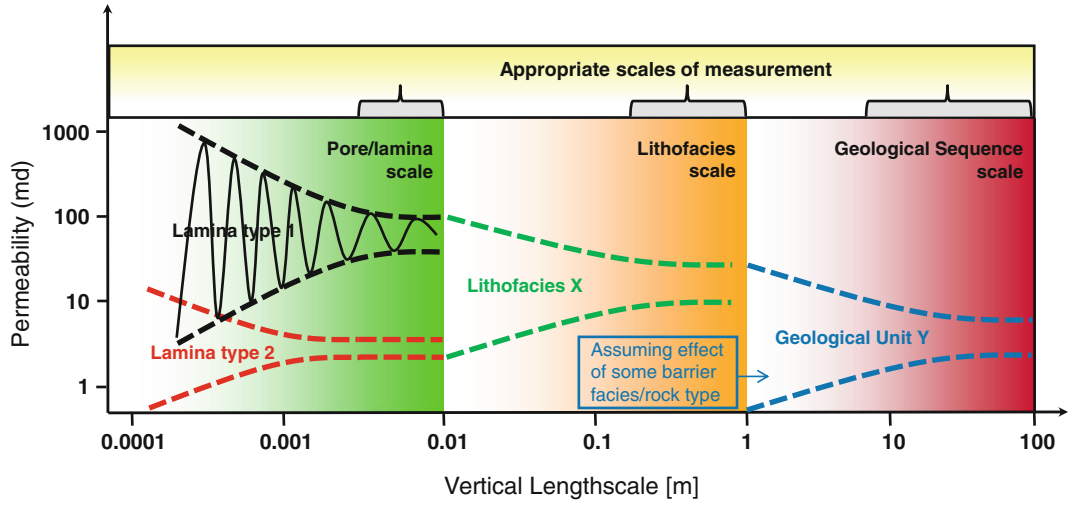

Index

P. Ringrose and M. Bentley, *Reservoir Model Design*, DOI 10.1007/978-94-007-5497-3,